SYNTHETIC APERTURE RADAR FOR A CROP INFORMATION SYSTEM: A MULTIPOLARIZATION AND MULTITEMPORAL APPROACH

by

Yifang Ban

A thesis
presented to the University of Waterloo
in fulfilment of the
thesis requirement for the degree of
Doctor of Philosophy
in
Geography

Waterloo, Ontario, Canada, 1996

© Yifang Ban 1996

National Library of Canada
Acquisitions and Bibliographic Services
395 Wellington Street
Ottawa ON K1A 0N4
Canada

Bibliothèque nationale du Canada
Acquisitions et services bibliographiques
395, rue Wellington
Ottawa ON K1A 0N4
Canada

Your file Votre référence

Our file Notre référence

The author has granted a non-exclusive licence allowing the National Library of Canada to reproduce, loan, distribute or sell copies of his/her thesis by any means and in any form or format, making this thesis available to interested persons.

L'auteur a accordé une licence non exclusive permettant à la Bibliothèque nationale du Canada de reproduire, prêter, distribuer ou vendre des copies de sa thèse de quelque manière et sous quelque forme que ce soit pour mettre des exemplaires de cette thèse à la disposition des personnes intéressées.

The author retains ownership of the copyright in his/her thesis. Neither the thesis nor substantial extracts from it may be printed or otherwise reproduced with the author's permission.

L'auteur conserve la propriété du droit d'auteur qui protège sa thèse. Ni la thèse ni des extraits substantiels de celle-ci ne doivent être imprimés ou autrement reproduits sans son autorisation.

0-612-21331-5

Canada

I hereby declare that I am the sole author of this thesis.

I authorize the University of Waterloo to lend this thesis to other institutions or individuals for the purpose of scholarly research.

I further authorize the University of Waterloo to reproduce this thesis by photocopying or by other means, in total or in part, at the request of other institutions or individuals for the purpose of scholarly research.

The University of Waterloo requires the signatures of all persons using or photocopying this thesis. Please sign below, and give address and date.

ABSTRACT

Acquisition of timely information is a critical requirement for successful management of an agricultural monitoring system. Crop identification and crop-area estimation can be done fairly successfully using satellite sensors operating in the visible and near-infrared (VIR) regions of the spectrum. However, data collection can be unreliable due to problems of cloud cover at critical stages of the growing season. The all-weather capability of synthetic aperture radar (SAR) imagery acquired from satellites provides data over large areas whenever crop information is required. At the same time, SAR is sensitive to surface roughness and should be able to provide surface information such as tillage-system characteristics. With the launch of ERS-1, the first long-duration SAR system became available. The analysis of airborne multipolarization SAR data, multitemporal ERS-1 SAR data, and their combinations with VIR data, is necessary for the development of image-analysis methodologies that can be applied to RADARSAT data for extracting agricultural crop information.

The overall objective of this research is to evaluate multipolarization airborne SAR data, multitemporal ERS-1 SAR data, and combinations of ERS-1 SAR and satellite VIR data for crop classification using non-conventional algorithms.

The study area is situated in Norwich Township, an agricultural area in Oxford County, southern Ontario, Canada. It has been selected as one of the few representative agricultural 'supersites' across Canada at which the relationships between radar data and agriculture are being studied. The major field crops are corn, soybeans, winter wheat, oats, barley, alfalfa, hay, and pasture.

Using airborne C-HH and C-HV SAR data, it was found that approaches using contextual information, texture information and per-field classification for improving agricultural crop classification proved to be effective, especially the per-field classification method. Results show that three of the four best per-field classification accuracies ($\hat{K}$=0.91) are achieved using combinations of C-HH and C-VV SAR data. This confirms the strong potential of multipolarization data for crop classification.

The synergistic effects of multitemporal ERS-1 SAR and Landsat TM data are evaluated for crop classification using an artificial neural network (ANN) approach. The results show that the per-field approach using a feed-forward ANN significantly improves the overall classification accuracy of both single-date and multitemporal SAR data. Using the combination of TM3,4,5

and Aug. 5 SAR data, the best per-field ANN classification of 96.8% was achieved. It represents an 8.5% improvement over a single TM3,4,5 classification alone.

Using multitemporal ERS-1 SAR data acquired during the 1992 and 1993 growing seasons, the radar backscatter characteristics of crops and their underlying soils are analyzed. The SAR temporal backscatter profiles were generated for each crop type and the earliest times of the year for differentiation of individual crop types were determined. Orbital (incidence-angle) effects were also observed on all crops. The average difference between the two orbits was about 3 dB. Thus attention should be given to the local incidence-angle effects when using ERS-1 SAR data, especially when comparing fields from different scenes or different areas within the same scene.

Finally, early- and mid-season multitemporal SAR data for crop classification using sequential-masking techniques are evaluated, based on the temporal backscatter profiles. It was found that all crops studied could be identified by July 21.

ACKNOWLEDGEMENTS

I would like to express my sincere thanks to many individuals who have assisted me during the preparation of this thesis.

First of all, I would like to thank my supervisor, Dr. Philip J. Howarth, for his continual support, guidance and encouragement throughout this research. I am specially appreciative of his editorial efforts on proof-reading my thesis.

I would also like to thank my thesis committee, Dr. Jane Law, Dr. Ellsworth LeDrew, and Dr. Ric Soulis for their constructive suggestions and comments. I am very grateful to them for reviewing my thesis at such short notice and offering effective feedback. In addition, I would like to thank my external examiner, Dr. Richard Protz of the Department of Land Resource Science at the University of Guelph, for reviewing my thesis and for the philosophical discussion during my defence regarding SAR and VIR remote sensing.

I would like to express my special thanks to Mr. Aldo Argentieri, Manager of the ERS Help Desk at ESRIN, ESA for making the calibration of the ERS-1 SAR data possible. Thanks also go to DLR, RADARSAT International and Eurimage on the SAR data calibration.

I appreciate the assistance of colleagues at both the University of Waterloo and elsewhere:

- The OXSOME and ERSOME field data collection teams for collecting the ground data during 1990, 1992 and 1993 growing seasons.
- Mr. Paul Treitz at the Department of Geography, York University for providing the airborne SAR textural images.
- Dr. Bas Bouman at Centre for Agrobiological Research and Dr. Maurice Borgeaud at ESTEC, ESA for the insightful discussions during my visit to the Netherlands.
- Dr. Tom Lukowski, Ms. Heather McNairn, Mr. Julius Printz and Mr. Mike Manore at CCRS, and Dr. Dave Barber at the University of Manitoba for discussing the Gatineau Processor, the Atlantis Processor, and the calibration of ERS-1 SAR data with me.
- Dr. Greta Reynolds, Manager of User Services and Mission Planning and Jason Williams, SAR Calibration Engineer at Alaska SAR Facility for their willingness to help me on ERS-1 SAR calibration.
- Dr. Joe Piwowar for his great help on image analysis software and hardware. Thanks also go to colleagues at WATLEO and MAD office.

I am very thankful to the University of Waterloo and the Government of Ontario for the various scholarships which made my Ph.D. study possible. Funding for this project has been provided by a Centre of Excellence Grant from the Province of Ontario to the Institute for Space and Terrestrial Science and through an NSERC Research Grant awarded to Dr. Howarth. The support of the Canada Centre for Remote Sensing through the RADARSAT Data Development Program is also gratefully acknowledged.

I would also like to thank the International Space University and the Canadian Foundation for ISU for the rewarding experiences during the ISU 1994 and 1995 Summer Sessions in Barcelona, Spain and Stockholm, Sweden.

Finally, I would like to thank Jonas, my fiancé for his unconditional love, support and understanding during the writing of this thesis. Also, I would like to express my deep gratitude for the constant inspiration and support of my parents.

DEDICATION

To my parents
献 给 我 敬 爱 的 父 母
for your constant inspiration for excellence

till min älskade Jonas
för ditt villkorslösa stöd och din kärlek

and to women and men
who are working towards preserving our home planet

We do not inherit the Earth from our ancestors, but borrow it from our children

- D. Brower

TABLE OF CONTENTS

LIST OF TABLES

LIST OF FIGURES

CHAPTER 1: INTRODUCTION

1.1 Motivations for the Research

As the 20th century draws to a close, pressures on agriculture can only increase with the exponential growth of world population, urbanization, desertification, deforestation, soil erosion, and other environmental stresses. It is projected that, by the year 2000, the amount of arable land per capita will be only about 0.2 ha, as compared with about 0.5 ha in 1950 (Avery *et al.*, 1992). For example, Java loses nearly 20,000 hectares of cropland annually to urban growth - enough to grow rice for some 378,000 Indonesians each year (Gardner, 1996). Each and every day, world demand for food increases by 250,000 mouths; at this rate, world demand for food will increase by as much as three times its current level in the next 50 years (Park *et al.*, 1980; Gilson, 1989; The Toronto Star, July 18, 1993). According to the World Food Council, 550 million people were too undernourished to "sustain an active, healthy life" in 1989 (Kutzner, 1991). These and other factors underscore the need for agricultural information systems that can provide accurate and timely information on crop type, area and location, crop growing condition, crop production, and the extent and severity of catastrophic events (e.g. tornadoes, hail, floods, droughts, crop diseases and insect infestation) on regional, national, and global scales, such that domestic and world agricultural policy planners can more effectively manage agricultural resources.

At present, a central world agricultural information system does not exist; thereby making it difficult for commodities to move within world food markets in a timely and efficient manner. For instance, advanced information concerning food production is important for providing the timely, accurate information necessary to stabilize fluctuations in commodity markets, which are especially sensitive to uncertainties or fluctuations in supply and demand (Campbell, 1987). Evidence of this was provided by the entrance of the USSR into the world wheat market in 1975

as an unexpected buyer rather than a seller. This caused world wheat prices to soar and a general disruption of normal market conditions (Park *et al.*, 1980).

Timely and accurate crop area and production information must be relayed at least on a country-by-country or region-by-region basis in order for world food markets to operate at an acceptable level of efficiency. The ability of a country or region to accurately forecast the harvest of its major crops, coupled with the ability to analyze its position with respect to the current world market, would enable agricultural planners to make more rational and economically rewarding export-import decisions. Indeed, the lack of current and accurate agricultural information can be a major obstacle to economic development. In fact, improvements in the timeliness and accuracies of crop production data can translate into substantial economic benefits. Cost-benefit studies for earth-resources data have shown that more timely and accurate crop production statistics could be worth billions of dollars[1] (Park *et al.*, 1980). This is especially true in developing countries where agriculture dominates the economy and employs most of the population. A good knowledge of cultivated areas and agricultural production is absolutely indispensable to major policy decisions concerning national or regional development and planning, trade-balance management and, in times of crisis, international food-aid management, to avoid not only shortages but also surpluses, the secondary effects of which are just as damaging (FAO, 1993).

A crop information system is one way that remote sensing can provide valuable agricultural information to decision-makers. Remote sensing is presently the only technology that can provide timely and accurate crop inventory information. When the advantages of various remote sensing platforms are compared, it is clear that repetitive coverage is unique to the orbiting spacecraft, since it is comparatively much more expensive to acquire the same coverage with

[1] For example, advanced knowledge of the U.S. crop yield is strategic information in maintaining a positive balance of agricultural exports: US$13 billion in 1989, with a surplus of US$3.7 billion (RSI, 1995a).

aircraft. Effective monitoring of crop growth requires that the coverage is repeated at least four times during the growing season. This is problematic on a global scale because the growing season is unique to *both* geographic location (latitude, longitude and altitude) and to the crop. Furthermore, the observation and control of crops is useful only at specific, well-determined points in time during the growing season (Myers *et al.*, 1983). The weather in Canada and in many other parts of the world, however, often makes this impossible using sensors operating in the visible and near-infrared (VIR) bands, as is demonstrated by the relatively few cloud-free images obtained by Landsat and SPOT (Blakeman, 1990). Thus, there is a need for a remote sensing system which can be employed in all weather conditions. Radar has great potential to provide information in such a manner.

The 1990s have been, and will continue to be, the decade of spaceborne synthetic aperture radar (SAR). In 1991 and 1995, the European Space Agency (ESA) launched the European Remote Sensing Satellites, ERS-1 & 2. In 1992, the Japanese Earth Resources Satellite (JERS-1) was launched. The third shuttle SAR missions, SIR-C/X SAR, were flown in 1994 for limited durations on two separate shuttle missions, and the Canadian RADARSAT was launched on Nov. 4, 1995. In the later part of this decade and early next decade, the future advanced SAR missions such as ESA ENVISAT ASAR and the U.S. Shuttle Radar Topography Mission will be launched (Ferster, 1996). All of these spaceborne SAR systems provide an excellent opportunity to develop an operational crop information system to support decision-making.

1.2 Problem Statement and Objectives

1.2.1 Problem Statement

As discussed earlier, acquisition of timely information is a critical requirement for successful management of an agricultural monitoring system. Crop identification and crop-area estimation

can be done fairly successfully using satellite sensors operating in the visible and near-infrared regions of the spectrum. However, data collection can be unreliable due to problems of cloud cover at critical stages of the growing season. The all-weather capability of synthetic aperture radar (SAR) imagery acquired from satellites provides data over large areas whenever crop information is required. At the same time, SAR is sensitive to surface roughness and should be able to provide surface information such as tillage-system characteristics. With the launch of ERS-1, the first long-duration SAR system became available. The analysis of multitemporal ERS-1 SAR data, and their combinations with VIR data, is necessary for the development of image-analysis methodologies that can be applied to RADARSAT data for extracting agricultural crop information.

Previous research has demonstrated the large potential for using radar remote sensing for various agronomic applications, as summarized by Holmes (1990) and Ban and Howarth (1996a). SAR data are so complex, however, that the interaction of the radar signal with agricultural targets is not fully understood. In addition, with the current state-of-the-art of interpretation methods for SAR imagery, the accuracies of crop classification are not always as high as required for successful operation of a crop information system (Brisco and Protz, 1982; Brown, 1987; Foody, 1988; Foody *et al.*, 1989; Brisco *et al.*, 1989a; Ban *et al.*, 1995). To be able to increase the accuracies of crop identification and area estimation, and thus develop a viable crop information system that makes use of SAR imagery as the primary data source, we need to:

1. have a better understanding of the crop and underlying soil characteristics that influence radar backscatter throughout the growing season;
2. identify suitable methodologies to extract crop information from SAR imagery;
3. evaluate multipolarization airborne SAR for crop identification;
4. evaluate multitemporal ERS-1 SAR for crop identification; and
5. evaluate combinations of satellite SAR and VIR for crop identification.

1.2.2 Research Objectives

The overall objective of this research is to evaluate multipolarization airborne SAR data, multitemporal ERS-1 SAR data, and combinations of ERS-1 SAR and satellite VIR data for crop classification using non-conventional algorithms. To achieve this objective, five major issues need to be addressed.

The first objective is to perform a comparative analysis of classification algorithms that incorporate tonal, contextual, and/or textural information. The specific objectives are:

- to determine the accuracy of crop classification, using standard per-pixel classification procedures such as a maximum likelihood classifier (MLC)
- to evaluate non-parametric and non-statistical classification algorithms based on contextual, textual, and per-field approaches for crop identification.

The second objective is to evaluate multipolarization (C-HH and C-HV) airborne SAR data for crop classification. The specific objectives are:

- to evaluate single polarization C-HH and C-HV SAR for crop classification
- to evaluate the combination of C-HH and C-HV SAR for crop classification.

The third objective is to evaluate the synergistic effects of multitemporal ERS-1 SAR and satellite VIR data for crop classification. The aims will be:

- to evaluate early- and mid-season crop classification accuracies using a single-date SAR image alone and also using multitemporal SAR data
- to evaluate the synergism of multitemporal ERS-1 SAR and Landsat TM data for improving crop classification, and
- to evaluate an ANN algorithm as a post-segmentation classifier in comparison to the conventional maximum-likelihood classifier.

The fourth objective is to develop a better understanding of the interaction of microwave energy with crops and their underlying soils over the growing season. This will involve:

- absolute calibration and geometric correction of ERS-1 SAR data
- generation of ERS-1 SAR temporal backscatter crop profiles for both 1992 and 1993 data
- identification of fields that display anomalous radar backscatter characteristics, statistically describing the anomalous fields, and attempting to identify reasons for these anomalies
- recommendations for the earliest time of the year to differentiate agricultural crops.

The fifth objective is to evaluate multitemporal ERS-1 SAR data for crop classification based on SAR temporal backscatter profiles. The satellite SAR data selected for multitemporal analysis will be representative of the different stages of development of crops. Furthermore, the classification procedures identified in the third objective as being the most appropriate for crop classification will be used in the analysis. The work will involve:

- analysis of ERS-1 SAR temporal backscatter crop profiles
- evaluation of multitemporal ERS-1 SAR for crop classification using sequential masking.

1.3 Implications of the Research

1.3.1 Scientific Perspective

The proposed research will contribute to two main theoretical developments. The application of satellite radar remote sensing to agriculture is still in its infancy. Thus, the proposed study aims, first, to provide a better understanding of the interaction of microwave energy with agricultural crops and soils throughout the growing season and, second, to develop optimal methodologies to extract agricultural information from SAR data.

From an applied perspective, the findings of this study are of practical significance since the Canadian RADARSAT was successfully launched on November 4, 1995. RADARSAT is designed to meet the data requirements and data-delivery requirements demanded by operational programs. The earlier satellites, such as ERS-1, were primarily intended to fulfill the needs of the research community. To be ready to use RADARSAT SAR as a primary data source for an operational crop information system, a concentrated research effort is necessary to gain experience using ERS-1 SAR as a research tool, since both RADARSAT and ERS-1 SAR operate at the same wavelength (C-band). In addition, multipolarization airborne SAR studies will benefit future spaceborne SAR missions; for example, ESA's ENVISAT Advanced SAR system will operate in alternating polarization modes.

1.3.2 Industrial and Socio-Economic Implications

Agriculture is one of the most important industries in the Canadian economy, employing 14.5% of Canadians in the agri-food sector and generating about 10% of the Gross Domestic Product. The $6.8 billion of agricultural products exported in 1989 exceeded imports by $3.5 billion, resulting in a significant contribution to the balance of trade. Of the total of 997 million ha of land in Canada, 76.8 million ha are in farmland, a large area managed by only 4% of the population. Although Canada's contribution to world food production is modest, it is still an important player in the world market, exporting 40 to 50% of its total agricultural production. A strong agricultural industry is vitally important to the Canadian economy and to the world. Satellite SAR, such as RADARSAT, is perceived by the agricultural community as a potentially important tool for supplying data to meet its timely and accurate informational requirements in agricultural resource management (Brown *et al.*, 1993b).

Timely and accurate information on crop type and area estimation is not only a basic need for crop inventory and monitoring, but also for crop production forecasting. A crop information system is needed for a variety of reasons. Government departments, such as Agriculture Canada and Statistics Canada, require a system for administrative purposes, possibly for measures to regulate quantities and prices, or for external trade settlements. Private firms, particularly those engaged in wholesale and external trade, are interested in timely and accurate data for their marketing and storage arrangements. Farmers themselves may use harvest data calculated for their country and region as a basis for their seasonal sales in order to obtain particularly favourable prices (Thiede, 1981). In addition, information on the extent and severity of catastrophic events is important for damage assessment and relief planning (Werle, 1992). The benefits of a crop information system can therefore be summarized as: 1. accurate estimates resulting in price stability; 2. timely and accurate forecasts of production allowing governments to plan domestic and foreign policy and actions; 3. accurate forecasts enabling optimal utilization of storage, transportation, and processing facilities; and 4. detection and timely knowledge of harmful effects on crop growth to assist in taking remedial measures.

1.4 Organization of the Thesis

The thesis is organized into eight chapters. In the first chapter, the motivations for the research, the achievements and problems using SAR for crop classification, the objectives of the research and its scientific and socio-economic implications have been introduced.

In Chapter 2, conventional agricultural inventory, airborne VIR remote sensing and satellite VIR remote sensing for agriculture are reviewed. Their roles as an input into an operational crop information system are evaluated.

Chapter 3 provides a detailed review of the state-of-art of SAR in agricultural applications, focusing specifically on crop identification. The advantages of radar remote sensing, fundamental theories of the interaction between SAR and agricultural parameters, airborne SAR agricultural studies, and spaceborne SAR agricultural studies are summarized. Methodologies to extract crop information from SAR data are also evaluated. An overview of achievements, limitations and the future potential of SAR data for agricultural crop identification, as explained in the existing literature, is presented.

In Chapter 4, the geographical characteristics of the study area are discussed. The characteristics of the airborne SAR data, ERS-1 SAR data and the ground information are described. The important aspects of calibration of ERS-1 SAR data are discussed and procedures for derivation of the calibration constant σ° are presented.

In Chapter 5, the multipolarization airborne SAR is evaluated for crop classification. The effectiveness of C-HH and C-HV SAR for crop classification are compared. Methodologies to improve the classification accuracies, such as filtering, texture analysis and a per-field approach, are tested.

In Chapter 6, the synergistic effects of ERS-1 SAR and Landsat TM data for crop classification are evaluated. Combinations of single-date SAR and TM data, and multitemporal ERS-1 SAR and TM data are compared with TM data alone for crop classification.

In Chapter 7, the use of multitemporal ERS-1 SAR for crop identification is presented. Specifically, SAR temporal backscatter profiles for major crops during the 1992 and the 1993 growing seasons are generated and the earliest times of the year to distinguish crop types are

identified. Multitemporal SAR data are evaluated for crop classification using sequential-masking techniques.

In the final chapter, Chapter 8, the major findings of this research are summarized. Conclusions are presented and future research directions are suggested.

CHAPTER 2: VIR REMOTE SENSING IN AGRICULTURE

2.1 Conventional Agricultural Inventory

In the past, information on crop type and area has often been compiled by conducting personal interviews with farm operators or by conducting mail surveys. Despite the valiant efforts that reporting agencies have made from time to time to acquire information on crop type and acreage, whether from questionnaires sent to farmers or from direct on-the-ground surveys, it is often uncertain whether a satisfactory estimate has been obtained. Returns from questionnaires have often been too few, too inaccurate, and too late. Returns from direct on-the-ground surveys, due to limitations of both time and funds, have sometimes constituted too small a sample of the vast agricultural area of interest for them to be used with confidence (Colwell *et al.*, 1970). At regional and (inter-) national levels, the processing of these sample data is an expensive and time-consuming procedure (Bouman, 1991b).

Agriculture is a dynamic system whose control and management call for rapid, regular, and reliable acquisition of a great many data on the growth cycle of crops, and their sequence in time and space (Gillot, 1980). Remote sensing is presently the only technology that can provide timely, regular, and accurate crop inventory information. In fact, agricultural crops and forest species were two areas of investigation to which remote sensing applications were initially directed (MacDonald, 1984).

2.2 Airborne VIR Remote Sensing for Agriculture

2.2.1 Aerial Photography

Aerial photography using the visible and the near-infrared bands for surveying agricultural crops is well-established. The earliest research report describing an attempt to identify crops using

black-and-white aerial photographs was by Goodman (1959) who used a multitemporal approach. Since then, conventional, medium-scale aerial photographs have been used in some regions for the identification of major crops and the monitoring of crop-area allotments.

The history of remote sensing in agriculture contains a comprehensive record of exploitation of panchromatic photos, largely by the United States Department of Agriculture (USDA); the use was virtually exclusively for measuration. During the 1950s, the Economic Research Service of USDA became the first to use historic as well as current air photos to perform land use and land use change analysis in an operational context. In the last twenty-five years, the technology of crop identification has advanced from utilization of broad-band black-and-white to black-and-white infrared photos; then to narrower band color and then to color-infrared photographs (Myers *et al.*, 1983).

Crop identification by manual airphoto interpretation is accomplished by application of the elements of photo interpretation in the context of knowledge of the local environmental setting and the local crop calendar (i.e., typical dates of planting and harvesting). In many settings, crops are usually observed planted in uniform, distinct fields, a single crop to a field. Precise identification of specific crops may be difficult in the absence of detailed knowledge of local cropping practices, such as crop rotation. For example, it is usually easy to separate small-grain crops (wheat, oats, barley, rye) from large-grain crops (corn or sorghum), although even experienced photo interpreters may have difficulty distinguishing crops within these classes (e.g., wheat and barley). Therefore, careful timing of the date and season of the aerial photographs and knowledge of the crop calendar are essential for crop identification and area estimation (Campbell, 1987).

Although black-and-white aerial photography is usually suitable for crop identification and distinction between small-grain crops and large-grain crops, difficulty has been encountered in

making distinctions within small grains and large grains. If color or color infrared (CIR) photographs are available, it may be possible to interpret information concerning crop maturity, as the time for harvest approaches. In addition, CIR photographs may permit interpretation of the presence, location, and nature of insect infestations or diseases (Campbell, 1987). Crop discrimination using CIR photography has been studied closely and it has been found that the percentage accuracy depends on time of year, location and the environment. For example, in some regions crops are planted in very small fields, or many different kinds of plants are planted together in a single field. Under such conditions, crop identification may be much more difficult than in the typical mid-latitude situation where fields are large and crops are homogeneous within fields (Campbell, 1987).

At the present time, aerial photography is by far the most widely used remote sensing technique in agriculture (Pacheco, 1980). The major advantages of conventional aerial photography are the high resolution, the wide choice of methods, the availability of instruments, and the knowledge of trained personnel. Aerial photographs also have the advantage of providing large-scale information, indispensable when mapping at scales above 1:25,000 (Lantieri, 1993). The major disadvantages of applying aerial photos to agriculture result from uneconomic repetitive coverage (within a year), non-uniform and uncalibrated intensity measurements that obstruct automated density processing, and the relatively high cost per km^2, especially for large-scale aerial surveys (Pacheco, 1980; see Appendix A for cost-benefit analysis).

2.2.2 Airborne Multispectral Sensors for Agriculture

Since the 1960s, a major thrust of an element of the U.S. civilian remote sensing research program has been advancing the techniques for machine processing of satellite-acquired multispectral data. The program's primary focus has been the use of multispectral data to identify crop type, condition, and ontogenetic stages of cultural vegetation. The research began

as a result of a National Academy of Science (NAS) study on the applicability of remote monitoring (NAS, 1970). It was given impetus in the mid-1960s with the introduction of the first airborne multispectral scanner (MSS) operated by the University of Michigan. In this period, narrow-band multispectral data were evaluated. In a separate advance, thermal infrared technology was developed. The two technologies were combined in the 18-channel (between 0.32 and 14 μm) University of Michigan Scanner. In 1970, the University of Michigan's airborne MSS and NASA's high-altitude photography were used in the Corn Blight Watch Experiment - the first large-scale application of remote sensing in agriculture (Myers *et al.*, 1983; MacDonald, 1984). In the 1970 report of the Laboratory for Applications of Remote Sensing (LARS) at Purdue University, results of a study were reported in which MSS data were analyzed using pattern recognition techniques. The overall validation classification accuracies for corn, soybeans, water and a mixture of pasture and other crops were 82.8% (3 V & 1 NIR), 83.9% (3 V & 2 NIR) and 86.4 % (3 V, 2 NIR & 1 TIR)[1].

Using data acquired in the 1971 Corn Blight Watch Experiment, Kumar (1977) evaluated 12 spectral channels in the visible, near infrared, middle infrared and thermal infrared (from 0.4-11.7 μm) for discriminating agricultural cover types consisting of corn, soybeans, green forage and forest. Overall separability of green forage (hay and pasture) from the other agricultural cover types was found to be considerably lower than the corresponding separability of corn, soybeans and forest. The author found that maximum separability of the agricultural cover types was obtained when using all twelve channels. Kumar (1977) further stated that the greatest overall statistical separability of agricultural cover types was obtained with data from the red channel (0.61-0.70 μm). Also, the overall statistical separability of the agricultural cover types was found to be greater for the data of August 12 than the data acquired on July 16.

[1] V, NIR, and TIR denote the visible, near infrared, and thermal infrared regions of the electromagnetic spectrum, respectively.

Multispectral scanners have certain advantages and disadvantages when compared with photography. Particularly important advantages are (i) having the capability to provide spectral data in wavelengths not available from photography, and (ii) being able to provide precision radiometric data on computer compatible tape (CCT). The major disadvantages are much higher cost and lower spatial resolution (Pacheco, 1980).

Recently, new airborne sensors have been developed which are capable of sensing vegetation and other targets at a much finer spectral resolution. Such sensors are capable of collecting more detailed reflectance spectra and in spectral regions outside those collected by the broad-band instruments (Malthus *et al.*, 1993). Such sensors include the Multi-detector Electro-optical Imaging Sensor (MEIS II, 8 channels from 0.39μm to 1.1μm) (Lillesand and Kiefer, 1994), the Advanced Visible-Infrared Imaging Spectrometer (AVIRIS, 224 contiguous channels from 0.41μm to 2.45μm) (Staenz and Teillet, 1993), the Compact Airborne Spectrographic Imager (CASI, 288 channels from 0.38μm to 0.89μm) (Babey and Anger, 1989), and the Geophysical and Environmental Research Corp. Scanner (GER, 63 channels from 0.47μm to 2.44μm) (Bach and Mauser, 1995), The uses of such data for the remote sensing of vegetation have focused particularly on the "red-edge," the transition from low reflectances in the visible region of the spectrum to high NIR reflectance (Malthus *et al.*, 1993). For example, Clevers *et al.* (1994) used AVIRIS data to monitor crop growth by using the red edge index to estimate the leaf optical properties during the MAC Europe 1991 campaign. A number of papers on forestry applications using these sensors were found in the literature; however, few applications in agriculture were documented. Possible reasons are the high costs and complexity of these sensors.

2.3 Satellite VIR Remote Sensing for Agriculture

2.3.1 Earth-Observation Satellites

The advent of earth-observation (EO) satellites led to the ability to cover much larger ground areas than could be achieved using aircraft in a given time. The ability to examine vegetation patterns, combined with the synoptic view and repetitive coverage of satellite sensors, provides an opportunity to survey agricultural resources in a manner that has not been possible in the past. The launch of Landsat-1 in July 1972 began a new era for the acquisition of information about the earth. Although early satellites suffered from relatively poor resolution by aircraft standards, system developments have led to the production of high-resolution images and the ability of computers to process the high volume data at a fast rate, an essential requirement with high-resolution images. A major breakthrough was made with the launch of Landsat-4 in 1982 and the French SPOT satellite in 1986, which carried higher radiometric, spectral, and spatial resolution sensors such as the Thematic Mapper (TM) and High Resolution Visible instruments (HRV). Satellite remote sensing technology has continued to advance, particularly in the area of sensor systems. These advances combined with rapid developments in the field of digital computing, have increased the potential to derive information of value for agricultural decision-makers (Ehrlich *et al.*, 1990). The fundamental characteristics of the data acquired by the major earth-observation satellites are listed in Table 2.1 (Campbell, 1987; Lillesand and Kiefer, 1994; ESA, 1995a; RESTEC, 1996a; 1996b; Satellitbild, 1996).

Studies aimed at perfecting techniques for identifying crops, and estimating acreage and yield of crops, have intensified with these improvements in technology and the increased availability of satellite imagery. The procedures for identifying crops and for estimating acreage and yield, utilizing remote sensing techniques, are frequently complex. Yet, the accuracy of crop identification with present Landsat data has been reported as being 90 percent or higher in studies

Table 2.1. Characteristics of Earth-Observation Satellite Data

Satellite	Sensor	Spectral Range *μm*	Spatial Resolution *m*	Temporal Resolution *days*
Landsat	MSS (Multispectral Scanner)	0.5-0.6 0.6-0.7 0.7-0.8 0.8-1.1	80	16
Landsat	TM	0.45-0.52 0.52-0.60 0.63-0.69 0.76-0.90 1.55-1.75 10.4-12.5 2.08-2.35	30 120 30	16 16 16
SPOT	HRV (XS)[1] HRV(PAN)[1]	0.49-0.59 0.61-0.68 0.79-0.89 0.51-0.73	20 10	26 (Nadir)[2] 26 (Nadir)[2]
IRS-1A/1B	LISS[3]-I LISS[3]-II	0.46-0.52 0.52-0.59 0.62-0.68 0.77-0.86 same as above	72.5 36.25	22 for individual satellite 11 for IRS-1a/1b together same as above
JERS-1	VNIR[4] SWIR[4]	0.52-0.60 0.63-0.69 0.76-0.86 0.76-0.86 1.60-1.71 2.01-2.12 2.13-2.15 2.27-2.40	18 18	44 44
RESURS-1	MSU-SK	0.5-0.6 0.6-0.7 0.7-0.8 0.8-1.1 10.4-12.6	160 600	4

1. SPOT has two identical HRV sensors which operate in two modes, i.e., Multispectral Mode (XS) and Panchromatic Mode (PAN).
2. Off-nadir viewing capability increases the repeat coverage at intervals of 1 to 5 days, depending upon latitude.
3. LISS: Linear Imaging Self-Scanning System.
4. VNIR: Visible and Near-Infrared; SWIR: Short-Wave Infrared. SWIR ceased to observe in December, 1993.

of areas where there are large, homogeneous, rectilinear fields with few competing crops, such as irrigated rice in California, potatoes in New Brunswick or wheat in Western Canada. Relatively few areas in other parts of the world, however, are structured as simply as wheat

fields in Canada and the United States. In the developing countries, cropland is frequently interspersed with non-cropland, fields are small and irregularly shaped, and numerous crops have similar spectral responses. In such complex environments, a single Landsat image may not provide enough data to be useful for purposes of crop identification (Myers *et al.*, 1983; Avery and Berlin, 1992). Selected studies on crop identification accuracies in different geographic regions using Landsat MSS, TM, SPOT and IRS data are presented in Table 2.2.

In the 1970s and early 1980s, a series of large-scale agricultural satellite remote sensing projects were implemented. The Large Area Crop Inventory Experiment (LACIE) was the first comprehensive study to perform wheat-area estimation and production forecasting at the regional/country level (MacDonald and Hall, 1978; Erb, 1980). Other notable projects were the Agriculture and Resource Inventory Surveys Through Aerospace Remote Sensing Program (AgRISTARS) in the U.S. (Myers *et al.*, 1983) and the Agricultural Resource Investigations in Northern Italy and Southern France (AGRESTE) (Dejace and Megier, 1980; Berg, 1981; Meyer-Roux and King, 1992). In the late 1980s and early 1990s, agricultural inventories using remote sensing have been quite successful worldwide. Among numerous studies described in the literature, the major agriculture application programs are presented in Table 2.3.

The potential of satellite remote sensing for the monitoring of agricultural crops and for estimating crop production was recognized by Canadian scientists in the early 1970s. Shortly after the launch of Landsat-1, several investigations were undertaken to evaluate the feasibility of crop-area estimation using satellite data (e.g., Atkinson *et al.*, 1975; Crosson *et al.*, 1975; Mack *et al.*, 1975; Mosher *et al.*, 1978; Ryerson *et al.*, 1979; Goodenough *et al.*, 1980; Ryerson *et al.*, 1981a; Ryerson *et al.*, 1981b; Ryerson *et al.*, 1985). Of special interest were cereal crops which are a major Canadian commodity on the domestic as well as international markets (Atkinson *et al.*, 1975; Crosson *et al.*, 1975; Mack *et al.*, 1975). Other studies focused on crop-condition monitoring (Mack *et al.*, 1977, Brown, 1986; Cihlar *et al.*, 1986b).

Table 2.2. Applications of Landsat MSS, TM, SPOT and IRS Data for Crop Identification in Different Geographic Regions: Selected Studies (ESA, 1995b)

Subject	Sensor	Study Area	Description	Accuracy	Reference
Cereal crop (wheat, oats, barley) classification	Landsat MSS	Melfort test site & Delisle test site, North America	Classification of cereal crops at 14 locations in the spring wheat area of North America for over 42 Landsat images. The level of accuracy varied with the date of image selected and with the criteria to characterize accuracy.	50.9-100%	Mack *et al.*, 1975
Crop identification & area estimation	Landsat MSS	California, USA	Addressing applicability of Landsat imagery and digital data to aid in the mapping and estimation of irrigated land and specific crop types.	Crop groups: 90% individual: 5-56%	Sharon *et al.*, 1984
Classification of summer crops	Landsat TM	Argentina	TM data were evaluated for classification of summer crops including soybean, corn, sorghum, sunflower, winter wheat, oats, and pasture. The average field size is 150 ha.	80% - 100%	Badhwar *et al.*, 1987
Large-area crop classification	Landsat MSS	New South Wales Australia	Digital classification techniques were developed for Australian conditions. Landsat data for 5 dates were used to classify winter crops and other land cover types.	92% (wheat/non-wheat) 97.5% (winter crops/ non- winter crops)	Dawbin & Evans, 1988
Crop monitoring and classification	Landsat MSS & TM	Provinces of Scania & Östergötland, Sweden	MSS and TM data were used to study the relationships between Landsat-based spectral differences and crops, and to evaluate mono- and multi-temporal classification accuracy, and area estimation accuracy.	Rye: 90% grazing crop & potatos: 70% winter & summer wheat, barley & oats: 40-60%	Hall-Könyves, 1990
Improving crop-type determination	Landsat TM	The Regione del Veneto, Italy	Two strategies to improve crop classification accuracies were explored: (i) use of digital ancillary data, (ii) use of multitemporal data.	Soybeans: 91% corn: 78% small grains: 94% sugar beets & orchards: 85.6%	Ehrlich *et al.*, 1990
Estimation of cropped area & yield of rice	Landsat TM	North of Bangkok, Thailand	Multitemporal TM data were used to estimate rice cultivated area. An attempt was made to develop a relationship between reflectance values and actual rice yield. A plant process model was adopted for estimation of rice yield.	Rice cultivated area: > 90%	Tennakoon *et al.*, 1992.
Spectral indices & crop discrimination	SPOT HRV (MS)	Thessaloniki-Giannitsa plain, Greece	Multitemporal and multispectral SPOT data were used to calculate three spectral indices, (i) radiometric means (C1, C2, C3), (ii) vegetation index (NDVI), (iii) brightness index (BI); & to study their relationships to crop discrimination.	Rice (C1-3): 100% sugar beets (BI): 83% maize (BI): 82% alfalfa (NDVI, BI): 72% cotton (NDVI): 33%	Silleos *et al.*, 1992
Pre-harvest state-level wheat acreage estimation	IRS-1A LISS-I	State of Punjab, India	Wheat acreage was estimated using single-acquisition IRS-1A LISS-I data. February 1989 data were used and the results were available by 11 April 1989, before the start of harvesting.	90% at 90% confidence level	Mahey *et al.*, 1993

Table 2.3. Major Agriculture Application Programs Using EO Data (ESA, 1995b)

Project Title	Agency	Instrument (Satellites)	Description	Benefits/Impact	Program Start Date (Duration)
CAPE - crop acreage estimation & production forecasting in India	ISRO (India Space & Research Organiza -tion)	LISS-I (IRS-1A) MSS (Landsat)	Provision of timely information on production of major crops to assist in policy decisions such as buffer stock level, important requirements, and price level. Operational since 1986.	Accurate prediction of crop yield is now possible. This is extremely important as 75% of population depend upon agriculture. Accurate data on crop acreage are now available for use in agriculture planning.	1986 (on-going)
MARS - monitoring agricultural statistics in the EC	JRC (EC's Joint Research Center)	TM (Landsat) HRV (SPOT) SAR (ERS-1/2) AVHRR (NOAA)	Project to use satellite EO data to provide quantitative estimations of crop acreage and thereby to provide yield estimates.	Project has resulted in the introduction of remote sensing techniques to verify the implementation of the common agricultural policy of the EU.	1988 (10 years)
Main crop yield estimation in China	Dept. of Develop- ment and Research CNRSCC	TM (Landsat) AVHRR (NOAA)	This project used remote sensing to develop several crop-yield estimation models, establish crop-yield estimation software and an integrated system. The main crops include wheat, rice and maize in China.	Through this project, a crop-yield estimation system was developed, and crop distribution maps and yield forecasts were verified. In the future, the system may be expanded to the whole country.	1991 (4 years)
ALIS - Egyptian agricultural land information system	SPOT IMAGE	HRV (SPOT-2)	Agricultural Land Information System data, produced for Nile Valley area of Egypt for Soil and Water Research Institute, Egyptian Ministry of Agriculture. It provides capability to measure crop progress, land potential and urban encroachment on to farmland.	EO image data allows a more accurate assessment of the agricultural land use and a detailed forecasting of area yields for the main crops. Detailed monitoring of urban enroachment on to Nile valley farmland is also now possible.	July 1991 (on-going)
Sugar beet monitoring	Logica DRA BNSC	HRV XS (SPOT) TM (Landsat)	EO images of crop areas are used to generate sugar beet yield forecasts for factory catchment areas. The end user is British Sugar.	Saving of £1.8 million per annum for British Sugar plc from improvements in beet delivery planning, operational factory management and marketing non-quota sugar.	1992 (4 years)
Inventory of agriculture and irrigated lands in Kansas	NASA University of Kansas	TM (Landsat)	Program uses Landsat scenes to identify the spatial distribution of farm lands as part of the Conservation Reserve Program which encourages farmers to convert erodable agriculture land into grassland.	Inventory using remote sensing is quicker and more cost effective than traditional methods, allowing better land management.	1994 (2 years)
Control of area-based arable and forage subsidies	NRSC Hunting Technical Services	TM (Landsat) Pan & XS (SPOT) SAR (ERS-1/2)	Contract to use satellite imagery to check claims for agriculture support payments under the European Commission's Integrated Administration and Control System (IACS)	Project has enabled standardization of controls. Also cost and efficiency savings.	1994 (on-going)

In addition to demonstrating the potential of visible and near-infrared (VIR) data for agriculture, these studies highlighted the limitations of Landsat and SPOT data caused by relatively infrequent revisits and cloud cover. This is particularly relevant in higher middle latitudes where the growing season is short and crop development is therefore rapid. For example, in the prairie region of Canada, 85 percent of the days during the growing seasons from 1980 to 1985 were affected to some extent by cloud cover (Brown, 1986). This impairs data acquisition by means of VIR sensors at important stages of crop development (Myers *et al.*, 1983). Agricultural applications need adequate temporal resolution since some of the critical and indicative changes in crop phenology take place over a period of as little as four days. Therefore, the ideal potential temporal resolution should be less than four days, even if this frequency is only needed during critical periods of the growing season (Allen, 1990; Figure 2.1).

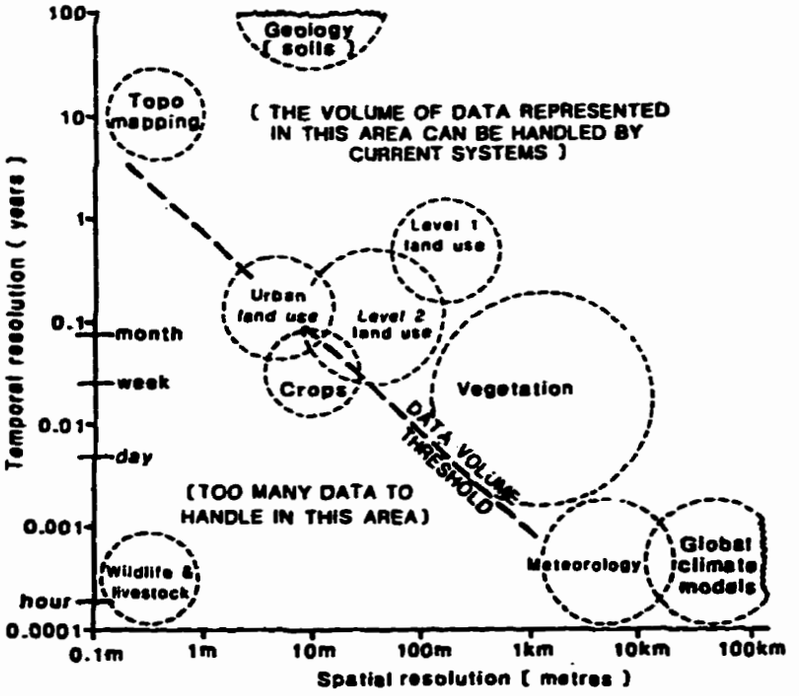

Figure 2.1. Remote sensing applications in relation to spatial and temporal resolution, illustrating the factors limiting their suitability (Allen, 1990).

2.3.2 Environmental/Meteorological Satellites

Environmental/Meteorological satellites such as METEOSAT, GOES, NOAA (see Table 2.4 for system characteristics) are best suited to frequent (hourly, daily or weekly) monitoring of relatively large areas, such as continents, subregions or countries. Although they are designed primarily for meteorological and oceanographic studies, these operational satellites provide rapid, continuous global coverage which was not previously feasible. Data from these satellites have been used successfully for vegetation and environmental monitoring over very broad geographic regions at scales from 1:10,000,000 to 1:2,000,000 (Lantieri, 1993). Table 2.5 shows selected studies of agricultural monitoring using environmental satellite systems. The major agricultural monitoring programs using these satellite systems are presented in Table 2.6 (Philipson *et al.*, 1988; Manore and Brown, 1990; Hutchinson, 1991; Kalensky, 1992; Hielkema and Snijders, 1993; ESA, 1995b; FAS, 1996; Rashid, 1996).

Table 2.4. Example of Environmental Satellite Systems
(Yates *et al.*, 1984; Kramer, 1993; TELSAT, 1995, ESA, 1996a & 1996b)

Satellite	Sensor	Spectral Range *μm*	Spatial Resolution *km*	Temporal Resolution
NOAA-POES*	AVHRR**	0.58-0.68	1.1 at nadir 8 at the border of the images	12 hours, 11 days
		0.725-1.10	same as above	12 hours, 11 days
		3.55-3.93	same as above	12 hours, 11 days
		10.3-11.3	same as above	12 hours, 11 days
		11.5-12.5	same as above	12 hours, 11 days
NOAA-GOES*	VISSR**	0.55-0.70	1	30 minutes
		10.5-12.5	8	30 minutes
METEOSAT	MVIRI	0.5-0.9	2.5	30 minutes
		5.7-7.1	2.5	30 minutes
		10.5-12.5	5	30 minutes

* POES: Polar-Orbiting Operational Environmental Satellite, a NOAA weather satellite series.
GOES: Geostationary Operational Environmental Satellite, a NOAA weather satellite series.

** AVHRR: Advanced Very High Resolution Radiometer.
VISSR: Visible and Infrared Spin Scan Radiometer.
MVIRI: METEOSAT Visible and Infrared Imager, similar to VISSR.

Table 2.5. Agricultural Monitoring Using Environmental Satellite Systems: Selected Studies

Subject	Sensor	Study Area	Description	Reference
Examination of crop phenology and agricultural practices	AVHRR	Nile Delta Egypt	Fifteen dates of AVHRR data between May and October 1981 were collected. For each date, a Normalized Difference Vegetation Index (NDVI) for each pixel was calculated. For each of the 15 dates, a map of the vegetation index was prepared. Individually, the maps show patterns of vegetation and agriculture; in sequence, seasonal patterns in irrigation, crop growth, maturity and harvest were revealed.	Tucker *et al.*, 1984
Monitoring U.S. crops during 1988 drought	AVHRR	U.S. Corn Belt	Effects of the 1988 drought on crops in the U.S. Corn Belt were assessed and monitored by the Foreign Crop Condition Assessment Division (FCCAD), U.S. Department of Agriculture (USDA). Using vegetation index numbers (VIN), FCCAD was able to detect the existence of drought early in the season, monitor changing conditions, and provide objective assessments of the drought's extent & severity.	Teng, 1990
Interpretation of crop growth patterns	AVHRR Landsat MSS	Zambia	A method to correlate crop production in Zambia to the yearly evolution of the NDVI is proposed. The method consists of the analysis of remote sensing data together with meteorological data and simulated crop production to obtained indicators of crop production. Landsat MSS data were used first to locate the agricultural area, then the NDVI time series of the "agricultural" pixels were used to calculate crop growth indicators which can be applied to assess crop production.	Azzali, 1991
Wheat yield estimate and forecast	AVHRR	Emilia Romagna Italy	The NDVI profiles were used as a tool for wheat monitoring in Italy between 1986 and 1989. NDVI has been found to be highly representative of plant photosynthetic capacity and efficiency. Based on NDVI integration during the wheat grain filling period, a simple linear regression model has been derived for wheat yield estimate and forecast.	Benedetti & Rossini, 1993
Crop monitoring & early yield assessment	AVHRR	Burkina Feso	On a 1984-1989 series of ARTEMIS-NDVI data derived from the AVHRR sensor, a case study on crop monitoring and early crop yield forecasting was elaborated for the provinces of Burkina Feso.	Groten, 1993
Rice paddy inventory	AVHRR	Yangtze delta region in Eastern China	Time series NDVI, computed from AVHRR data, were used in an attempt to locate areas of rice cultivation in China. NDVI dynamics were examined using 16 km global area coverage data from 1988 composited into 12 monthly images.	Bachelet, 1995
Spring wheat yield prediction	AVHRR	Western Canada	Weekly maximum value AVHRR NDVI composites were used to predict spring wheat yield for Western Canada. Results for 1991 & 1992 growing seasons show that early season NDVI yield estimates are within 5% of official yield estimates released 3 months following harvest.	Hochheim *et al.*, 1996

Table 2.6. Major Agricultural Monitoring Programs Using Environmental Satellite Systems

Project Title	Agency	Instrument (Satellites)	Description	Benefits/Impact	Program Start Date (Duration)
International crop condition and production analyses	Production Estimates & Crop Assessment Division (PECAD). FAS, USDA	AVHRR (NOAA) MSS/TM (Landsat) HRV (SPOT)	Operational outgrowth of LACIE, PECAD analyzes, satellites images & supporting information to monitor and assess crop conditions worldwide, and to analyze world agricultural production and supply.	Worldwide crop assessments and production forecasting by PECAD provides advance information on areas which may experience food shortages. Timely information on a worldwide basis is also important to stabilize fluctuations in commodity markets.	1978 (on-going)
Famine Early Warning System (FEWS)	US Agency for International Developmen (USAID)	AVHRR (NOAA)	FEWS considers rainfall, yield estimates, production estimates market prices, other social indicators, and AVHRR data. Confronted with such a wide array of different data types, FEWS analysts have come to rely more heavily on AVHRR GAC NDVI data than any other single type of information.	Decadal (10-day composite) NDVI images for large regions help to reveal regional patterns that might not be readily observed in precipitation station data alone. AVHRR NDVI time series for administrative units are compared to historical means and extremes (e.g., the 1984 drought) to gauge the current conditions.	1984 (on-going)
Crop information system	CCRS Agriculture & Agri-Food Canada Canadian Wheat Board	AVHRR (NOAA)	Monitoring vegetation & crop condition for all Canada. Operational since 1987, after pilot project 1985-86. Product is NDVI map used by Agriculture Division of Statistics Canada to generate yield forecasts.	Capability for cost-effective wide-area vegetation condition monitoring. Early season wheat yield indicators are produced allowing the improved management & planning of marketing & distribution facilities.	1987 (on-going)
ARTEMIS - Africa Real Time Environmental Monitoring Information System	FAO, UN NASA/GFSC University of Reading (UK) National Aerospace Laboratory of the Netherlands	AVHRR (NOAA) MVIRI (METEOSAT)	Crop conditions, drought levels and locust threat are determined from EO images. In addition, estimates of rainfall can be generated from cold-cloud images. Data obtained via High Resolution Picture Transmission (HRPT) & Primary Data User Station (PDUS).	ARTEMIS has been used successfully by FAO & national governments for monitoring cereal production in Africa & as an early warning tool in assessment of food aid/import requirements (e.g. it provides timely information to GIEWS). This system can generate timely images over entire region required thus removing dependence on sparse ground-based observations.	1988 (on-going)
MARS - monitoring agricultural statistics in the EC	JRC (EC's Joint Research Center)	AVHRR (NOAA)TM (Landsat) HRV (SPOT) SAR (ERS-1/2)	Project to use satellite EO data to provide quantitative estimations of crop acreage & thereby to provide yield estimates.	Project has resulted in the introduction of remote sensing techniques to verify the implementation of the common agricultural policy of the EU.	1988 (10 years)
Main crop yield estimation in China	Department of Development & Research CNRSCC	AVHRR (NOAA) TM (Landsat)	This project used remote sensing to develop several crop-yield estimation models, establish crop-yield estimation software and an integrated system. The main crops include wheat, rice and maize in China.	Through this project, a crop-yield estimation system was developed and crop distribution maps & yield forecasts were verified. In the future, the system may be expanded to the whole country.	1991 (4 years)

From the above selected studies, it is clear that AVHRR data are adequate for large-area, operational monitoring of crops due to the sensor's wide swath and excellent temporal resolution which increases the likelihood of cloud-free observations during the growing season. It is also clear, however, that AVHRR data are much too coarse to attempt mapping of individual crops and fields. Cropping in most agricultural areas of the world is neither monocultural nor in fields with sides larger than 1.1 km (AVHRR local area coverage) or 4.4 km (AVHRR global area coverage). Vegetation indices of nearly all cells of AVHRR pixels are derived from a preponderance of mixed pixels. Researchers (e.g., Philipson *et al.*, 1988; Azzali, 1991; Bachelet, 1995) found that, despite the preponderance of mixed pixels, useful global or continental crop information can be reliably and efficiently derived from AVHRR data. The usefulness of AVHRR data is most apparent in monitoring the effects of episodic weather events on crops (Teng, 1990).

2.3.3 High-Resolution Satellite Systems

In the past two years, the declassification of U.S. spy satellite technology has stimulated the development of high-resolution commercial remote sensing satellite systems, such as ORBIMAGE, Space Imaging, and EarthWatch. Geophysical & Environmental Research Corp. (GER) announced recently its plan to develop a satellite system for crop monitoring. The GER Earth Resource Observation System (GEROS) is a constellation of six to eight satellites. Each satellite will be equipped with a panchromatic and a multispectral sensor. The multispectral sensor will have 10 m resolution and the panchromatic will have better than 10 m resolution. GER intends to offer farmers affordable products on a rapid revisit cycle. GER is also developing a ground system that will get the satellite data and crop information to the farmers fast enough to save stressed crops. High cost and slow turnaround time have impeded widespread imagery use by individual farmers for monitoring the health of their crops up to present (GER,

1995). This and other high-resolution systems will be important data sources for precision farming - an information and technology-based agricultural management system (Robert, 1996).

2.4 Crop Information Extraction from Satellite VIR Data

2.4.1 Temporal-Spectral Profiles for Global Based Crop Identification

The identification of cultivated crops from satellite VIR imagery has been accomplished by the recognition of a temporal pattern of crop characteristics through the growing season of a particular crop of interest. The main idea is to infer the time of occurrence of a particular feature that is stable from year to year and does not overlap with similar characteristics from other crops growing in the same geographic region. If such feature(s) could be identified, the crop of interest could be accurately and consistently identified (Badhwar, 1984a & 1984b). Experience with Landsat data in the LACIE and other studies demonstrated that the use of multitemporal data greatly enhances the ability to distinguish between various crop spectral patterns. In the late 1970s and early 1980s, interest developed in utilizing characterizations of continuous patterns of crop spectral development over time, termed "spectral profiles", in automated crop identification techniques (Tucker *et al.*, 1979; Crist and Milila, 1980; 1981; Badhwar, 1982; Badhwar *et al.*, 1982; Badhwar, 1984a; 1984b; Crist, 1984; Odenweller, 1984; Turner, 1986; Hall and Badhwar, 1987). In the early stage of development, these techniques relied on the temporal sequences of colors (i.e., non-red/red/non-red) indicating non-vegetation/vegetation/non-vegetation in the false-color products. They also depended greatly on human analysis and interpretation of film products and were not very effective or objective (Badhwar, 1984a; 1984b). A breakthrough in this field was made by Kauth and Thomas (1976) who developed a technique called the Tasselled Cap. The greenness component of Tasselled Cap is the most appropriate indicator for crop identification because it measures infrared reflectance relative to that in the visible band (Odenweller, 1984; Hall and Badhwar, 1987).

Although temporal-spectral profiles contain information to support crop identification at various levels, some caveats must be attached to the use of profiles. The overall appearance of a profile is highly dependent upon data acquisition history. If key observations are missing, discrimination features may not be detected. Furthermore, if the labeling target is misregistered on any acquisition, the resulting profile will be inaccurate. These are generic difficulties related to the analysis of multitemporal satellite VIR data (Odenweller, 1984).

2.4.2 Vegetation Indices

Vegetation index (VI), a measure of "greenness," is directly related to the health and vigor of vegetation. It is described in the literature as a good indicator of biomass and as an indicator of photosynthetic activity (Ehrlich *et al.*, 1990). Various vegetation indices have been developed including the Ratio Vegetation Index (RVI), the Normalized Difference Vegetation Index (NDVI), the Transformed Vegetation Index (TVI), the Tasselled Cap Transformation (for MSS), the Crist and Cicone Transformation (for TM), Perpendicular Vegetation indices (PVIs), the Greenness above bare soil (GRABS), and the Cereals Leaf Area Index (CLAI) (Crist and Cicone, 1984; Jensen, 1986; Wiegand *et al.*, 1991). VIs have been used extensively to monitor agriculture. For example, NOAA provides standard vegetation index maps compiled weekly for both hemispheres from AVHRR data (Jensen, 1986). Although the spectral bands of AVHRR are not ideally positioned for vegetation analysis, as they are rather broadly defined and are not focused on the spectral regions of maximum interest, the meaning of the vegetation index derived is the same (Campbell, 1987).

Vegetation indices have been employed in two separate kinds of applications. Many of the first studies defining applications of vegetation indices attempted to "validate" their usefulness by establishing that values of the VIs are closely related to biological properties of plants. Typically, such studies examined test plots during an entire growing season, then compared values of the

VIs, measured throughout the growing season, to in-situ measurements of leaf-area index (LAI), the area of leaf surface per unit area of soil surface. The objective of such studies was ultimately to establish use of VIs as a means of remote monitoring of the growth and productivity of specific crops, or of seasonal and yearly fluctuations in productivity in a timely and accurate manner.

A second category of applications uses VIs as a mapping device - much more of a qualitative, rather than a quantitative, tool. Such applications use VIs to assist in image classification, to separate vegetated from non-vegetated areas, to distinguish between different types and densities of vegetation, and to monitor seasonal variations in vegetative vigor, abundance, and distributions (Campbell, 1987).

2.4.3 Classification Algorithms

Many forms of classification algorithm have been used in agricultural crop identification, including supervised/unsupervised, parametric/non-parametric, per-pixel/per-field, textural and contextual. The supervised maximum likelihood classifier is the most commonly used parametric, per-pixel classifier. In contrast, however, cluster analysis is commonly used for unsupervised, per-pixel classifications. A per-field classifier, known as ECHO (Extraction and Classification of Homogeneous Objects), was developed by Ketting and Landgrebe (1975). ECHO classifies a digital image into fields of spectrally similar pixels before the pixels are assigned to categories. Classification is then conducted using the fields, rather than individual pixels.

New developments in image classification include a knowledge-based approach through integration of ancillary data from a GIS. For example, Janssen and Middelkoop (1992) designed a knowledge classification method to improve crop classification. Crop data of preceding years,

stored in a GIS, were used as ancillary data. Knowledge about crop succession, determined from crop-rotation schemes, was formalized by means of transition matrices. The spectral data, the data from the GIS and the knowledge represented in the transition matrix were used in a modified Bayesian classification algorithm. Depending on the spectral class discrimination, the accuracy of the knowledge-based classification was 6% to 20% better compared with a maximum likelihood classification. Kontoes *et al.* (1993) also used a knowledge-based system to improve remote sensing image classification for estimates of crop acreage through the integration of easily available geographic context information from a GIS, such as soil maps and buffered road networks. Ehrlich *et al.* (1994) developed an advanced agricultural information system (AAIS) for operational agricultural crop area estimation by integrating a variety of data types including satellite imagery.

2.5 VIR Spectral Vegetation Identification: A Hope Unfulfilled

Early in remote sensing, and persisting to this day, investigators have tried to establish a characteristic pattern of reflectance (a spectral "signature") to associate with specific types of vegetation. In some cases, results were excellent; in others, very poor. In fact, this approach was not robust - it depended too much on luck and fortuitous circumstances. As a general class of objects, green vegetation itself can be identified as a spectrally unique object. Nevertheless, the whole scheme of converting MSS, and especially TM, data to a single vegetation measure (index) rests on the fact that vegetation has a unique composition compared to objects such as soils and rocks. Specific types of vegetation (e.g. corn and soybeans) however, can (and do) have similar optical broad band spectral properties at a given location and given time in the season. In a particular region, one might count on a particular vegetation type having a particularly high value of a primary measure, such as alfalfa having a very high near-infrared reflectance compared to many other crops. Nevertheless, the successful spectral identification of

a crop, like alfalfa, depends on a set of circumstances that may not hold in the next region or at a different stage of growth (Paris, 1990).

What are the alternatives to the identification of crops based on single-date spectral measurements? The answer seems to be the element of time (seasonal or temporal change). In the AgRISTARS Project, researchers found that one could relate to crop type the seasonal patterns of emergence of a crop, its growth and its senescence to harvest, as seen by Landsat MSS or TM (or any other sensor that responds to changes in standing biomass, especially foliage biomass). An excellent example was the identification of corn and soybeans. Using the greenness measure from the Kauth-Thomas Tasselled Cap or the Crist and Cicone Transformation (MSS and TM, respectively), it is possible to fit a two-parameter model to the seasonal variations of changes in greenness in a particular field. Then, using a crop-calendar model incorporating a non-linear distribution in greenness having characteristics of emergence-date peak greenness and length of season, corn could be distinguished from soybeans in every crop-growing region without changing the decision rule or its parameters. This "Temporal-Spectral Profile" approach is robust - it works everywhere for global-based crop recognition (Hall and Badhwar, 1987; Paris, 1990).

There are two major problems, however, associated with using EO satellite VIR data as a monitoring tool over a large area. One is the sheer volume (revisit) of imagery which must be analyzed, while the other is the uncertainty of actually acquiring the imagery due to cloud cover. For example, in Oxford County, southern Ontario, Canada, cloud-free SPOT imagery were not available during the growing seasons of 1988, 1989, 1991, 1993 and 1995 (see Appendix B for SPOT search results). In the Canadian prairies, 85% of the days during the growing season from 1981 to 1985 were affected by cloud cover (Cihlar *et al.*, 1986b). Most parts of western Europe have a cloud cover of 6/8 to 8/8 for at least 50% of the time (De Loor, 1980). In general, tropical and semi-tropical crop environments have inescapable cloud problems at least 75% of the

time, while other areas in the world often have cloud problems from 30% to 50% of the time (Myers *et al.*, 1983).

As a partial solution to the cloud-cover problem, a thorough evaluation of the information content of the NOAA AVHRR data was desirable. However, AVHRR data also suffer from serious limitations. They have wide scan angles and low spatial resolution (1.1 km - LAC or 4.4 km - GAC) which distort the crop information present, and they can be acquired only when the sky is clear. Cihlar *et al.* (1986) concluded that the data are not suitable for crop-area estimation or for other assessments requiring field-by-field analysis (Figure 2.1). Microwave instruments, such as imaging radar, are very attractive data sources from the timeliness standpoint since these data can be acquired virtually independent of the weather conditions.

2.6 Summary

The recognition of crop type, estimation of crop acreage, and timely and accurate prediction of crop yield are matters of critical interest everywhere in the world. Perhaps no information is more basic for yield predictions, agricultural planning, and export-import negotiations of agricultural commodities, than data on crops being grown in a region or a country. Acquisition of timely and regular information is a critical requirement for successful management of a crop information system. Unfortunately, farm questionnaires are too time-consuming to administer and there is a considerable delay in processing the information.

The use of aerial photographs recording in the visible and the near-infrared bands for surveying agricultural crops is well established. The use of more sophisticated techniques (e.g., high-altitude colour-infrared photography, multispectral scanning, and earth satellite imagery) offers the potential for macroscopic agricultural surveys on a synoptic basis, along with detailed observations of selected croplands (Avery and Berlin, 1992). Quantitative measurements of key

agricultural crop properties, the identification of crop types, and the estimation of their areal extents using EO satellite data have been major goals of remote sensing for several decades. Many investigators have pursued these goals by studying the information content of VIR sensors, such as the Landsat MSS, TM, SPOT HRV and IRS-1 LLIS (Colwell, 1983; Paris, 1990). Crop identification and crop-area estimation can be done fairly successfully using satellite sensors operating in the VIR regions of the spectrum (accuracies of about 80%, very site-specific). Data collection, however, can be unreliable due to problems of cloud cover and infrequent revisits at critical stages of the growing season. AVHRR provides rapid, continuous global coverage and is adequate for large-area, operational monitoring of crops; however, the data are much too coarse to attempt mapping of individual crops and fields, and the data can only be acquired when the sky is clear. Use of airborne imagery for data collection is technically feasible, but costs become prohibitive and speed is a concern when large areas are being studied (Howarth and Protz, 1991). Microwave instruments, such as imaging radar, appear to be very attractive data sources from the timeliness standpoint since these data can be acquired virtually independent of the weather conditions.

CHAPTER 3: SYNTHETIC APERTURE RADAR FOR AGRICULTURE

3.1 Introduction

Radar remote sensing has the potential to play an important role in agricultural crop mapping and monitoring for several reasons. In particular, radar permits the acquisition of high-resolution data at optimal times during the crop growth cycle, regardless of atmospheric or solar illumination conditions. This results in a high degree of *timeliness* or synchronization between the Synthetic Aperture Radar (SAR) data collection and the crop calendar. Thus, growing conditions of different crops can be monitored during crucial periods of their growth cycles. Subsequently, crop classifications can be improved by selecting data acquisition dates to correspond with times when the variation in radar backscatter response of dominant crops is at a maximum (Werle, 1992).

Sensitivity refers to the ability of radar to respond to differences in crop type, growth stages, moisture conditions, soil roughness, soil moisture and row direction. Radar is sensitive to a variety of agricultural targets (*geometric*) and to moisture differences in the soil, as well as to plant material (*dielectric*) (Brisco, 1993). Our understanding of the backscatter characteristics of these agricultural targets, however, is still rudimentary. It should not be inferred that these parameters can be extracted easily from SAR imagery. One of the major tasks is to remove the effects of backscatter contributions from the underlying soil, including its roughness, moisture content and directional biases. This is necessary to isolate the information of interest, such as crop type, for operational use (Werle, 1992).

Starting in the mid-1960s, a group of scientists at the University of Kansas used aircraft-based radar imagers (Ka- and Ku-bands) to investigate the potential of radar for crop identification, mapping and condition assessment (Simonett *et al.*, 1967; Haralick *et al.*, 1969-70; Paris, 1983).

Since then, radar remote sensing techniques have been investigated for a variety of applications in agriculture (e.g., Ulaby and Batlivala, 1975; Ulaby *et al.*, 1978; Ulaby *et al.*, 1979; Brisco and Protz, 1980a; 1980b; Ulaby, 1981; Brisco *et al.*, 1984; De Loor, 1984; Cihlar *et al.*, 1986a; Ulaby *et al.*, 1986a; Brisco *et al.*, 1989a; 1989b; Brisco and Brown, 1990; Brisco *et al.*, 1990; Bouman, 1991a; 1991b; Brisco *et al.*, 1991; Engman, 1991; Ferrazzoli *et al.*, 1992; McCulloch and Yates, 1992; Bouman and Hoekman, 1993; Kohl *et al.*, 1993; Ban *et al.*, 1995; Ban and Howarth, 1995; Ban and Howarth, 1996b; Chen *et al.*, 1996; Filho *et al.*, 1996). Numerous campaigns and investigations have been conducted by research laboratories in North America and Europe using ground-based scatterometers and airborne imaging radars, as well as spaceborne SARs (Holmes, 1990; Werle, 1992; Ban and Howarth, 1996a).

In Canada, the status of radar applications is still restricted, as it is elsewhere, to the research and development stage. The scientific objectives have been clearly oriented towards future operational use of SAR data as an input to crop information systems, with a focus on the study of radar backscatter characteristics of crops and soils in various geographic regions. This includes assessing the feasibility of monitoring crop conditions, crop practices, crop rotation, soil and land deterioration (Brown, 1987; Werle, 1992). The Canadian Surveillance Satellite Program (SURSAT) provided the first opportunity to acquire airborne and, in some cases, spaceborne SAR data and simultaneous ground data. Several test sites were selected representing agricultural regions both in the prairies and in the eastern portion of Canada. The experimental program was later expanded as part of the RADARSAT project, which began in 1981, and the Radar Data Development Program (RDDP), introduced in 1986. The RDDP was aimed at establishing a comprehensive coordinated program within Canada, designed to develop the necessary knowledge for reliable interpretation of SAR imagery and to use these data for the benefit of Canadian users (Brown, 1987).

In the fall of 1993, the Canada Centre for Remote Sensing (CCRS), in cooperation with the Canadian Space Agency (CSA), RADARSAT International Inc. (RSI) and the International Development Research Centre (IDRC) embarked upon a world-wide demonstration, training and applications-development program labelled GlobeSAR. The former CCRS-owned Convair 580 aircraft, equipped with a C/X SAR, undertook data-collection flights in 13 countries in Europe, Africa, the Middle East and Asia. The purpose of these flights was to acquire multidisciplinary radar data to be evaluated for various applications, as well as to simulate the data of the Canadian RADARSAT (Campbell *et al.*, 1995; Petzinger, 1995).

Recently, two major programs were initiated to stimulate research, applications and commercialization of RADARSAT data. The CSA's Applications Development Research Opportunity (ADRO), jointly sponsored by the governments of Canada, United States and the licensed commercial distributor of RADARSAT data, RSI, supports two types of projects: 1. those which exhibit innovative scientific research utilizing RADARSAT data; and 2. demonstrations of new radar applications or the development of products for specific applications (CSA, 1996a). The RADARSAT User Development Program (RUDP) aims to help the Canadian value-added industry to develop products and services that will result in greater RADARSAT benefits and data sales, both in Canada and abroad (CSA, 1996b).

3.2 Important Parameters Affecting Radar Backscatter

An understanding of the relationships between agricultural parameters and radar backscatter is of key importance in assessing the usefulness of SAR. It can provide the confidence required for extending from limited test sites to larger geographic regions, and it is necessary for constructing inversion models whereby SAR might be used, for example, as a crop monitoring tool (Cihlar, 1986; Cihlar *et al.*, 1987).

A wide range of parameters affect the backscatter of microwaves from vegetation and soil. In a recent study undertaken for ESA, for example, it was concluded that a minimum of four instrument parameters, 28 vegetation parameters, 13 soil parameters, and 12 environmental parameters needed to be included in a database designed for interpreting the mechanisms controlling backscatter from vegetation (Holmes, 1990). The important characteristics of the radiation are frequency, polarization and incidence angle. The crucial features of the target in determining the proportion of radiation returning to the instrument are plant canopy and the underlying soil. Key parameters of the plant canopy are: plant height, plant cover, plant density, leaf area index (LAI), plant biomass and water content, plant row direction, growing stage, canopy structure and weed infestation. Key parameters of soil are: soil moisture, soil roughness, soil texture and tillage direction (Holmes, 1990, Werle, 1992).

3.2.1 SAR System Parameters

3.2.1.1 Frequency

Frequency has the greatest effect on radar backscatter because the choice of Ka-, Ku-, X-, C-, L- or P- band is the main determinant of the type and strength of the radar backscatter from an agricultural scene. In general, the use of shorter wavelengths, such as X-band, results in direct backscatter from the canopy and provides little information about the internal structure of a dense canopy and the surface below the canopy layer. Longer wavelengths, such as L-band, have the capability to penetrate the crop canopy layer and provide returns from the soil surface (Werle, 1992). In fact, soil parameters are dominant in determining the broad characteristics of co- and cross-polar backscattering at the lower radar frequencies (e.g., L-band) (De Matthaeis *et al.*, 1991). The two-way attenuation of longer wavelengths by the canopy may also result in volume-scattering effects which may become the prominent backscatter response for some crops such as broadleaf crops. C-band has shown sensitivity to both the internal structure of the crop canopy layer and, to a limited extent, to the soil surface underneath (Werle, 1992).

There are reports which conclude that each of the Ku-band (e.g., Ulaby and Batlivala, 1975; Bush and Ulaby, 1978; Ulaby, 1981; Mehta, 1983; Bouman, 1987), or the X-band (e.g., Ulaby and Batlivala, 1975; Ulaby, 1981; Guindon *et al.*, 1984; Hoogeboom, 1983; 1986; Pei-yu and De-li, 1983; Bouman, 1987; Bouman and Van Kasteren, 1990a; 1990b; Brown *et al.*, 1992; Wever *et al.*, 1995), or the C-band (e.g., Mehta, 1983; Paris, 1983; Brown *et al.*, 1992; Baronti *et al.*, 1995; Wever *et al.*, 1995) or the L-band (e.g., Mehta, 1983; McCulloch and Yates, 1992; De Matthaeis *et al.*, 1994; Lemoine *et al.*, 1994; Baronti *et al.*, 1995) or P-band (Chen *et al.*, 1996) provided best discriminations among crops. It is clear that an optimum wavelength for general crop studies cannot be defined because the optimum waveband depends on crop type, growth stage, conditions of test sites, etc.

While the conclusions arrived at by the many investigators are application-dependent, direct comparison is not usually possible between crops due to the lack of studies that eliminate all variables, including soil dielectric properties, soil roughness, plant age, etc. As Churchill *et al.* (1985) pointed out, the results of individual investigations can be seen to be unique to individual test sites due to crop stage and test-area conditions at the time of measurement. Thus, recommendations as to which frequency is most appropriate in all circumstances are not possible, and no individual wavelength can be singled out as being optimum for agricultural studies (Holmes, 1990).

Another possible reason for the conflicting findings is that many of the results have been achieved with uncalibrated SAR data. Comparisons of different sensors, different dates, and different sites, however, are not possible without calibrated data (Freeman, 1992). Yanasse *et al.* (1992), for instance, reported that some data suffered from several serious radiometric distortions, in addition to those caused by the antenna pattern, which might affect the conclusions made by investigators.

The long-established Canadian remote sensing program offers some experience in the identification of optimal frequency for discrimination of crop type. Cihlar *et al.* (1986b) summarized findings to that date. It was found that, whereas X-band provides good discrimination, L-band was very useful for separating broad-leaved crops and fallow in some sites. L-band did have the disadvantage of sensitivity to row direction, however, which X-band did not exhibit. The ability of C-band to discriminate was intermediate between the X- and L-band. Recently Brown *et al.* (1992) examined the similarities and differences between imagery acquired at X-, C- and L-bands by calculating the correlations between X-, C- and L-bands in airborne SAR data. It was found that the correlations between C- and L-band and between X- and L-band data were very low indicating that the radar backscatter at different frequencies is caused by different mechanisms. The correlation between X- and C-band data was low for grains (a well-defined vertical structure), but higher for canola and peas (broad-leaved plants with little definite structure). For L-band data, the primary cause of the radar backscatter is probably from the underlying soil and is thus largely influenced by soil properties. For C- and X-band data, the vegetation parameters are probably the predominant factors, particularly for the July data set. In addition, similar crop-classification accuracies were obtained with the X- and C-band data (with C-band being slightly better), but the classification accuracies for L-band data were considerably lower. This analysis supports the previous conclusions that vegetation cover is the dominant agricultural parameter driving radar backscatter at X- and C-bands, but not at L-band.

The inherent disadvantage of using only a single frequency is obvious and the potential for having multifrequency satellite capability in the future cannot be ignored (Holmes, 1990). There are many recommendations that multifrequency studies are required for crop classification (e.g., Drake *et al.*, 1974; Parashar *et al.*, 1979; Ulaby *et al.*, 1981; Van Kasteren, 1981; Freeman *et al.*, 1994) and many studies have demonstrated large improvements in classification by using multifrequency (and multipolarization) measurements (e.g. Brisco and Protz, 1980a; 1980b;

Guindon *et al.*, 1984; Bouman, 1987; Thomson *et al.*, 1990; Ferrazzoli *et al.*, 1992; Freeman *et al.*, 1994; Wever *et al.*, 1995; Chen *et al.*, 1996).

3.2.1.2 Polarization

The polarization of an electromagnetic wave describes the orientation of the electric-field vector at a given point in space during one period of oscillation. The penetration depth of an incident microwave source depends on its polarization and frequency, such that the optical thickness of the vegetation layer increases with increasing frequency. Whereas L-band observations are influenced by the entire crop canopy, X-band observations are generally governed by the top layers. Horizontally polarized (HH) radar couples weakly to vertical stalks, resulting in low attenuation. Vertically polarized (VV) microwaves, however, are attenuated to a greater extent causing a reduction in the penetration depth (Figure 3.1). Measurements using HH, therefore, give information primarily about the underlying soil, while VV data are related more to canopy structure. This statement, however, must be considered in the context of the wavelength used. Longer wavelengths, such as L-band, tend to penetrate deeply into vegetation, whereas shorter wavelength, such as X-band, are scattered in the upper layers. As a result, discrimination between polarizations may be impossible at the shorter wavelengths (Bouman and Van Kasteren, 1990a; 1990b; Holmes, 1990).

There are reports which conclude that each of the HH (Ban *et al.*, 1995), or the VV (Ulaby, 1981; Thomson *et al.*, 1992; Anys and He, 1995), or the HV (De Matthaeis *et al.* 1994; Foody *et al.*, 1994), or the depolarization ratio (defined as the like-polarization measurement divided by the cross-polarized measurement) (Paris, 1983), or the polarization ratio (Le Toan and Laur, 1988) provide the best discrimination among crops. It is clear that an optimal polarization for general crop studies cannot be defined because the optimal polarization depends on wavelength, crop type, growth stage, conditions of test sites, etc. The following general statements,

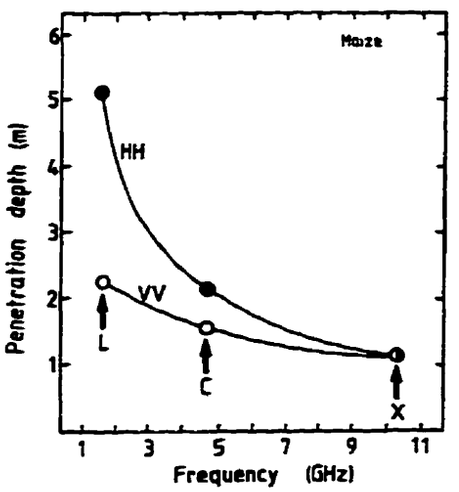

Figure 3.1. Frequency dependency for microwave penetration into a corn canopy. Penetration depth is defined as the depth at which the incidence power is reduced to 37% (1/e) of that incidence. The data presented are for an incidence angle of 40°, LAI = 2.8, plant height = 2.7 m, leaf volumetric moisture content = 0.65, stalk volumetric moisture content = 0.47 (Holmes, 1990)

however, can be made. The degree of inhomogeneity of a surface or volume is strongly associated with the cross-polarization scattering coefficient of that surface or volume. The separation of crop types can be enhanced using cross-polarization data; for example, two crops having similar geometries, such as wheat and barley, may have similar like-polarization backscatter, but it is possible to separate them with observations from cross-polarization studies. Similarly, the distinction between bare soil and vegetation-covered surfaces is made easier using cross-polarization, due to the fact that the vegetation canopies depolarize the incident radiation more strongly than the bare surfaces. The cross-polarization ratio (ratio of σ°_{HV} to σ°_{HH}) is the useful discriminating parameter in these studies. Earlier studies were based on higher frequency (> 8 GHz) observations and led to the conclusion that little was to be gained using cross-polarization. Lower-frequency studies at C-band by Paris (1982) demonstrated the advantage of using cross-polarization for discriminating corn and soybeans which could not be achieved with like-polarization (Holmes, 1990).

Several researchers (e.g., Ulaby, 1981; Megier *et al.*, 1984; Foody *et al.*, 1994; Anys and He, 1995; Ban *et al.*, 1995; Chen *et al.*, 1996) found that multipolarization analysis greatly improved the ability to discriminate between crops. This demonstrated that agricultural crop studies require multipolarization radar if maximum information about crops is to be achieved. Since target structure influences the extent of radiation depolarization, there is a need to understand the depolarization on the basis of each individual crop structure. This implies that multipolarization studies need to be made of different crops, and at different growth stages for each crop, if the factors that influence depolarization are to be understood (Holmes, 1990).

3.2.1.3 Incidence angle

The influence of incidence angle depends on the polarization of the microwave source and the canopy orientation under examination. If a fully grown corn canopy is considered, using L-band radar, an increase in incidence angle from 0° to 90° has little effect on the penetration depth of HH polarized radiation due to its low attenuation, whereas it decreases with VV polarization as incidence angle increases (Figure 3.2). This phenomenon can be used to help to choose the most suitable incidence angle and polarization, depending on the application and information required (Holmes, 1990).

There is no conclusive evidence that any one angle, or narrow range of angles, is optimal for species classification purposes. Ulaby (1981) suggested that the observation angle should be in the 50° - 70° range (from nadir). Bouman and Van Kasteren (1990a; 1990b) confirmed Ulaby's suggestion. They found that the different backscattering levels at medium-to-high angles of incidence of sugar beet and potato would result in a high probability of discrimination between these two crops. The best angle of observation for discrimination appeared to be a high one. At 70° incidence angle, possible disturbing effects on radar backscatter such as ridge orientation in potato and canopy architecture of sugar beet, are minimal. On the other hand,

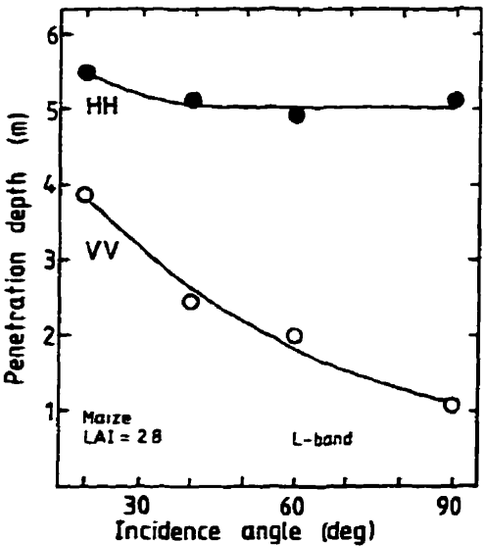

Figure 3.2. Polarization and incidence angle dependency for microwave penetration into a corn canopy. Penetration depth is defined as the depth at which the incident power is reduced to 37% of that incident. LAI = 2.8, plant height = 2.7 m, leaf volumetric moisture content = 0.65, stalk volumetric content 0.47 (Holmes, 1990)

Shanmugan *et al.* (1983) noted an improvement in the ability to classify crops with increasing incidence angle up to 40°, but found no improvement with higher angles. This ties in with the conclusion of Pei-yu and De-li (1983) that angles between 42° to 72° are optimal for rice, while Paris (1982) concluded that the optimal angle for delineating corn and soybeans with C-band is 50°. Poirier *et al.* (1988) reported the multiangle combinations (53° + 30°) improved crop classification using C-VV SAR data, and accuracy at an incidence angle of 53° was more influenced by vegetation than the data at 30° incidence angle. For monitoring of crop growth, Bouman (1987) concluded that with the X-band wavelength, steep incidence angles are most suitable (Holmes, 1990).

The above studies show that our knowledge of the influence of incidence angle is still very poor. Almost all incidence-angle studies have been restricted to correlative field observations and few substantive studies aimed directly at understanding incidence effects have been made. The optimal incidence angle for applied studies depends on the application. As with analysis of

optimal polarization, the lack of comprehensive information for all wavebands tends to limit interpretation. Thus, there is a clear need for future studies at all incidence angles to understand the incidence-angle effects. The multi-incidence angle capability of RADARSAT provides an excellent opportunity for such studies.

3.2.2 Agricultural Target Parameters

The total radar backscatter (δ°) from a vegetated agricultural field is a function of the vegetation canopy (volume scattering), the soil surface (surface scattering) as well as the interaction of the radar signal between the vegetation component and the soil component (Ulaby *et al.*, 1984; Dobson *et al.*, 1986a; 1986b; Figure 3.3). The total backscatter is also incidence-angle (θ) dependent and can be expressed as:

$$\delta^\circ_{total}(\theta) = \delta^\circ_{vol.}(\theta) + \delta^\circ_{surf.}(\theta) + \delta^\circ_{int.}(\theta)$$

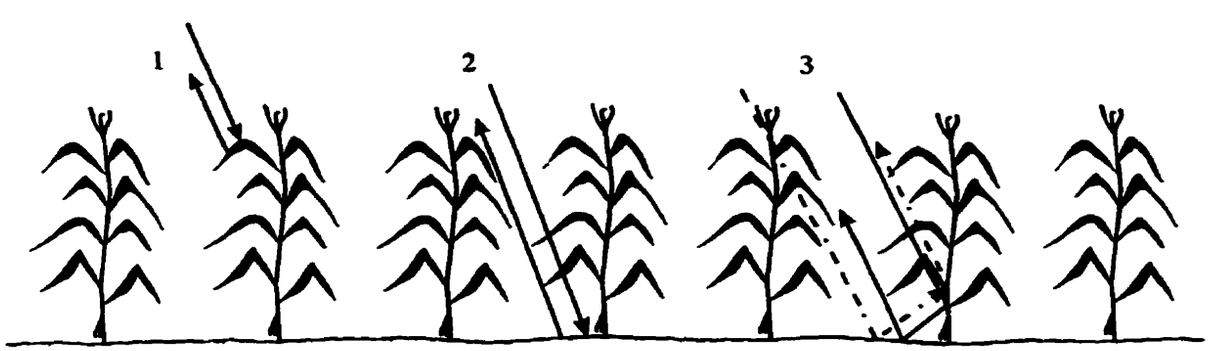

Figure 3.3. Three Sources contributing to δ°_{total} from a crop canopy (Ulaby *et al.*, 1984)

3.2.2.1 Vegetation Component

The interaction of microwave energy and crops in the canopy layer is not only strongly influenced by crop species, plant geometry and its dielectric constant, but it is also frequency-, polarization- and incidence angle- dependent.

Crop Morphology

Radar backscatter from crops is strongly dependent on the size of the scattering elements within a crop. This can be seen in Figure 3.4, where the size of the elements that cause maximum backscatter varies with the wavelength of the radiation. In most instances, the greatest response is shown to scatterers that are of a similar size to the wavelength. This is one of several crop characteristics that contribute to the ability of multifrequency imagery to discriminate between targets. In addition, crops usually exhibit preferential orientations in their geometry. This results in polarization-dependent differences in the penetration and return of microwaves from the canopy (Holmes, 1990).

Bouman and Van Kasteren (1990a; 1990b) reported that the geometrical architecture of the crop canopy is a major factor that influenced the X-band radar backscattering of wheat, barley, oats, sugar beet and potatoes. Row spacing, crop variety, lodging and ear orientation of barley had a large effect on radar backscattering. The architecture of the canopy also influences the impact of soil background on radar backscattering from the whole crop. Even stubble and straw, which are theoretically relatively transparent to microwaves, largely determine the radar backscattering of harvest fields.

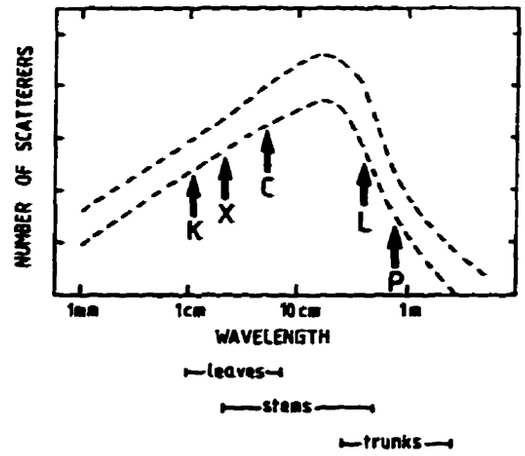

Figure 3.4. Radar response as a function of the size-distribution of scatterers in the canopy (Holmes, 1990)

Crop canopies can generally be divided into several components including leaves, stalks, stems and fruit. For example, a corn canopy can be regarded as a two-layer system with the upper layer dominated by leaves and stems and the lower layer dominated by stalks or stems, while a wheat canopy (after heading) can be regarded as a three-layer system with a head layer added on top (Ulaby *et al.*, 1984; Ulaby *et al.*, 1986a). Krul (1988) suggested that the structure of the crop canopy (shape, size, orientation of canopy components) will primarily influence the spatial distribution of the scattered energy, while the material constituents of the canopy components (internal microstructure, moisture, etc.) will change the magnitude of the scattered energy in all directions (Ban *et al.*, 1993).

Plant Leaves

Canopy leaves tend to attenuate the incident radar beam, particularly as frequency increases (Chuah and Tan, 1990; Van Kasteren, 1981; Ulaby and Wilson, 1985). The radar pulse is first attenuated when the energy initially passes through the canopy. After surface and volume scattering has occurred, the energy is again attenuated as it passes back through the canopy on its

way to the sensor (i.e., two-way attenuation). The attenuation versus scattering of microwave energy by leaves is likely related to the penetration ability of the energy, which is in turn related to wavelength and leaf size. Bouman (1987) has shown that at short wavelengths, radar return is sensitive to leaf size; while the longer wavelengths are less sensitive to the changes in geometry, particularly with respect to sugar beet and potatoes. Brisco (1993) suggested that broad-leaved plants such as corn are more likely to increase backscatter as a result of canopy structure whereas small-leaved plants such as alfalfa are more likely to attenuate the incident energy and therefore decrease backscatter.

Leaf area and vegetation water content also affect the proportion of incident energy that is absorbed and scattered. For all parts of the plant, an increase in moisture content generally leads to an increase in backscatter (Ulaby and Bush, 1976). Stem moisture content, however, has a stronger effect on the magnitude of the cross-polarized return compared to leaf moisture (Chuah and Tan, 1990). When a leaf is comparable in size to the incident wavelength, the shape, density and orientation of the leaf can have a major impact on radar return (Morton, 1987). In fact, Van Kasteren (1981) noted that a single leaf can attenuate incident energy by as much as 4-7 dB.

Plant Stems and Stalks

Similar to leaves, plant stems and stalks tend to scatter and absorb microwave energy (Chuah and Tan, 1990). The importance of stems and stalks to the attenuation and/or scattering of microwaves varies depending upon frequency, polarization, incidence angle and crop structure as well as crop developmental stage (Ulaby *et al.*, 1978; Ulaby *et al.*, 1982; Ulaby *et al.*, 1984; Ulaby and Wilson, 1985; Chuah and Tan, 1990; Engman, 1991; Coppo *et al.*, 1992). For example, Chuah and Tan (1990) found that stems contribute more to total like- and cross-polarized backscatter as frequency increases. Also, for cross-polarized returns, stems and stalks appear to contribute more to total backscatter than leaves, especially at higher frequencies.

Contradictory evidence exists regarding the contribution of plant stalks to radar backscatter. For instance, when corn canopies are fully developed, the majority of scattering in C-band (HH polarization) originates in the top 1 m of a 2.8 m corn canopy and little backscatter was measured below that level for view angles of 30° or greater (Daughtry *et al.*, 1991).

Plant Fruit and Seeds

Detailed research has been conducted on the relationships between radar return and fruit and seed development in crops. Allen and Ulaby (1984), for example, conducted attenuation measurements on wheat heads and found that the average attenuation of the head layer of the canopy was about 8.3 dB at θ=60°. Paris (1986) also observed a rapid fall in the corn-canopy backscatter coefficient shortly after tasselling and cob formation. Bouman and Van Kasteren (1990b), however, found the lack of pronounced response of radar backscattering was due to the emergence of wheat ears. Other researchers have ignored the contribution of fruit and seeds to total backscatter, in part to simplify the model and in part because of the results of defoliation experiments which showed that the backscattering contribution of the fruit is much smaller than that of stalks and leaves (Ulaby *et al.*, 1986a).

Crop Species

Studies to date have indicated that crop species is the single most important parameter among those recorded in the field (e.g., Brown *et al.*, 1984; Cihlar and Hirose, 1984; Cihlar, 1986; Bouman and Van Kasteren, 1990a; 1990b; Brown *et al.*, 1992; Ban *et al.*, 1995). Crop type can result in a unique radar return. For example, Bouman (1987) attributed the highest radar return in beets using X-VV to its relatively higher water content or to its general geometry and larger leaves when comparing beets, potatoes and peas. Although the reasons for many of the

observed relationships between crops and backscatter are not fully understood, there is general agreement that broad-leaved crops produce higher signal returns than other crops for L-, C-, and X-band with parallel polarization. The approach of considering the cross-polarization ratio is a useful method for species identification. Although two different crop species may exhibit similar backscatter in one polarization mode, there is usually a morphology-dependent difference in another mode (Holmes, 1990).

Plant Moisture (Dielectric) Content

Plant moisture content, as an indicator of stage of growth, was found to be highly correlated with δ°, based on the measurement of δ° of wheat acquired during the final month of its growing cycle using a truck-mounted Microwave Active Spectrometer (MAS) at 8-18 GHz (Ulaby and Bush, 1976). Their results indicated that δ° is quite sensitive to the physiological and morphological changes which wheat undergoes as it ripens, particularly during the one-week period prior to harvest. In terms of the range of sensor parameters examined, 9.4 GHz δ°v nadir data showed the highest sensitivity to plant moisture variations and to the passage of time. At angles away from nadir, however, higher frequencies were found more suitable.

Plant Density and Biomass

De Matthaeis *et al.* (1995) reported that a combined use of L- and C-band allowed discrimination between low-density and high-density crops. To monitor biomass, L-band was more effective for crops with low plant density, while C-band was better for high plant density crops. HV, circular copolar and 45° crosspolar polarizations were found to be important for biomass retrieval.

Dubois *et al.* (1995) compared the L-band $\sigma^{\circ}_{HV}/\sigma^{\circ}_{VV}$ ratio image and a SPOT-derived NDVI image over the same area. Their results showed that the L-band parameter did not have a good sensitivity to vegetation with NDVI below 0.2. This indicated that the scattering at L-band was dominated by interactions with the underlying surface and not with vegetation when the vegetation was very sparse. Although the correspondence between the two indices was noisy with a wide standard deviation, their results indicated a definite correlation between the two indices confirming the potential of the $\sigma^{\circ}_{HV}/\sigma^{\circ}_{VV}$ ratio to be a good vegetation index. Their results also indicated that the copolarized channels were less sensitive to vegetation than the cross-polarized channels.

Plant Growth Stage

Bouman and Van Kasteren (1990a; 1990b) conducted a ground-based experiment on radar backscattering (X-band) and crop growth. It was found that the possibilities of X-band radar for the monitoring of crop growth were different for sugar beets and potatoes. For both crops the backscattering increased with crop growth until a saturation level was reached at about 80% crop cover. At full crop cover radar backscattering no longer reacted to any further increase in biomass. Therefore, the possibilities seemed good for monitoring the early growth of sugar beet; however, the monitoring of the growth of potatoes would be more troublesome than that of sugar beet because the ridge orientations of potatoes (with respect to the incidence microwave) dominated radar backscattering from bare soil stage to an 80% crop cover. In an airborne scatterometer study, Bouman and Hoekman (1993) concluded, however, that all frequencies (1.2-17.25) were equally useful to indicate qualitatively the growth of beet and potato in the early growing season. The backscattering of wheat appeared not to be related to crop growth in any of the frequencies.

It was also found that both VV and HH backscattering of wheat and barley decreased at all incidence angles with crop growth until it fluctuated around a stable level from grain filling to dying of the canopy. The decrease in radar backscattering, as opposed to the increase observed for sugar beets and potatoes, was caused by the relative open structure of the canopy and the small dimensions of its elements. Microwaves penetrate relatively deeply into the canopy where they eventually become extinct through absorption by the canopy elements (stems, leaves). The VV backscattering of oats at low to medium angles of incidence decreased during vegetation growth and sharply increased to a steady level with the appearance of panicles. This was due to high reflection of panicles with their cloud of small, elongated grains for VV polarized microwaves (Bouman and Van Kasteren, 1990b). Schmullius and Nithack (1992) also noted that the VV-polarized C- and X-band scattering is dependent on the different degrees of maturity in the barley fields.

Van Kasteren (1981) reported that maturity was the best phase to distinguish crops from each other on radar images. The differences in reflection level between crops were greatest at that time. On the other hand, Foody *et al.* (1989) and Fischer *et al.* (1992) found that the crop separability is optimal in the mid-growing season.

3.2.2.3 Soil Component

Soil roughness, soil moisture content and row direction can have a significant impact on the magnitude of backscatter depending upon incidence angle, polarization and frequency, as well as the amount of vegetative cover.

Soil Roughness

If the radar frequency is short relative to the surface roughness, the surface will appear smooth and little energy is backscattered to the sensor (Curlander and McDonough, 1991). Surfaces are considered smooth, specular reflectors if:

$$h < 1/25\sin T,$$

where, T is the depression angle and h is the vertical relief of the surfaces (Werle, 1992). If the wavelength is roughly the same as the average surface height, a significant fraction of incident energy will be reflected back to the sensor (Curlander and McDonough, 1991). If the average surface height (h) exceeds $1/4.4\sin T$, then the surface is considered rough and will be a diffuse reflector (Werle, 1992).

Scatterometer measurements (Figure 3.5) have demonstrated that the effects of roughness are minimal at incidence angles of about 10° (Holmes, 1990). Several researchers (Dobson and Ulaby, 1986b; Beaudoin *et al.*, 1990; Chuah and Tan; 1990; Daughrty *et al.*, 1991) found that backscatter is dominated by rough-surface scattering at low incidence angles, even in the presence of vegetation. Another notable aspect of the observations was that the effects of different roughnesses were least with shorter wavelengths; this is because all the surfaces are relatively rough for shorter wavelengths (Holmes, 1990).

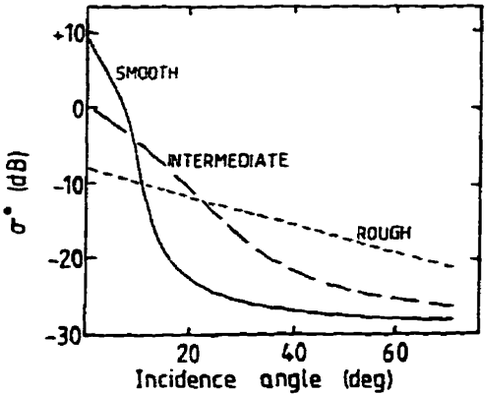

Figure 3.5. The typical backscatter curves against angle of incidence for smooth, intermediate and rough surfaces (Holmes, 1990)

Soil texture was also found to be important to determine the radar backscatter. For example, Proud *et al.* (1990) examined temporal changes in radar backscatter of crop canopies due to soil effects using C- and X-band airborne SAR and found that the sandy loam transects had the most significant results (highest R^2) compared to the clay loam and silt loam transects. Sandy loam soils are well drained; thus soil moisture conditions fluctuate rapidly compared to the clay loam and silt loam transects.

Soil Moisture

In general, an increase in the amount of soil moisture results in an increase in backscatter at all incidence angles and all frequencies (Ulaby *et al.*, 1978; Engman, 1990). The magnitude of the increase however, is incidence-angle, polarization-, frequency- and roughness-dependent (Schmullius and Furrer, 1992a; 1992b). Microwaves are generally sensitive to moisture in the 0-10 cm surface layer (Bruckler *et al.*, 1988).

The effect of soil moisture on backscatter is also dependent upon the amount and condition of surface vegetation cover (Pultz *et al.*, 1990; Schmullius and Furrer, 1992a; 1992b; Baronti *et al.*, 1995). In mid-season, the full vegetation canopy attenuates incident radar and therefore soil moisture variations have little effect on backscatter (Paris, 1986). At the end of the season however, the dry canopy is nearly transparent to microwaves and soil moisture conditions may again influence total backscatter.

Paris (1983) reported that wet-surface soil moisture conditions resulted in significantly poorer separability of corn and soybeans as compared to dry-soil conditions. On the dry-soil date, the best separation between corn and soybeans was achieved with a C-band cross-polarized measurement at a look angle of 50 degrees. Ulaby *et al.* (1981) suggested that through proper

choice of radar parameters, radar could be used to provide quantitative information on the soil moisture content of both bare and vegetation-covered soil.

Row Direction

There are reports that both cropped-land row direction (e.g., Mehta, 1983; Wooding, 1983) and the soil row direction (e.g., Bradley and Ulaby, 1981; Ulaby, 1981) affect radar backscatter. Although some researchers have concluded that the row direction effect is insignificant for frequencies greater than 4 GHz, other observations do not fully support this hypothesis. There is circumstantial evidence regarding the row effects on polarization. Bradley and Ulaby (1981) and Paris (1982) noted the effects of row direction using like-polarization; Batlivala and Ulaby (1976) noted row effects were much stronger with HH than HV.

Recent studies by Michelson (1994) have indicated that significant differences in δ° occur for fields tilled to and perpendicular to the look direction. Linear relationships between row direction and δ°, however, were weak. The ERS-1 SAR appeared sensitive to differences in the tillage row directions, but factors influencing this sensitivity must be analyzed before definite conclusions are drawn. A study using airborne C-band SAR data (Brisco *et al.*, 1991) showed significant differences in δ° between parallel and perpendicular row directions using like-polarized data from grain stubble fields; cross-polarized data were less sensitive to the influence of row direction. Dubois *et al.* (1992) reported that the radar backscatter of agricultural fields is very sensitive to the angle between the radar plane of incidence and the furrow direction. The variation is fairly sharp, up to 19 dB decrease in backscatter, when the radar incident plane is 5° off the perpendicular to the furrow plane. The observed variations are fairly independent of the incidence angle. Using both airborne X- and L-band SAR and SEASAT L-band SAR, Cihlar and Hirose (1984) noted that row direction effects were dominant in some crop/site combinations

but absent in others, even for the same crop in the northern prairies of Canada. Guindon *et al.* (1984) noted anomalously bright grain fields on some SAR passes at L-band. Bright returns were only observed when the aircraft heading and crop row direction directions were parallel.

It should be emphasized that row direction does not inevitably affect backscatter to a significant degree. For example, Sieber *et al.* (1982) concluded from analyzing three wavelengths (X-, C- and L-band) that row direction does not affect SAR images in a way that will cause changes of average backscatter cross-section. Canadian studies underline the apparent confusion about the effects of row direction on backscatter in grain fields at one test site (especially with airborne L-band), but no effect for equivalent fields at another test site. Also, there are no consistent conclusions to be drawn on which crop types results in row direction having an effect on radar return signal (Holmes, 1990).

3.2.2.2 Vegetation and Soil Interaction Component

The contribution of canopy and soil constituents to total backscatter is dependent upon polarization, incidence angle and frequency, as well as vegetation growth and development stages. For instance, Daughtry *et al.* (1991) reported that, at $\theta<20°$, soil conditions dominate backscatter coefficients; but at $\theta>20°$, the influence of vegetation on total backscatter increases and the soil contribution decreases. Daughtry *et al.* (1991) also found that polarization has little effect on penetration into dense corn canopies. Conversely, Holmes (1990) reported that horizontally polarized (HH) L-band radar couples weakly to vertical stalks resulting in low attenuation. Vertically polarized (VV) microwaves, however, are attenuated to a greater extent causing a reduction in the penetration depth.

3.2.3 Effects of Rain, Dew, Wind and Other Environmental Factors

Effects of rain (e.g., Fischer *et al.*, 1992; Schmullius and Nithack, 1992) , dew (e.g., Ulaby *et al.*, 1986a; Gillespie *et al.*, 1990a; 1990b; Schmullius and Furrer, 1992a) and wind (Ulaby *et al.*, 1986a; Bouman and Van Kasteren, 1990a; 1990b) on radar backscatter have been reported by some researchers. For example, Brisco *et al.* (1989b) reported that wheat separability may be increased when the crop canopies contain free water, and this phenomenon may also be enhanced using VV polarization. Bouman and Van Kasteren (1990a; 1990b) reported changes in canopy structure due to strong winds which in turn affected radar backscatter by 1-2 dB for both sugar beets and potatoes.

3.3 Ground-Based Scatterometer in Agriculture

Much of the knowledge available today on the interaction of microwaves with agricultural targets has been obtained through scatterometer experiments over small test plots. These detailed experiments have the advantage that both radar parameters and the agricultural target parameters can be carefully controlled and measured. Scatterometer studies of this kind have been carried out mainly by researchers in North America and western Europe including research groups affiliated with the University of Kansas, the Radar Observation of Vegetation (ROVE) team in the Netherlands, a French multi-disciplinary team, and the Canadian Center for Remote Sensing (e.g., Attema, 1980; Lannelongue, 1981; Krul, 1987; 1988; Bouman and Van Kasteren, 1990a; 1990b; Bouman, 1991a; Brisco *et al.*, 1992). The results from these ground based scatterometer studies represent a backbone of radar remote sensing research in agriculture since data provided by ground based scatterometers are necessary for the calibration of other sensors and serve as an important data base for quantitative SAR investigations in agriculture (Werle, 1992). Due to the scope of this review, studies using ground-based scatterometer data are not detailed here.

3.4 Airborne SAR in Agriculture

Most of the research in the past three decades has used airborne radar. The notable airborne radar campaigns includes the Canadian GlobalSAR (Campbell *et al.*, 1995; Petzinger, 1995), Multisensor Airborne Campaign (MAC) Europe-91 (Wooding and Attema, 1995), ESA and Joint Research Center's (JRC) Multiple Airborne Experiments Toward Radar Observations (MAESTRO-1) Campaign (Wooding and Attema, 1992; Churchill and Attema, 1994; Lemoine *et al.*, 1994), and US' AIRSAR Campaign (JPL, 1996).

3.4.1 Airborne SAR Systems

A wide variety of radars were used to acquire data including X-Band, C-Band, and L-band. Major airborne SAR systems are listed in Table 3.1. (Wooding and Attema, 1992; Geomatics Canada, 1994; Schmullius *et al.*, 1994; Horn, 1996)

Table 3.1. Major Airborne SAR Systems

Airborne SAR Systems	Frequency	Polarization
CCRS C/X-SAR (Canada)	X- and C-band	HH, HV, VH, and VV
NASA/JPL SAR (U.S.)	C-, L-, and P-band	HH, HV, VH, and VV
DLR E-SAR (Germany)	X-, C-, L-, and P-band	HH and VV

3.4.2 Airborne SAR Data for Agricultural Crop Classification

3.4.2.1 Multiparameter Airborne SAR Data for Crop Classification

Multifrequency, multipolarization and multi-incidence angle airborne SAR data have been studied intensively for crop classification in the past three decades. The interpretation success is based

entirely on each specific investigation, which can be time specific, site specific, SAR-parameter specific, or image-quality specific, as discussed in Section 3.2.1. In general, the results indicated that multiparameter airborne SAR data significantly improved crop classification accuracies. For example, Wever *et al.* (1995) reported that no class could be clearly separated using monotemporal classification with one single frequency. The use of four frequencies, however, resulted in a very good classification. Brisco and Protz (1980) also demonstrated greater than 90% correct classification of corn fields using single-date dual-channel (X- and L-band) SAR. Table 3.2 shows the selected studies of multiparameter airborne SAR data for agricultural crop classification.

3.4.2.2 Multitemporal Airborne SAR Data for Crop Classification

The potential of multitemporal data has been explored and is considered a necessity especially for crop classification. Indeed, the crop calendar and crop phenological development are some of the most important considerations to make when classifying crops from remotely sensed data. Improvement in crop discrimination has been achieved by synchronization of SAR data collection with growth stages of crops since multitemporal imagery maximizes the differences in the geometric and dielectric properties of crops. Research conducted by Bush and Ulaby (1978), for example, showed that 90% correct classification of crop type was possible using multitemporal radar with four revisits approximately 10 days apart. Some classification results suggest that a single data acquisition taken during peak growth stage is of primary importance, while others suggested during plant maturity. Data acquisition dates range from late May just after crops have been planted to September when crops are fully grown and perhaps even harvested. The majority of the studies, however, used data that were collected during one or more of the summer months of June, July and August. In general, the use of multitemporal imagery has improved classification accuracies over single-date input especially when single-date classification

Table 3.2. Multiparameter Airborne SAR Data for Crop Classification: Selected Studies

Major Crops	SAR Mode & Parameters	Study Area	Description	Overall Accuracy	Reference
Corn, soybeans, small grains, pasture	ERIM SAR L-band HH, HV	Huntington County, Indiana, USA	Crop classification with multipolarization L-band radar	L-HH & L-HV: 71% L-HH: 65%	Ulaby *et al.*, 1980
Corn, grains, hay-pasture,	ERIM SAR X-, L-band HH, HV	Univ. of Guelph test strip, Ontario, Canada	Manual and automatic crop identification with airborne radar imagery	Corn: >90% Hay-pasture & grains: 50%	Brisco & Protz, 1982
Sugar beets, potatoes, winter wheat, winter barley, oats	CCRS SAR X-,C-, L-band HH, VV	Danube River Valley, Germany	Evaluation of the crop classification performance of X-,L-, and C-band SAR imagery	X-HH, C-VV, L-HH, & L-HV: >90%	Guindon *et al.*, 1984
Wheat, barley, canola, fellow	CCRS SAR C-VV 30° & 53°	Melfort, Saskatchewan, Canada	A comparison of steep and shallow mode (30° & 53° incidence angles) data for crop classification	53°: 95% 30°: 72% for site 25, July SAR data	Poirier *et al.*, 1988
Corn, barley, oats, potatoes, forage crops, pasture, etc.	CCRS SAR X- & C-band HH	Municipality of Saint-Léonard d'Aston, Quebec, Canada	Multiband SAR: comparison of per-pixel classification and a classification using segmentation results	X- & C-band: up to 53% X- or C-band alone: <45%	Thomson *et al.*, 1990
Sugar beet, potatoes, carrots, wheat, beans, grass, etc.	NASA/JPL AIRSAR C-band, polarimetric	Feltwell, Norfolk, UK	Crop classification from C-band polarimetric radar data	9 classes (80 cases): 79% 7 classes (388 cases): 61% 15 classes (412 cases): 37%	Foody *et al.*, 1994
Corn, wheat, soybeans, pasture, alfalfa	CCRS SAR C-band HH, HV & VV 45°-76°	Oxford County, Ontario, Canada	Evaluation of textural and multipolarization radar features for crop classification	supervised: 86% unsupervised: 75%	Anys & He, 1995
Wheat, barley, lucerne, peas, potatoes, stem beans, rapeseed, sugar beet, grass	NASA/JPL AIRSAR C-, L- & P-band, polarimetric 20°-55°	Flevoland, the Netherlands	Classification of multifrequency polarimetric imagery using a dynamic learning neural network	95% for all covers except peas	Chen *et al.*, 1996

accuracies are low. Table 3.3 shows the selected studies of multitemporal airborne SAR data for agricultural crop classification.

Table 3.3. Multitemporal Airborne SAR Data for Crop Classification: Selected Studies

Major Crops	SAR Sensor & Data	Study Area	Description	Overall Accuracy	Reference
Corn, forest, grain, & other cover types	ERIM SAR X-, L-band HH, HV June 20 & Sept. 3	Univ. of Guelph test strip, Ontario, Canada	Improving crop classification through attention to the timing of airborne radar acquisition	Multidate: 83% Corn: 92% Grain: 51%	Brisco *et al.*, 1984
Wheat, canola, fallow	ERIM SAR C-VV, 53° June 26, July 31 & Aug. 13, 1983	Melfort, Saskatchewan, Canada	Crop type determination from multitemporal SAR imagery	Filtered data: June: 60±23% July: 87±7% Aug.: 65±24% July & Aug.: 87±7%	Brown *et al.*, 1984
Wheat, barley, canola, fellow	ERIM SAR C-VV 30° & 53° June 26, July 31 & Aug. 13, 1983	Melfort, Saskatchewan, Canada	Multitemporal SAR for crop classification: a comparison of steep and shallow mode (30° & 53° incidence angles) data	At 53°: June: 62% July: 91% Aug.: 80% July & Aug.: 96%	Poirier *et al.*, 1988
Spring wheat, winter wheat, spring barley, sugar beet, potatoes, carrots, grass	VARAN SAR X-HH 29°-67° 4 dates from early June to late Aug., 1986	Feltwell, Norfolk, UK	Multitemporal airborne SAR data for crop classification using a per-field approach	3 classes: 4 dates: 90% 2 dates: 88% 7 classes: 4 dates: 69% 2 dates: 55%	Foody *et al.*, 1989
Potatoes	CCRS C/X SAR C-band HH & VV June 27, Aug. 8 & Sept. 11,1990	Queens County, PEI, Canada	A comparison between multidate C-HH & C-VV SAR imagery for potato crop monitoring	C-VV: June & Aug.: 81% 3 dates: 79% C-HH: 3 dates: 73%	Dobbins *et al.*, 1992

3.4.2.3 Integration of Airborne SAR and VIR Data for Crop Classification

The synergistic effect of integrating SAR data and imagery acquired in the visible and infrared (VIR) portions of the spectrum has been recognized as important for two main reasons. First,

timeliness of SAR fills information gaps during overcast or hazy periods at critical stages of the growing season and second, the combination of data from different parts of the spectrum often leads to increased classification accuracy. Several researchers have demonstrated that combining airborne SAR and satellite VIR data improves crop classification accuracies (e.g., Brisco *et al.*, 1989a, Fiumara and Pierdicca, 1989; Brisco and Brown, 1995). For example, Brisco and Brown (1995) evaluated the synergistic effects of multidate airborne SAR and Landsat TM data for crop classification in western Canada. Four dates of C-HH SAR data (May 25, June 24, July 21 & Aug. 10) and two dates of TM data (May 28 & July 16) were acquired over an agricultural area near Saskatoon, Saskatchewan, Canada during the 1988 growing season. The major crops investigated were canola, barley, wheat, summerfallow and alfalfa. The results showed that VIR data were superior to the SAR data for single date classifications due to the multispectral information content. Multidate SAR data improved the classification accuracy from 30 to 74% although multidate VIR produced the highest single sensor result of 90% correct classification. This was slightly improved to 92% by including the SAR data with the VIR data. The best two SAR channels and the best two VIR channels, based on their transformed divergence statistics, produced an overall classification accuracy of 85%. Furthermore, the May TM data combined with SAR data yielded an 87% correct classification because the grain and alfalfa classes were much better separated when VIR data were combined with SAR data. These results demonstrated significant synergism between the two sensors.

3.5 Spaceborne SAR in Agriculture

3.5.1 Spaceborne SAR Systems: Past, Present and Future

The first spaceborne imaging radar was launched in 1978 on-board the SEASAT satellite. It operated for 105 days, pioneering spaceborne radar and many other microwave instruments (NASA and JPL, 1994). As part of a radar evaluation program, the U.S. carried out two additional spaceborne radar missions, SIR-A and SIR-B. SIR-A and SIR-B orbited the Earth only for a number of consecutive days in 1981 and 1984, respectively (Werle, 1992). Despite their overall technological and scientific success, the relatively short lifetime precluded the acquisition of seasonal data sets; for example, of vegetation-canopy phenology. Moreover, the SEASAT and SIR-A SARs were "single-parameter" instruments; i.e., they used a fixed wavelength, a fixed polarization, and a fixed incidence angle (NASA, 1988). The SIR-B SAR provided the first multi-incidence angle data set for surface feature (particularly forest) mapping and topographic mapping. Also, the SIR-B data were the first to be digitally encoded and digitally processed; they represented a significant advance in SAR image processing technology. The sensor stimulated interesting research and applications, but the research and applications have been limited in scope due to its short lifetime. The past spaceborne SAR system parameters are summarized in Table 3.4 (NASA, 1988; Werle, 1992). The detailed information on spaceborne SAR systems can be found in Appendix C.

Table 3.4. Past Spaceborne SAR System Parameters

Parameters	SEASAT	SIR-A	SIR-B
Frequency or Wavelength	1.275 GHz (23.5 cm) (L-Band)	1.275 GHz (23.5 cm) (L-Band)	1.275 GHz (23.5 cm) (L-Band)
Polarization	HH	HH	HH
Incidence Angle	23°	47°	15° - 60°
Swath Width (km)	100	50	20 - 50
Azimuth Resolution (m)	25 (4 looks)	40 (6 looks)	20 - 30 (4 looks)
Range Resolution (m)	25	40	58 - 16

The 1990s is the decade of spaceborne SAR systems with the launch of ALMAZ-1, ERS-1 and ERS-2, JERS-1, SIR-C/X-SAR and RADARSAT. With the launch of ALMAZ-1 on March 31, 1991, the former Soviet Union (just prior to its dissolution) became the first country to operate a spaceborne radar system (Lillesand and Kiefer, 1994). Although this system initiated a new era in operational remote sensing from space with the ability to provide high-resolution data independent of weather conditions and time of day, ALMAZ-1 was not well known in the SAR research and application community due to lack of promotion by Russia. With the launch of the European Space Agency (ESA)'s ERS-1 in July, 1991, the first long-duration spaceborne SAR system became available. Carrying the same SAR instrument as ERS-1, the second European Earth Resources Satellite was successfully launched in April, 1995 (ESA, 1992; Eurimage, 1994; ESA, 1995a). In February, 1992, the Japanese Earth Resources Satellite JERS-1 was launched. ERS-1&2 and JERS-1 SARs are single-parameter SAR systems with fixed wavelengths, incidence angles and polarizations (ESA, 1992; NASDA, 1993; Eurimage, 1994; RESTEC, 1996b). Thus, their capabilities are limited for experimental and research use. The geometry of ERS-1 and ERS-2 SAR imaging mode is shown in Figure 3.6.

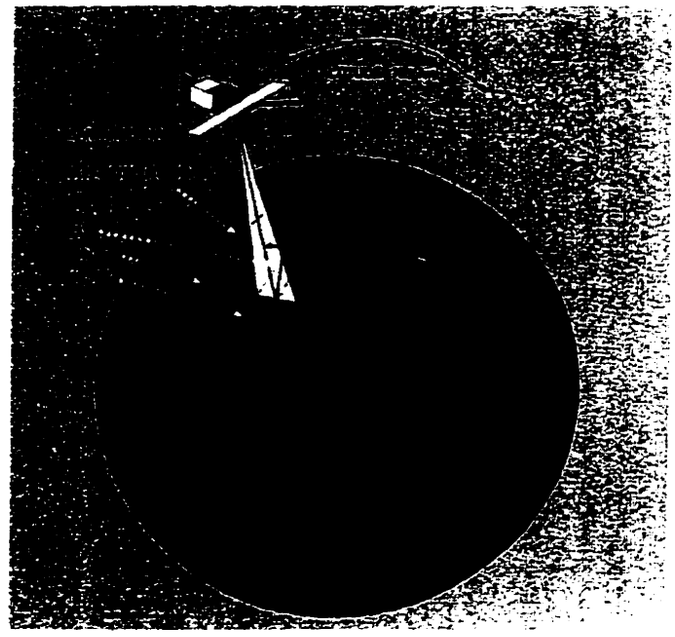

Figure 3.6. ERS-1 SAR imaging mode geometry (ESA, 1989)

The SIR-C/X-SAR system marked a big step forward with advanced SAR technologies. SIR-C/X-SAR's unique contributions to earth observation and monitoring are its capability to measure, from space, the radar signature of the surface at three different wavelengths, and to make measurements for different polarizations at two of those wavelengths (NASA/JPL, 1994; JPL, 1996). The applications of SAR-C/X-SAR, again, are limited due to its short lifetime.

Successfully launched on November 4, 1995, the Canadian RADARSAT is the first long-duration spaceborne system with multincidence angle, multiresolution, and multiswath width capability (CSA *et al.*, 1994). It provides an excellent opportunity for operational environmental monitoring and resource management, including agricultural monitoring. The present spaceborne SAR system parameters are summarized in Table 3.5 (ESA, 1992; Luscombe *et al.*, 1993; NASDA, 1993; CSA *et al.*, 1994; Eurimage, 1994; Lillesand and Kiefer, 1994; ESA, 1995a; Jordan, 1995; RSI, 1995b; CSA, 1996c; JPL, 1996; RESTEC, 1996b). The RADARSAT SAR operating modes are shown in Figure 3.7.

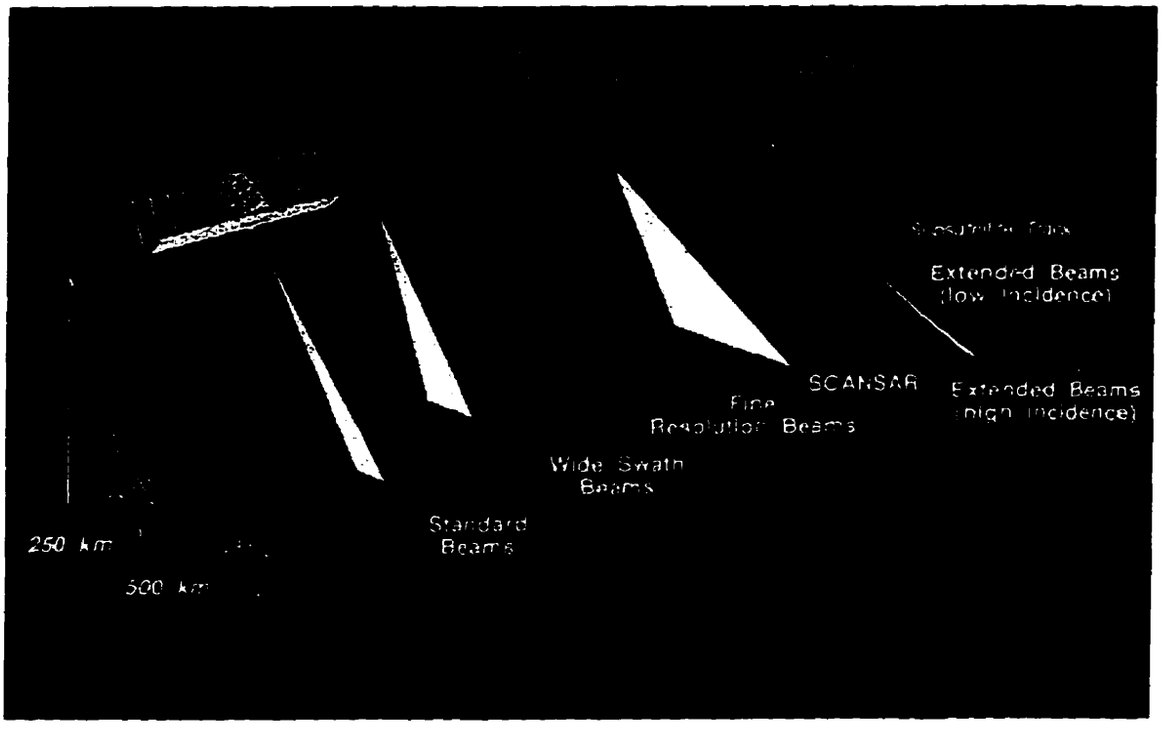

Figure 3.7. RADARSAT SAR operating modes (CSA, 1996c)

Table 3.5. Present Spaceborne SAR System Parameters

Parameters	ALMAZ-1 SAR	ERS-1 & 2 SAR	JERS-1 SAR	SIR-C/X-SAR	RADARSAT SAR
Band Frequency or Wavelength	S-Band 3 GHz or 10 cm	C-Band 5.3 GHz or 5.7 cm	L-Band 1.3 GHz or 23 cm	L-Band: 23.5 cm C-Band: 5.8 cm X-Band: 3.1 cm	C-Band 5.3 GHz or 5.7 cm
Polarization	HH	VV	HH	L & C-Band: Polarimetric X-Band: VV	HH
Incidence Angle	30° - 60°	23°	38.5°	17° - 63°	20° - 60°
Swath Width (km)	350 (left/right)	100 (right)	75 (right)	L:15 - 90 C:15 - 90 X:15 - 40	50 - 500 (right)
Revisit Period (days)	1-3	16-18	44	-	3+
Spatial Resolution (m)	10-30	30	18	30	10 - 100
Lifetime (years)	1.5	3	4	10 days (April) 10 days (October)	5

Later this century or early next century, a few proposed spaceborne missions with advanced multiparameter SAR systems will be launched. The operational use of SAR data will be enhanced by the launch of these future spaceborne advanced SAR systems. Their multifrequency, multipolarization, multiresolution, multiswath width and multitemporal capability will provide unbiased and consistent real-time information for an operational agricultural monitoring system and other operational environmental monitoring systems. The future SAR missions and systems characteristics are summarized in Tables 3.6 and 3.7 (Dornier Deutsche Aerospace and British Aerospace Space Systems, 1994; Bartholomä *et al.*, 1995; ESA, 1995a; Brown *et al.*, 1996).

Table 3.6. Future Spaceborne SAR Missions

Mission (Agency)	SAR Instrument	Status	Launch Date/ Duration	Orbit	Primary Applications
ALMAZ-1B (Russia)	SAR-10 SAR-3 SAR-70 SLR-3	Proposed	1997 3 years	Circular, 73°, 400 km, 92 mins	Agriculture, forestry, cartography, oceans
SICH-2 (NSAU)	SAR	Firm/ approved	1997 3 years	Sun-synchronous, near-polar, 98°, 670 km, 98 mins	Agriculture, forestry, hydrology, environmental monitoring, forest and tundra fires
ENVISAT-1 (ESA)	ASAR	Firm/ approved	1998 5 years	Sun-synchronous, polar, 780-820 km, 100.59 mins	Environmental monitoring, physical oceanography, ice and snow, land surface
RADARSAT-3 (CSA/CNES)	SAR	Proposed	2005	TBD	Operational sea-ice reconnaissance, structural geologic mapping, and land-use mapping

Table 3.7. Future Spaceborne SAR System Parameters

Parameters	ALMAZ-1B SAR	SICH-2 SAR	ENVISAT-1 ASAR	RADARSAT-3 SAR (TBD)
Frequency or Wavelength	SAR-10: 9.6 cm SAR-3: 3.5 cm SAR-70: 70 cm SLR-3: 3.5 cm	23 cm (L-Band)	5.3 GHz (C-Band)	L-Band and C-Band
Polarization			HH & VV	HH, VV, HV and HV (TBD)
Incidence Angle				L-Band: 20° - 50° C-Band: 15° - 65°
Swath Width (km)	SAR-10: 30 - 170 SAR-3: 20-35 SAR-70: 120-170 resight swath 330 for all above SLR: 450	40 km (detailed) 80-120 (Survey)	100-400	L-Band: 100-300 C-Band: 25-800
Spatial Resolution (m)	SAR-10: 5-7 (detailed), 15 (intermediate), & 15-40 (survey) SAR-3: 5-7 SAR-70: 20-40 SLR: 190-250 range, 1200-2000 azimuth	10-50	30, 100, 1000	C-Band: Standard: 5 or 10 Spotlight: 3 x 1.7 ScanSAR: 5-10 x 45-90 Twin Pol: 10-20 x 5-10 Quad Pol: 10-20 x 5-10

3.5.2 Spaceborne SAR for Agricultural Crop Classification

3.5.2.1 Early Spaceborne SAR Data for Crop Classification

Compared to the numerous airborne studies, little research has been done using early spaceborne SAR in agriculture due to the very limited amount of data collected by these short-lived missions. An overview of past spaceborne imaging radar studies in agriculture is given in Table 3.8. A discussion of selected studies can be found in Appendix D.

3.5.2.2 Multitemporal Spaceborne SAR Data for Crop Classification

Spaceborne SAR is potentially an important new data source for agricultural applications. It satisfies a basic agricultural requirement for reliable and frequent imaging through the crop growing season, which cannot be met by optical satellites such as SPOT or Landsat. Agricultural interest focuses on the use of multitemporal ERS-1 and other spaceborne SAR images (Wooding and Laur, 1993).

Before the launch of the long-duration spaceborne SAR systems, airborne studies had demonstrated that multitemporal SAR data could enhance the ability to distinguish between various crop spectral patterns (see Section 3.4.2 for details). However, comparatively few datasets have been available for study due to the increased cost and logistics of generating multitemporal SAR data with airborne platforms. With the launch of ALMAZ-1, ERS-1, JERS-1, and RADARSAT, world-wide spaceborne SAR data are now routinely available. They provide researchers with an excellent opportunity for developing multitemporal SAR agricultural applications (Ban and Howarth, 1995). Table 3.9 presents an overview of multitemporal studies using these SAR data. A discussion of selected studies can be found in Appendix D.

Table 3.8. Overview of Early Spaceborne Imaging Radar Studies in Agriculture

Subject	Mission	Band/ Pol.	Test Area	Investigation	Reference
Crop-Type Classification	SEASAT CCRS SAR-580	L-HH X-HH L-HH	Swift Current, Outlook, Raymond, Melfort, western Canada	Determination of relationships between image tones & parameters describing agricultural cover types and comparison of classification accuracies (visual/digital)	Cihlar and Hirose, 1984
Backscatter & Agricultural Target Parameters	SEASAT CCRS SAR-580	L-HH X-HH L-HH	Swift Current, Outlook, Raymond, Melfort, western Canada	Determination of relationships between image tones & parameters describing agricultural cover types (visual/digital)	Cihlar, 1986
Land-Cover Types	SIR-B	L-HH	Hoosier & Lake Diefenbaker, Saskatchewan, Canada	Discrimination of prairie land-cover types: feasibility study (visual/digital)	Cihlar *et al.*, 1986a
SAR & Soil Moisture, Surface Roughness & Crop Canopy	SIR-B	L-HH	West-central Illinois, U.S.A.	Evaluation of the effects of soil moisture, surface roughness, and crop canopy cover on radar backscattering (digital)	Dobson and Ulaby, 1986a
Backscatter & Agricultural Cover Types	SIR-B CCRS SAR-580	L-HH L-HH	Napierville, Quebec, Canada	Determination of the influence of ground features on radar return & comparison of relative backscattering coefficients collected by space and airborne radar (visual/digital)	Hutton and Brown, 1986
Backscatter & Soil Moisture, Surface Roughness & Vegetation	SIR-B	L-HH	San Joaquin Valley, near Fresno, California, U.S.A.	Observations of microwave backscatter dependence on soil moisture, surface roughness, and vegetation covers (digital)	Wang *et al.*, 1986
SAR for Agriculture, Forestry & Settlements	SEASAT	L-HH	The region of Bonn, Germany	Qualitative and quantitative interpretation for applications in agriculture, forestry and urban areas (visual/digital)	Bönsch *et al.*, 1988

Table 3.9. Overview of Multitemporal Agriculture Studies Using ERS-1, JERS-1 & SIR-C/X-SAR Data

Subject	Mission/ SAR	Images	Test Area	Investigation	Reference
Crop Discrimination	ERS-1 C-VV	3 (1992 growing season)	Melfort, Saskatchewan, Canada	Evaluation of different filtering algorithms and sizes for ERS-1 SAR, comparison of the separability between crops on multitemporal ERS-1 SAR data, and assessment of principle components as a mean of providing information in class separability	Brown *et al.*, 1993a
Rice-Crop Monitoring	ERS-1 C-VV	8 (1992 growing season)	Test field of Akita Prefectural College of Agriculture, Japan	Investigation of the feasibility of spaceborne microwave remote sensing for rice-crop monitoring	Kurosu *et al.*, 1993; 1995
Agricultural Land-Use Mapping	ERS-1 C-VV	3 (1992 growing season)	Northwest of Bonn, Germany	Investigation of suitability of unitemporal and multitemporal ERS-1 SAR data for land-use inventories	Müller *et al.*, 1993
Crop Monitoring	ERS-1 C-VV E-SAR (airborne) C-VV	3 (SAR) & 5 (TM) (1992 growing season)	Lechfeld, near Munich, Germany	Comparison of multitemporal ERS-1 and airborne DLR E-SAR data for crop monitoring	Schmullius *et al.*, 1993
Crop Discrimination	ERS-1 C-VV	10 (1992 growing season)	Four test sites in eastern England	Study of changes in the backscatter of agricultural crops throughout a growing season	Wooding *et al.*, 1993
Crop Monitoring	ERS-1 C-VV	10 (1992 growing season)	East Anglia UK	Assessment of the feasibility of using spaceborne SAR data for crop-type discrimination.	Wright *et al.*, 1993
Agricultural Land Applications	ERS-1 C-VV JERS-1 L-HH	10 (ERS-1) & 3 (JERS-1)	Flevoland, the Netherlands	Comparison of multitemporal ERS-1 and JERS-1 SAR data for agricultural land applications	Borgeaud *et al.*, 1994
Rice-Crop Mapping & Monitoring	ERS-1 C-VV	8 (1991, 1992 & 1993)	Kanchanaburi Province, West Thailand	Investigation of the potential of ERS-1 SAR data for rice-field mapping and rice-crop monitoring	Aschbacher *et al.*, 1995
Crop Identification	ERS-1 C-VV	6 (1992 growing season)	Oxford County, southern Ontario, Canada	Investigation of ERS-1 SAR temporal backscatter profile for crop identification	Ban & Howarth, 1995
Agricultural Land-Use	SIR-C/X-SAR; L- &C-band, polarime-tric, X-VV	? (April 11 & 13, 1994)	Oltrepo Pavese, northern Italy & Oberpfaffenhofen, Germany	Investigation of agricultural landuse in Italy and Germany by means of the multi-frequency SIR-C/X-SAR system	Kühbauch *et al.*, 1995
Agricultural Crop Discrimination	ERS-1 C-VV	14 (1992 growing season)	South Flevoland, The Netherlands	Assessment of the capability of ERS-1 SAR precision data to discriminate between crop types using field-based classification and determination of the earliest possible stage in the growing season at which crop type can be distinguished	Schotten *et al.*, 1995

3.5.2.3 Integration of Spaceborne SAR and VIR Data for Crop Classification

Previous studies have shown that the integration of airborne SAR and satellite VIR data improves crop classification accuracies (see Section 3.4.2 for details). Attempts have also been made by a few researchers to improve crop classification accuracies using data from two satellite sensors (Ban and Howarth, 1995). Table 3.8 is an overview of the synergism of SAR and VIR for crop classification. A discussion of selected studies can be found in Appendix D.

Table 3.10. Overview of Integration of SAR and VIR Data for Crop Classification

Subject	Missions /Sensors	Dates	Test Area	Investigation	Reference
Crop Classification	ERS-1 C-VV SPOT XS	3 1	Southern part of Fyn, Denmark	Evaluation of combinations of ERS-1 SAR and SPOT data for crop classification	Fog *et al.*, 1993
Agricultural Statistics: Crop Acreage Estimation	ERS-1 C-VV SPOT XS	6 4	Seville, Spain; Great Driffield, UK	Comparison of ERS-1 and SPOT for crop acreage estimation of the MARS project	Kohl *et al.*, 1993
Monitoring Grassland & Detecting Changes in Agricultural Use	ERS-1 C-VV Landsat TM	6 3	Weilheim, near Munich, Germany	Comparison of ERS-1 and Landsat TM data for monitoring grassland and detecting changes in agricultural use.	Schadt *et al.*, 1993
Crop Classification	ERS-1 C-VV Landsat TM	3 1	Oxford County, Ontario, Canada	Evaluation of the synergistic effects of integrating satellite SAR and VIR data for crop classification	Ban and Howarth, 1995

3.5.2.4 Summary

The spaceborne SAR is potentially an important data source for agricultural applications. It satisfies a basic agricultural requirement for reliable and frequent imaging through the crop growing season, which cannot be met by optical satellites such as SPOT or Landsat.

Agricultural interest focuses on the use of multitemporal ERS-1 and other spaceborne SAR images.

There have been significant developments in our understanding of the radar backscatter of agricultural crops over the lifetime of ERS-1. Prior to the launch of ERS-1 in July 1991, research had been concentrated on experimental programs using airborne radar systems, and involvement in space had been limited to the brief-duration SEASAT and Shuttle Imaging Radar (SIR-A and SIR-B) missions. The availability of frequent and reliable satellite radar data from ERS-1 has provided new insights into the potential of multitemporal radar imaging for monitoring agricultural crops. The excellent stability of the ERS-1 SAR calibration has been another important factor, facilitating comparisons of crop backscatter measurements across different test sites and over different years (Wooding, 1995).

Spaceborne SAR agricultural research has been concentrated on using ERS-1 data, although a few studies have made use of the combinations of ERS-1 and JERS-1, and the SIR-C/X-SAR. Most of the research has been carried out in Europe through ESA's programs and the European Community's MARS projects. In Canada, research has been supported through the Radar Data Development Program (RDDP) and the ERS-1 Soil Moisture Experiment (ERSOME). Very few papers, however, were found from the rest of the world.

From these studies, temporal backscatter profiles for a large number of different fields have been analyzed. It has been found that some crops generate distinctive temporal backscatter profiles which can be exploited for crop-classification purposes. For example, rice, wheat, barley, oilseed rape and grass, all show particularly distinctive behaviour. Time-windows exist in which these crops are separable on the basis of their backscatter and differences in backscatter between dates. This allows them to be classified with high orders of accuracy. All studies reported that multitemporal SAR data improve crop classification accuracy (Wooding, 1995).

The synergistic effects of integrating satellite SAR data and VIR data have also been investigated by researchers. Both combinations of ERS-1 SAR/TM and SAR/SPOT data have been evaluated. Most of the studies reported an increase in crop classification accuracy, with the combinations of SAR and VIR data compared with either SAR data or single VIR data alone. Surprisingly, in some cases a decrease of the classification accuracy was found by adding ERS-1 to SPOT data (Wooding, 1995).

Experience with ERS-1 has established the potential of satellite radar for agricultural applications. With ERS-2, JERS-1, RADARSAT, ENVISAT ASAR and other spaceborne SAR systems providing continuity of data into the next century, there are excellent opportunities for exploiting the potential of satellite radar for operational crop monitoring. Operational multifrequency, multipolarization radar systems being planned for early next century will extend the capabilities even further

3.6 Crop Information Extraction from Digital SAR Data

Extensive maximum likelihood classification (MLC) experiments have been performed on agricultural targets. In general, SAR has been out-performed by optical sensors when data acquired on the same date(s) and multi-spectral VIR data are used. Crop classification in SAR images using pixel-by-pixel comparisons have been found too inappropriate (less than 50% accuracy with single-band SAR), due to problems associated with image speckle (Cihlar *et al.*, 1986b). Durand (1987), however, suggests that crop classification is possible using this technique, as long as the image is filtered. In fact, it has been suggested that filtering significantly improves visual aspects and pixel-by-pixel classification results, without losing textural information and edges (Shi and Fung, 1994). Median filtering, for instance, has been successfully applied to reduce SAR speckle and, hence to improve the classification accuracy

(Goodenough *et al.* 1980; Brown *et al.*, 1984; Ban *et al.*, 1995). Even with filtering, some classes, such as grain varieties, still remain confused.

A variety of efforts have been made to improve crop classification, including: 1. generation of various texture measurements and segmentation techniques or per-field classifiers for crop discrimination (e.g., Ulaby *et al.*, 1986b; Dubé *et al.*: 1986; Pultz and Brown, 1987; Vallée *et al.*, 1987; Bénié *et al.*, 1989; Treitz *et al.*, 1993; Foody *et al.*, 1994; Anys and He, 1995; Ban *et al.*, 1995; Treitz *et al.*, 1996); 2. the use of multiparameter (i.e., multifrequency, multipolarization, multi-incidence angle, and multitemporal) SAR data (e.g., Brisco and Protz, 1982; Brisco *et al.*, 1984; Brown *et al.*, 1984; Guindon *et al.*, 1984; Foody *et al.*, 1989; Brown *et al.*, 1992; Wooding *et al.*, 1993; Baronti *et al.*, 1995; Kühbauch *et al.*, 1995); 3. the combinations of SAR and VIR data for crop identification (e.g., Brisco *et al.*, 1989a; Fiumara and Pierdicca, 1989; Fog *et al.*, 1993; Brisco and Brown, 1995; Ban and Howarth, 1996b); 4. incorporation of crop rotation practices into crop classification of SAR imagery with a knowledge-based approach (e.g., Bedard *et al.*, 1992; Ban, 1993). These approaches have proven effective for improving crop classification to a certain degree, however, comprehensive understanding of the radar backscatter from crops, and the systematic, optimal methodology to extract SAR information for input into a crop information system still remain problems.

3.7 Achievements and Limitations

Studies conducted in the past three decades have provided valuable initial insights into the potential usefulness of SAR for agricultural applications. The findings to date can be summarized in the following broad statements:

- Crop canopy and soil parameters: Crop type is the most important field parameter. No definite relationships between SAR intensities and individual canopy parameters have been

established to date, although some progress has been made. Research has indicated relationships between radar backscatter intensities and various crop variables, including crop type, moisture content, and leaf area index (LAI) or percent cover. Surface roughness and moisture content are the dominant soil parameters affecting radar backscatter. The underlying soil will have a varying contribution to the backscatter throughout the crop-growth period. It is difficult to identify different crop types on the basis of their microwave backscatter characteristics because we do not fully understand how varying crop and soil conditions affect the backscatter.

- Crop identification: Research has demonstrated the value of radar data in identifying crop types. High accuracy can be achieved with SAR (particularly multifrequency and multipolarization) data under some conditions. Classification accuracies often vary among sites and between dates at one site. The extension of test site results to larger areas has not been carried out.

- Digital classification methodology: Digital filtering prior to classification improves results. Per-field classifiers are generally preferable to per-pixel classifiers. Image texture offers some potential, but has not been thoroughly explored. Image segmentation followed by classification appears to offer an effective approach to digital analysis of SAR data; however, segmentation of SAR imagery is difficult because of speckle. Incorporating crop rotation information using an expert system has proven to be a promising approach to certain extent, however, the incorporation of crop rotation knowledge into an expert system for crop classification could be troublesome because crop rotations are strongly influenced by market prices and the local climate.

- Integration of SAR and VIR: VIR image data from Landsat TM and SPOT XS have increasingly been merged with SAR data to take advantage of the best qualities of both types

of imagery for agricultural crop identification. The synergism of SAR and VIR data has been demonstrated by several researchers using airborne SAR and satellite VIR data. Very little research, however, has been done to improve crop classification accuracies using data from two satellite sensors. Thus, the potential of satellite SAR and VIR synergism still needs further investigation.

- Multitemporal approach: There are no clear-cut conclusions as to optimal timing of measurements for classification accuracy. For example, studies with C-VV imagery indicated that the highest accuracy in crop separation was obtained before three general vegetation classes reached maturity (Cihlar *et al.*, 1986b). Van Kasteren (1981) on the other hand, concluded that greatest accuracy in crop type separation was obtained when the crop had reached maturity. Contrasting studies such as these reaffirm the need for a better understanding of the parameters which influence the image. Furthermore, an inadequate amount of airborne SAR data acquired during the growing season has limited multitemporal studies. With the launch of ERS-1, ERS-2, JERS-1 and RADARSAT, the long-duration spaceborne SAR data became routinely available to provide researchers with an excellent opportunity for developing multitemporal SAR agricultural applications.

3.8 Summary

Radar remote sensing has the potential to play an important role in agricultural crop mapping and monitoring due to its independence from solar illumination and cloud cover. Starting in the mid-1960s, a group of scientists at the University of Kansas used aircraft-based radar imagers (Ka- and Ku-bands) to investigate the potential of radar for crop identification, mapping and condition assessment. Since then, radar remote sensing techniques have been investigated for a variety of applications in agriculture. Major campaigns and investigations conducted by research

laboratories in North America and Europe using ground-based scatterometers and airborne imaging radars, as well as spaceborne SARs, have been reviewed in this chapter.

Previous research has demonstrated the large potential for using radar remote sensing for various agronomic applications. SAR data are so complex, however, that their interaction with agricultural crop targets is not fully understood; and with the current state-of-the-art of interpretation methods for SAR imagery, the accuracies of crop classification are not always as high as required for successful operation of a crop information system. To be able to increase the accuracies of crop identification and area estimation, and thus develop a viable crop information system that makes use of SAR imagery as the primary data source, we need to:

1. have a better understanding of the crop and underlying soil characteristics that influences the radar backscatter throughout the growing season;
2. identify the suitable methodologies to extract crop information from SAR imagery;
3. evaluate multipolarization airborne SAR for crop identification;
4. evaluate the synergistic effects of satellite SAR and VIR for crop identification; and
5. evaluate multitemporal ERS-1 SAR for crop identification.

CHAPTER 4: EXPERIMENTAL DESIGN

In this chapter, the geographical characteristics of the study area are discussed. The characteristics of the airborne SAR data, ERS-1 SAR data and the ground information are described. The important aspects of calibration of ERS-1 SAR data are discussed and procedures for derivation of the calibration constant σ° are presented.

4.1 Study Area

The study area is situated in Norwich Township, an agricultural area in Oxford County, southern Ontario, Canada. Approximately 15 km x 4 km and centred at 42° 57' N, 80° 38' W (UTM 530 000 E; 4 755 000 N), this area has been selected as one of the few representative agricultural 'supersites' across Canada at which the relationships between radar data and agriculture are being studied (Brown *et al.*, 1991). As part of the Radar Data Development Program (RDDP), the **OX**ford County **SO**il Moisture Experiment (OXSOME) and the **ERS**-1 **SO**il Moisture Experiment (ERSOME) experiments were conducted at this site. Figure 4.1 shows the location of the study area.

4.1.1 Relief and Drainage

Oxford County has a varied relief and possesses typical landform features associated with continental glaciation. Elongated hills, known as drumlins, occupy much of the central part of the county, while the southern half consists of sand plains of deltaic origin interleaved with morainic ridges. The most continuously rugged relief is associated with the Waterloo Hills, near the border of Waterloo and Brant Counties on the northern margin of the county (Wicklund and

Richards, 1961). In the southeast part of the county, the relief of the study area is relatively smooth. Overall elevation is about 260 m.

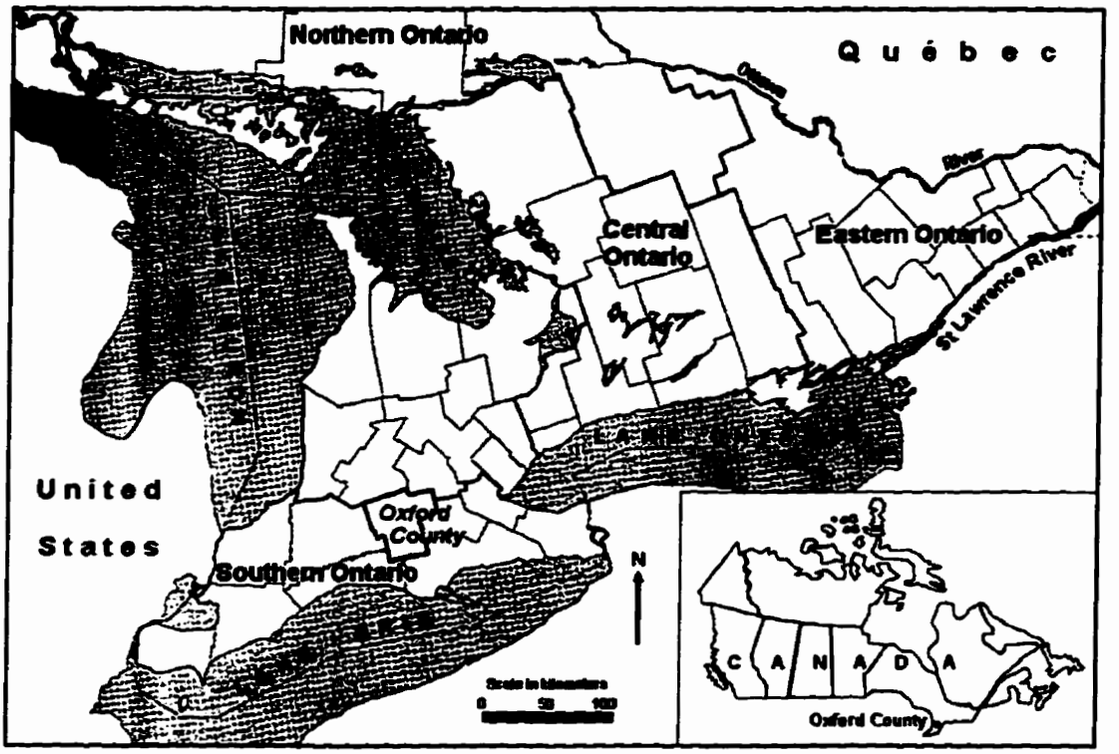

Figure 4.1. Location of the study area

Figure 4.2 shows some of the external drainage features within Oxford County. There are no major rivers in the southern half of the county, but the study area is drained by small intermittently flowing creeks that run in south, southeast and southwest directions.

4.1.2 Climate

Situated in the peninsular region of southwestern Ontario, Oxford County has a climate that is strongly influenced by the Great Lakes. One of the most important aspects of climate in relation to agriculture is the length of the growing season, i.e., the interval between the last killing frost in the spring and the first in the autumn. In general, with increasing distance from the lakes,

there is a shorter frost-free season. Another important aspect of climate in relation to agricultural crops is precipitation. This region has a fairly uniform pattern of precipitation distribution throughout the year. It has no marked wet or dry season. The region is traversed alternately by cool dry air from the north and warm humid air from the south and southwest. Variations in the frequency of these air currents can produce a humid hot month or an unseasonably cool month with too much cloud and rain in the summer. The latter results in a condition of slow growth of those crops, such as wheat and corn, that require high temperatures for maturity (Wicklund and Richards, 1961).

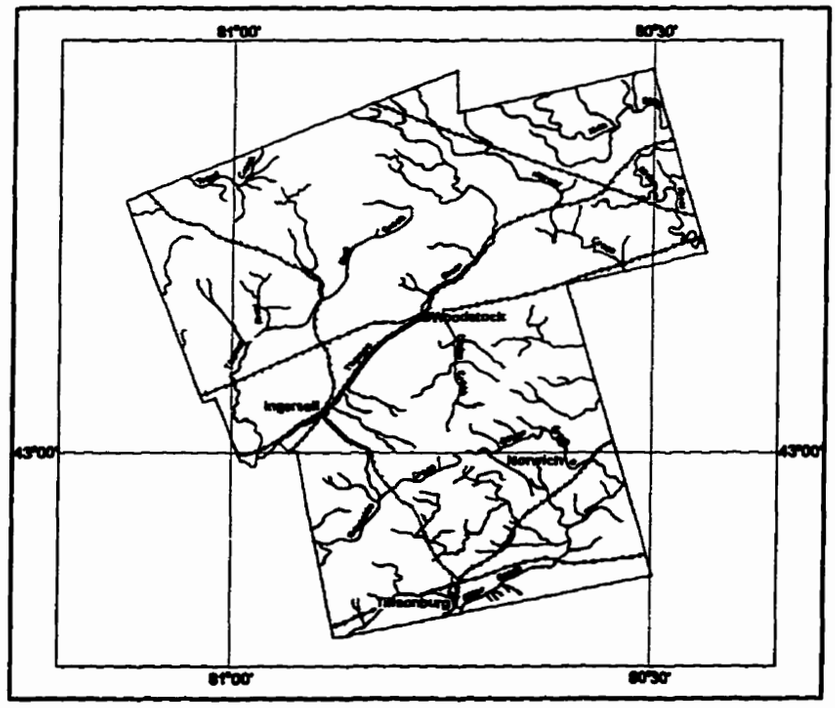

Figure 4.2. Drainage systems of Oxford County (Wicklund and Richards, 1961)

4.1.3 Soils and Land Use

Soils in the study area range from silt loam in the west to clay loam in the center and loamy sand in the east (Figure 4.3). A change in soil types runs diagonally through blocks one and seven.

This boundary change can be located approximately by the location of strip-farming areas (principally tobacco), which are indicative of a sandy, well-drained soil. A till plain with clay and silty loams exists in the western end of the study area (Gardell *et al.*, 1993).

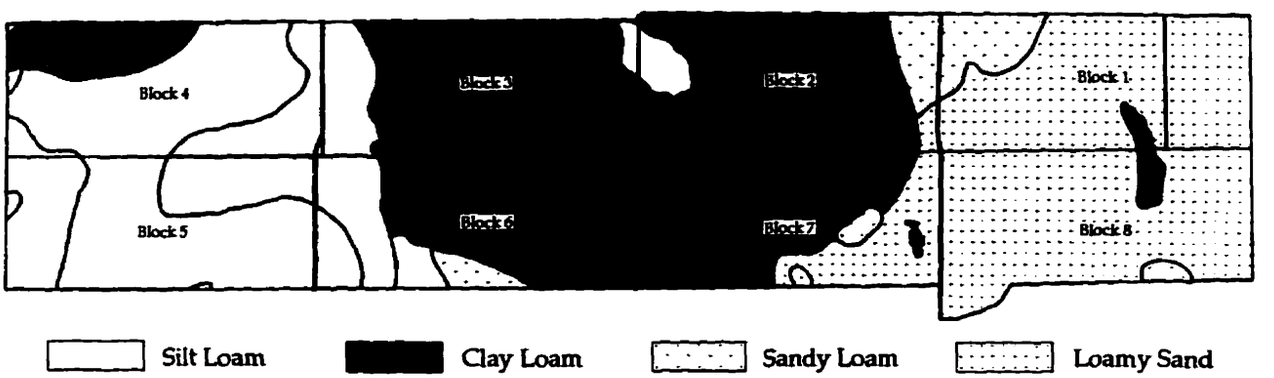

Figure 4.3. Soil classification of the study area (Wicklund and Richards, 1961)

The major field crops of Oxford County include corn, soybeans, winter wheat, oats, barley, alfalfa, hay, pasture, tobacco and rye. Statistics (Statistics Canada, 1992) show that improved land[1] occupies 86% of the total farm-land area, unimproved pasture occupies 2.8% and all other land occupies 11.4%. Of the improved land, 96% is devoted to crop production, 0.6% to summer fallow, and 3.4% to improved pasture. Of total crop land, 43.2% is corn, 16% is soybeans, 14.5% is hay, 7.2% is winter wheat, 1.7% is oats, 1.8% is barley, 3% is mixed grain, 1.7% is tobacco, 1.5% is rye and small areas of other crops (Statistics Canada, 1992). In the study area there are notable variations. Towards the west on silt-loam and clay-loam soils, fields are bigger and dominated by corn, soybeans, winter wheat, hay and alfalfa. Towards the east, on loamy sand, fields are smaller and grow mostly tobacco and rye.

[1] For 1991, the figures shown were derived by summation of cropland, summer fallow and improved pasture. The 1991 census did not include a separate question on "other" improved land. Therefore, some other types of improved land (e.g., land on which buildings, barnyards, home gardens, and greenhouses are located, newly broken land or land left idle for more than one year) will not be included in these totals.

4.2 Data Description

4.2.1 Airborne SAR Data

Narrow-swath, C-band SAR data were collected for the study area by the CCRS Convair 580 aircraft in 1990 as part of the OXSOME project (Table 4.1). The aircraft acquired SAR data in C-band and four polarizations (HH, HV, VH and VV). The specifications are listed in Table 4.2 (Geomatics Canada, 1994; Livingstone *et al.*, 1987; 1988).

Table 4.1 Remotely Sensed Data of the Study Area

Sensor	Spatial Resolution	Date of Acquisition
Airborne SAR C-HH, C-HV	6 m x 6 m (8 looks)	July 10, 1990
ERS-1 SAR C-VV	30 m x 30 m	May 27, 1992
		June 15, 1992
		July 24, 1992
		Aug. 5, 1992
		Sept. 28, 1992
		Oct. 14, 1992
		May 12, 1993
		June 16, 1993
		July 5, 1993
		July 21, 1993
		Aug. 9, 1993
		Aug. 25, 1993
		Sept. 13, 1993
		Sept. 29, 1993
		Oct. 18, 1993
Landsat TM	30 m x 30 m	Aug. 6, 1992
SPOT HRV(XS)	20 m x 20 m	June 15, 1992
		Aug. 26,1993

Table 4.2. CCRS Airborne C/X-SAR System Characteristics

Frequency	5.3 GHz (C-band) and 9.25 GHz (X-band)
Polarization	horizontal or vertical
Incidence Angles	nadir mode = 0 - 74°, narrow mode = 45 - 76°, wide mode = 45 - 85°
Resolution	nadir- and narrow-swath (high) resolution: 6m in azimuth & range wide-swath (low) resolution: 10m in azimuth and 20m in range
Swath Width (with 6 km aircraft altitude)	nadir = 22 km, narrow = 18 km, wide = 63 km

4.2.2 ERS-1 SAR Data

Multitemporal ERS-1 SAR data were acquired during the 1992 and 1993 growing seasons (Table 4.1). The SAR system characteristics are listed in Section 3.5.1 in Chapter 3.

The fifteen scenes of ERS-1 SAR signal data were received on High Density Digital Tape (HDDT) at the Canadian Data Reception Facility at the Gatineau Satellite Station (GSS). Among them, six scenes of 1992 signal data were correlated to imagery using the Canadian ERS-1 SAR Processor (CERS-1) at GSS. These SAR georeferenced fine-resolution (SGF) ground-range images were neither radiometrically calibrated nor corrected for changes in system gain (see Section 4.3 for details). The SGF product parameters are listed in Table 4.3 (CCRS, 1992; Livingstone *et al.*, 1992).

In order to gain a precise understanding of multitemporal radar backscatter properties of agricultural crops and soils, and to develop methodologies for classification of agricultural crops, accurate absolute calibration of SAR is necessary. The nine scenes of 1993 signal data, therefore, were processed at the ESA Processing and Archiving Facility at the German Aerospace Research Establishment (DLR) (D-PAF). The ESA SAR Precision (PRI) product is a multilook (speckle-reduced), ground-range, system-corrected image (see Table 4.4). The product is

calibrated and corrected for the SAR antenna pattern and range-spreading loss; i.e. radar backscatter can be derived from the product for geophysical modelling, but no correction is applied for terrain-induced radiometric effects. The image is not geocoded and terrain distortion (foreshortening and layover) has not been removed (ESRIN/ESA, 1996). The calibration principles are detailed in Section 4.3.

Table 4.3. The ERS-1 SGF Product Parameters

Coordinate system	zero Doppler, ground range
Number of lines	8000 (image) variable swath
Number of pixels	8000
Spatial resolution	nominal 30 m at azimuth by 30 m at ground range
Incidence angle	19.5° to 27°
Absolute geometric accuracy (flat terrain)	1100 m
Relative geometric accuracy (flat terrain)	40 m
Number of looks	6 (3.3 looks effective)
Type of pixel	16-bit detected
Pixel spacing	12.5 m x 12.5 m

Table 4.4. ESA ERS-1 SAR PRI Product Parameters

Pixel size	12.5 m at range and azimuth
Scene area	100 km at range and at least 102.5 km at azimuth
Scene size	8000 pixels and at least 8200 lines
Pixel depth	16 bits
Product location accuracy	100 m at range and 200 m at azimuth
Projection	ground-range
Number of looks	3
Incidence angle	19.5° to 26.6°
Annotation in image	lat./long. of scene centre and the four corners

4.2.3 Landsat TM and SPOT Data

Landsat TM and SPOT data were also collected in 1992 and 1993 (Table 4.1). The systems' characteristics are described in Section 2.3.1 in Chapter 2.

4.2.4 Ground Information

Ground data were collected by field teams during OXSOME in May and July, 1990 (Hutton *et al.*, 1990; Brown *et al.*, 1991) and ERSOME during the 1992 and 1993 growing seasons. The field boundaries were digitized into a PAMAP GIS from a SPOT image acquired during the 1990 growing season. The boundaries were updated using 1992 and 1993 SPOT images.

The study area is subdivided into eight blocks (Figure 4.3) for the convenience of the field work. Each field has been assigned a block and a field number. Extensive ground data (known as "green sheets") were collected for agricultural fields and included: crop type, plant growth stage, canopy height, percentage cover, row spacing, row direction, plant condition, and ground photographs (Figure 4.4). Intensive sampling for soil moisture, surface roughness and/or residue amounts were also made on some "priority fields" during May and October, 1992. As a result of these field observations, an extensive GIS database has been developed for this area, including agricultural field boundaries, crop information (i.e., green sheets), airborne SAR and ERS-1 data. An example of the "green sheets" can be found in Appendix E.

Winter Wheat

Barley/Oats

Corn

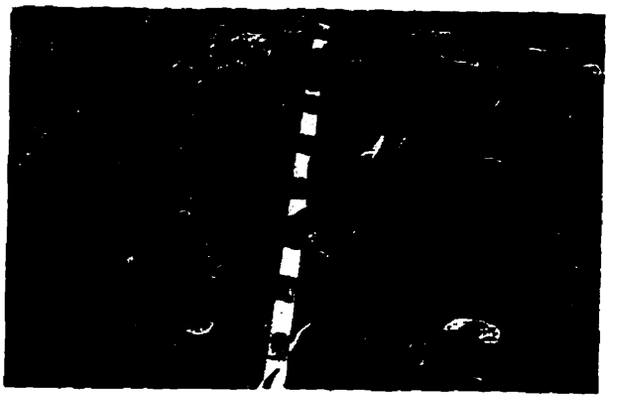

Soybeans

Alfalfa

Pasture

Figure 4.4. Major crops in the study area

4.3 SAR Radiometric Calibration

4.3.1 Introduction

The quantitative use of SAR data requires calibrated images. Researchers who want to carry out multitemporal studies over large areas, compare data from different sensors, extract geophysical parameters from backscatter measurements using models, build up a database of backscatter measurements for different types of terrain/incidence angle, etc., can only do so using calibrated SAR data products. Also, the full benefit of the new multichannel SARs will not be realized unless the different channels can be properly compared to one another (Freeman, 1992).

The radiometric fidelity of SAR imagery is affected by intensity variations resulting from surface scattering geometry and antenna pattern variations. The surface scattering geometry causes radiometric distortions, because at increasing incidence angle down-range less power is received. This results in less intense signal returns and less image brightness. The following radar equation (4.1) states that the power received is inversely proportional to the fourth power of the range. This relationship is known as R^4 power loss.

$$P_r = \frac{P_t G_t}{4\pi R^2} \sigma_{rt} \frac{A_r}{4\pi R^2} \qquad \text{Equation 4.1}$$

(with the two way path losses neglected)

where
- P_r = received power at polarization r,
- P_t = transmitted power at polarization t,
- G_t = gain of the transmitting antenna, in direction of target, at polarization t,
- R = distance between the radar and the target (slant range),
- σ_{rt} = radar cross-section, the area intercepting that amount of power of polarization t which, when scattered isotopically, produces an echo at polarization r equal to that observed from the target,
- A_r = effective receiving area of radar antenna aperture at polarization r, and
- $1/4\pi R^2$ = isotropic spreading.

The antenna pattern causes radiometric distortion in the range dimension, because an antenna transmits more power from the center of the antenna than from its edges. This results in more intense radar returns in the middle-range of the image swath relative to the near- and far-range edges where illumination is less intense (Werle, 1992). Figures 4.5 & 4.6 show the azimuth cut of the SAR antenna pattern.

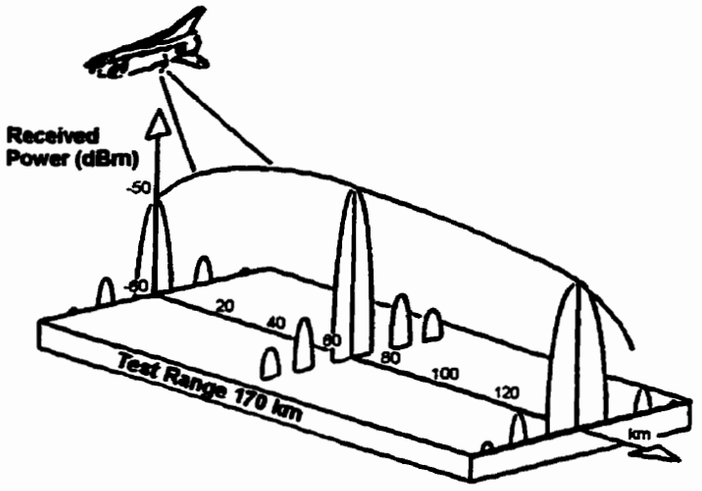

Figure 4.5. Measurements of the SAR antenna pattern, using azimuth cuts (Lentz, 1993)

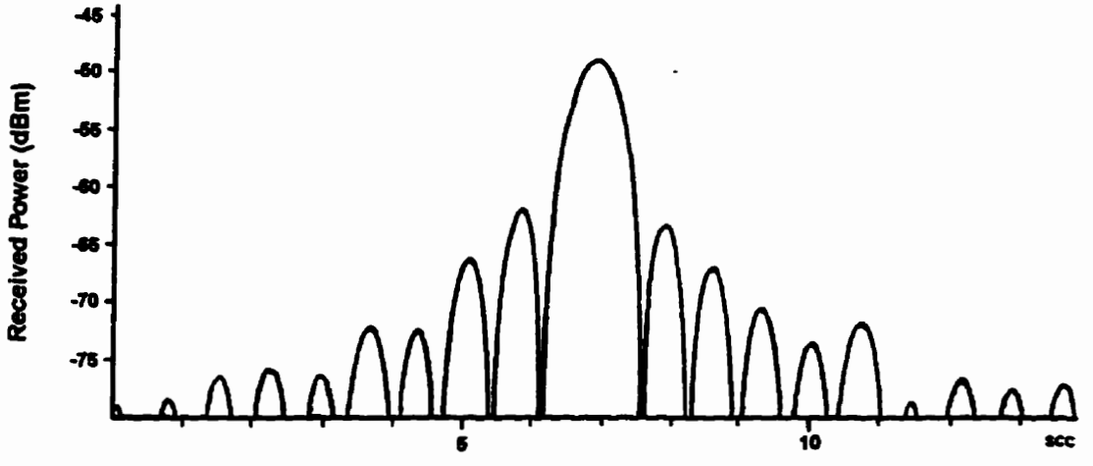

Figure 4.6. One antenna azimuth cut of ERS-1 (Lentz, 1993)

These distortions can be compensated by calculating the range power loss and by measuring the antenna pattern cross the image swath. Range spreading loss can be compensated in the pixel digital number using the following equation:

$$DN^2_{comp} = DN^2 \frac{R^3}{R^3_{ref}} \qquad \text{Equation 4.2}$$

where R is the slant range distance at the distributed target location and R_{ref} is a reference slant range distance; i.e., the mid-swath slant-range distance $R_{ref} = 847.0$ km (Laur, 1992).

The antenna pattern (Figure 4.7) can be applied to the pixel digital number using the following equation:

$$DN^2_{comp} = \frac{DN^2}{g^2(\theta)} \qquad \text{Equation 4.3}$$

where $g^2(\theta)$ is the two-way antenna pattern profile (to be applied on power data) and θ is the look angle at the distributed target location (Laur, 1992).

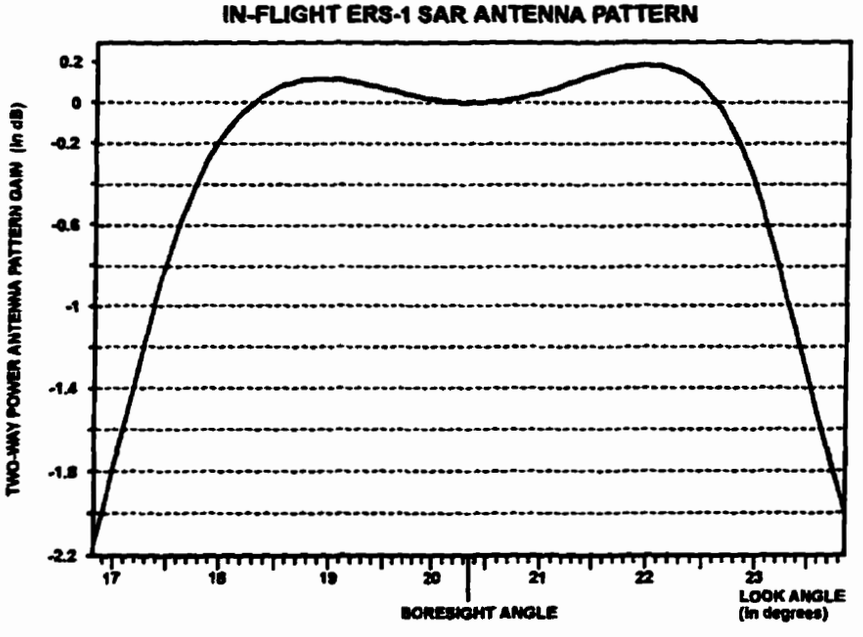

Figure 4.7. Measured antenna pattern for ERS-1 SAR (Laur, 1992)

4.3.2 ERS-1 SAR Radiometric Calibration

4.3.2.1 Canadian ERS-1 SAR Processor

The Canada Centre for Remote Sensing (CCRS) has been receiving ERS-1 SAR data and recording them on HDDTs at the Canadian Data Reception Facility at the GSS and Prince Albert, Saskatchewan Satellite Station since the launch of ERS-1 in 1991. These data are correlated to imagery by the CERS-1 located at GSS. Because ERS-1 was initially an experimental satellite, the design and development of the CERS-1 processor were carried out prior to the growth of requirements in the scientific community for radiometrically calibrated imagery. As a result, the CERS-1 processor was not designed to perform radiometric calibration and performs no corrections for changes in system gain. The intention was rather to allow all fluctuations in the sensor to flow through to the data. Any stability that it does produce is therefore inherent in the sensor itself. There are no normalizations for slant range, incidence angle or antenna pattern dependencies (Lukowski *et al.*, 1993).

Since the Gatineau processor supplies much of the North American SAR data from ERS-1, CCRS gave a contract to the Noetix Research Inc. in 1993 to develop ERS-1 SGF Image Calibration Software based on the paper by Livingstone *et al.* (1992) to calibrate the ERS-1 SGF images by removing the effects of the illumination antenna and by providing the coefficients which convert the digital numbers on a SGF image to total power, or the normalized backscatter coefficient σ° (Noetix Research Inc., 1993). The calibration software, however, does not compensate for range spreading loss. Livingstone *et al.* (1992) estimated the accuracy for this calibration is at +/- 2 dB.

4.3.2.2 ESA Processing and Archiving Facilities (PAF) SAR Processor

The ERS-1 SAR PRI product is radiometrically calibrated and corrected for the SAR antenna pattern and range-spreading loss at one of the ESA PAFs. The calibration measurements were performed using transponders deployed by ESA/ESTEC in Flevoland, the Netherlands, a joint effort between the ESA PAF and the ERS Central Facility at ESA/ESRIN. The combination of internal calibration parameters and accurate on-ground measurements gives the ERS-1 user community the first opportunity to work with precisely calibrated SAR products acquired over a long period (Laur *et al.*, 1993).

Internal Calibration Parameters

Two types of internal calibration parameters are measured in the ERS-1 SAR Active Microwave Instrument (AMI). At the start and end of each SAR imaging sequence, a set of four calibration pulse measurements and eight noise measurements is made. During the imaging sequence, copies of the transmitted pulses (replicas) are generated and appended to the raw data. One complete replica pulse is transmitted with every 24 raw-data range line records. These two stage internal calibration parameters are required to ensure that the ERS-1 SAR image products are internally calibrated, especially as the ERS-1 AMI does not have an automatic gain-control system. The system gain can drift due to temperature changes and aging. The gain changes are monitored via the replica pulse powers as they are passed through the SAR system. The calibration pulse measures the majority of the gain drift with the replica pulse being used to monitor the gain drift during the imaging sequence when the more representative pulse is not available. The thermal noise is measured when pulses are not being transmitted at the start and end of each imaging sequence.

Within ESA SAR processors, a *single* replica pulse associated with the image product being processed is extracted and used for gain normalization and range compression. Two problems were identified with replica pulses. The first was that the replica pulses were being extracted from the raw data incorrectly such that the start of the replica was misidentified by one or two range line records. The second problem was associated with the fact that the replica pulse itself is corrupt in that one or more of the 704 samples that make up the replica can have spurious values. Quality checking has been introduced at the ESA PAFs including D-PAF to identify the two problems and, if found, to select another suitable replica pulse to be used for image generation (Laur *et al.*, 1993).

A further problem was found. The use of a replica pulse within a processor assumes that the replica pulse power is directly proportional to the transmitted pulse power. If this were the case, any transmitter pulse power variations would be compensated for in the resultant SAR image. It was found, however, that the above assumption is invalid (i.e., there is no direct relationship between the replica pulse and the calibration pulse power). The consequence of this is that any replica pulse power variations introduced by a SAR processor need to be removed (Laur *et al.*, 1993). It was suggested by Laur *et al.* (1993) that users of ERS-1 SAR imagery need to correct their imagery to obtain correctly calibrated results. This is done by comparison of the replica pulse power used to generate the image in question with that used to generate the reference image of Flevoland from which the calibration constant was derived. The replica pulse power used for image generation is given in the CEOS header of each image product. The expression used for this correction is:

$$\frac{\text{image replica power}}{\text{reference replica power}} \qquad \text{Equation 4.4}$$

(The reference replica power is 205229.)

No corrections are made for the calibration pulse power variations within the ESA ground segment SAR processors. Because the calibration pulse power information is difficult to access for users and corrections of its variations do not improve the calibration measurements, it is not proposed to apply such a correction in the derivation of σ° in ESA SAR products generation (Laur *et al.*, 1993).

Raw Data Quality Parameters

SAR data obey a certain statistical distribution (zero mean, Gaussian amplitude and uniform phase). Statistical checks on the data can establish whether the data are corrupted during on-board processing such as in-phase (I) and quadrapture (Q) channel separation and analogue to digital conversion (ADC) (Laur *et al.* 1993).

Laur *et al.* (1993) identified the ADC non-linearity as the main source of error in the measurement of radar cross-sections or backscattering coefficients. The ADC non-linearity occurs over large distributed targets having high backscattering levels, such as sea surfaces. Examinations of ERS-1 SAR raw data for the period January 1992 to September 1993 indicate an average I channel standard deviation of 6.15 (corresponding to a power loss of 0.1 dB) together with a range of approximately 2 to 12. These findings indicate that a significant proportion (22%) of ERS-1 SAR raw data suffers from an ADC power loss higher than 0.5 dB. Thus, these findings clearly indicate the need to correct for ADC non-linearities when measuring the radar cross-sections of calibration targets, especially when the targets are in a coastal area.

Table 4.5 shows the radiometric stability and the radiometric accuracy measured with the transponder 2 before and after the ADC correction. From these results, it appears that the ADC non-linearities correction gives *substantial improvement* in the precision of the radar cross section

measurements. The derived radiometric parameters such as the radiometric stability and the radiometric accuracy are *reduced by half.*

Table 4.5. Radiometric Calibration Parameters with Correction of ADC Non-Linearities

Transponder 2 (38 measurements over 2 years)	*Before* correction of ADC power loss estimate	*After* correction of ADC power loss estimate
Radiometric stability	0.38 dB	0.18 dB
Radiometric accuracy	0.32 dB	0.16 dB
Max. variation of the measured RCS*	$\pm$ 0.75 dB	$\pm$ 0.42 dB

* RCS: radar cross-section

Antenna Pattern Correction

The in-flight ERS-1 SAR antenna elevation pattern has been estimated by ESA/ESRIN using images over the Brazilian Amazon rain-forest (isotropic targets method). The derivation of the antenna pattern was done using the mean range profile of 10 images of uniform rain-forest with the assumption that $\gamma = \sigma^{\circ}/\cos\alpha$ is a constant value for the rain-forest (for the ERS-1 SAR incidence angle α). The derived mean polynomial of range profiles was set to zero at the boresight angle (look angle $\theta = 20.35^{\circ}$). Noise compensation was applied. In order to check the effect of ADC non-linearities over the rain-forest, a raw data image was analyzed and the ADC power-loss in the scene was derived. The estimated ADC power loss correction was then applied to the previously derived in-flight antenna pattern. The estimated in-flight antenna pattern was then compensated in ESA PRI products (Laur *et al.*, 1993; Laycock and Laur, 1994). The in-flight ERS-1 SAR antenna pattern is shown in Figure 4.7.

The Derivation of the Calibration Constant

The calibration constants for ESA ERS-1 products are derived from the Transponder 2 radar cross-section on October 13, 1991. Table 4.6 gives K values (±0.75 dB) for all PRI products processed after September 1, 1992. The calibration constant is valid for *one specific product and one specific SAR processor.* The different values of K between PAFs arise from the different gains of the PAF processors (Laur, 1992).

Table 4.6. Calibration Constant K for ESA ERS-1 SAR PRI Products

ESRIN/EECF*	D-PAF	UK-PAF
K = 58.24 dB	K = 58.24	K = 59.49 dB

* EECF: ESRIN ERS-1 Central Facility

The estimation of ADC non-linearity corrections (computed from the raw block power analysis) to apply to the Transponder 2 radar cross-section for this date is 0.39 dB. A confirmation of the estimate is given by the mean ADC correction of 0.45 dB (measurements over 2 years). An updated calibration constant is obtained when applying the ADC correction:

$$K(\text{update}) = K + 0.39 \text{ dB} \qquad \text{Equation 4.5}$$

The updated calibration constant K is *consistent* with previous K estimated error bounds at the end of the commissioning phase. The updated K error bounds (± 0.42 dB) are indeed within the previous estimation of ±0.75 dB. The updated radiometric stability is 0.18 dB compared to a previous figure of 0.38 dB (Laur *et al.*, 1993).

4.3.3 Derivation of the Radar Backscatter Coefficient σ°

The generation of ERS-1 SAR temporal backscatter profiles of agricultural crops requires relating pixel digital numbers (DN) on SAR images to backscatter coefficients of corresponding distributed targets in the scene. The aim of this section is to describe the methodology for deriving backscatter coefficients in ERS-1 SAR PRI products.

The relationship between image intensity and backscatter coefficient is given in its simplest form:

$$\langle I \rangle = K * \sigma^\circ \qquad \text{Equation 4.6}$$

where: $\langle I \rangle$ is the average pixel intensity measurements,

σ° is the backscatter coefficient of the distributed target, and

K is the calibration constant.

To derive a local estimate $K(\alpha)$ of the calibration constant, the following equation should be applied:

$$K(\alpha) = K * \frac{\sin\alpha_{ref}}{\sin\alpha} \qquad \text{Equation 4.7}$$

The calibration constant, K, given in ESA SAR PRI products is $K = K(\alpha_{ref} = 23^\circ)$. The local incidence angle α can be determined by the following equations:

$$\cos\alpha_n = \frac{(R_T + h)^2 - R_n^2 - R_T^2}{2 R_n R_T} \qquad \text{Equation 4.8}$$

where R_T is the earth radius, R_n is the distance between radar and the target (Figure 4.8).

The complete equation to be applied in order to determine the backscatter coefficient σ° of an area located at incidence angle α is:

$$\sigma^\circ = \frac{\langle I \rangle}{K(\alpha)} = \frac{\langle I \rangle}{K} \bullet \frac{\sin\alpha}{\sin\alpha_{ref}} \bullet \frac{R^3}{R^3_{ref}} \bullet \frac{1}{g^2(\theta)} \qquad \text{Equation 4.9}$$

Since the ESA SAR PRI products have compensated for range spreading loss and antenna pattern, the equation can be simplified to:

$$\sigma^\circ = \frac{\langle I \rangle}{K} \bullet \frac{\sin\alpha}{\sin\alpha_{ref}} \qquad \text{Equation 4.10}$$

where :

$$\langle I \rangle = \frac{1}{N} \bullet \sum_{i=1}^{i=N} DN_i^2$$

DN_i is the digital number of a given pixel *i* and is proportional to the square-root of the intensity I_i received from the ground resolution cell corresponding to pixel *I*.

N is a large pixel number (more than 500) to ensure statistical validity to the estimation of the mean intensity.

Expressed in decibels ($\sigma^\circ_{(dB)} = 10 \bullet \log_{10} \sigma^\circ$), we have:

$$\sigma^\circ_{(dB)} = (10 \bullet \log_{10}\langle I \rangle) - (10 \bullet \log_{10} K) + \{10 \bullet \log_{10}(\frac{\sin\alpha}{\sin\alpha_{ref}})\} \qquad \text{Equation 4.11}$$

$$\sigma^\circ_{(dB)} = \langle I \rangle_{(dB)} - K_{(dB)} + \beta_{(dB)} \qquad \text{Equation 4.12}$$

$$\text{where } \beta_{(dB)} = 10 \bullet \log_{10}(\frac{\sin\alpha}{\sin\alpha_{ref}})$$

In PRI images, the range of incidence angles α is typically from 19.5° at the near-range to 26.6° at the far-range. The correction factor β can vary from - 0.7 dB to +0.6 dB with image swath.

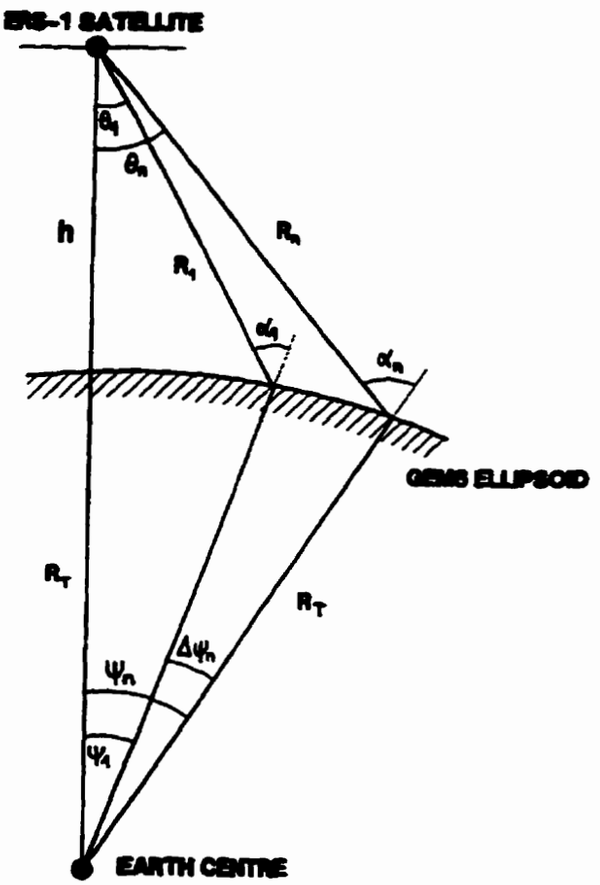

Figure 4.8. ERS-1 SAR Imaging Geometry (Laur, 1992)
(*GEM6: Goddard Earth Model 6)

4.4 Summary

In this chapter, the geographical characteristics of the study area have been discussed. The characteristics of the airborne SAR data, ERS-1 SAR data and the ground information have been described. The important aspects of calibration of ERS-1 SAR data were discussed and procedures for derivation of the calibration constant σ° were presented.

CHAPTER 5: AIRBORNE SAR FOR CROP CLASSIFICATION: A MULTIPOLARIZATION APPROACH

5.1 Introduction

As discussed in Chapter 3, airborne SAR data have been used by researchers to identify crops for the past two decades (e.g., Brisco *et al.*, 1984; Brown *et al.*, 1984; Foody, 1988; Brisco *et al.*, 1989a; Fischer and Mussakowski, 1989; Brown *et al.*, 1993a; Foody *et al.*, 1994). The accuracy of SAR crop classification, however, varies and is not always sufficiently high for crop inventory and analysis. This can be attributed, in part, to the performance of per-pixel classifiers when applied to SAR data because the results of such classifications are often noisy. In order to reduce noise and improve classification accuracy, it is necessary to take into account the spatial correlation among pixels (Qiu and Goldberg, 1985). A per-field classification approach should improve classification accuracy since fields in Canada are generally planted with a single crop (Brown *et al.*, 1984; Brisco *et al.*, 1989a). Therefore, efforts have been directed towards development of techniques to extract and classify homogeneous segments on SAR images (Bénié *et al.*, 1989; Fiumara and Pierdicca, 1989; Thomson *et al.*, 1990).

The objective in this chapter is to evaluate spatial information processing and classification methods for improving crop classification using multipolarization airborne SAR data. Specifically, contextual (filtering) and textural processing techniques are investigated to examine their effects on improving classification accuracy. Per-pixel and per-field classification approaches are tested to determine the most appropriate classification method for use in an agricultural environment; and co-polarization (C-HH), cross-polarization (C-HV) SAR data and their combinations are evaluated for crop classification.

5.2 Data Description

The C-HH and C-HV airborne SAR amplitude data used in this study were acquired in narrow mode by the Convair 580 aircraft of CCRS on July 10, 1990 (Livingstone *et al.*, 1987; 1988). The detailed characteristics of the SAR systems are described in Section 4.2.1. Differentiation of crops, based on their stage of development, is greatest in mid-July for Oxford County. As a result, it was anticipated that crop separability in the microwave region would be optimum at this time (Foody *et al.*, 1989; Fischer *et al.*, 1992). The incidence angles in the narrow mode of collection ranged from 45 to 76 degrees for the swath width. The study site, however, fell within approximately 15 degrees of the incidence-angle range. As a result, backscatter variation within this range was assumed to be indicative of surface variation, rather than of incidence-angle effects. The spatial resolution of the data was approximately 6 m (Figure 5.1).

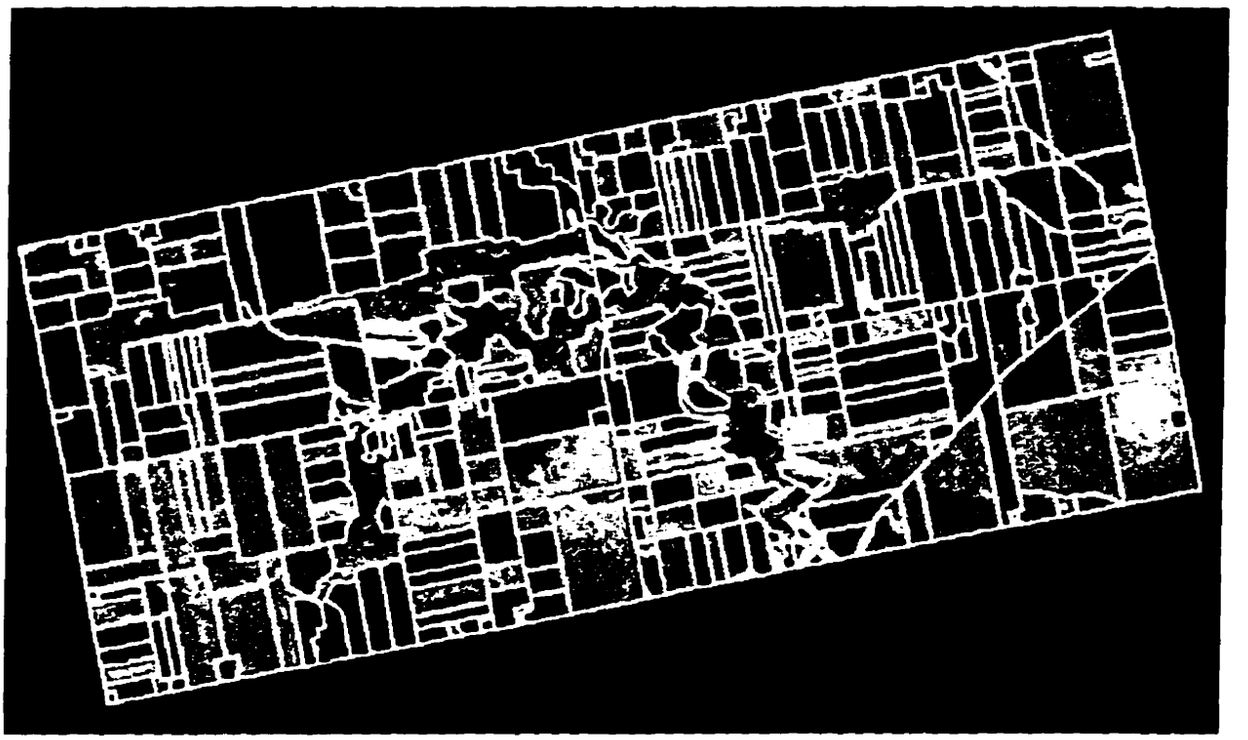

Figure 5.1. Colour composite of C-HH texture (red), C-HV texture (green), and C-HH (blue) for the study area acquired on July 10, 1990

Ground data were collected by field teams during the Oxford County Soil Moisture Experiment (OXSOME) in July, 1990 (Hutton *et al.*, 1990; Brown *et al.*, 1991). The field boundaries were digitized at CCRS from SPOT satellite data acquired during the 1990 growing season. Extensive ground data were collected for agricultural fields and included: crop species, plant maturity, percentage cover, canopy height, row spacing, row direction and plant condition.

5.3 Methodology

Both contextual (filtering) and textural processing techniques are investigated to examine their effects on improving classification accuracy. Per-pixel and per-field classification approaches are tested to determine the most appropriate classification method for agricultural crop identification. The per-field classification method was performed using field-boundary data to define homogeneous areas. Mean and modal values for each field were calculated and used to replace the pixel values in the field. The classifications based on field means, modes and their combinations were performed using a non-parametric classifier. The classification accuracies achieved using the per-pixel and per-field classification approaches, in conjunction with the various processing methods using spatial information, are the emphasis in this study.

5.3.1 Preprocessing

Since the development of image segmentation techniques is not the aim of this study, field boundaries for the study area were extracted from a geographic information system (GIS) and were used to define homogeneous areas. The geocoded (i.e., Universal Transverse Mercator (UTM) coordinates) field-boundary file for the study area was generated using a PAMAP GIS. First, the field-boundary file was converted from a vector format to a raster format with a pixel size of 4 m by 4 m; then a 10-pixel buffer was applied to the field boundaries to eliminate the effects of field boundary pixels and minor image registration errors on crop discrimination. The

file was then imported into the PCI EASI/PACE image processing system, and the C-HH and C-HV images were geometrically corrected to the geocoded field boundaries using a second-order polynomial and a nearest-neighbour resampling algorithm. The accuracy of the geometric corrections was within one pixel.

5.3.2 Contextual Information in Classification

In order to reduce speckle and within-field variability, a 5x5 median filter was applied to the raw C-HH and C-HV data. These images were used to determine the effectiveness of simple filtering on classification accuracy, particularly in conjunction with the field-classification approach.

5.3.3 Texture Information in Classification

A grey-level co-occurrence matrix (GLCM) is a two-dimensional array that can provide conditional joint probabilities of all pairwise combinations of pixels within a computation window (Haralick *et al.*, 1973; Haralick, 1979). The co-occurrence of grey values represents the probability of any two pairs of grey values occurring at a user-defined interpixel sampling distance and orientation. Texture statistics generated from the GLCM represent a single spatial measure of image texture from which the GLCM is computed (Barber and LeDrew, 1991). The mean texture features based on GLCMs were generated using PCI EASI/PACE software (PCI, 1994). The GLCMs used in this analysis consisted of the conditional joint probabilities of neighbouring grey values from the 8-bit SAR image at an interpixel sample distance of 1 and orientation perpendicular to the azimuth/flight direction. An 11x11 moving window was used in the generation of the texture statistics. This window size was found to produce superior results to a 7x7 window (Treitz *et al.*, 1993).

The pixel values of the texture images were 16-bit, so they were scaled to 8-bit values in order to be compatible with other data types for the subsequent image processing. A supervised maximum-likelihood classification of the four crops performed on both the 8-bit and the 16-bit images resulted in similar classification accuracies (i.e., Kappa coefficient ($\hat{K}$) = 0.69), indicating that the information content remained similar after linear scaling. Schmullius *et al.* (1994) also used linear scaling of 16-bit airborne SAR data to 8-bit in their study of variations of radar backscatter over time for agricultural crops in Germany.

5.3.4 Per-Pixel Classification

In order to assess the effectiveness of the per-field classification approach, a comparison with a traditional per-pixel classification was required. For this reason, a number of per-pixel classifications were performed using C-HH and C-HV raw and preprocessed data (e.g., Figures 5.2 to 5.5).

The four major crops classified in this study were winter wheat, corn, soybeans, and alfalfa. For each crop, pixel sample blocks were randomly extracted within representative fields in order to calibrate the classifiers. To assess the accuracy of the classifications, validation pixels, independent from the calibration pixels, were randomly selected for each crop. Fields that exhibited anomalies, such as backscatter that deviated significantly from the norm of a particular class, were excluded from both the calibration and validation samples. These anomalies usually resulted from crop management and/or soil drainage characteristics. Calibration and validation pixels were extracted from different fields, a requirement for the per-field approach where a field was defined as a homogeneous area and all pixels were assigned the value of either the mean or mode. This reduced the number of fields that could be used for calibration and validation, so

Figure 5.2. C-HH image for the study area acquired on July 10, 1990

Figure 5.3. C-HH texture image (using the mean texture statistics of the GLCM)

Figure 5.4. C-HV image for the study area acquired on July 10, 1990

Figure 5.5. C-HV texture image (using the mean texture statistics of the GLCM)

calibration had to be restricted to three winter wheat fields, eight corn fields, five soybean fields and seven alfalfa fields. Other crops in the study area were too few in number or size to be included.

Calibration data were extracted for each of the crops from the imagery and the histograms were examined in order to determine whether a parametric or non-parametric classifier was more suited to the data distribution. The calibration data did not follow a Gaussian distribution, particularly for the texture images, indicating that a non-parametric classifier was better suited. The minimum-distance-to-means (MD) assigns each pixel to the class which has the minimum distance between the pixel value and the class mean. In situations where the maximum-likelihood classifier's (MLC) multivariate normal distribution assumption does not hold, the MD may perform better than the MLC. This is because the MD does not require assumptions. In this study, the MINDIS program in the EASI/PACE software was used (PCI, 1994).

Tests were performed to compare a MD (non-parametric classifier) and a MLC (parametric classifier). The results indicated that the MD classifier performed better under most circumstances (Tables 5.1 and 5.2). In all cases, Kappa coefficients ($\hat{K}$) were higher for the MD classification than for the maximum-likelihood classification. For example, the per-field classification accuracy ($\hat{K}$) for the C-HH texture image increased from 0.81 to 0.91 when using the MD as a post-segmentation classifier as opposed to the maximum-likelihood classifier. For this reason, the MD classifier was used for the remaining analyses.

Table 5.1. Comparison of MD and MLC: Per-Pixel Classifications (%)

Image	Classifier	Winter Wheat	Corn	Soybeans	Alfalfa	Overall	Kappa Coefficient
C-HH	MD	61.10	23.30	22.00	91.20	49.36	0.37
C-HH	*MLC*	*55.40*	*0.00*	*55.90*	*91.20*	*50.63*	*0.35*
C-HV	MD	35.30	56.40	18.00	69.80	45.41	0.33
C-HV	*MLC*	*40.60*	*52.20*	*14.50*	*74.50*	*45.85*	*0.28*
C-HH filtered	MD	89.50	55.30	60.60	100.00	75.51	0.70
C-HH filtered	*MLC*	*89.50*	*21.50*	*75.30*	*99.50*	*69.27*	*0.59*
C-HH texture	MD	99.70	63.90	68.40	100.00	82.26	0.78
C-HH texture	*MLC*	*99.70*	*43.20*	*69.70*	*100.00*	*76.69*	*0.69*

Table 5.2. Comparison MD and MLC: Per-Field Classifications (%)

Image - Segmentation	Classifier	Winter Wheat	Corn	Soybeans	Alfalfa	Overall	Kappa Coefficient
C-HH - mean	MD	100.00	75.00	80.00	100.00	88.20	0.85
C-HH - mean	*MLC*	*100.00*	*58.30*	*80.00*	*100.00*	*83.47*	*0.78*
C-HH - mode	MD	80.50	66.70	100.00	100.00	85.84	0.82
C-HH - mode	*MLC*	*80.50*	*66.70*	*70.00*	*100.00*	*78.75*	*0.72*
C-HV - mean	MD	100.00	100.00	60.00	80.20	85.84	0.83
C-HV - mean	*MLC*	*100.00*	*83.30*	*60.00*	*80.20*	*81.11*	*0.75*
C-HV - mode	MD	100.00	91.70	60.00	100.00	88.20	0.86
C-HV - mode	*MLC*	*100.00*	*91.70*	*60.00*	*100.00*	*88.20*	*0.84*
C-HH texture - mean	MD	100.00	83.30	90.00	100.00	92.92	0.91
C-HH texture - mean	*MLC*	*100.00*	*66.70*	*80.00*	*100.00*	*85.84*	*0.81*
C-HH texture - mode	MD	100.00	75.00	80.00	100.00	88.20	0.85
C-HH texture - mode	*MLC*	*100.00*	*75.00*	*60.00*	*100.00*	*83.47*	*0.78*

5.3.5 Per-Field Classification

Field boundaries permitted segmentation of the C-HH and C-HV data into homogeneous fields using an image-polygon-growing algorithm and homogeneous classifier (PCI, 1994). A unique grey level was assigned as a label to each output polygon of the field-boundary file which was then input to the homogeneous classifier as a theme channel. The homogeneous classifier then defined the homogeneous segments of interest. There were two values that could be assigned to segments, namely the mean and the mode. Both were tested in this study. The pixel values in each field were replaced with mean and modal values for that field. Post-segmentation classifications using the MD were then performed on field means and modes of C-HH and C-HV data.

5.4 Results and Discussion

5.4.1 Per-Pixel Classification

Both single-channel C-HH and C-HV SAR data had poor validation accuracies (Table 5.3). The overall validation accuracy for C-HH SAR data was 49.36% ($\hat{K}$=0.37), while the overall validation accuracy for C-HV was 45.41% ($\hat{K}$=0.33) (Table 5.3). The lower accuracy for C-HV, however, is contrary to what one would expect from the microwave theory and the conclusions drawn by other researchers. According to Holmes (1990), the degree of inhomogeneity of a surface or volume is strongly associated with the cross-polarization scattering coefficient of that surface or volume. The separation of crop types can be enhanced using cross-polarization data. A possible reason for the contradiction is the low signal-to-noise ratio which occurred with the C-HV data.

The application of a 5x5 median filter to the raw data improved classification accuracies significantly for both the C-HH and C-HV images. For example, the validation accuracies of the filtered C-HH and C-HV images increased to 75.51% ($\hat{K}$=0.70) and 64.55% ($\hat{K}$=0.57) respectively (Table 5.3). The C-HH texture image provided the highest validation accuracy of 82.26% (K=0.78) and the C-HV texture image produced a validation accuracy of 74.18% (K=0.68) (Table 5.3). In all cases, the C-HH image provided better validation accuracies than its C-HV equivalent. It is evident that texture statistics are able to improve classification accuracies significantly for mapping agricultural crops. However, texture statistics in combination with a per-pixel classifier did not appear to provide sufficient accuracy for operational mapping of crops in southern Ontario.

Table 5.3. Validation Accuracies (%) for Per-Pixel Classifications

Image	Winter Wheat	Corn	Soybeans	Alfalfa	Overall	Kappa Coefficient
C-HH	61.10	23.30	22.00	91.20	49.36	0.37
C-HV	35.30	56.40	18.00	69.80	45.41	0.33
C-HH filtered	89.50	55.30	60.60	100.00	75.51	0.70
C-HV filtered	70.20	71.40	30.60	84.30	64.55	0.57
C-HH texture	99.70	63.90	68.40	100.00	82.26	0.78
C-HV texture	87.60	79.30	38.10	90.10	74.18	0.68

5.4.2 Per-Field Classification

The per-field validation accuracies for single-channel C-HH, C-HV (mean and mode trials) and their combinations were inconclusive as to whether the mean or the modal value for defining homogeneous areas provided the best classification results. For example, classifications based on the field mean provided a slightly higher accuracy for the C-HH data, whereas the field mode provided a slightly higher accuracy for the C-HV data (Table 5.2). For the majority of trials,

particularly with image combinations, the field mean was used and applied to the post-segmentation classifier.

All per-field classifications improved validation accuracies to varying degrees. The highest per-field classification accuracy ($\hat{K}$=0.91) was achieved in four separate classifications; C-HH texture mean; C-HH filtered + C-HV filtered mean; C-HH texture + C-HV texture mean; and C-HH + C-HV mean (Figure 5.6). This represents more than a 40% increase in validation accuracy over the single-channel C-HH or C-HV per-pixel classifications (Tables 5.3 and 5.4). Among the four highest classification accuracies, three are achieved with the combinations of CHH and C-HV data. This confirms the strong potential of multipolarization data for crop classification.

Table 5.4. Validation Accuracies (%) for Field Classifications

Image - Segmentation	Winter Wheat	Corn	Soybeans	Alfalfa	Overall	Kappa Coefficient
C-HH - mean	100.00	75.00	80.00	100.00	88.20	0.85
C-HH - mode	80.50	66.70	100.00	100.00	85.84	0.82
C-HV - mean	100.00	100.00	60.00	80.20	85.84	0.83
C-HV - mode	100.00	91.70	60.00	100.00	88.20	0.86
C-HH median filter - mean	100.00	66.70	90.00	100.00	88.20	0.85
C-HV median filter - mean	100.00	100.00	60.00	80.20	85.84	0.83
C-HH texture - mean	100.00	83.30	90.00	100.00	92.92	0.91
C-HV texture - mean	100.00	100.00	50.00	80.20	83.47	0.80
C-HH + C-HH filter - mean	100.00	75.00	80.00	100.00	88.20	0.85
C-HH + C-HH texture - mean	100.00	83.30	90.00	100.00	92.92	0.91
C-HV + C-HV filter - mean	100.00	100.00	60.00	80.20	85.84	0.83
C-HV + C-HV texture - mean	100.00	100.00	60.00	80.20	85.84	0.83
C-HH + C-HV - mean	100.00	100.00	70.00	100.00	92.92	0.91
C-HH filter + C-HV filter - mean	100.00	100.00	70.00	100.00	92.92	0.91
C-HH texture + C-HV texture - mean	100.00	100.00	70.00	100.00	92.92	0.91
C-HH - mean + C-HV - mode	100.00	91.70	70.00	100.00	90.56	0.88

The reason these four classifications exhibited similar classification accuracies is due, in part, to the high correlations ($r \geq 0.98$) between these images after segmentation. Crop characteristics analyzed on a per-field basis generally display reduced spectral variance within a crop while leaving the mean relatively unchanged. This provides better classification decision rules for the MD classifier. It must be remembered, however, that these accuracies are artificially high, since in the MD classification there are no unclassified pixels, meaning that all crops within the study area are classified into one of four classes. For example, pasture and oats are grouped into one of the four classes. These assignments are not evident in the validation data. It is desirable, therefore, to develop better measures for the classification accuracy in a per-field classification. In most classifications, wheat and alfalfa are easily separated. The majority of confusion among the four major crops occurred with corn and soybean, due to these two crops possessing similar tones and textures.

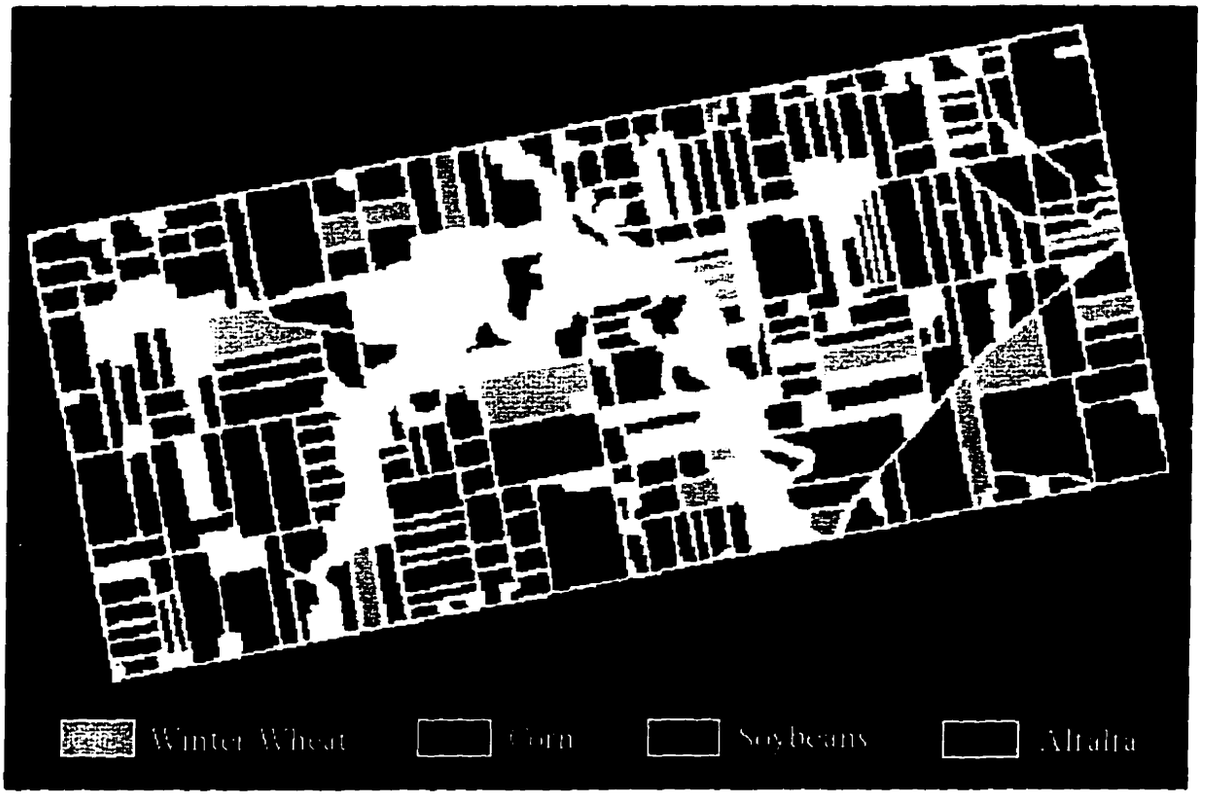

Figure 5.6. Per-field classification results of a C-HH mean and C-HV mean combination

The user must also be aware that some of these processes are more computationally intensive than others and must be applied appropriately. For example, in this study, texture statistics (a very CPU-intensive process) produced 5-10% improvement over simple median filtering. It may be judged that this level of improvement is not justified based on the amount of computer processing required. Alternatively, per-field classification of multiple polarizations provide classification accuracies similar to those which include texture features and are therefore a viable alternative to calculating texture features.

5.5 Summary

Operational methodologies for improving agricultural crop identification have been tested using C-HH and C-HV airborne SAR data collected on July 10, 1990. Raw SAR data, filtered SAR data and SAR texture statistics were classified using per-pixel and per-field classification approaches to determine their effectiveness for agricultural crop classification. The approaches presented for improving agricultural crop classification proved to be effective, especially the per-field classification method. Results indicate that C-HH and C-HV data, classified using a standard per-pixel MD classifier, provide relatively poor classification accuracies. Inclusion of texture statistics in the per-pixel classification improves accuracies by approximately 30% and simple median filtering boosts accuracies by approximately 25%. However, using a per-field classifier, the classification accuracies improve by about 40%.

Multipolarization SAR data were also evaluated for crop classification. Results indicated that C-HV SAR data yielded lower overall classification accuracy (45.41%) than C-HH SAR data (49.36%). The lower accuracy for C-HV is contradicting conclusions put forward by other researchers. A possible reason for the contradiction is the low signal-to-noise ratio with C-HV data. It was also found that three of the four best per-field classification accuracies ($\hat{K}$=0.91) were achieved using combinations of C-HH and C-VV SAR data. This confirms the strong potential of multipolarization data for crop classification.

CHAPTER 6: INTEGRATION OF SATELLITE SAR AND VIR DATA FOR CROP CLASSIFICATION

6.1 Introduction

The synergistic effects of SAR data and imagery acquired in the visible and infrared (VIR) portions of the spectrum have been recognized as important for two main reasons. First, timeliness of SAR fills information gaps during overcast or hazy periods at the critical stages of the growing season, and second, the combination of data from different parts of the spectrum often leads to increased classification accuracy. Previous studies have shown that combining airborne SAR and satellite VIR data improves crop classification accuracies (Brown *et al.*, 1984; Guindon *et al.*, 1984; Hirose *et al.*, 1984; Brisco *et al.*, 1989a; Fiumara and Pierdicca, 1989; Dixon and Mack, 1990; Brisco and Brown, 1995). Very little research, however, has been done to improve crop classification accuracies using data from two satellite sensors (Fog *et al.*, 1993; Kohl *et al.*, 1993). Thus, the potential of satellite SAR and VIR synergism still needs further investigation.

Conventional statistical classifiers, such as the maximum-likelihood classifier (MLC), make a number of untenable assumptions about the dataset to be classified (Foody *et al.*, 1995). For example, this parametric approach requires data to have a Gaussian distribution. SAR data, however, are not normally distributed due to speckle. Therefore, the accuracies of SAR crop classification using conventional statistical classifiers are often not sufficiently high for crop inventory and analysis. In order to improve classification accuracy, it is necessary to explore robust classifiers using non-parametric and non-statistical approaches.

The artificial neural network (ANN) classifier presents a distribution-free approach to image classification. It also has the special advantages of simple local computations and parallel

processing (Schalkoff, 1992). In the past few years, studies have shown that neural networks compare well to statistical classification methods in the classification of multidate, multisource remote sensing/geographic data, very high dimensional data, and when classification is done with a large number of classes (e.g., Benediktsson *et al.*, 1990a; 1990b; Kanellopoulos *et al*, 1991; Paola and Schowengerdt, 1995). When applied to airborne SAR data, it was found that for the classification of agricultural crops ANN algorithms produced higher classification accuracies in general than those derived from statistical classifiers (Foody *et al.*, 1994; 1995). Therefore, it is desirable to investigate the effectiveness of ANN algorithms for crop classifications using satellite SAR and VIR data.

The objective of this chapter is to evaluate the synergy of multitemporal ERS-1 SAR and Landsat TM data for crop classification using an artificial neural network approach. The specific objectives are:

- to evaluate early- and mid-season crop classification accuracies using a single-date SAR image alone and also using multitemporal SAR data,
- to evaluate the synergism of multitemporal ERS-1 SAR and Landsat TM data for improving crop classification, and
- to evaluate an ANN algorithm as a post-segmentation classifier in comparison to the conventional maximum-likelihood classifier.

6.2 Data Description

Three dates of early- and mid-season ERS-1 C-VV SAR data were acquired during the 1992 growing season (June 15, July 24 and August 5). The July 24 SAR image was acquired in ascending mode, while the others were recorded in descending mode. One date of Landsat TM data was also acquired on August 6, 1992. The ERS-1 SAR and Landsat TM images are shown in Figure 6.1 and 6.2. The charateristics of the data are described in Chapters 2 and 3.

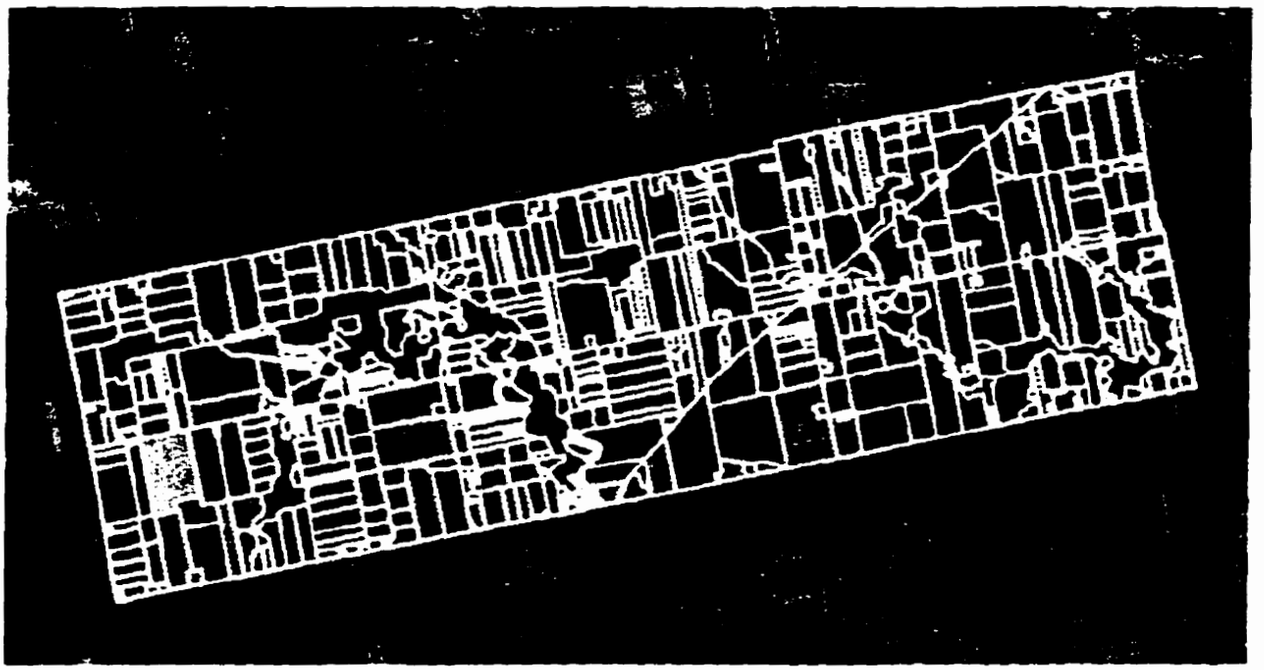

Figure 6.1. Landsat TM imagery of the study area acquired on August 6, 1992
Red:TM4, Green:TM5, and Blue:TM3

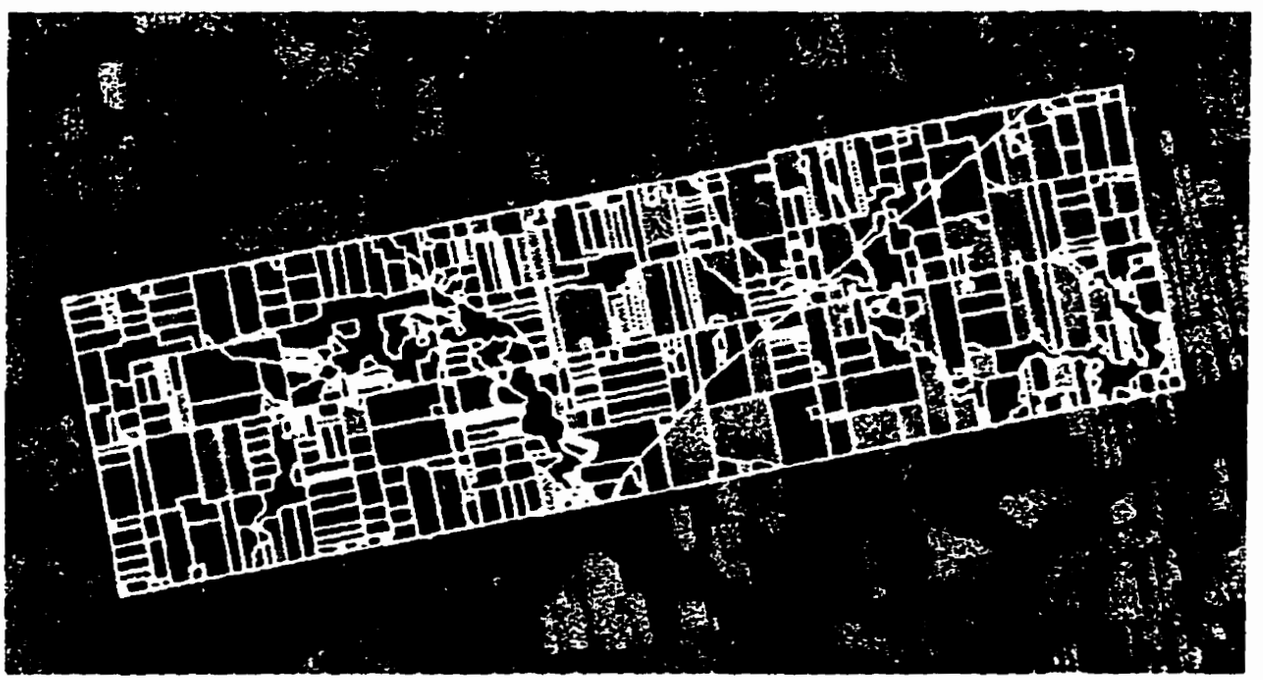

Figure 6.2. Multitemporal ERS-1 SAR imagery of the study area, acquired during the 1992 growing season - Red:August 5, Green:July 24, and Blue:June 15

Detailed field information was collected at the time of the overpasses and was input to a geographic information system (GIS) to aid in developing and understanding the classifications.

6.3 Methodology

In the analyses presented in this chapter, single-date SAR data, multitemporal SAR data, and combinations of SAR and TM data are classified. In all cases, a per-field classification approach is adopted since this conforms to conventional mapping strategies and has been widely used in radar remote sensing as a means of reducing the effect of speckle (Foody *et al.*, 1994; Ban *et al.*, 1995). The ANN classifier is used in post-segmentation classifications. Also, per-pixel classifications using the MLC are performed for comparison purposes.

6.3.1 Preprocessing

The raw-signal SAR data were processed by the Atlantis Processor at the Canada Centre for Remote Sensing and were geometrically corrected to the 1992 field boundaries (Universal Transverse Mercator -UTM projection) to a sub-pixel accuracy. The geocoded field-boundary file for the study area was digitized from a SPOT image in a PAMAP GIS and was then imported into a PCI EASI/PACE image processing system. To eliminate the effects of field-boundary pixels and minor image registration errors on crop discrimination, a 5-pixel buffer was applied to the field boundaries. This procedure is similar to the one described in Chapter 5.

6.3.2 Selection of Calibration and Validation Blocks

The major crops classified in this study were winter wheat, corn, soybeans, barley/oats, alfalfa and pasture/cut-hay/cut-alfalfa. Due to the differences in growing stages and ground-cover density, corn and soybeans were further divided into two classes: good growth and poor growth.

For each crop, pixel sample blocks were randomly extracted within representative fields in order to calibrate the maximum-likelihood classifier and to train the artificial neural network.

To assess the accuracy of the classifications, validation pixels, independent from the calibration pixels, were randomly selected for each crop. Fields that exhibited anomalies, such as spectral reflectance/backscatter that deviated significantly from the norm of a particular class, were excluded from both the calibration and validation samples. These anomalies usually resulted from weed infestations, crop management and/or soil-drainage characteristics. The calibration and validation block selections were based on the crop information; i.e., crop type, crop growth stage, ground cover, height, row direction, etc. These data were stored in a PAMAP GIS.

Calibration and validation pixels were extracted from different fields, a requirement for the per-field approach where a field is defined as a homogeneous area and all pixels are assigned the mean value of the field. This reduced the number of fields that could be used for calibration and validation, so calibration had to be restricted to fewer fields than preferable.

6.3.3 Per-Pixel Classification

In order to assess the effectiveness of the non-parametric and non-statistical approaches, a comparison with the results of an MLC was required. A number of classifications for SAR, TM and their combinations were performed using the MLC.

6.3.4 Per-Field Classification

In Canada, a field only grows a single crop. Thus, it is desirable to use a per-field classification. Also a per-field approach reduces the SAR speckle effects, as discussed earlier.

6.3.4.1 Segmentation

A per-field classifier permits segmentation of the ERS-1 SAR image into homogeneous fields using field boundaries. A unique grey level was assigned as a label to each output polygon of the field-boundary file which was then input to the homogeneous classifier as a theme channel. The homogeneous classifier defined the homogeneous segments of interest. There were two values that could be assigned to segments, namely the mean and the mode. Only the mean was tested in this study. The pixel values in each field were replaced with the mean value for that field.

6.3.4.2 Post-segmentation Classification

A post-segmentation classifier, an ANN, was investigated. An artificial neural network consists of interconnected processing elements called units ("nodes" or "neurons"). These are organized in two or more layers. There is an input layer of units which is activated by the input image data. The output layer of units represents the output classes to train for. In between, there is usually one or more hidden layers of units (PCI, 1994; Paola and Schowengerdt, 1995; Foody, 1996). A feed-forward neural network structure is shown in Figure 6.3. A specific artificial neuron computational structure is shown in Figure 6.4.

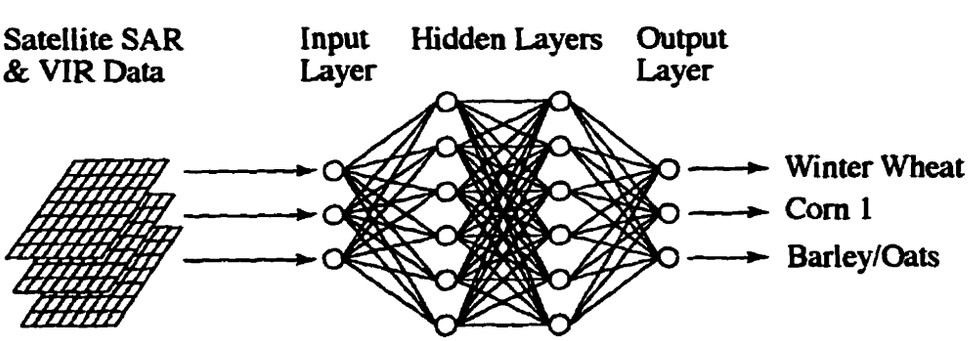

Figure 6.3. A feed-forward Artificial Neural Network structure (Foody, 1996)

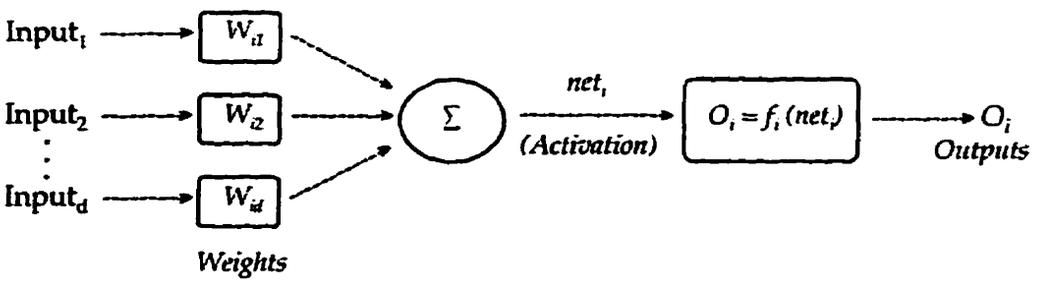

Figure 6.4. A specific artificial neuron computational structure, where

$$net_i = \sum_j W_{ij} O_{ij},\ O_i = f(net_i) = \frac{1}{1 + e^{-\lambda net_i}}$$ (Schalkoff, 1992)

The programs use a back-propagation network that learns using the Generalized Delta Rule:

$$\Delta W_{jk} = \eta\ \delta_k\ O_j + \alpha\ \Delta\ W_{jk}$$

where η = learning rate, α = momentum, δ_k = error at the kth-layer, O_j is the output of layer j, and W_{jk} is the connection weight between the jth-layer node and the kth-layer node (Li and Si, 1992).

The back-propagation learning algorithm has been widely used in pattern recognition applications of artificial neural networks. The term "back-propagation" refers to the training method by which the connection weights of the network are adjusted. It iteratively minimizes an error function over the network outputs and a set of target outputs, taken from a training data set. The process continues until the error value converges to a (possibly local) minimum. The error function is given as:

$$E = 1/2 \sum_i (T_i - O_i)^2$$

where T_i is the target output vector for the training set (T_1, ..., T_n) and O_i is the output vector from the network for the given training set. On each iteration, back-propagation recursively computes the gradient or change in error with respect to each weight in the network, $\partial E/\partial W$, and these values are used to modify weights. Adding a fraction of the negative gradient to each

weight is equivalent to performing a steepest-descent minimization of the error function with respect to each weight in the network (Foody, 1996).

The training of the network is similar to any supervised classification procedure i.e., calibration blocks have to be selected and used to adapt the classifier. In this case, network weights were adapted. The back-propagation learning procedure is shown in Figure 6.5 (Schalkoff, 1992).

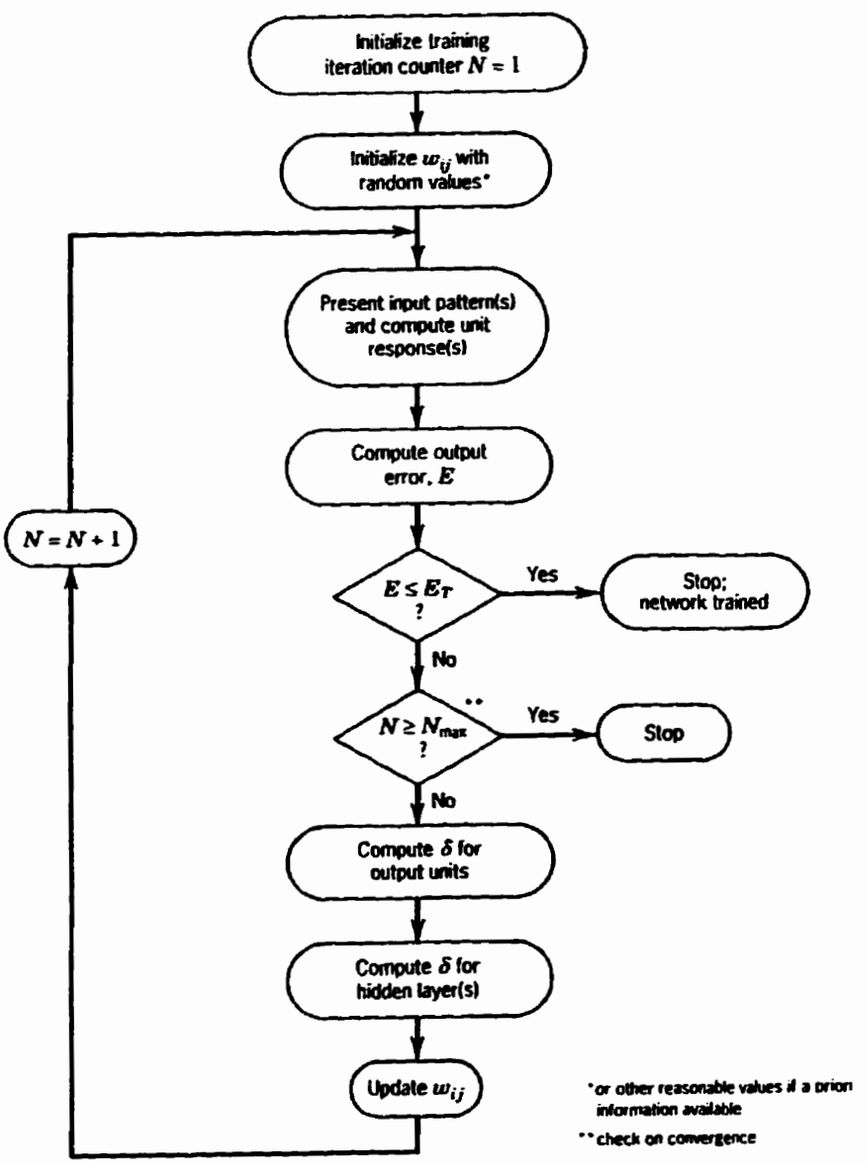

Figure 6.5. A summary of the back-propagation learning procedure (Schalkoff, 1992)

In this study, EASI/PACE software NNCREAT, NNTRAIN and NNCLASS (PCI, 1994) were used to evaluate a multilayer feed-forward neural network using back-propagation.

6.4 Results and Discussion

6.4.1 Per-Pixel Classification

Although three-date SAR combination displayed a 4% improvement for classification accuracy over the best single-date classification alone, the overall validation accuracies for both single-date SAR and multitemporal SAR were very low (see Table 6.1). The first reason for the poor accuracies is that the MLC is not an effective classifier for SAR data classifications, due to speckle. The second reason for the poor performances is that the single-parameter, high incidence angle ERS-1 SAR system does not provide sufficient differences for eight crop classes. Satellite SAR systems with multi-incidence angle, multiresolution, multiwavelength, and multipolarization, such as the Canadian RADARSAT, are very desirable to improve the performance of satellite SAR data for crop classification. The third reason for the poor accuracies is that the calibration and validation blocks were selected based on the August 5 field data, but the change of crop cover over the growing season can cause confusion. For example, an alfalfa class in June was shown as a pasture/cut-hay/cut-alfalfa class in August.

Landsat TM3,4,5 alone produced an 89.8% classification accuracy (Table 6.1). Combinations of SAR and TM data improved the classification accuracies in general. The best overall accuracy (91.85%) was for the combination of all three dates of SAR and TM3,4,5 imagery. This represents a 2% increase over the TM3,4,5 classification alone.

Table 6.1. MLC Classifications for SAR, TM Data and their Combinations

SAR, June 15	SAR, July 24	SAR, Aug. 5	TM345, Aug. 6	Overall Accuracy (%)	Kappa Coefficient
x				30.32	0.07
	x			28.75	0.18
		x		33.68	0.09
x	x	x		37.66	0.28
			x	89.81	0.88
x			x	90.30	0.89
	x		x	91.40	0.90
x	x	x	x	91.85	0.91

6.4.2 Per-Field Classification

Per-field classification with an ANN proved to be very effective. The best single-date (Aug. 5) SAR classification using per-field ANN improved the overall accuracy by about 26% compared to that of the per-pixel classification (Tables 6.1 and 6.2). The crop classification accuracies improved by almost 20% using the combination of June, July and August SAR data (Tables 6.1 and 6.2) Although these overall classification accuracies (<60%) are not sufficiently high for operational crop inventory and analysis, both single-date and multitemporal SAR data have demonstrated their abilities to discriminate certain crops in the early- and mid-season. For instance, winter wheat, poor-growth corn and alfalfa could be differentiated perfectly from others using the combination of the three-date SAR (Table 6.3).

The best per-field classification of 96.8% with an ANN classifier was achieved using the combination of TM3,4,5 and Aug. 5 SAR data (Table 6.2, Figure 6.6). It represents an 8.5% improvement over a single TM3,4,5 classification alone. It also represents a 5% increase over

the best per-pixel classification. In this classification, accuracies of 100% were achieved for all crops except the alfalfa and pasture/cut-hay/cut-alfalfa classes (Table 6.4). Alfalfa had a 16.3% commission error to the first corn class (i.e., good growth), and pasture/cut-hay/cut-alfalfa had a 15.1% commission error with the second class of soybeans (i.e., poor growth). The second-best classification accuracy of 95.9% was achieved using the combination of TM3,4,5 and the July 24 SAR image (Table 6.2). These results indicate that a combination of mid-season SAR and VIR data is very well suited for crop classification. The success of this combination may have been because the ground conditions were similar since the SAR data and TM data were acquired only one day or a few days apart.

All classification accuracies improved using the per-field ANN except that of TM3,4,5 (Tables 6.1 and 6.2). This is possibly because the neural network for the second corn class (i.e., poor growth) was not well trained. It resulted in poor accuracy for the second corn class (only 25.9%) with a commission error to the barley/oat class of 62.1%, while all other classes were 100% correctly classified (Table 6.5).

Table 6.2. ANN Per-Field Classifications for SAR, TM Data and their Combinations

SAR, June 15 Mean	SAR, July 24 Mean	SAR, Aug. 5 Mean	TM345, Aug. 6 Mean	Overall Accuracy (%)	Kappa Coefficient
	x			41.66	0.30
		x		59.94	0.46
x	x	x		57.24	0.51
			x	88.48	0.87
x			x	88.08	0.86
	x		x	95.92	0.95
		x	x	96.81	0.96
x	x		x	93.62	0.93
x	x	x	x	93.89	0.93

Table 6.3. ANN Per-Field Classification for the Combinations of the Three-Date SAR (%)

	Winter Wheat	Corn 1	Corn 2	Soybeans 1	Soybeans 2	Alfalfa	Pasture/ cut-hay-alf	Barley/ Oats
W. Wheat	*100.0*	0.0	0.0	0.0	0.0	0.0	0.0	0.0
Corn 1	13.2	*60.4*	26.4	0.0	0.0	0.0	0.0	0.0
Corn 2	0.0	0.0	*100.0*	0.0	0.0	0.0	0.0	62.1
Soybeans 1	16.1	32.2	7.6	*44.1*	0.0	0.0	0.0	0.0
Soybeans 2	0.0	58.5	0.0	0.0	*41.5*	0.0	0.0	0.0
Alfalfa	0.0	0.0	0.0	0.0	0.0	*100.0*	0.0	0.0
P/cut-hay-alf	0.0	0.0	0.0	61.8	0.0	27.7	*0.0*	10.5
Barley/Oats	0.0	0.0	0.0	0.0	0.0	86.8	0.0	*0.0*

Table 6.4. ANN Per-Field Classification for the Combination of TM3,4,5 and Aug. 5 SAR Data (%)

	Winter Wheat	Corn 1	Corn 2	Soybeans 1	Soybeans 2	Alfalfa	Pasture/ cut-hay-alf	Barley/ Oats
W. Wheat	*100.0*	0.0	0.0	0.0	0.0	0.0	0.0	0.0
Corn 1	0.0	*100.0*	0.0	0.0	0.0	0.0	0.0	0.0
Corn 2	0.0	0.0	*100.0*	0.0	0.0	0.0	0.0	0.0
Soybeans 1	0.0	0.0	0.0	*100.0*	0.0	0.0	0.0	0.0
Soybeans 2	0.0	0.0	0.0	0.0	*100.0*	0.0	0.0	0.0
Alfalfa	0.0	16.3	0.0	0.0	0.0	*83.7*	0.0	0.0
P/cut-hay-alf	0.0	0.0	0.0	0.0	15.1	0.0	*84.9*	0.0
Barley/Oats	0.0	0.0	0.0	0.0	0.0	0.0	0.0	*100.0*

Table 6.5. ANN Per-Field Classification for TM3,4,5 (%)

	Winter Wheat	Corn 1	Corn 2	Soybeans 1	Soybeans 2	Alfalfa	Pasture/ cut-hay-alf	Barley/ Oats
W. Wheat	*100.0*	0.0	0.0	0.0	0.0	0.0	0.0	0.0
Corn 1	0.0	*100.0*	0.0	0.0	0.0	0.0	0.0	0.0
Corn 2	0.0	12.0	*25.9*	0.0	0.0	0.0	0.0	62.1
Soybeans 1	0.0	0.0	0.0	*100.0*	0.0	0.0	0.0	0.0
Soybeans 2	0.0	0.0	0.0	0.0	*100.0*	0.0	0.0	0.0
Alfalfa	0.0	0.0	0.0	0.0	0.0	*100.0*	0.0	0.0
P/cut-hay-alf	0.0	0.0	0.0	0.0	0.0	0.0	*100.0*	0.0
Barley/Oats	0.0	0.0	0.0	0.0	0.0	0.0	0.0	*100.0*

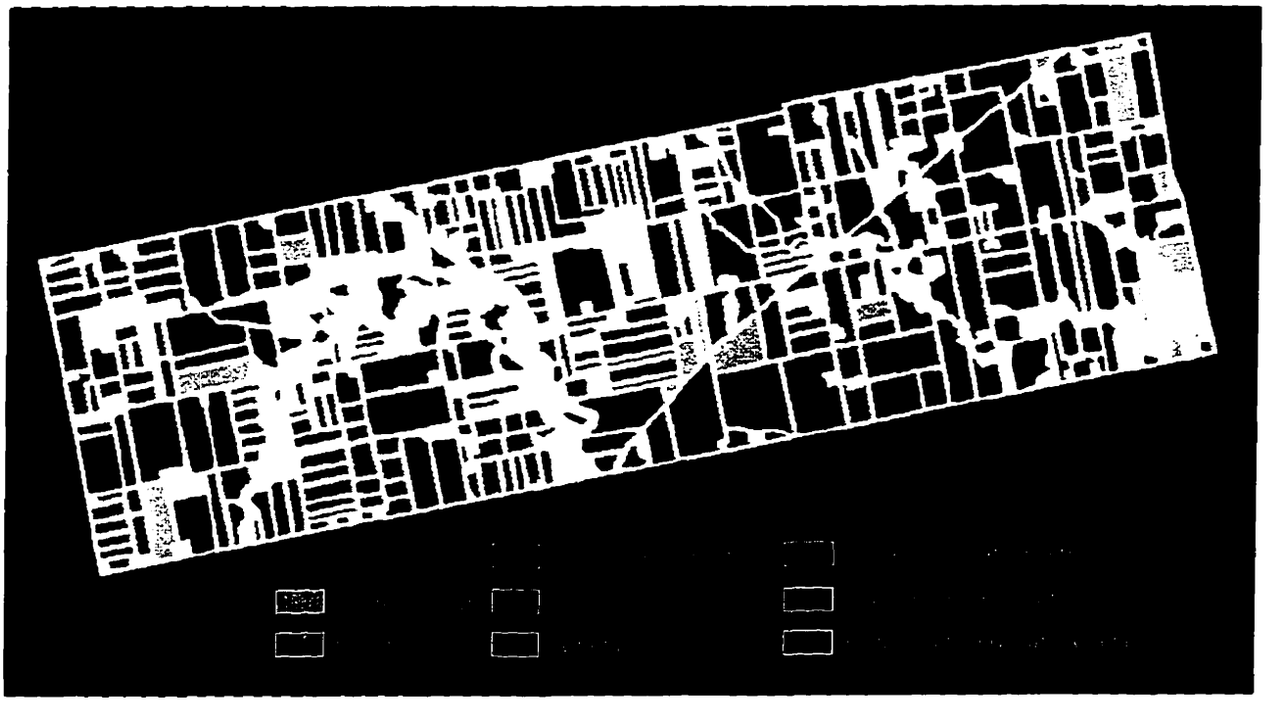

Figure 6.6. ANN per-field classification for the combination of ERS-1 SAR (Aug. 5) and TM3,4,5 (Aug. 6) data

6.5 Summary

The synergistic effects of multitemporal ERS-1 SAR and Landsat TM data were evaluated for crop classification using an artificial neural network (ANN) approach. Eight crop types and conditions were identified: winter wheat, corn (good growth), corn (poor growth), soybeans (good growth), soybeans (poor growth), barley/oats, alfalfa, and pasture/cut-hay/cut-alfalfa. The results show that both single-date and multitemporal SAR data yielded poor classification accuracies using a maximum-likelihood classifier (MLC). With the per-field approach using a feed-forward artificial neural network, the overall classification accuracy of three-date SAR data improved almost 20%, and the best classification of a single-date (Aug. 5) SAR image improved the overall accuracy by about 26%. Although these overall classification accuracies (<60%) were not sufficiently high for operational crop inventory and analysis, both single-date and multitemporal SAR data demonstrated their abilities to discriminate certain crops in the early- and mid-season. Using the combination of TM3,4,5 and Aug. 5 SAR data, the best per-field ANN classification of 96.8% was achieved. It represents an 8.5% improvement over a single TM3,4,5 classification alone. This indicates that a combination of mid-season SAR and VIR data is very well suited for crop classification.

CHAPTER 7: ERS-1 SAR FOR CROP IDENTIFICATION: A MULTITEMPORAL APPROACH

7.1 Introduction

Past studies have demonstrated that multitemporal SAR data can enhance the ability to distinguish between crop spectral patterns (e.g., Brisco *et al.*, 1984; Brown *et al.*, 1984; Fischer and Mussakowski, 1989; Foody *et al.*, 1989; Dobbins *et al.*, 1992; see Section 3.4.2 in Chapter 3 for the detailed review). However, comparatively few datasets have been available for study because of the increased cost and logistics of generating multitemporal SAR data with airborne platforms (Brisco *et al.*, 1992). With the launch of the European Remote Sensing Satellite (ERS-1), the first long-duration spaceborne imaging SAR system became available to provide researchers with an excellent opportunity for developing agricultural applications of remote sensing data using multitemporal SAR imagery (e.g., Brown *et al.*, 1993a; Kurosu *et al.*, 1993; Wooding *et al.*, 1993; Borgeaud *et al.*, 1994).

The objectives of this study are to understand and analyze the multitemporal radar backscatter characteristics of crops and their underlying soils over the growing season and to determine the earliest time of the year for differentiation of individual crop types. The specific objectives are: 1. to generate ERS-1 SAR temporal backscatter profiles for each crop type; to identify fields displaying anomalous radar backscatter characteristics, statistically describe the anomalous fields, and discuss reasons for those anomalies; and 2. to evaluate early- and mid-season multitemporal SAR data for crop classification using sequential masking techniques.

7.2 Data Description

The ERS-1 C-Band (5.3 GHz) VV polarization SAR data used in this study were acquired on six dates during the growing season in 1992 and on nine dates during the 1993 growing season.

Except for July 24, 1992, all data were acquired during two descending passes (Figures 7.1, 7.2, 7.3, 7.4, 7.5 and 7.6; Table 7.1). The 1992 images were received and processed at the Gatineau Receiving Station in Canada, while the 1993 data were processed and fully calibrated at D-PAF, Germany. The detailed characteristics of the ERS-1 SAR data are described in Chapter 4.

Ground data were collected by field teams during the ERS-1 Soil Moisture Experiment (ERSOME) in the 1992 and 1993 growing seasons (Gardell *et al.*, 1993). The 1992 field boundaries were digitized from a SPOT satellite image at CCRS and were updated at the University of Waterloo using a 1993 SPOT image. Extensive ground data were collected for agricultural fields and included crop type, growth stage, percentage cover, canopy height, row spacing, row direction and plant condition.

Table 7.1 Fifteen Dates of ERS-1 Data

Date	Orbit	Mode
May 27, 1992	2	Descending
June 15, 1992	1	Descending
July 24, 1992	?	Ascending
Aug. 5, 1992	2	Descending
Sept. 28, 1992	1	Descending
Oct. 14, 1992	2	Descending
May 31, 1993	2	Descending
June 16, 1993	1	Descending
July 5, 1993	2	Descending
July 21, 1993	1	Descending
Aug. 9, 1993	2	Descending
Aug. 25, 1993	1	Descending
Sept. 13, 1993	2	Descending
Sept. 29, 1993	1	Descending
Oct. 18, 1993	2	Descending

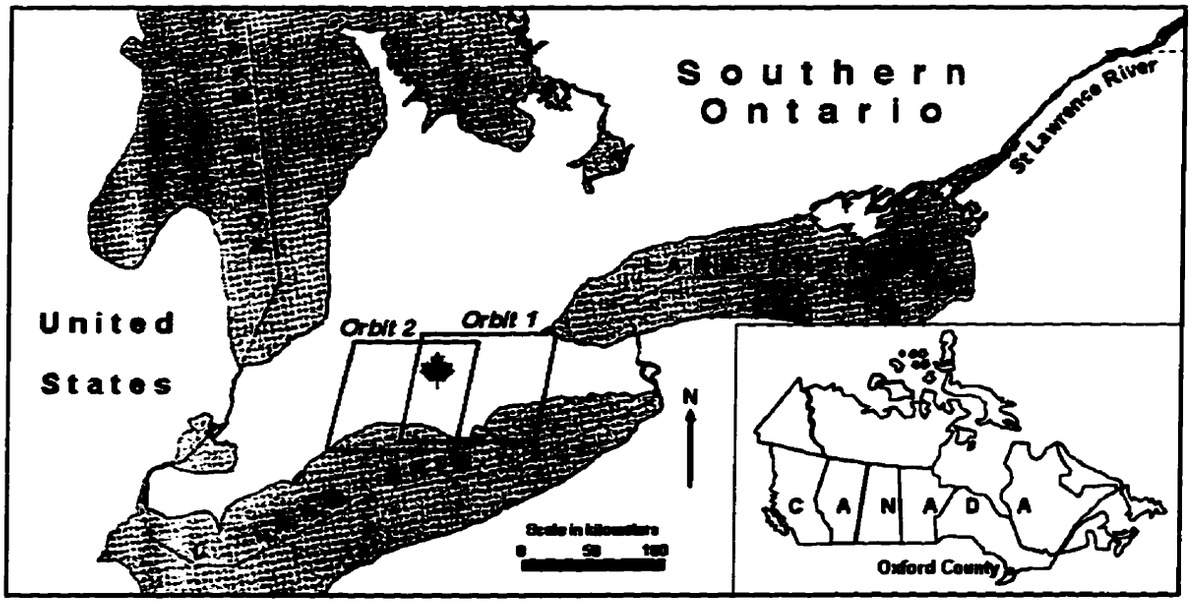

Figure 7.1. ERS-1 satellite orbits of the study area

Figure 7.2. Multitemporal ERS-1 SAR imagery of the study area, acquired during the 1992 growing season - Red: July 24, Green: June 15, and Blue: May 27

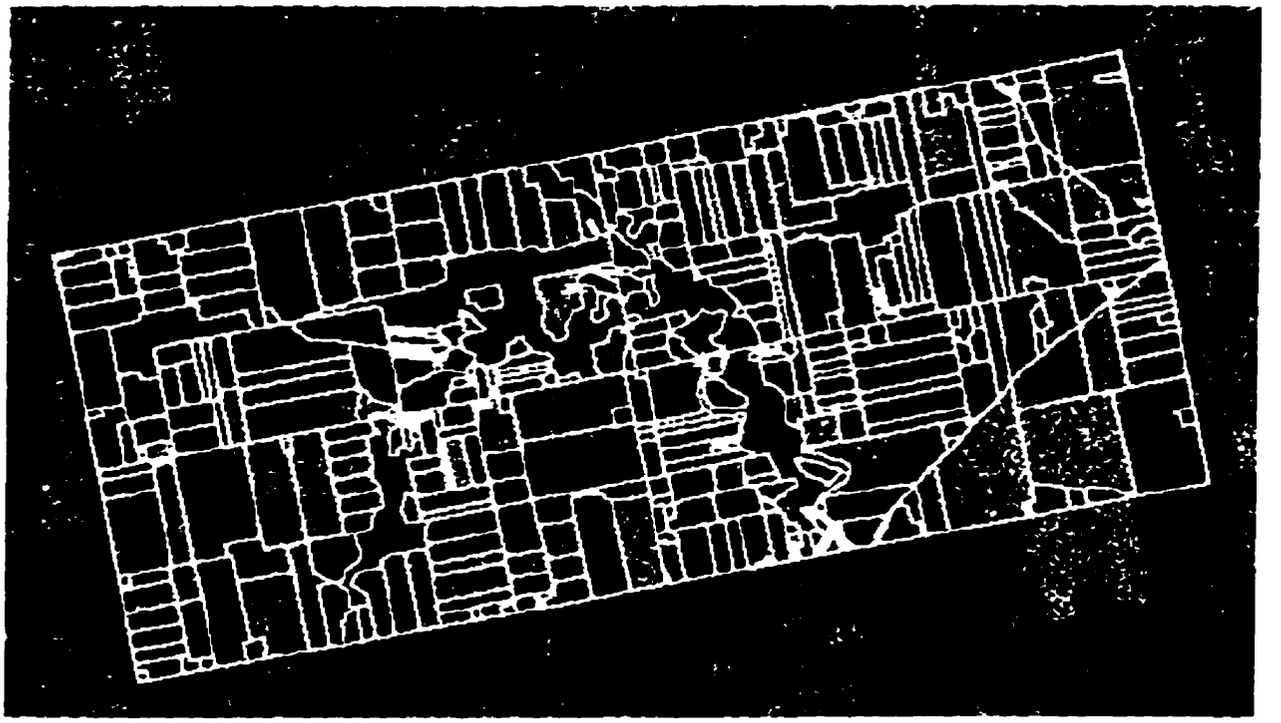

Figure 7.3. Multitemporal ERS-1 SAR imagery of the study area, acquired during the 1992 growing season - Red: Oct. 14, Green: Sept. 28, and Blue: Aug. 5

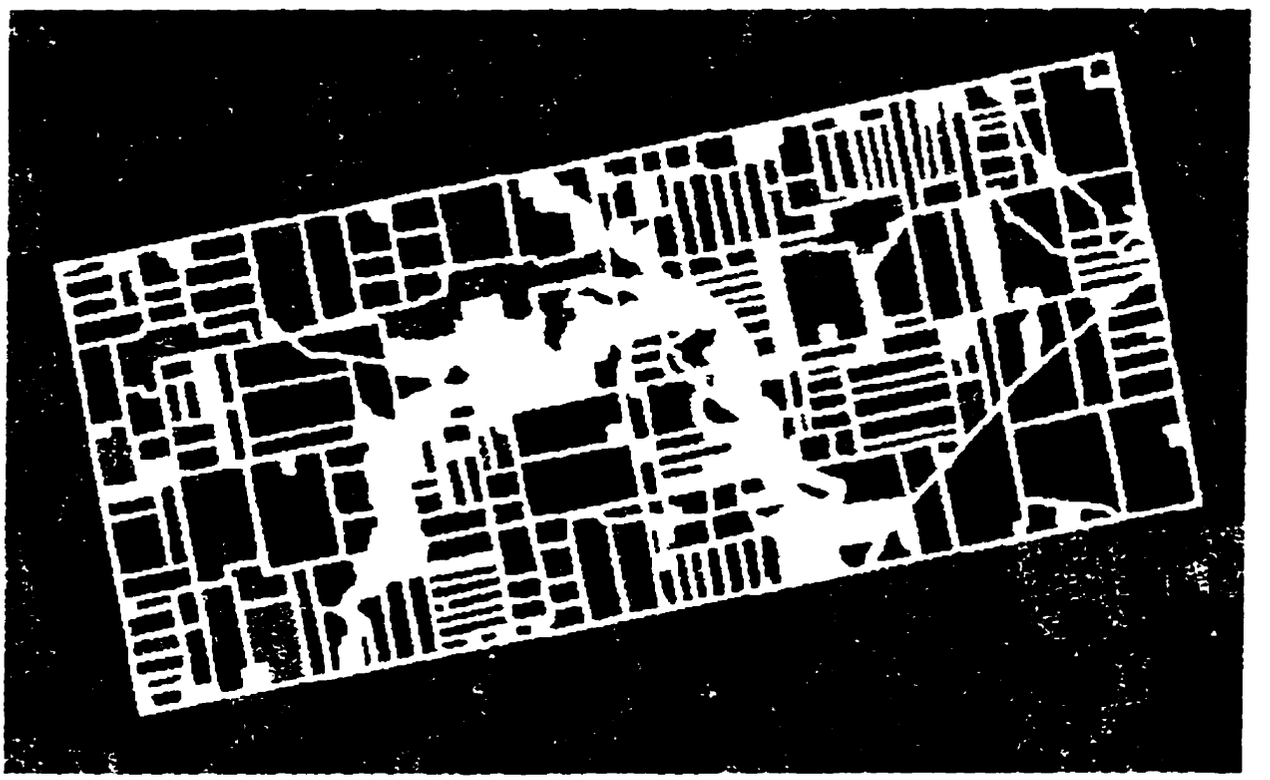

Figure 7.4. Multitemporal ERS-1 SAR imagery of the study area, acquired during the 1993 growing season - Red: July 5, Green: June 16, and Blue: May 31

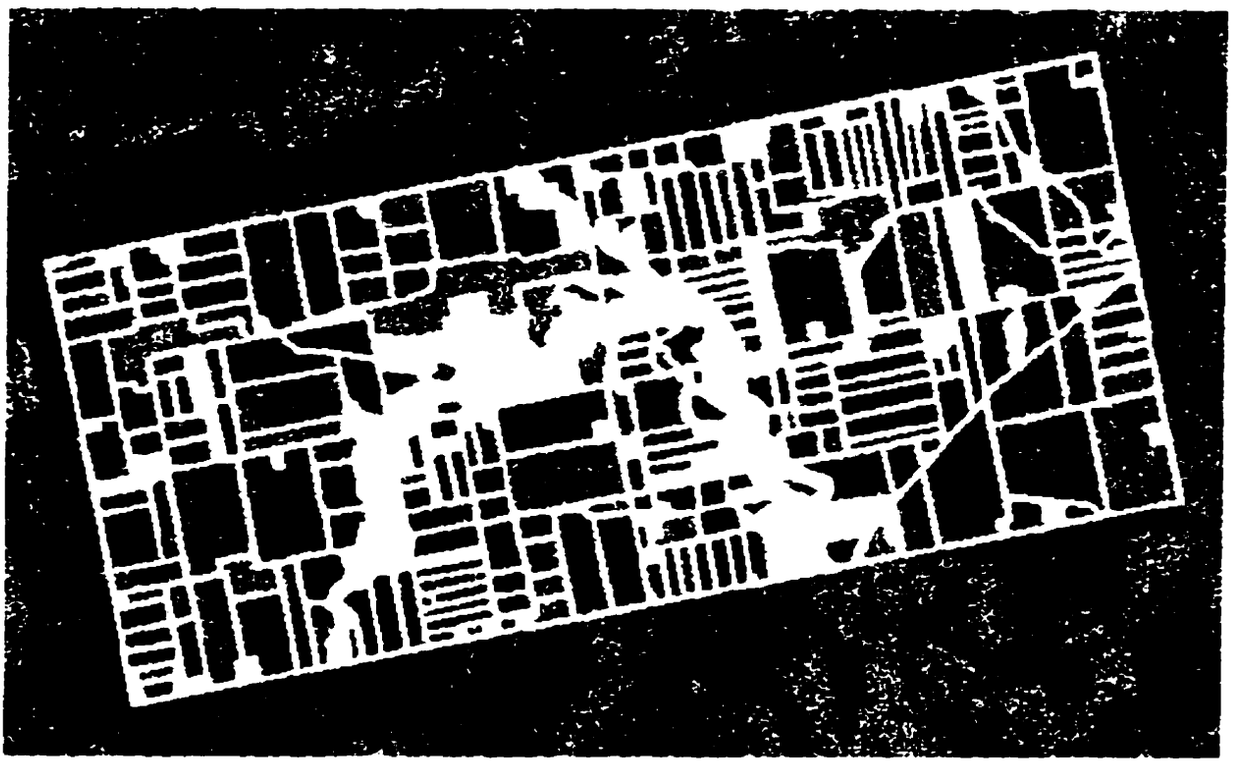

Figure 7.5. Multitemporal ERS-1 SAR imagery of the study area, acquired during the 1993 growing season - Red: Aug. 25, Green: Aug. 9, and Blue: July 21

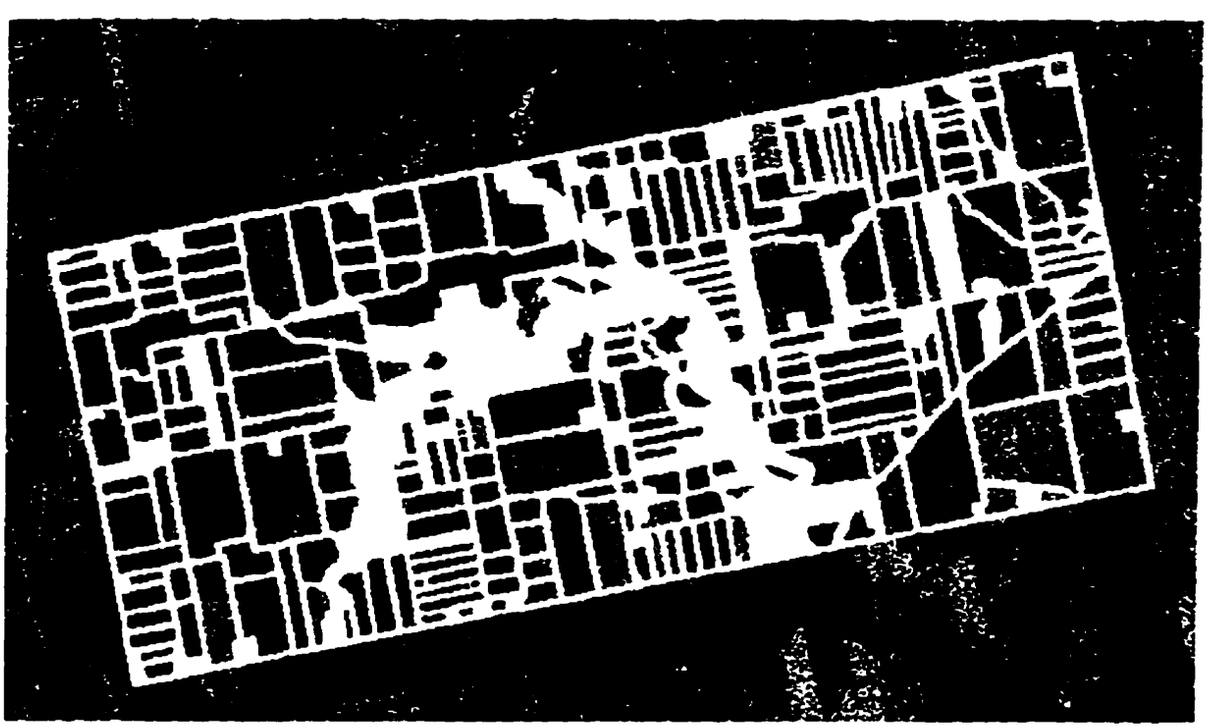

Figure 7.6. Multitemporal ERS-1 SAR imagery of the study area, acquired during the 1993 growing season - Red: Oct. 18, Green: Sept. 29, and Blue: Sept. 13

7.3 Methodology

7.3.1 Field-Boundary Preparation

Since the development of image segmentation techniques is not the aim of this study, field boundaries for the study area were extracted from a geographic information system (GIS). The geocoded field-boundary file for the study area was generated using a PAMAP GIS. The file was then imported into the PCI EASI/PACE image processing system. To eliminate the effects of field-boundary pixels and minor image registration errors on crop discrimination, a 5-pixel buffer was applied to the field boundaries. This procedure is similar to the one described in Chapter 5.

7.3.2 SAR Data Radiometric Calibration And Geometric Correction

Quantitative comparisons of the multitemporal SAR data require calibrated images. The ERS-1 SAR calibration principles and procedures are described in Chapter 4. For the 1992 data, the effects of the illumination antenna were removed, but range-spreading loss was not compensated (Noetix Research Inc., 1993). The accuracy for this calibration was conservatively estimated at $\pm$ 2 dB (Livingstone *et al.*, 1992; Brown *et al.*, 1993a). The 1993 data were radiometrically calibrated, i.e., corrected for the SAR antenna pattern and compensated for range-spreading loss. The calibration accuracy is $\pm$ 0.42 dB (Laur *et al.*, 1993).

The SAR images were then geometrically corrected to field boundaries (Universal Transverse Mercator - UTM projection) with a 12.5 m pixel spacing using a second-order polynomial and a nearest-neighbour resampling algorithm.

7.3.3 Derivation of the Radar Backscatter Coefficient σ°

The generation of ERS-1 SAR temporal backscatter profiles of agricultural crops requires relating pixel digital numbers (DN) on SAR images to backscatter coefficients of corresponding distributed targets in the scene. The detailed methodology for deriving backscatter coefficients in ERS-1 SAR PRI products is described in Chapter 4.

Using both 1992 and 1993 field-boundary files, radar backscatter characteristics for each field were analyzed for each date using PCI EASI/PACE. First, the DN values on each image were converted to power (amplitude squared), then the mean backscatter of each field (> 500 pixels) was calculated in the power domain and imported to EXCEL. For 1993 data, the local incidence angles of the study area for each scene were calculated using the central pixel numbers of the study area from the near range. Then the local estimate $K(\alpha)$ of the calibration constants was determined using Equation 4.7. Finally, the σ° (dB) of each field for both 1992 and 1993 data was derived using Equation 4.10.

7.3.4 Temporal Backscatter Profile Generation

SAR temporal backscatter profiles for both the 1992 and the 1993 growing season were generated in EXCEL for major crop types (i.e., corn, soybeans, winter wheat, barley/oats, alfalfa and pasture). First, the temporal backscatter profile for each individual field was generated; then the general temporal backscatter profile for each crop was generated by averaging the σ° of all fields for that crop on each date.

7.3.5 Classification of Multitemporal SAR Data: A Sequential-Masking Approach

7.3.5.1 Selection of Calibration and Validation Blocks

For each crop, pixel sample blocks were randomly extracted within representative fields in order to calibrate the maximum-likelihood classifier (MLC). To assess the accuracy of the classifications, validation pixels, independent of the calibration pixels, were randomly selected for each crop. Fields that exhibited anomalies, such as backscatter that deviated significantly from the norm of a particular class, were excluded from both the calibration and validation samples. Calibration and validation pixels were extracted from different fields, a requirement for the per-field approach where a field is defined as a homogeneous area and all pixels are assigned the value of the mean. This reduced the number of fields that could be used for calibration and validation (Ban *et al.*, 1995).

7.3.5.2 Per-Pixel Classification

In order to assess the effectiveness of the field-classification approach, comparison with a traditional per-pixel classification was required. For this reason, MLC classifications were performed using early- and mid- season ERS-1 SAR data in 1992 and 1993.

7.3.5.3 Per-Field Classification

Field boundaries permitted segmentation of the ERS-1 SAR data into homogeneous fields using an image-polygon-growing algorithm and homogeneous classifier (PCI, 1994). A unique grey level was assigned as a label for each output polygon of the field-boundary file which was then input to the homogeneous classifier as a theme channel. The homogeneous classifier defined the homogeneous segments of interest. There were two values that could be assigned

to segments, namely the mean and the mode. Only the mean was tested in this study. The pixel values in each field were replaced with the mean value for that field. Post-segmentation classifications using an ANN algorithm were then performed on field means of the ERS-1 SAR data. The procedure is similar to the one described in Chapter 6.

7.3.5.4 Sequential-Masking Classification

The sequential-masking classification procedure is an interactive human/computer interface patterned after photointerpretation techniques in which the most distinct image features are labelled (classified) first. Image analysis is then carried out on the less-interpretable image features until the entire image is classified. Sequential masking employs image-processing techniques and GIS operations simultaneously to classify multitemporal images. Sequential masking also allows incorporation of ancillary spatial data such as thematic maps (e.g., soil maps) into the classification process (Ehrlich *et al.*, 1994). The classification logic of the sequential-masking procedure is summarized in Figure 7.7. Although sequential-masking techniques were developed using satellite VIR data for land-use mapping, the potential has not been fully explored due to lack of multitemporal datasets (i.e., the problem of cloud cover). The availability of multitemporal satellite SAR data provides an excellent opportunity to investigate sequential-masking techniques for crop classification.

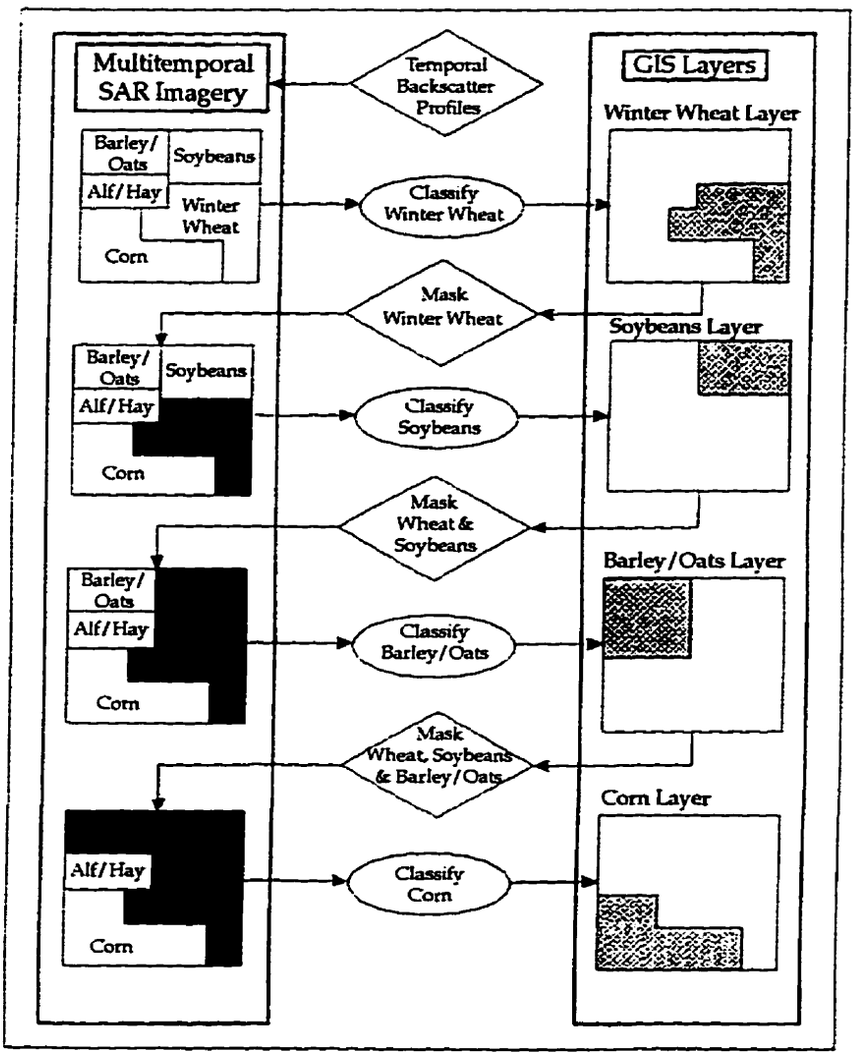

Figure 7.7. Summary of the classification logic of the sequential masking procedure (modified from Ehrlich *et al.*, 1994)

7.4 Results and Discussion

7.4.1 ERS-1 SAR Temporal Backscatter Profiles

As discussed in Chapter 3, a wide range of parameters affects the backscatter of microwaves from vegetation and soil. The important instrument parameters, however, are frequency, polarization and incidence angle. The crucial features of the target in determining the proportion of radiation returning to the instrument are plant canopy (e.g., plant type, height, density, biomass, water content and growth stage) and soil parameters (e.g., soil moisture content, roughness and tillage direction). The SAR temporal backscatter profiles for each crop show the complexity of the relationship between microwave and agricultural parameters over the growing season.

7.4.1.1 ERS-1 SAR Temporal Backscatter Profiles for Major Crops: 1992

ERS-1 SAR Temporal Backscatter Profiles

The ERS-1 SAR temporal backscatter profiles for major crops are shown in Figure 7.8. From this figure, it is possible to make the following observations for the earliest differentiation of crop types:

- Winter wheat can be successfully separated from other crops in May and June since it is at a very different growth stage from other crops.
- Alfalfa and pasture can be separated from other crops in the mid-season, but they both have very similar profiles throughout the growing season.
- Corn and soybeans have similar profiles in the early and mid- season, but can be separated from each other in the late season.

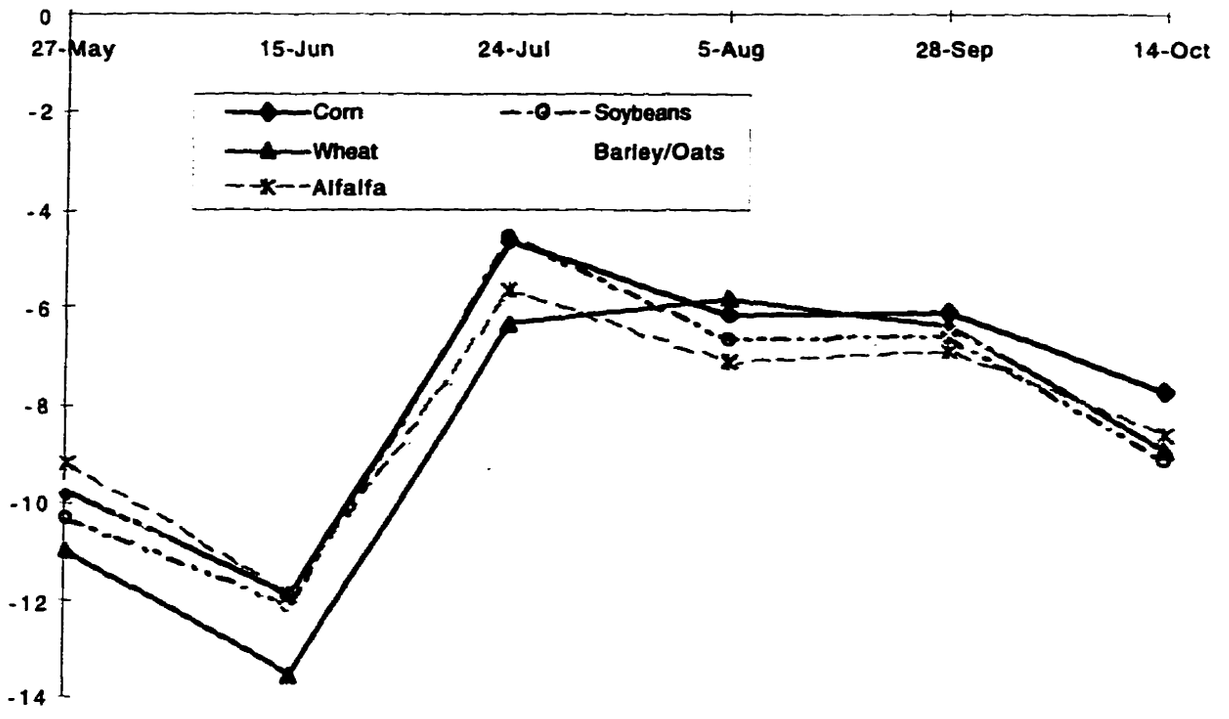

Figure 7.8. ERS-1 SAR temporal backscatter profiles for major crops during the 1992 growing season

Anomalous Fields

Some anomalous fields were observed during the analysis. For example, on July 24, there was more than 2 dB of difference for the backscatter of an anomalous corn field (4-31) when compared with the average corn backscatter of more than 20 fields (Figure 7.9). This was caused by the differences in ground coverage, growth conditions and local climate. According to field observations, the normal fields were densely covered by corn (>90%), while the anomalous field only had 70% of corn coverage and was infested by weeds (Figure 7.10). The fields were wet because of rain. Other anomalies observed are mainly caused by changes in the fields. For example, one of the harvested small-grain fields (with residue) was ploughed before the data acquisition on October 14 (Figure 7.11). This caused a 2 dB increase in radar backscatter when compared with that of other harvested small-grain fields. There was another 2 dB increase in radar backscatter when an alfalfa field was ploughed (compared with

backscatter of the alfalfa fields). These indicate that close attention should be given to the changes of the field status over the growing season. In general, the anomalies usually resulted from crop condition and crop management, and/or soil drainage and soil roughness characteristics. These anomalies can cause confusion during classification and they should be excluded from the selection of calibration and validation fields if a supervised classification is used.

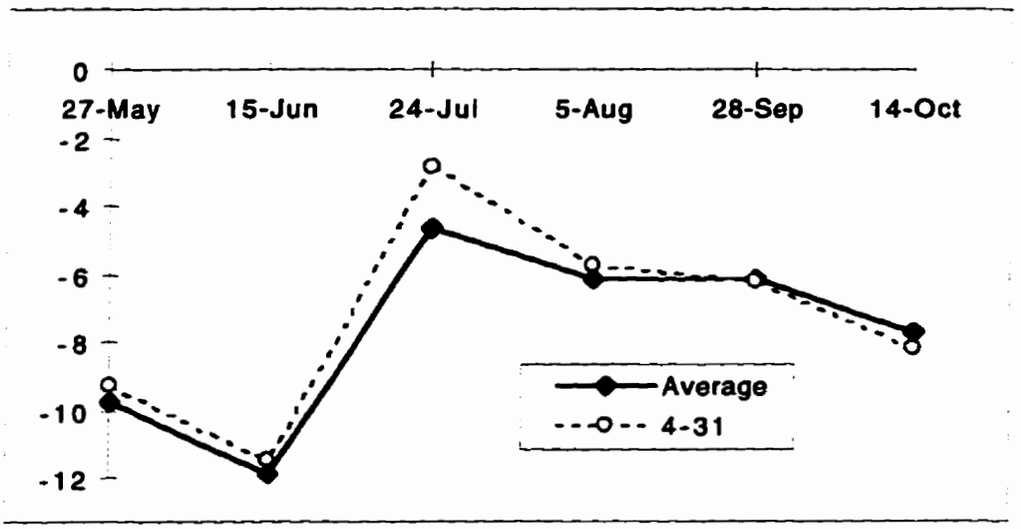

Figure 7.9. Comparison of a corn anomaly and the corn average

Figure 7.10. Corn: poor growth and good growth (July 20, 1992)

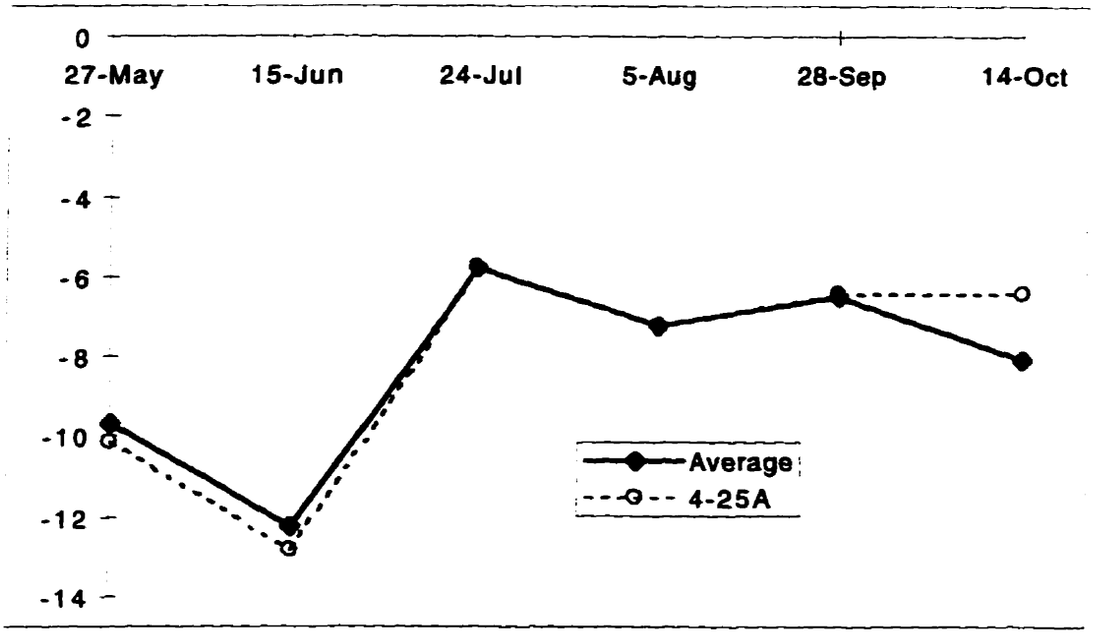

Figure 7.11. Comparison of a barley/oats anomaly and the barley/oats average

7.4.1.2 ERS-1 SAR Temporal Backscatter Profiles for Major Crops: 1993

ERS-1 SAR Temporal Backscatter Profiles

Using multitemporal ERS-1 SAR data during the 1993 growing seasons, the radar backscatter characteristics of crops and their underlying soils were analyzed. The SAR temporal backscatter profiles were generated for each crop type (Figure 7.12). Using corn as an example, radar backscatter was high in the early season when fields were relatively rough with bare soil. With crop development, backscatter decreased due to attenuation and absorption by the vegetation canopies. The decreasing trend continued until August 9, when corn was at cob development stage. Then the backscatter started to increase as the crops reached the senescent stage (Figures 7.13 & 7.14).

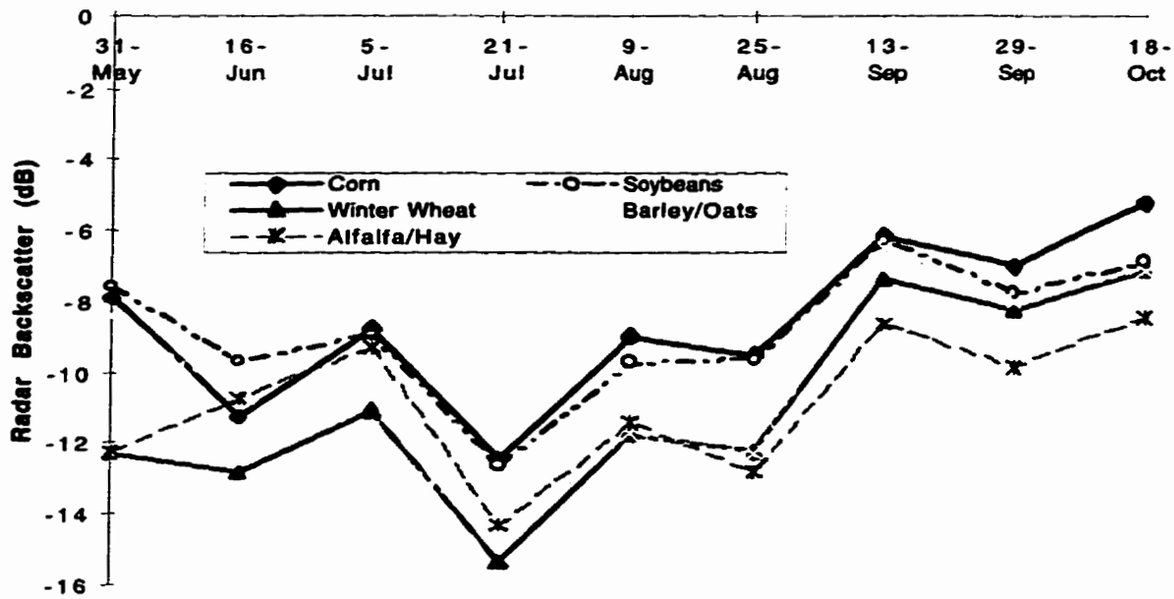

Figure 7.12. ERS-1 SAR temporal backscatter profiles for major crops during 1993 growing season

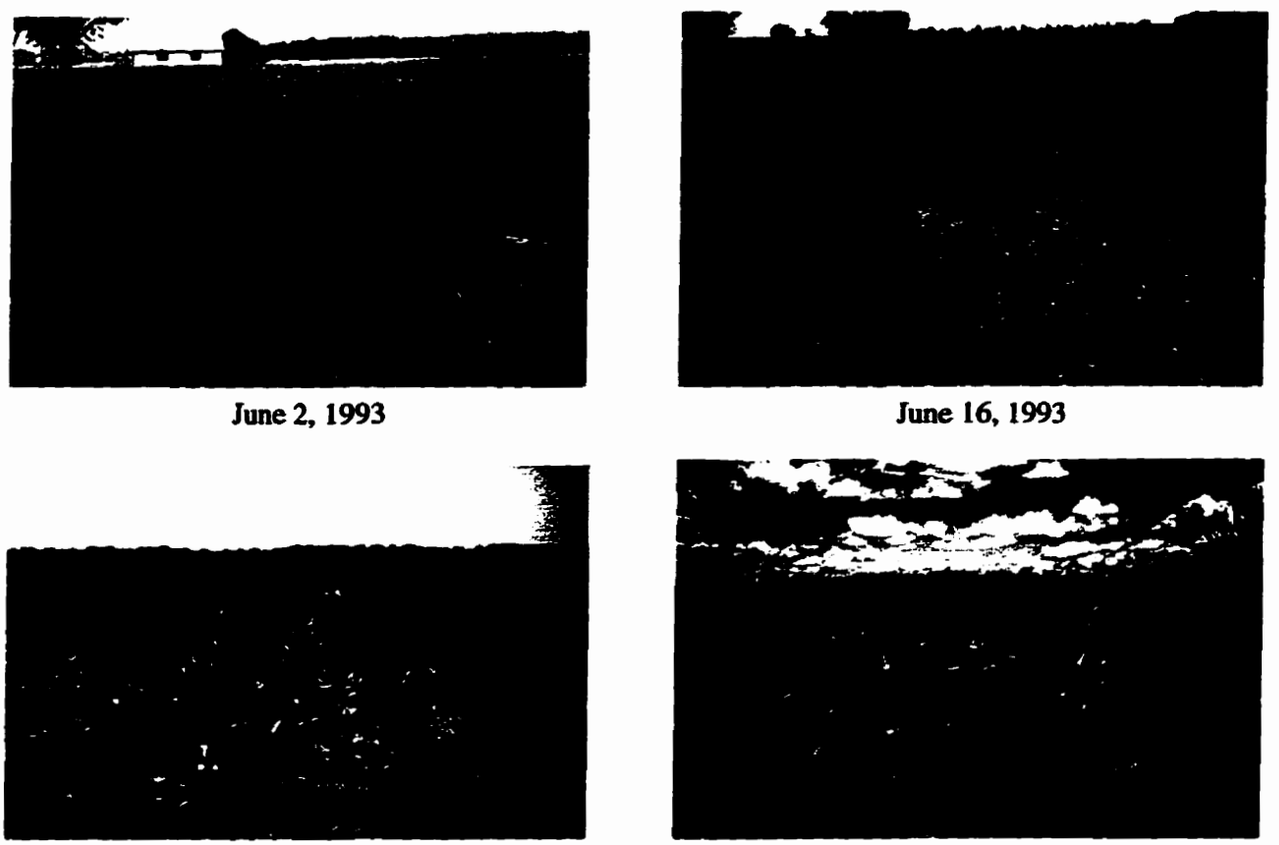

June 2, 1993

June 16, 1993

July 5, 1993

July 21, 1993

Figure 7.13. Corn development during the 1993 growing season

Aug. 9, 1993

Aug. 25, 1993

Sept. 13, 1993

Sept. 29, 1993

Oct. 18, 1993

Oct. 18, 1993

Figure 7.13. Corn development during the 1993 growing season (cont.)

The temporal backscatter profiles shown in Figures 7.12 and 7.14, however, do not match the general findings described earlier. Efforts were made to explain ups and downs in the backscatter patterns. ERS-1 radiometric calibration accuracies, local climatic conditions, crop growth conditions, etc. were taken into account, but none of these were found to be responsible for such temporal backscatter behaviours. When the two ERS-1 orbits were separated, however, the temporal backscatter profiles started to make sense (Figure 7.15).

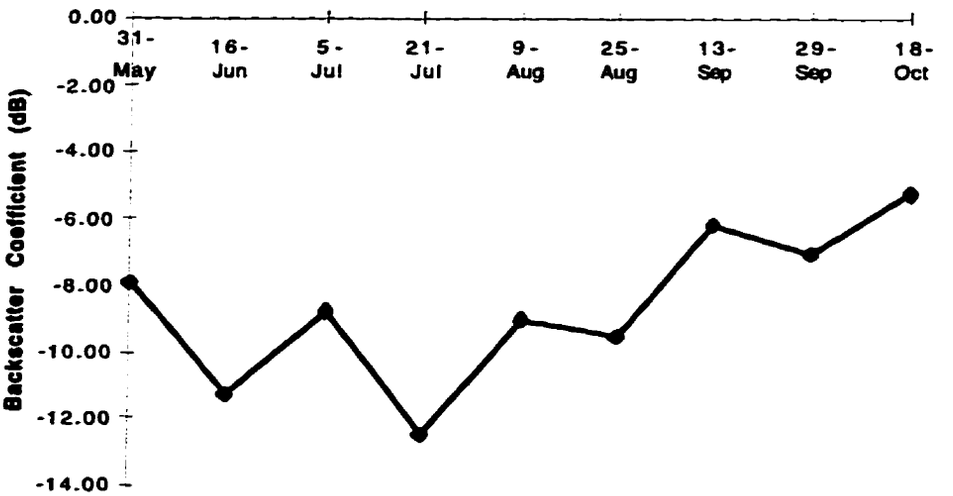

Figure 7.14. ERS-1 SAR temporal backscatter profile for corn - 1993

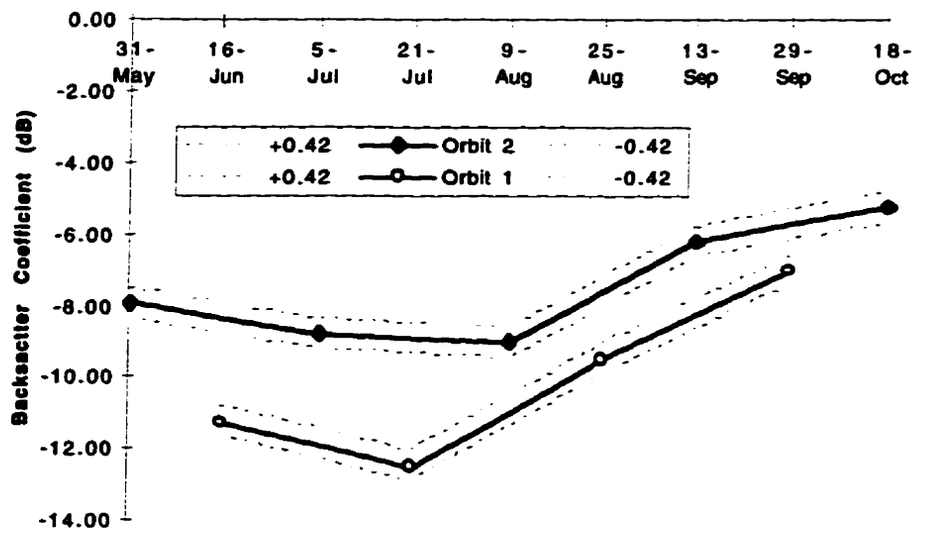

Figure 7.15. ERS-1 SAR temporal backscatter profiles for corn derived from two orbits: error buffers included

Orbital (Incidence Angle) Effects

No previous research on the relationship of C-VV backscatter coefficient δ° and angle of incidence for crops has been found in the literature. However, Ulaby *et al.* (1986a) measured incidence-angle effects on a corn canopy using C-HH. Although C-VV penetrates less into the crop canopy than C-HH, it is clear that at higher incidence angles (>30°), the backscatter coefficient decreases sharply when the incidence angle increases. The estimated change of backscatter is about 3-4 dB from 20° to 25° (Figure 7.16).

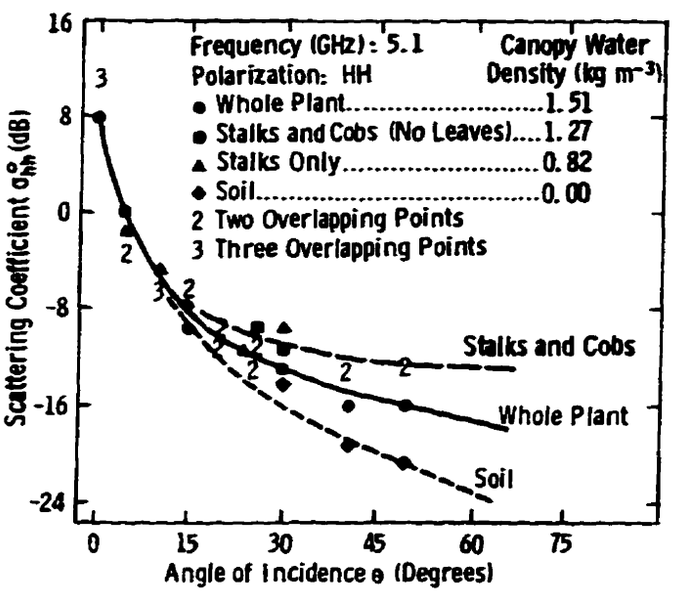

Figure 7.16. Measured δ° of a fully mature corn canopy in four consecutive stages of defoliation; all the measurements were made on the same day (Ulaby *et al.*, 1986a)

ERS-1 orbital (incidence angle) effects were observed on all crops (Figures 7.15 & 7.17-7.20). For 4° difference of incidence angles between the two orbits (about 21.5° and 25.5°), the average difference of radar backscatter was about 3 dB. This is similar to the findings of Ulaby *et al.* (1986a). Thus attention must be given to the local incidence effects when using ERS-1 SAR data, especially when comparing fields from different scenes or different areas within the same scene.

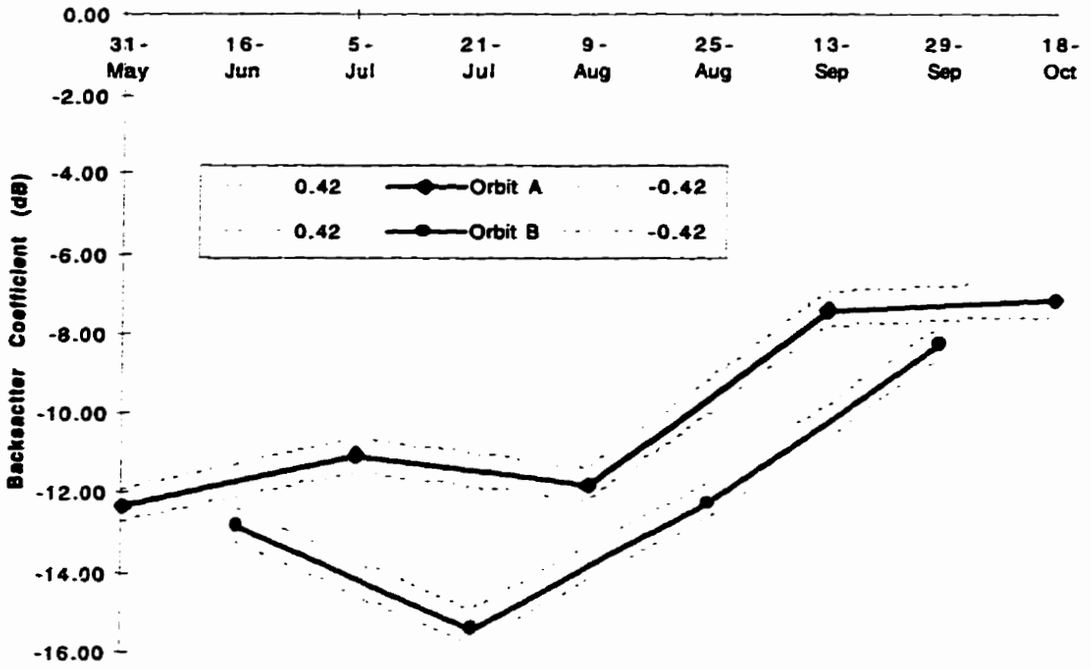

Figure 7.17. ERS-1 SAR temporal backscatter profiles for wheat derived from two orbits: error buffers included

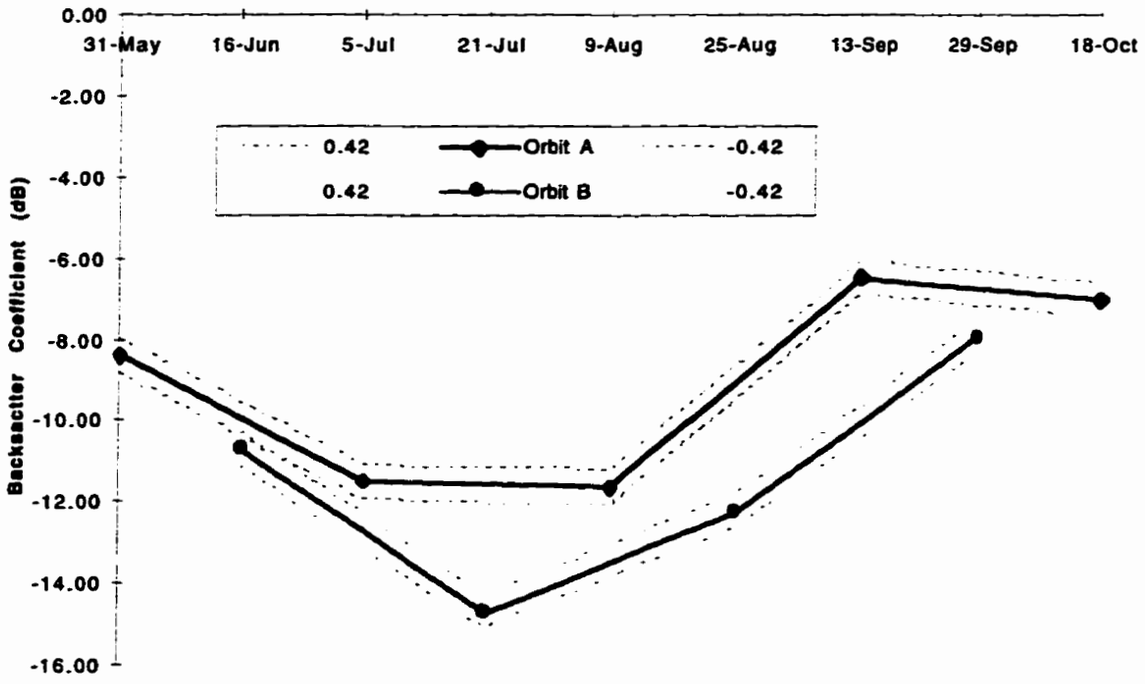

Figure 7.18. ERS-1 SAR temporal backscatter profiles for barley/oats derived from two orbits: error buffers included

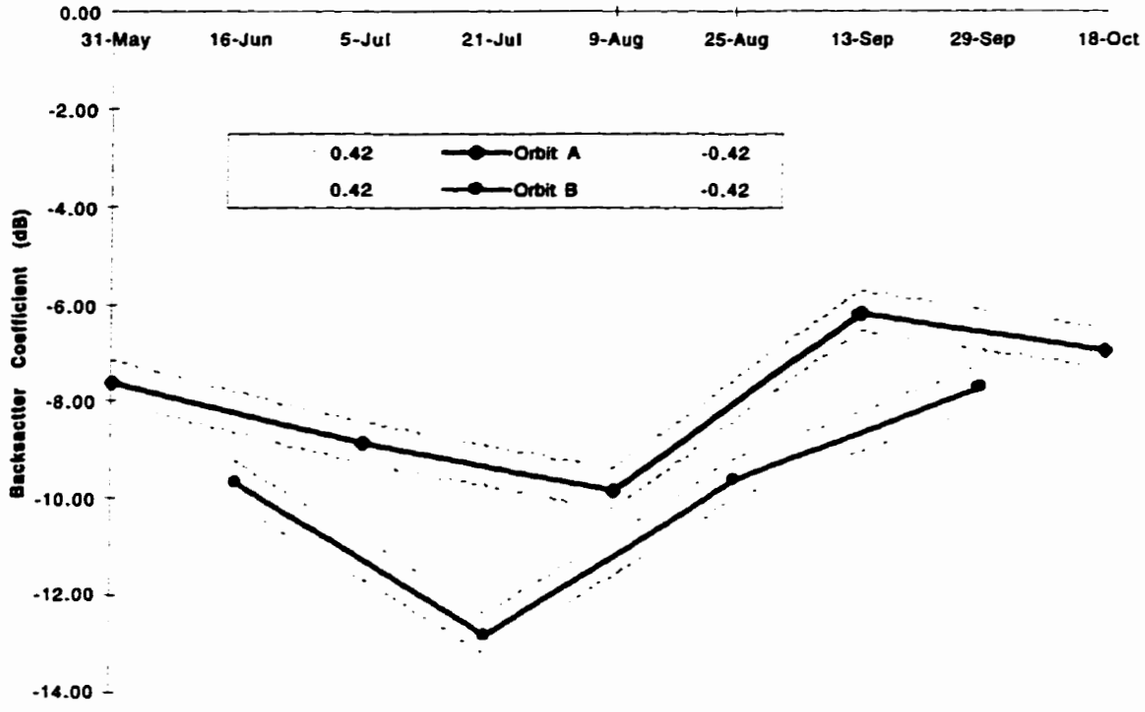

Figure 7.19. ERS-1 SAR temporal backscatter profiles for soybeans derived from two orbits: error buffers included

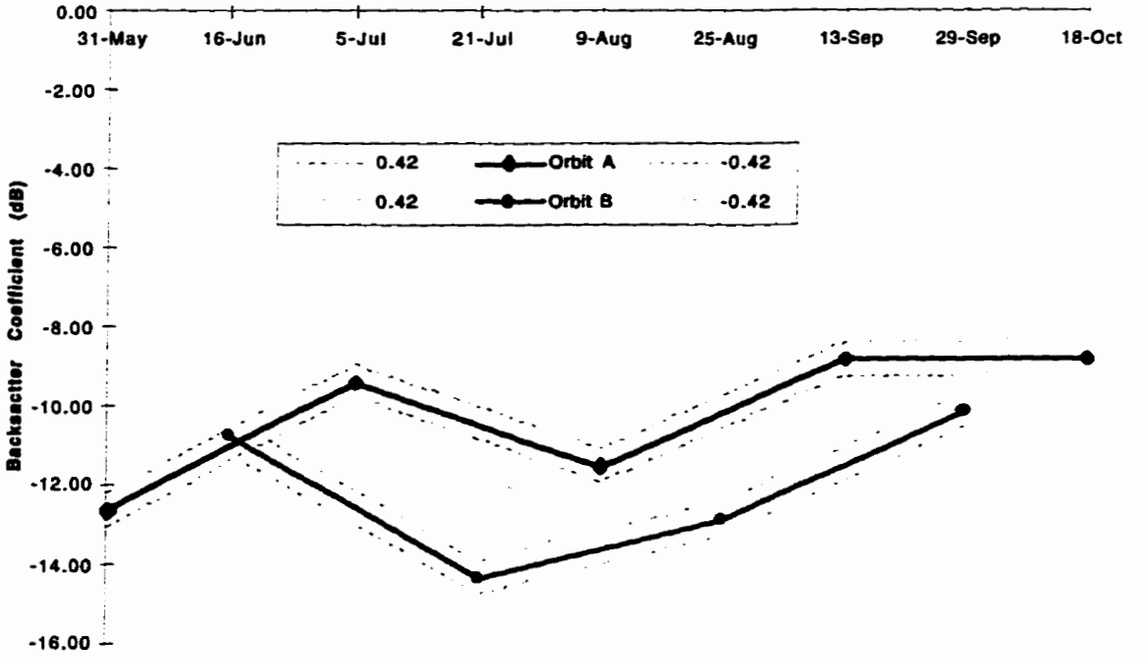

Figure 7.20. ERS-1 SAR temporal backscatter profiles for alfalfa/hay derived from two orbits: error buffers included

Earliest Time of Year for Differentiation of Crops

Based on the SAR temporal backscatter profiles (Figure 7.12), the earliest time of the year for differentiation of individual crop types was investigated. The results showed there were 4 dB of difference in backscatter between wheat and corn (or soybeans or barley/oats) on May 31. This is mainly due to the crops were at differenct development stages. For example, winter wheat was at the stage of vegetation growth on May 31 while corn, soybeans and barley/oats were at the stage of seed-bed preparation. Thus winter wheat could be easily separated from all crops in the early season (May 31 and June 16). Soybeans could only be separated from the rest of the crops on June 16 since soybeans and corn had similar backscatter profile on all dates, except on June 16 (Figure 7.21). This was due to the effect of litter in soybeans fields so that soybeans had a higher radar backscatter than corn on June 16. Barley/oats could be distinguished from corn, soybeans and alfalfa/hay on July 5 and dates thereafter. However, from July 5 on, barley/oats had a similar profile to wheat. In turn, wheat and barley/oats displayed similar patterns to alfalfa/hay after July 21. The earliest time to differentiate corn from other crops was July 21.

Corn Soybeans

Figure 7.21. Corn and Soybeans on June 16, 1993

Within crop variations

Within crop variations for corn and barley/oats are illustrated in Figures 7.22 and 7.23. Corn fields had larger variations at the beginning of the growing season (Figure 7.22 and Table 7.2). The variation decreased during the mid-season and the late season. There was no clear trend, however, for barley/oats variations mainly due to anomalous fields. The highest standard deviation was 2.56 dB on July 21 (Figure 7.23 and Table 7.3). It was because Field 4-25 was beginning to senesce and turn brownish yellow, while average barley/oats fields were still in the stage of seed development. Thus such variations can be major sources of mis-classification and attention should be given to this during crop classifications.

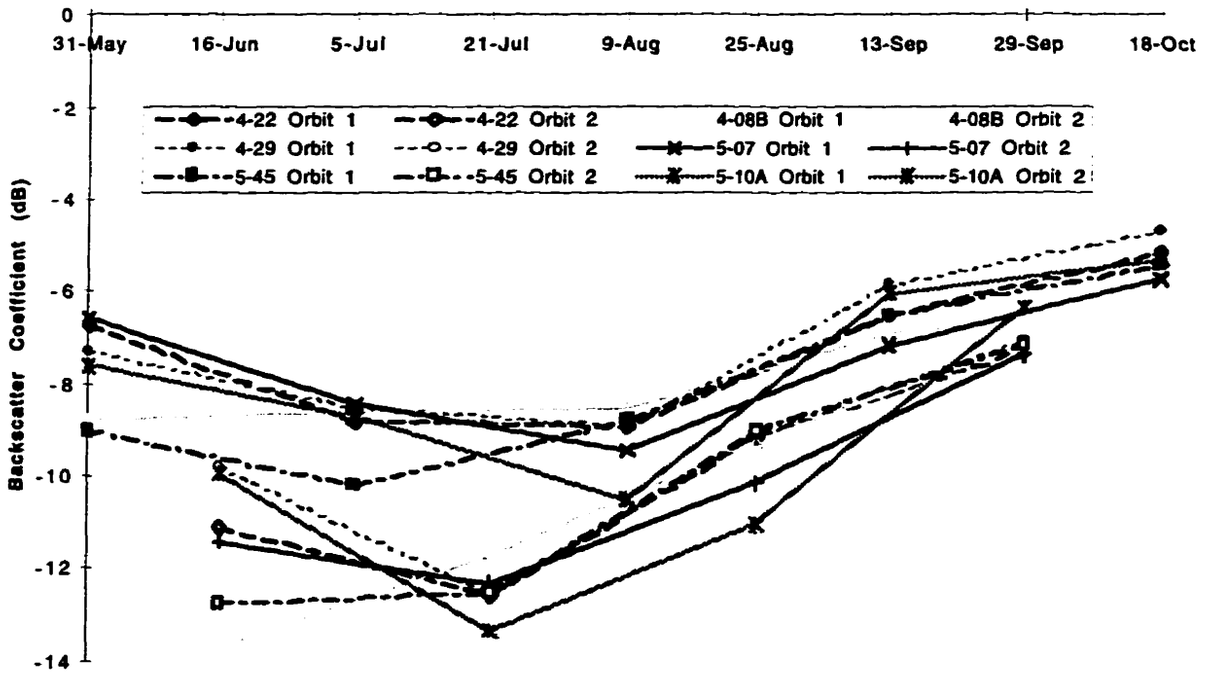

Figure 7.22. ERS-1 SAR temporal backscatter profiles for corn derived from two orbits: within crop variations

Table 7.2. Within Crop Variations (dB): Corn

Field #	31-May	16-Jun	5-Jul	21-Jul	9-Aug	25-Aug	13-Sep	29-Sep	18-Oct
3-10	-6.91	-12.19	-9.05	-11.15	-7.62	-8.77	-5.43	-6.70	-4.52
3-11B	-9.46	-11.32	-8.90	-12.00	-9.42	-9.59	-6.36	-7.55	-4.83
3-12	-8.11	-10.99	-8.62	-13.07	-9.14	-9.99	-5.66	-7.31	-5.41
3-32A	-7.52	-11.26	-8.31	-12.69	-9.38	-9.58	-6.48	-7.43	-4.53
4-12	-5.88	-9.42	-7.56	-12.96	-10.24	-9.6	-7.32	-8.1	-5.6
4-22	-6.7	-11.11	-8.79	-12.56	-8.95	-9.15	-6.52	-7.3	-5.17
4-29	-7.27	-9.80	-8.49	-12.57	-8.95	-9.07	-5.84	-7.08	-4.70
4-08B	-8.74	-13.71	-8.58	-11.72	-8.56	-9.24	-6.9	-7.15	-6.28
5-07	-6.54	-11.41	-8.41	-12.30	-9.45	-10.15	-7.16	-7.38	-5.72
5-10A	-7.57	-9.93	-8.70	-13.37	-10.48	-11.07	-6.01	-6.32	-5.28
5-21	-6.54	-10.91	-7.49	-11.58	-9.01	-9.4	-6.17	-6.69	-5.08
5-45	-9.02	-12.75	-10.18	-12.51	-8.81	-9.01	-6.48	-7.16	-5.41
6-13	-7.99	-10.44	-8.50	-12.39	-9.34	-9.77	-6.33	-7.36	-5.12
6-20	-7.63	-10.77	-7.95	-12.82	-9.39	-9.43	-5.04	-5.93	-4.33
6-24A	-9.29	-12.27	-9.34	-13.32	-9.28	-9.80	-5.95	-6.98	-5.75
6-25	-7.20	-11.56	-8.09	-13.18	-9.28	-9.53	-5.86	-6.92	-5.03
Average	**-7.65**	**-11.24**	**-8.56**	**-12.51**	**-9.21**	**-9.57**	**-6.22**	**-7.09**	**-5.17**
STDEV	**1.06**	**1.11**	**0.66**	**0.64**	**0.64**	**0.54**	**0.61**	**0.51**	**0.52**
Average*	**-7.91**	**-11.23**	**-8.77**	**-12.45**	**-9.00**	**-9.48**	**-6.17**	**-7.00**	**-5.22**

* Derived from all corn fields using Equation 4.10.

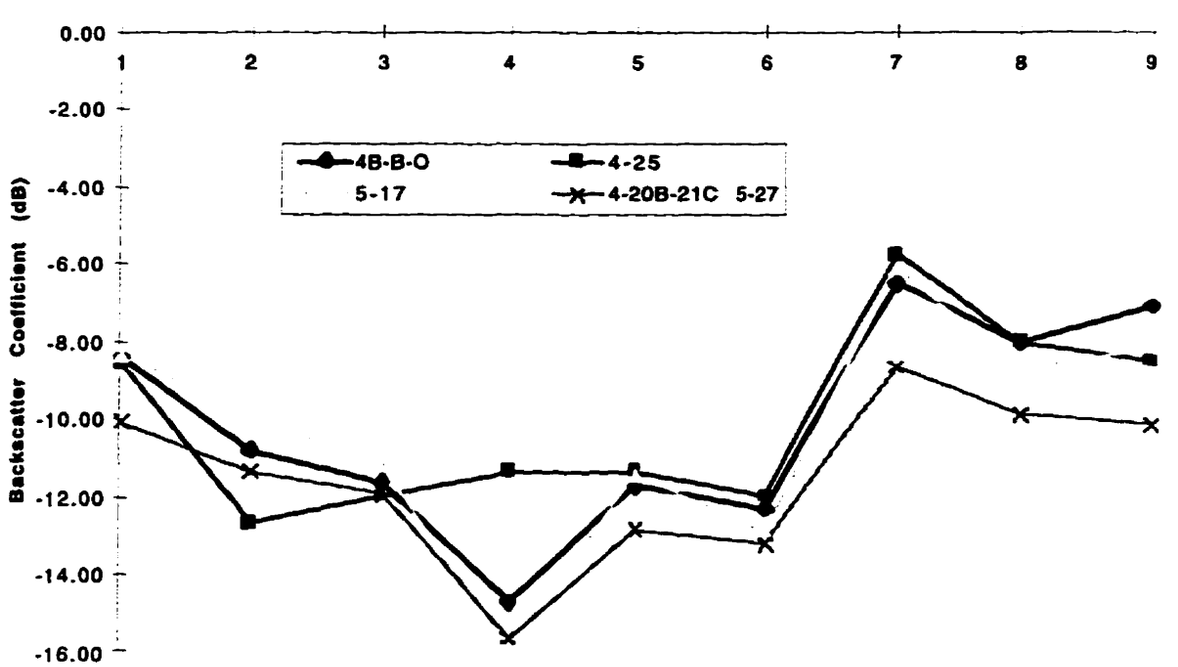

Figure 7.23. ERS-1 SAR temporal backscatter profiles for barley/oats: within crop variations

Table 7.3. Within Crop Variations (dB): Barley/Oats

Field #	31-May	16-Jun	5-Jul	21-Jul	9-Aug	25-Aug	13-Sep	29-Sep	18-Oct
4-25	-8.53	-12.66	-11.99	-11.32	-11.32	-11.97	-5.73	-8.02	-8.50
5-17	-8.32	-9.94	-11.23	-15.87	-11.45	-12.96	-6.13	-8.70	-8.16
4-20B-21C 5-27	-10.03	-11.33	-11.94	-15.63	-12.84	-13.23	-8.66	-9.87	-10.14
Average	**-8.96**	**-11.31**	**-11.72**	**-14.27**	**-11.87**	**-12.72**	**-6.84**	**-8.86**	**-8.93**
STD DEV	**0.9326**	**1.3601**	**0.425**	**2.56**	**0.8426**	**0.663**	**1.5888**	**0.936**	**1.0587**
Average*	**-8.39**	**-10.79**	**-11.60**	**-14.72**	**-11.72**	**-12.30**	**-6.51**	**-7.99**	**-7.11**

* Derived from all barley/oats fields using Equation 4.10.

7.4.2 ERS-1 SAR Data for Crop Classifications: A Multitemporal Approach

7.4.2.1 Multitemporal SAR Classifications: 1992

The overall validation accuracy for single-channel ERS-1 SAR data (Aug. 5) using a per-field classifier was 57.7% (Table 7.4, Figure 7.24). Alfalfa had the highest validation accuracy (91.7%). The overall validation accuracy for three-date (May 27, June 15 and July 24) SAR in early and mid- season using a per-field classifier was 74.3%. This is a 16% improvement over the single-date classification. The highest validation accuracy (78.2%) was achieved by classifying four-date (May, June, July and Aug.- early and mid-season) SAR data using a per-field approach (Table 7.5). This is a 20.5% improvement over the best single-date SAR classification. It also represents a 30% improvement over per-pixel classification using the same four-date combination. Specifically, winter wheat had a validation accuracy of 100% while the alfalfa accuracy remained unchanged, but the accuracy for soybean classification improved significantly; corn, however, was still quite low (45.7%).

Table 7.4. Validation Accuracy for Single-Date (Aug. 5) SAR Per-Field Classification

	Winter Wheat (%)	Corn (%)	Soybeans (%)	Alfalfa (%)
Winter Wheat	**50.0**	30.0	0.0	20.0
Corn	8.7	**56.5**	26.1	8.7
Soybeans	16.3	42.9	**32.7**	8.2
Alfalfa	0.0	0.0	8.3	**91.7**
Overall Validation accuracy: **57.7%**				

Table 7.5. Validation Accuracy for a Four-Date (May 27, June 15, July 24 and Aug. 5) SAR Per-Field Classification

	Winter Wheat (%)	Corn (%)	Soybeans (%)	Alfalfa (%)
Winter Wheat	**100.0**	0.0	0.0	0.0
Corn	8.7	**45.7**	17.4	0.0
Soybeans	0.0	0.0	**75.5**	0.0
Alfalfa	0.0	0.0	8.3	**91.7**
Overall Validation accuracy: **78.2%**				

Figure 7.24. Per-field Classification for May 27, June 15, July 24 and Aug. 5 ERS-1 SAR

7.4.2.2 Multitemporal SAR Classifications: 1993

Based on the temporal backscatter profiles, early- and mid-season multitemporal SAR data for crop classification using sequential-masking techniques was evaluated. It was found that winter wheat and alfalfa/hay were confused with each other (Table 7.6), but could be identified from other crops because they were well into the vegetation development stage while other crops were at the stage of seed-bed preparation or emerging (Figures 7.25 & 7.26). Using a single-date June 16 image, winter wheat could be successfully identified (91.1%). Soybeans could be classified with some degree of success using the combination of May 31 and June 16 SAR data (94.9% accuracy, but with high commission errors from other crops) (Figure 7.27). After masking out wheat and soybeans, barley/oats could be identified on July 5 and July 21 (mid-season) (Figure 7.28). Again, after masking out wheat, soybeans and barley/oats, corn can be successfully separated from alfalfa/hay on July 21 (Figure 7.29). These results clearly indicate that crop classification can be carried out successfully using sequential-masking techniques with early-and mid-season multitemporal SAR.

Table 7.6. Validation Accuracy for a Per-Field Classification Using the May 31, 1993 Image

	Winter Wheat (%)	Corn (%)	Soybeans (%)	Barley/Oats (%)	Alfalfa/Hay (%)
Winter Wheat	**65.6**	0.0	0.0	0.0	34.4
Corn	5.1	**62.8**	0.0	32.1	0.0
Soybeans	11.0	67.5	**0.0**	21.5	0.0
Barley/Oats	12.7	51.3	0.0	**36.0**	0.0
Alfalfa	31.5	0.0	0.0	9.7	**57.8**
Overall Validation accuracy: **55.2%**					

Figure 7.25. Winter wheat and soybeans on June 2, 1993

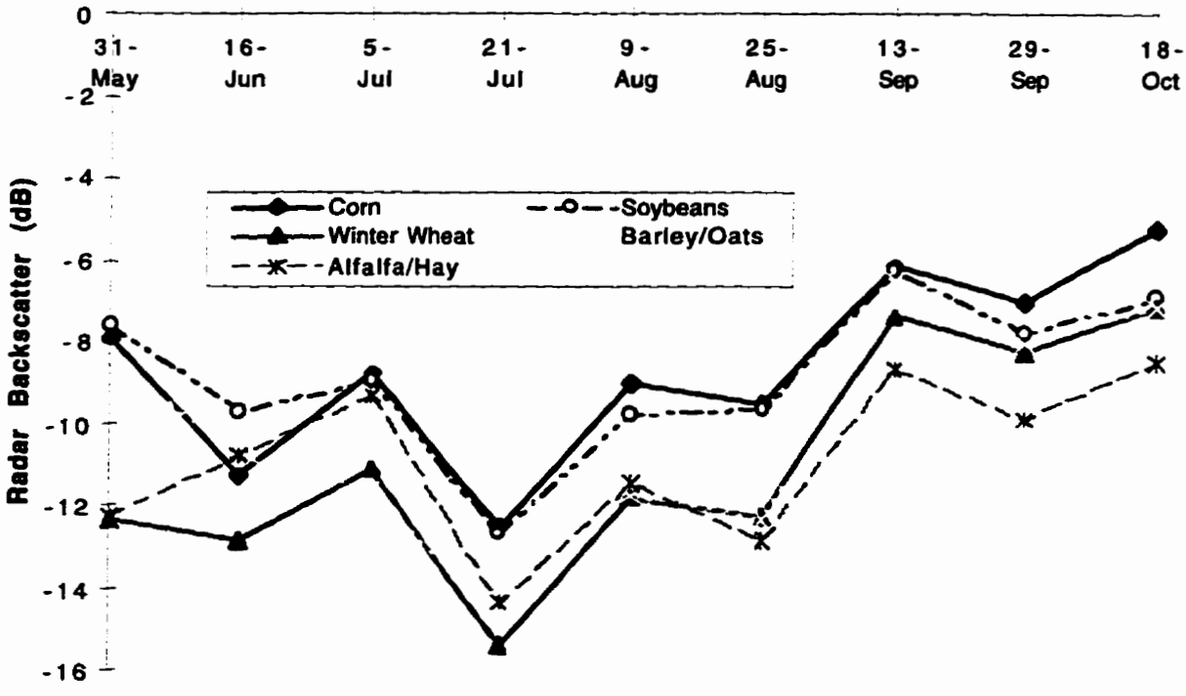

Figure 7.26. ERS-1 SAR temporal backscatter profiles for major crops during 1993 growing season

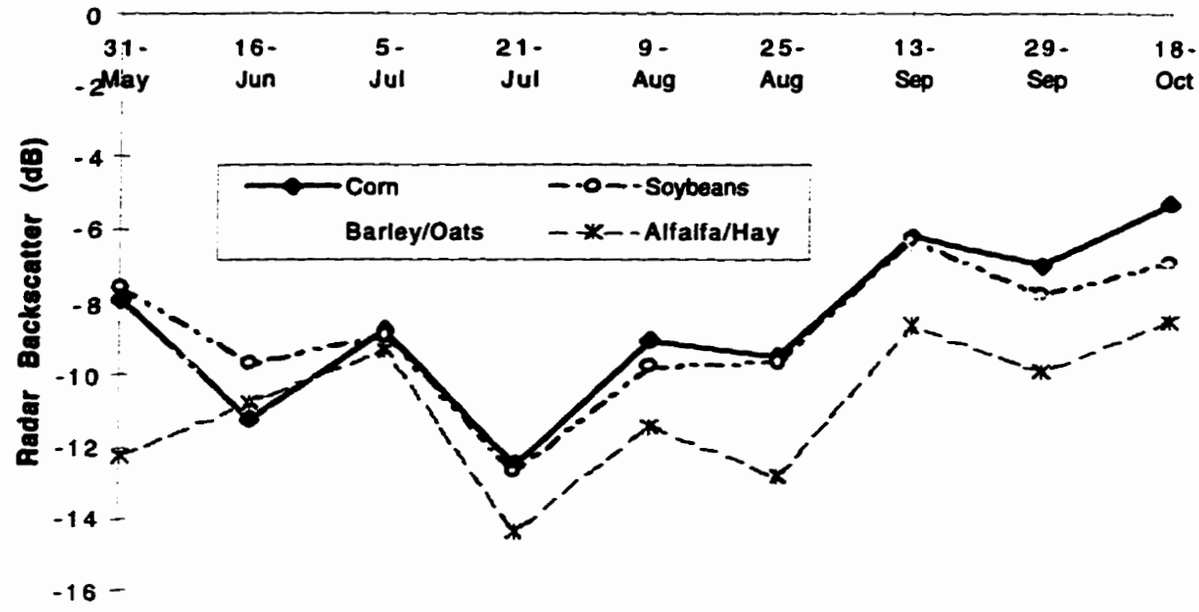

Figure 7.27. Crop separabilities after masking out winter wheat

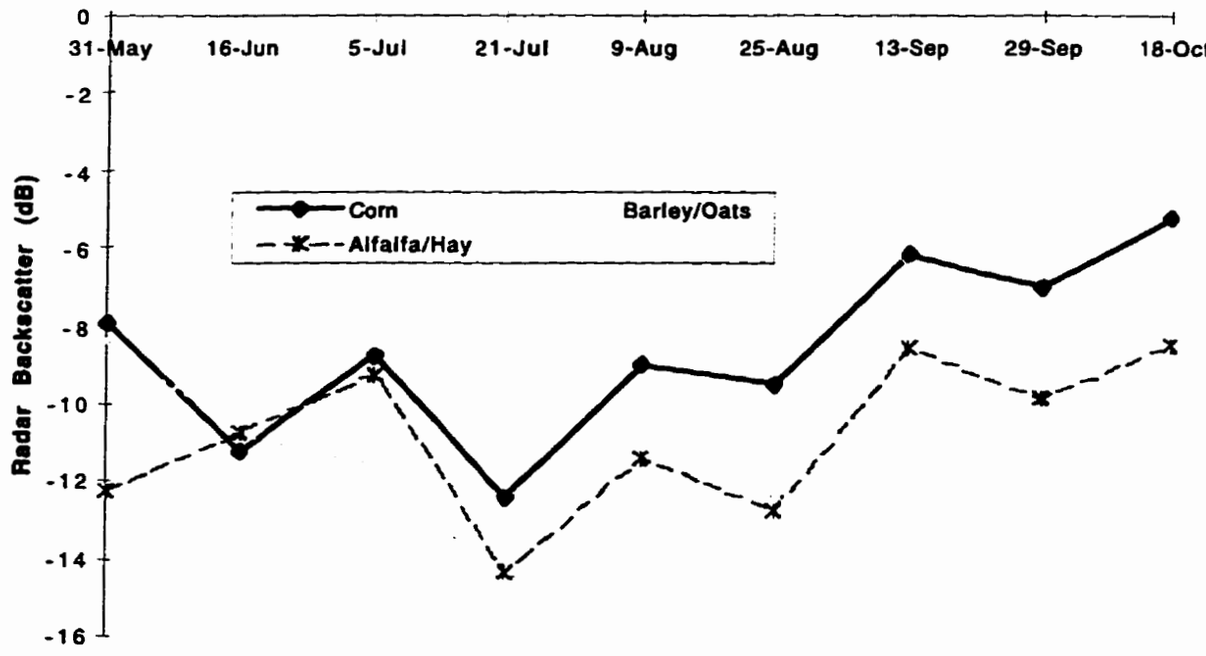

Figure 7.28. Crop separabilities after masking out winter wheat and soybeans

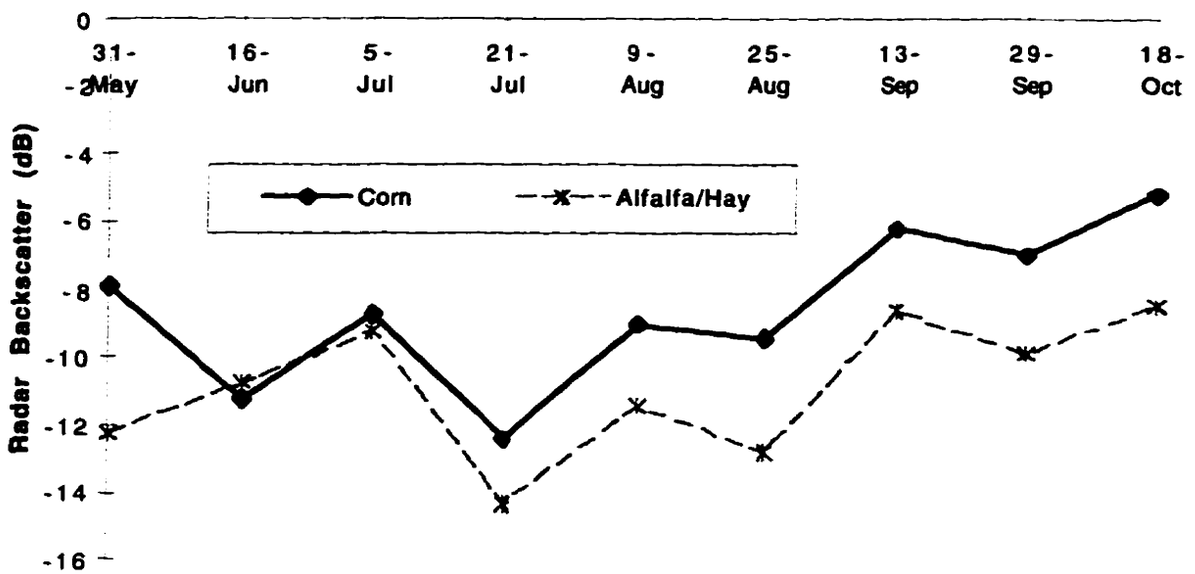

Figure 7.29. Crop separabilities after masking out winter wheat, soybeans and barley/oats

7.5 Summary

7.5.1 Summary: 1992 SAR Data

ERS-1 SAR temporal backscatter profiles indicate that winter wheat can be successfully separated from other crops in the early season. Alfalfa and pasture can be separated from others in the mid-season, but they both have very similar profiles throughout the growing season. Corn and soybeans have similar profiles in the early and mid- season, but can be separated from each other in the late season.

A multitemporal approach using a per-field classifier proved to be effective for crop identification. Using four dates of SAR data in the early and mid- season produced the highest validation accuracy of 78.2%. This is a 20.5% improvement over the best single-date SAR classification. It represents a 30% improvement over per-pixel classification using the same four-date combination.

7.5.2 Summary: 1993 SAR Data

Using multitemporal ERS-1 SAR data acquired during the 1993 growing season, the radar backscatter characteristics of crops and their underlying soils were analyzed. The SAR temporal backscatter profiles were generated for each crop type and the earliest time of the year for differentiation of individual crop types was determined. The results showed that winter wheat could be easily separated from all crops in the early season (May 31 and June 16). Soybeans could only be separated from the rest of the crops on June 16 since soybeans and corn had similar backscatter profile on all dates, except on June 16. Barley/oats could be distinguished from corn, soybeans and alfalfa/hay on July 5 and dates thereafter. However, from July 5 on, barley/oats had a similar profile to wheat. In turn, wheat and barley/oats displayed similar patterns to alfalfa/hay after July 21. The earliest time to differentiate corn from other crops was July 21.

Orbital (incidence angle) effects were observed on all crops. The average difference between the two orbits was about 3 dB. Thus attention must be given to the local incidence-angle effects when using ERS-1 SAR data, especially when comparing fields from different scenes or different areas within the same scene.

Based on the temporal backscatter profiles, early- and mid-season multitemporal SAR data for crop classification using sequential-masking techniques were evaluated. It was found that winter wheat could be easily identified using an early-season single-date SAR image (June 16). Soybeans could be classified with some degree of success using June 16 SAR data. After masking out wheat and soybeans, barley/oats could be easily classified on July 5 and July 21 (mid-season). Again, after masking out wheat, soybeans and barley/oats, corn can be successfully separated from alfalfa/hay on July 21 (mid-season). These results clearly indicate

that crop classification can be carried out successfully using sequential-masking techniques with early-and mid-season multitemporal SAR data.

CHAPTER 8: CONCLUSIONS AND RECOMMENDATIONS

8.1 Conclusions

The overall objective of this research was to evaluate multipolarization airborne SAR data, multitemporal ERS-1 SAR data, and combinations of ERS-1 SAR and satellite VIR data for crop classification using non-conventional algorithms. To achieve this objective, five major issues have been addressed.

The first objective was to perform a comparative analysis of classification algorithms that incorporate tonal, contextual, and/or textural information.

Operational methodologies for improving agricultural crop identification were tested using C-HH and C-HV airborne SAR data collected on July 10, 1990. Raw SAR data, filtered SAR data and SAR texture statistics were classified using per-pixel and per-field classification approaches to determine their effectiveness for agricultural crop classification. The approaches presented for improving agricultural crop classification proved to be effective, especially the per-field classification method. Results indicated that C-HH and C-HV data, classified using a standard per-pixel MD classifier, provided relatively poor classification accuracies. Inclusion of texture statistics in the per-pixel classification improved accuracies by approximately 30% and simple median filtering boosted accuracies by approximately 25%. However, using a per-field classifier, the classification accuracies improved by about 40%.

The second objective was to evaluate multipolarization (C-HH and C-HV) airborne SAR data for crop classification.

Multipolarization SAR data were evaluated for crop classification. Results indicated that C-HV SAR data yielded a lower overall classification accuracy (45.41%) than C-HH SAR data (49.36%). The lower accuracy for C-HV contradicts conclusions put forward by other researchers. A possible reason for the contradiction is the low signal-to-noise ratio with C-HV data. It was also found that three of the four best per-field classification accuracies ($\hat{K}$=0.91) were achieved using combinations of C-HH and C-VV SAR data. This confirms the strong potential of multipolarization data for crop classification.

The third objective was to evaluate the synergistic effects of multitemporal ERS-1 SAR and satellite VIR data for crop classification.

The synergistic effects of multitemporal ERS-1 SAR and Landsat TM data were evaluated for crop classification using an artificial neural network (ANN) approach. Eight crop types and conditions were identified: winter wheat, corn (good growth), corn (poor growth), soybeans (good growth), soybeans (poor growth), barley/oats, alfalfa, and pasture/cut-hay/cut-alfalfa. The results show that both single-date and multitemporal SAR data yielded poor classification accuracies using a maximum-likelihood classifier (MLC). With the per-field approach using a feed-forward artificial neural network, the overall classification accuracy of three-date SAR data improved almost 20%, and the best classification of a single-date (Aug. 5) SAR image improved the overall accuracy by about 26%. Although these overall classification accuracies (<60%) were not sufficiently high for operational crop inventory and analysis, both single-date and multitemporal SAR data demonstrated their abilities to discriminate certain crops in the early- and mid-season. Using the combination of TM3,4,5 and Aug. 5 SAR data, the best per-field ANN classification of 96.8% was achieved. It represents an 8.5% improvement over a single TM3,4,5 classification alone. This indicates that a combination of mid-season SAR and VIR data is very well suited for crop classification.

The fourth objective was to develop a better understanding of the interaction of microwave energy with crops and their underlying soils over the growing season.

Using multitemporal ERS-1 SAR data during the 1992 and 1993 growing seasons, the radar backscatter characteristics of crops and their underlying soils were analyzed. The SAR temporal backscatter profiles were generated for each crop type. For example, radar backscatter was high in early-season when fields of corn and soybeans were relatively rough with bare soils. With crop development, backscatter decreased due to attenuation and absorption by the vegetation canopies. The decreasing trend continued until August 9, when corn and soybeans were at cob or seed development stage. Then the backscatter started to increase as the crops reached the senescent stage.

The earliest time of the year for differentiation of individual crop types was determined. The results showed that winter wheat could be easily separated from all crops in the early season (May 31 and June 16). Soybeans could only be separated from the rest of the crops on June 16 since soybeans and corn had similar backscatter profile on all dates, except on June 16. Barley/oats could be distinguished from corn, soybeans and alfalfa/hay on July 5 and dates thereafter. However, from July 5 on, barley/oats had a similar profile to wheat. In turn, wheat and barley/oats displayed similar patterns to alfalfa/hay after July 21. The earliest time to differentiate corn from other crops was July 21.

Orbital (incidence angle) effects were observed on all crops. The average difference between the two orbits was about 3 dB. Thus attention must be given to the local incidence-angle effects when using ERS-1 SAR data, especially when comparing fields from different scenes or different areas within the same scene.

In addition, fields displaying anomalous radar backscatter characteristics were also identified and statistically described. Anomalies were caused by differences in ground coverage, growth conditions, tillage practice and local climate

The fifth objective was to evaluate multitemporal ERS-1 SAR data for crop classification.

Based on the temporal backscatter profiles, early- and mid-season multitemporal SAR data for crop classification using sequential-masking techniques were evaluated. It was found that winter wheat could be easily identified using an early-season single-date SAR image (June 16). Soybeans could be classified with some degree of success using June 16 SAR data. After masking out wheat and soybeans, barley/oats could be easily classified on July 5 and July 21 (mid-season); Again, after masking out wheat, soybeans and barley/oats, corn can be successfully separated from alfalfa/hay on July 21 (mid-season). These results clearly indicate that crop classification can be carried out successfully using sequential-masking techniques with early- and mid-season multitemporal SAR data.

8.2 Recommendations for Future Research

The following recommendations can be made for future research:

- For a better understanding of the interactions of microwave energy with crops and the underlying soils over the growing season, more detailed ground information on crop growth, within-field variation, local climate, etc. are needed. Also, more fields should be included in ground data collection for the calibration and validation of a per-field classifier.
- Field-boundary information is costly to obtain over large areas. Image segmentation is a relatively new image-analysis technology which offers solutions to the problem of identifying boundaries. Further investigations on image segmentation are needed.

- Incidence angle (orbital) effects should also be further investigated for crop classification using RADARSAT multi-incidence angle SAR data.

REFERENCES

Allen, C.T. and F.T. Ulaby. 1984. Modeling the polarization dependence of the attenuation in vegetation canopies. *IGARSS'84*, Strasbourg, France, August, 20-30.

Allen, J.A. 1990. Sensors, platforms and applications: acquiring and managing remotely sensed data. *Applications of Remote Sensing in Agriculture*, Butterworths: London, Boston, pp. 3-18.

Anys, H. and D. He. 1995. Evaluation of textural and multipolarization radar feature for crop classification. *IEEE Transactions on Geoscience and Remote Sensing*, Vol. 33, No. 5, pp. 1170-1181.

Aschbacher J., A. Pongsrihadulchai, S. Karnchanasutham, C. Rodprom, D. R. Paudyal & T. Le Toan. 1995. Assessment of ERS-1 SAR data for rice crop mapping and monitoring. *Proceedings, IGARSS'95*, Florence, Italy, July 10-14, pp. 2183-2185.

Aschbacher, J. 1995. Rice mapping and crop growth monitoring: an ERS/SAR demonstration project. *Earth Observation Quarterly No. 49.* http://esapub.esrin.esa.it/pointtoeoq/eoq49.html.

Atkinson, T.G., M.D. Rigby, and A.D. Kuzyk. 1975. Monitoring cereal cover crops in south western Alberta using colour-infrared aerial photography and Landsat-I data. *Proceedings of the 3rd Canadian Symposium on Remote Sensing*, Edmonton, Alberta, pp. 435-447.

Attema, E.P.W. 1980. Radar signature studies: radar measurements on vegetation, crops and soils, done in the Netherlands from 1975 to 1980 by ROVE team. *EARSel News*, published by the European Association of Remote Sensing Laboratories, pp. 20-31.

Avery, T.E. and G.L. Berlin. 1992. *Fundamentals of Remote Sensing and Airphoto Interpretation*, 5th Ed. New York: Macmillan Publishing Company.

Azzali, S. 1991. Interpretation of crop growth patterns by means of NDVI-time series in Zambia. *Geocarto International*, Vol. 6, No. 3, pp. 15-26.

Babey, S.K. and C.D. Anger. 1989. A compact airborne spectrographic imager (CASI). *Proceedings, IGARSS'89*, Vol. 2, pp. 1028-1031.

Bach, H. and W. Mauser. 1995. Multisensoral approach for the determination of plant parameters of corn. *Proceedings, IGARSS'95*, Florence, Italy, July 10-14, pp. 960-966.

Bachelet, D. 1995. Rice paddy inventory in a few provinces of China using AVHRR data. *Geocarto International*, Vol. 10, No. 1, pp. 23-38.

Badhwar, G.D. 1982. Profile modeling for crop discrimination. *Proceedings, Symposium on Machine Processing of Remote Sensing Data*, Purdue University, West Lafayette, IN, pp. 454-460.

Badhwar, G.D. 1984a. Automatic corn-soybean classification using MSS data. I. Near-harvest crop proportion Estimation. *Remote Sensing of Environment*, 14:15-29.

Badhwar, G.D. 1984b. Automatic corn-soybean classification using MSS data. II. Early season crop proportion Estimation. *Remote Sensing of Environment*, 14:31-37.

Badhwar, G.D., J.G. Garnes, and W.W. Austin. 1982. Use of Landsat-derived temporal profiles for corn-soybean feature extraction and classification. *Remote Sensing of Environment*, 12:57-79.

Badhwar, G.D., C.E. Garganti, and F.V. Redondo. 1987. Landsat classification of Argentina summer crops. *Remote Sensing of Environment*, 2:111-117.

Ban, Y. 1993. *Satellite Synthetic Aperture Radar for a Crop Information System: A Knowledge-Based Approach*, A Research Paper Submitted for a Ph.D. Comprehensive Exam, University of Waterloo, Canada, 45pp.

Ban, Y. and P.J. Howarth. 1995. Application of ERS-1 temporal-spectral SAR profiles for agricultural crop identification - preliminary results. *Proceedings, 17th Canadian Symposium on Remote Sensing*, Saskatoon, Saskatchewan, Canada, June 12-15. pp. 442-447.

Ban, Y. and P.J. Howarth. 1996a. *Spaceborne Radar Remote Sensing for Agricultural Crop Identification: Literature Review*, Prepared for the Canadian Space Agency, 23pp.

Ban, Y. and P.J. Howarth. 1996b. Integration of ERS-1 SAR and Landsat TM data for agricultural crop classification. *Proceedings, the 26th International Symposium on Remote Sensing of Environment/ 18th Canadian Symposium on Remote Sensing*, March 25-29, Vancouver, British Columbia, Canada, pp. 546-549.

Ban, Y., H. McNairn, K. Misurak and D. Wood. 1993. *Modelling C-Band Radar Backscatter from a Corn Canopy Using MIMICS*, Project Report for Geog. 675M, 38pp.

Ban, Y., P.M. Treitz, P.J. Howarth, B. Brisco and R. Brown. 1995. Improving the accuracy of synthetic aperture radar for agricultural crop classification. *Canadian Journal of Remote Sensing, Special Issue on Agriculture*, Vol.21, No. 2, pp. 158-164.

Barber, D.G. and E.F. LeDrew. 1991. SAR sea ice discrimination using texture statistics: a multivariate approach. *Photogrammetric Engineering and Remote Sensing*, Vol. 57, No. 4, pp. 385-395.

Baronti, S., F.D. Frate, P. Ferrazzoli, S. Paloscia, P. Pampaloni, and G. Schiavon. 1995. SAR polarimetric features of agricultural areas. *International Journal of Remote Sensing*, Vol. 16, No. 14, 2639-2656.

Bartholomä, K.-P., R. Benz, D. Denmuth, P. Dubock, B. Gardini, G. Graf and G. Ratier. 1995. ENVISAT-1: on its way to hardware. *Proceedings, IGARSS'95*, Florence, Italy, pp. 1560-1563.

Batlivala, P.P. and Ulaby, F.T. 1976. Radar look direction and row crops. *Photogrammetric Engineering and Remote Sensing*, 42:233-238.

Beaudoin, A., Q.H.J. Gwyn, and T. LeToan. 1989. C-band backscatter sensitivity to multi-scale geometry and soil moisture variability of agricultural surfaces. *Proceedings IGARSS'89 / 12th Canadian Symposium on Remote Sensing*, Vancouver, British Columbia, Vol. 4, pp. 2116-2121.

Beaudoin, A., T. LeToan, and Q.H.J. Gwyn. 1988. Observations on the effect of geometric properties of agricultural soils on radar backscatter, from C-SAR images. *Proceedings of IGARSS '88 Symposium*, Edinburgh, Scotland, Vol. 3, pp. 1595-1598.

Beaudoin, A., T. LeToan, and Q.H.J. Gwyn. 1990. SAR observations and modeling of the C-band backscatter variability due to multiscale geometry and soil moisture. *IEEE Transactions on Geoscience and Remote Sensing*, Vol. 28, No. 5, pp. 886-895.

Bedard, D., R. Brown, J. Naunheimer, B. Brisco, and S. Huang. 1992 Investigating crop rotation knowledge to improve agricultural SAR classifications. *Proceedings, 15th Canadian Symposium on Remote Sensing,* Toronto, Ontario, Canada, pp. 239-244.

Belward, A.S. and J.C. Taylor. 1986. The use of multitemporal Landsat data for improving crop mapping accuracy. *Remote Sensing for Resource Development and Environmental Management.* Eds. M.C. J. Damen, G.S. Smit, and H.T. Verstappen. A.A. Balkema Rotterdam Brookfield., Vol. 1, pp. 381-386.

Benedetti, R. and P. Rossini. 1993. On the use of NDVI profiles as a tool for agricultural statistics: the case study of wheat yield estimate and forecast in Emilia Romagna. *Remote Sensing of Environment*, 45:311-326.

Benediktsson J.A, P.H. Swain and O.K. Ersoy, 1990a. Neural networks approaches versus statistical methods in classification of multi-source remote sensing data. *IEEE Transactions on Geoscience and Remote Sensing*, GE-28(4), pp. 540-552.

Benediktsson J.A, P.H. Swain, O.K. Ersoy and D. Hong, 1990b. Classification of very high dimensional data using neural networks. *Proceedings, IGARSS'90*, May 20-24, College Park, Maryland, U.S. A., Vol.2, pp.1269-1272.

Bénié, G.B., K.P.B. Thomson, and M. Goldberg. 1989. A comparison of four segmentation algorithms in the context of agricultural remote sensing. *ISPRS Journal of Photogrammetry and Remote Sensing*, Vol. 44, pp. 1-13.

Berg, A. 1981. General results of a European remote sensing project (AGRESTE): agronomic considerations and needs of society. *Application of Remote Sensing to Agricultural Production Forecasting*, Berg, A. Ed., A.A. Balkema: Rotterdam, pp. 193-211.

Binder, A.K. 1978. Information requirements on basic food crops of the FAO global information and early warning system on food and agriculture. *Proceedings of the W. Nordberg Memorial Symposium of the Twentieth Plenary Meeting of COSPAR,* Tel Aviv, Israel. Eds. E.A. Godby and J Otterman. Vol. 2, pp. 33-42.

Binnenkade, P. 1986. The determination of optimum parameters for identification of agricultural crops with airborne SLAR data. *Remote Sensing for Resource Development and Environmental Management. Eds. M.C. J. Damen, G.S. Smit, H.T. Verstappen, Published by: A.A. Balkema Rotterdam Brookfield.* Vol. 1, pp. 111-114.

Blakeman, R.H. 1990. The identification of crop disease and stress by aerial photography. *Application of Remote Sensing in Agriculture*, Butterworths: London, Boston. pp. 229-254.

Bönsch, E., R. Winter and G. Schreier. 1988. Investigations of SAR backscatter for different test areas using two geocoded SEASAT SAR scenes. *Proceedings, IGARSS'88*, Edinburgh, Scotland, pp. 1-4.

Borgeaud, M., J. Noll and A. Bellini. 1994. Multi-temporal comparisons of ERS-1 and JERS-1 SAR data for land applications. *IGARSS'94*, Pasadena, California, USA, August 8-12, pp. 1603-1605.

Bouman, B.A.M. 1987. *Radar backscatter from three agricultural crops: beet, potatoes and peas.* Centre for Agrobiological Research (CABO) at Wageningen, the Netherlands, Verlag No. 71.

Bouman, B.A.M. 1991a. Crop parameter estimation from ground-based X-band (3-cm wave) radar backscattering data. *Remote Sensing of Environment*, 37:193-205.

Bouman, B.A.M. 1991b. *Linking X-Band Radar Backscattering and Optical Refelctance with Crop Growth Models*, Ph.D. Thesis, Centre for Agrobiological Research (CABO-DLO) at Wageningen, the Netherlands, 169pp.

Bouman, B.A.M and H.W.J. Van Kasteren. 1990a. Ground-based X-band (3-cm wave) radar backscattering of agricultural crops. I. sugar beet and potato; backscattering and crop growth. *Remote Sensing of the Environment.* 34:93-105.

Bouman, B.A.M and H.W.J. Van Kasteren. 1990b. Ground-based X-band (3-cm wave) radar backscattering of agricultural crops. II. wheat, barley, and oats; the impact of canopy structure. *Remote Sensing of the Environment*, 34:107-119.

Bouman, B.A.M. and D.H. Hoekman. 1993. Multi-temporal, multi-frequency radar measurements of agricultural crops during the Agriscatt-88 campaign in the Netherlands. *International Journal of Remote Sensing*, Vol. 14, No. 8, pp. 1595-1614.

Bowker, D.E. 1985. Priorities for worldwide remote sensing of agricultural crops. *Photogrammetric Engineering and Remote Sensing*, Vol. 51, No. 10, pp.1625-1631.

Bradley, G.A. and F.T. Ulaby. 1981. Aircraft Radar Response to Soil Moisture. *Remote Sensing of the Environment.* 11:419-438.

Brakke, T.W., E.T. Kanemasu, J.L. Steiner, F.T. Ulaby, and E. Wilson. 1981. Microwave radar response to canopy moisture, leaf-area index, and dry weight of wheat, corn and sorghum. *Remote Sensing of Environment*, 11:207-220.

Brisco, B. 1993. *Radar Imaging of Vegetation and Soil.* Guest lecture, Department of Geograpgy, University of Waterloo, Canada.

Brisco, B. and R.J. Brown. 1990. Drought stress evaluation in agricultural crops using C-HH SAR data. *Canadian Journal of Remote Sensing*, Vol. 16, No. 3, pp.56-62.

Brisco B. and R.J. Brown. 1995. Multidate SAR/TM synergism for crop classification in western Canada. Photogrammetric Engineering and Remote Sensing, 61(8), pp. 1009-1014.

Brisco, B. and R. Protz. 1980a. *Radar Image Tone and Texture Analysis of Agricultural Targets in the University of Guelph Test Strip.* Guelph: University of Guelph, 35pp.

Brisco, B. and R. Protz. 1980b. Corn field identification accuracy using airborne radar imagery. *Canadian Journal of Remote Sensing*, Vol. 6, No. 1, pp. 15-25.

Brisco, B. and R. Protz. 1982. Manual and automatic crop identification with airborne radar imagery. *Photogrammetric Engineering and Remote Sensing*, Vol. 48, No. 1, pp. 101-109.

Brisco, B, F.T. Ulaby, and R. Protz. 1984. Improving crop classification through attention to the timing of airborne radar acquisitions. *Photogrammetric Engineering and Remote Sensing*, Vol. 50, No. 6, pp. 739-745.

Brisco, B., R.J. Brown, and M.J. Manore. 1989a. Early season crop discrimination with combined SAR and TM data. *Canadian Journal of Remote Sensing* , Vol. 15, No. 1, pp. 44-54.

Brisco, B., R.J. Brown, and T.J. Pultz. 1989b. The effects of free canopy water on SAR crop separability. *Proceedings, IGARSS'89 / 12th Canadian Symposium on Remote Sensing*, Vancouver, British Columbia, Vol. 2, pp. 424-428.

Brisco, B., R.J. Brown, J. A. Koehler, G.J. Sofko, and M.J. McKibben. 1990. The diurnal pattern of microwave backscattering by wheat. *Remote Sensing of the Environment*, Vol. 34, No. 1, pp.37-47.

Brisco, B., R.J. Brown, B. Snider, G.J. Sofko, J.A. Koehlar, and A.G. Wacker. 1991. Tillage effects on the radar backscattering coefficient of grain stubbled fields. *International Journal of Remote Sensing*, Vol 12, pp. 2283-2298.

Brisco, B., R. J. Brown, J. G. Gairns and B. Snider. 1992. Temporal ground-based scatterometer observations of crops in western Canada. *Canadian Journal of Remote Sensing*. Vol. 18, No. 1, pp. 14-21.

Brown, R.J. 1986. An overview of remote sensing agricultural applications in North America: past, present and future. *Proceedings, IGARSS'86*. pp. 733-737.

Brown, R.J. 1987. Preparing for satellite microwave systems for renewable resource management. *Geocarto International*, Vol. 2, No. 3, pp. 31-37.

Brown, R. J., B. Guindon, P.M. Teillet and D. G. Goodenough. 1984. Crop type determination from multitemporal SAR imagery. *Proceedings, 9th Canadian Symposium on Remote Sensing*, St. John's, Newfoundland. pp. 683-691.

Brown, R.J., R. Leconte, B.G. Brisco, C.A. Hutton, D. Mullins, J.G. Gairns, Q.H.J. Gwyn, R. Protz, J. Fischer, P.J. Howarth, P.M. Treitz, J.B. Boisvert, and K.P.B. Thomson. 1991. Oxford County Soil Moisture Experiment (OXSOME) Overview. *Proceedings, 14th Canadian Symposium on Remote Sensing*, Calgary, Alberta, pp. 512-518.

Brown, R.J., M.J. Manore and S. Poirier. 1992. Correlations between X-, C-, and L-band imagery within an agricultural environment. *International Journal of Remote Sensing*, Vol. 13, No. 9, pp. 1645-1661.

Brown, R. J., D. Bedard, B. Brisco and J. Naunheimer. 1993a. Multi-temporal ERS-1 for crop discrimination. *Proceedings, the Second ERS-1 Symposium: Space at the Service of Our Environment*, ESA SP-361, Vol. 1, pp. 57-62. Hamburg, Germany.

Brown, R.J., B. Brisco, R. Leconte, D.J. Major, J.A. Fischer, G. Reichert, K.D. Korporal, P.R. Bullock, H. Pokrant, and J. Culley. 1993b. Potential applications of RADARSAT data to agriculture and hydrology. *Canadian Journal of Remote Sensing*, Vol. 19, No. 4, pp. 317-329.

Brown, R.J., J.S. Peterson and M. McKean. 1996. Benefits of RADARSAT - N Configurations for Future applications. *Proceedings, 26th International Symposium on Remote Sensing of Environment and 18th Annual Symposium of the Canadian Remote Sensing Society*, March 25-29, 1996, Vancouver, B.C., Canada.

Bruckler, L., H. Witono and P. Stengel. 1988. Near surface soil moisture estimation from microwave measurements. *Remote Sensing of Environment*, 26:101-121.

Bush, T.F. and F.T. Ulaby. 1978. An evaluation of radar as a crop classifier. *Remote Sensing of Environment*, 7:15-36.

Campbell, J.B. 1987. *Introduction to remote sensing*, New York, London: The Guilford Press.

Campbell, F.H.A., R.A. Ryerson and R.J. Brown. 1995. GlobeSAR: a Canadian radar remote sensing program. *Geocarto International*, Vol. 10, No. 3, pp. 3-7.

Canada Department of Agriculture. 1986. *Four Band Airborne Radar Imagery for Agricultural Applications*. Agriculture Canada, Research Branch, Technical Bulletin 1986-14E.

CCRS. 1992. *ERS-1: Canadian User Guide*, Canada Centre for Remote Sensing Brochure, 22pp.

Chen, K.S., W.P. Huang, D.H. Tsay, and F. Amar. 1996. Classification of multifrequency polarimetric SAR imagery using a dynamic learning neural network. *IEEE Transactions on Geoscience and Remote Sensing*, vol.34, No. 3, pp. 814-820.

Chen, S.C., G.T. Batista and A.T. Tardin. 1986. LANDSAT TM band combination for crop discrimination. *Remote Sensing for Resource Development and Environmental Management*. Eds. M.C. J. Damen, G.S. Smit, H.T. Verstappen, A.A. Balkema Rotterdam Brookfield, Vol. 1, pp. 211-214.

Chuah, H.T. and H.S. Tan. 1990. A multiconstituent and multilayer microwave backscatter model for a vegetative medium. *Remote Sensing of Environment*, 31:137-153.

Churchill, P.N. and E.P.W. Attema. 1994. The MAESTRO 1 European airborne polarimetric synthetic aperture radar campaign. *International Journal of Remote Sensing*, Vol. 15, No. 14, pp. 2707-2717.

Churchill, P.N., A.I.D. Horne and R. Kessler. 1985. A review of radar analysis of woodland. *Proceedings, EARSeL Workshop- Microwave Remote Sensing Applied to Vegetation*, Amsterdam, ESA Publication, SP-227, pp. 25-32.

Cihlar, J. 1986. On the relationship between agroclimatic region, crop parameters, and SAR image tone in Western Canada. *Canadian Journal of Remote Sensing* , Vol. 12, No. 2, pp. 81-93.

Cihlar, J. and T. Hirose. 1984. On the SAR response of agricultural targets in a northern prairie environment. *Proceedings of IGARSS '84 Symposium*, Strasbourg, France.

Cihlar, J., C. Prévost, and H. Vickers. 1986a. Interpretation of prairie land cover types from SIR-B data. *Proceedings 10th Canadian Symposium on Remote Sensing*, Edmonton, Alberta, pp. 885-894.

Cihlar, J., R.J. Brown, and B. Guindon. 1986b. Microwave remote sensing of agricultural crops in Canada. *International Journal of Remote Sensing*, Vol. 7, No. 2, pp. 195-212.

Cihlar, J., M.C. Dobson, T.J. Schmugge, P. Hoogeboom, A.R.P. Janse, F. Baret, G. Guyot, T. Le Toan, and P. Pampaloni. 1987. Procedures for the description of agricultural crops and soils in optical and microwave remote sensing studies. *International Journal of Remote Sensing*, Vol. 8, No. 3, pp. 427-439.

Clevers, J.G.P.W. 1986. The use of multispectral photography in agrcultural research. *Remote Sensing for Resource Development and Environmental Management.* Eds. M.C. J. Damen, G.S. Smit, H.T. Verstappen, A.A. Balkema Rotterdam Brookfield. Vol. 1, pp. 227-232.

Clevers, J.G.P.W., C. Büker, H.J.C. van Leeuwen, and B.A.M. Bouman. 1994. A framework for monitoring crop growth by combining directional and spectral remote sensing information. *Remote Sensing of Environment*, 50:161-170.

Colwell, R.N. 1983. *Manual of Remote Sensing*, Vol. I & II, Second Edition, Editor-in-Chief: Colwell, R.N, American Society of Photogrammetry, the Sheridan Press, Virginia.

Colwell, R.N., D. Carneggie, R. Croxton, F. Manzer, D. Simonett, and D. Steiner. 1970. Application of remote sensing in agriculture and forest. *Remote Sensing: With Special Reference to Agriculture and Forestry*, National Academy of Sciences:Washington, D.C., pp. 164-223.

Coppo, P., P. Ferrazzoli, G. Luzi, S. Paloscian and C. Susini. 1992. MAC-91 on Montespertoli: preliminary analysis of multifrequency SAR sensitiviti to soil and vegetation parameters. *Proceedings, IGARSS'92*, May 26-29, Houston, Texas, pp. 489-491.

Crist. E.P. 1984. Effects of cultural and environmental factors on corn and soybean spectral development pattern. *Remote Sensing of Environment*, 14:3-13.

Crist, E.P and R.C. Cicone. 1984. Application of the tasselled cap concept to simulated thematic mapper data. *Photogrammetric Engineering and Remote Sensing*, Vol. 50, pp. 343-352.

Crist, E.P. and W.A. Milila. 1980. A temporal-spectral analysis technique for vegetation applications of Landsat. *Proceedings, 14th International Symposium on Remote Sensing of Environment*, San Jose, Costa Rica, pp. 1031-1040.

Crist, E.P. and W.A. Milila. 1981. A technique for automatic labeling of Landsat agricultural scene elements by analysis of temporal-spectral patterns. *Proceedings, 15th International Symposium on Remote Sensing of Environment*, Ann Arbor, Michigan, pp. 1227-1236.

Crosson, L.S., F.G. Peet and D.W.L. Read. 1975. Agricultural crop reflectance studies using landsat-I data. *Proceedings of the 3rd Canadian Symposium on Remote Sensing*, Edmonton, Alberta, pp. 427-433.

CSA. 1996a. *RADARSAT's Application Development and Research Opportunity (ADRO)*. http://radarsat.space.gc.ca/ENG/Activities/Programs/adro.html

CSA. 1996b. *RADARSAT User Development Program (RUDP)*. http://radarsat.space.gc.ca/ENG/Activities/Programs/rudp.html

CSA. 1996c. *The Canadian Space Agency's Homepage*. http://radarsat.space.gc.ca/ENG/RADARSAT/description.html.

CSA, NASA and RSI. 1994. RADARSAT System Description. *RADARSAT: ADRO Program Announcement*, Volume II, 35pp.

Curlander , J.C. and R.N. McDonough. 1991. *Synthetic Aperture Radar: Systems and Signal Processing*, John Wiley and Sons, Inc., New York.

Daughtry, C.S.T., K.J. Ranson and L.L. Biehl. 1991. C-band backscattering from corn canopies. *International Journal of Remote Sensing*, 12(5):1097-1109.

Dawbin K.W. and J.C. Evans. 1988. Large area crop classification in New South Wales, Australia, using Landsat data. *International Journal of Remote Sensing*. Vol. 9 No. 2, pp.295-301.

De Loor, G.P. 1980. Survey of radar applications in agriculture. *Remote Sensing Application in Agriculture and Hydrology*, Fraysse, G. Ed., Netherland: A.A. Balkema/Rotterdam, pp. 215-232.

De Loor, G.P. 1984. Variation of the radar backscatter of vegetation through the growing season. *Proceedings, Microwave Remote Sensing Applied to Vegetation Workshop*, Amsterdam: European Space Agency - Scientific and Technical Publications, pp. 63-67.

De Matthaeis, P., P. Ferrazzoli, L. Guerriero, G. Schiavon, D. Solimini, and P. Tognolatti. 1991. Radar response to vegetation parameters: comparison between theory and MAESTRO-1 results. *Proceedings, IGARSS'91*, June 3-6, Espoo, Finland, pp. 685-687.

De Matthaeis, P., G. Schiavon, and D. Solimini. 1994. Effect of scattering mechanisms on polarimetric features of crops and trees. *International Journal of Remote Sensing*, Vol. 15, No. 14, pp. 2917-2930.

De Matthaeis, P., P. Ferrazzoli, G. Schiavon, and D. Solimini. 1995. Crop type identification and biomass estimation by SAR. *Proceedings, IGARSS'95*, Florence, Italy, pp. 957-959.

Dejace, J. and J. Megier. 1980. AGRESTE project: experience gained in data processing, main results on rice, poplar and beech inventories. *Remote Sensing Application in Agriculture and Hydrology*, Netherland: A.A. Balkema/Rotterdam, pp. 309-328.

Dixon, R. and A. Mack. 1990. Crop discrimination in the carberry area with combined SAR and TM data. *Proceeding, 14th Canadian Remote Sensing Symposium*, pp. 118-123.

Dobbins, R., K. Korporal, P. Nixon, B. Brisco and R. Brown. 1992. A comparison between multi-date C-HH and C-VV SAR digital imagery for potato crop monitoring. *Proceedings, 15th Canadian Symposium on Remote Sensing*. June 1-4, Toronto, Ontario, Canada. pp. 245-250.

Dobson, M.C. and F.T. Ulaby. 1986a. Preliminary evaluation of the SIR-B response to soil moisture, surface roughness, and crop canopy cover. *IEEE Transactions on Geoscience and Remote Sensing*, Vol. GE-24, No. 4, pp. 517-526.

Dobson, M.C. and F.T. Ulaby. 1986b. Active microwave soil moisture research. *IEEE Transactions on Geoscience and Remote Sensing*, GE-24:23-36.

Dobson, M.C., L.P. Pierce, K. Sarabandi, F.T. Ulaby, T. Sharik. 1992. Preliminary analysis of ERS-1 SAR for forest ecosystem studies. *IEEE Transactions on Geoscience and Remote Sensing*, GE-20:203-210.

Dornier Deutsche Aerospace and British Aerospace Space Systems. 1994. *ENVISAT-1 Mission System: Preliminary Design Review - Executive Summary*, 52pp.

Drake, B., R.A. Schuchman, M.L. Bryan, R.W. Larson, and C.L. Liskow. 1974. *The Application of Airborne Imaging Radars (L and X-band) to Earth Resources Problems*, Report No. NASA-CR-139385-1, Environmental Research Institute of Michigan.

Dubé, C., H. Proulx, and K.P.B. Thompson. 1986. Analysis of the spatial structure of synthetic aperture radar (SAR) imagery for a better separability of cereal crops, wheat and barley. *Proceedings of IGARSS '86 Symposium*, Zurich, Switzerland, Vol. 2, 745-750.

Dubois, P.C., E. Rignot, and J.J. van Zyl. 1992. Direction angle sensitivity of agricultural field backscatter with AIRSAR data. *Proceedings, IGARSS'92*, May 26-29, Houston, Texas, pp. 1680-1682.

Dubois, P.C., J. van Zyl, and T. Engman. 1995. Measureing soil moisture with imaging radars. *IEEE Transactions on Geoscience and Remote Sensing*, Vol. 33, No. 4, pp.915-926.

Durand, E.T. 1987. SAR data filtering for classification. *IEEE Transactions on Geoscience and Remote Sensing*, GE-25, pp. 629-637.

Ehrlich, D., J. Estes and J. Scepan. 1990. Improving crop type determination using satellite imagery: a study for the regione del Veneto, Italy. *Geocarto International*, (2):35-47.

Ehrlich, D. J. E. Estes, J. Scapan, and K.C. McGwire. 1994. Crop area monitoring within an advanced agricultural information system. *Geocarto International*, (4):31-41.

Engman, E. T. 1990. Progress in microwave remote sensing of soil moisture. *Canadian Journal of Remote Sensing*, Vol. 16, No. 3, 6-14.

Engman, E.T. 1991. Applications of microwave remote sensing of soil moisture for water resources and agriculture. *Remote Sensing of the Environment*, 35:213-226.

Erb, R.B. 1980. The large area crop inventory ecperiment (LACIE): methodology for area, yield and production estimation, results and perspectives. *Remote Sensing Application in Agriculture and Hydrology*, Fraysse ED. A.A. Balkema, Rotterdam, pp. 285-297.

ESA. 1989. *ERS-1: European Remote Sensing Satellite*, European Space Agency Publication, BR-36, 38pp.

ESA. 1992. *ERS-1 User Handbook*, European Space Agency Publication, SP-1148, 159pp.

ESA. 1995a. *Committee on Earth Observation Satellites: Coordination for the Next Decade (1995 CEOS Yearbook)*, Published by Smith System Engineering Limited, UK, pp. 61-120.

ESA. 1995b. *CEOS Special Report on Successful Applications of EO Satellite Data.* Published by Smith System Engineering Limited, UK.

ESA. 1996a. *Missions Completed: METEOSAT*, http://www.esoc.esa.de/external/mso/meteosat.html.

ESA. 1996b. *Meteosat Satellite Description*,. http://gds.esrin.esa.it/CMETEO.DES;sk=6598B307.

ESRIN/ESA. 1996. *ESRIN/ESA Earth Remote Sensing User Services*, http://gds.esrin.it:80/euro_ers.

Eurimage. 1994. *The ERS-1 Satellite: What's It All About?* Eurimage Brochure, 63pp.

Evans, D.L. 1992. Current status and future developments in radar remote sensing. *Journal of Photogrammetry and Remote Sensing*, 47:79-99.

FAO. 1993. *High Resolution Satellite Data for Agricultural Statistics*, Food and Agriculture Organization of the Unites Nations, Remote Sensing for Decision-Makers Series, No. 4.

FAS. 1996. *Remote Sensing: International Crop Condition and Production Analyses*, Foreign Agricultural Service, U.S. Department of Agriculture, http://ffas.usda.gov/ffas/fas-programs-services-resources/fas-programs/fas-commodity/remote.html.

Ferrazzoli, P., S. Paloscia, P. Pampaloni, G. Schiavon, D. Solimini, and P.Coppo. 1992 Sensitivity of microwave measurements to vegetation biomass and soil moisture content: a case study. *IEEE Transactions on Geoscience and Remote Sensing*, Vol. 30, No. 4, pp. 750-756.

Ferster, W. 1996. Pentagon Will Pay for Radar Imagery Mission. *Space News*, Vol. 7, No. 29, July 22-28. pp. 6

Filho, O.C. R., E. D. Soulis, N. Kouwen, A. Abdeh-Kolahchi, T.J. Pultz, and R. Crevier. 1996. Soil moisture in pasture fields using ERS-1 SAR data: preliminary results. *Canadina Journal of Remote Sensing, Special Issue on Hydrology Applications*, Vol. 22, No. 1, pp.95-107.

Fischer, J.A., and R.S. Mussakowski. 1989. Preliminary evaluation of multi-date SAR data for the identification of agricultural crops in Southern Ontario. *Proceedings*,

IGARSS'89 / 12th Canadian Symposium on Remote Sensing, Vancouver, British Columbia, Canada, Vol. 2, pp. 430-433.

Fischer, J.A., R.J. Brown, and B. Brisco. 1992. The effects of changes in soil moisture and rainfall on SAR data crop classification. *Proceedings, 15th Canadian Symposium on Remote Sensing*, Toronto, Ontario, Canada, pp. 221-226.

Fiumara, A., and N. Pierdicca. 1989. Evaluation of classification results obtained with combined multitemporal optical and microwave data. *Proceedings IGARSS'89 / 12th Canadian Symposium on Remote Sensing*, Vancouver, British Columbia, Vol. 2, pp. 787-790.

Fog B., J. Poulsen, I. Sandholt and H. M. Skriver. 1993. Monitoring land cover and crop types in Denmark using ERS-1 SAR and optical satellite images. *Proceeding, International Symposium from Optics to Radar, SPOT and ERS Applications*, Paris, France, CNES series no. 312, pp. 71-80.

Foody, G.M. 1988. Crop classification from airborne synthetic aperture radar data. *International Journal of Remote Sensing*, Vol. 9, No. 4, pp. 655-668.

Foody, G.M. 1996. Relating the land-cover composition of mixed pixels to artificial neural network classification output. *Photogrammetric Engineering and Remote Sensing*, 61(5):491-498.

Foody, G.M., P.J. Curran, G.B. Groom, and D.C. Munro. 1989. Multi-temporal synthetic aperture radar data for crop classification. *Geocarto International*, Vol. 4, No. 3, pp. 19-29.

Foody, G.M., M.B. McCulloch, and W.B. Yates. 1994. Crop classification from C-band polarmetric radar data. *International Journal of Remote Sensing*, 15(14), pp. 2871-2885.

Foody, G.M., M.B. McCulloch, and W.B. Yates. 1995. Classification of remotely sensed data by an artificial neural network: issues related to training data characteristics. *Photogrammetric Engineering and Remote Sensing*, 61(4):391-401.

Freeman, A. 1992. SAR calibration: an overview. *IEEE Transactions on Geoscience and Remote Sensing*, Vol. 30, No. 6, pp. 1107-1121.

Freeman, A. and J.C. Curlander. 1989. Radiometric correction and calibration of SAR images. *Photogrammetric Engineering and Remote Sensing*, 55(9):1295-1301.

Freeman, A., J. Villasenor, J.D. Klein, P. Hoogeboom, and J. Groot. 1994. On the use of multi-frequency and polarimetric radar backscatter features for classification of agricultural crops. *International Journal of Remote Sensing*, Vol. 15, No. 9, pp. 1799-1812.

Gandia, S., V. Caselles, A. Gilabert and J. Melia. 1986. Spectral signature of rice fields using Landsat-5 TM in the Mediterranean coast of Spain. *Remote Sensing for Resource Development and Environmental Management.* Eds. M.C. J. Damen, G.S. Smit, H.T. Verstappen, A.A. Balkema Rotterdam Brookfield, Vol. 1, pp. 257-260.

Gardell, F., R.J. Brown, B. Brisco and J. Naunheimer. 1993. *ERSOME 1992 Experiment Data Collection Report*, Canada Centre for Remote Sensing.

Gardner, G. 1996. Preserving agricultural resources. *State of the World 1996: A Worldwatch Institute Report on Progress Toward a Sustainable Society*, W W Norton & Company: New York, London. pp. 78-86.

Geomatics Canada. 1994. *Canada Centre for Remote Sensing Airborne C/X SAR*, Geomatics Canada Brochure.

GER. 1995. Sensor firm announces plan to develop satellite system for crop monitoring. *Earth Observations Magazine*, August, pp.7.

Gillespie, T.J., B. Brisco, R.J. Brown, and G.J. Sofko. 1990a. Radar detection of a dew event in wheat. *Remote Sensing of Environment*, Vol. 33, pp. 151-156.

Gillespie, T.J., R.J. Brown, B. Brisco, R. Protz, and S. Sweeney. 1990b. Plant surface wetness detection in an agricultural environment with SAR data. *Proceedings of the Thirteenth Canadian Symposium on Remote Sensing*, Fredericton, New Brunswick, pp. 183-189.

Gillot, J. 1980. Potential applications of remote sensing in agriculture. *Remote Sensing Application in Agriculture and Hydrology*. Fraysse ED. A.A. Balkema, Rotterdam. pp. 1-7.

Gilson, J.C. 1989. *World Agricultural Changes: Implications for Canada.* C. D. Howe Institute, Toronto and Calgary. pp. 28.

Giovacchini, A. 1986. An evaluation of different green vegetation indices for wheat yield forecasting. *Remote Sensing for Resource Development and Environmental Management.* Eds. M.C. J. Damen, G.S. Smit, H.T. Verstappen, A.A. Balkema Rotterdam Brookfield. Vol. 1, pp. 265-267.

Goodenough, D.G., P.M. Teillet, and B. Guindon. 1980. Integration and comparison of SAR and MSS data for potato crop area estimation. *Proceedings, 6th Canadian Symposium on Remote Sensing,* Halifax, Nova Scotia. pp. 127-142.

Goodman, M.S. 1959. A technique for the identification of farm crops on aerial photographs. *Photogrammetric Engineering*, 25: 131-137.

Groten, S.M.E. 1993. NDVI - crop monitoring and early yield assessment of Burkina Faso. *International Journal of Remote Sensing.* Vol. 14, No. 8, pp.1495-1515.

Guindon, B., P.M. Teillet, D. G. Goodenough, J.J. Palimaka and A. Sieber. 1984. Evaluation of the crop classification performance of X, L and C-band SAR imagery. *Canadian Journal of Remote Sensing*, 10(1):4-16.

Hall, F.G. and G.D. Badhwar. 1987. Signature-extendable technology: global crop recognition. *IEEE Transactions on Geoscience and Remote Sensing.* Vol. GE-25, No. 1, pp. 93-103.

Hall-Könyves, K. 1990. Crop monitoring in Sweden. *International Journal of Remote Sensing.* Vol. 11, No. 3, pp.461-484.

Haralick, R.M. 1979. Statistical and structural approaches to texture. *Proceedings of the IEEE*, Vol. 67, No. 5, pp.786-804.

Haralick, R.M., F. Caspall, and D.S. Simonett. 1969-1970. Using radar imagery for crop discrimination: a statistical and conventional probability study. *Remote Sensing of Environment*, 1:131-142.

Haralick, R.M., Shanmugam, K., and I. Dinstein. 1973. Textural features for image classification. *IEEE Transactions on Systems, Man, and Cybernetics*, Vol. 3, No. 6, pp. 610-621.

Heydorn, R.P. and H.C. Takacs. 1986. On the design of classifiers for crop inventories. *IEEE Transactions on Geoscience and Remote Sensing*, Vol. GE-24, No. 1, pp. 150-168.

Hielkema, J.U. and F.L. Snijders. 1993. *Operational Use of Environmental Satellite Remote Sensing and Satellite Communications Technology for Global Food Security and Locust Control by FAO: the ARTEMIS and DIANA Systems*, FAO Report, 22pp.

Hirose T., J. Cihlar, and A. Mack. 1984. Discrimination of agricultural crops in Canada with SAR plus VIR data: initial results. *Proceeding, 8th Canadian Remote Sensing Symposium*, pp. 387-403.

Hixson, M.M., B.J. Davis, M.E. Bauer. 1981. Sampling Landsat classifications for crop area estimation. *Photogrammetric Engineering and Remote Sensing*, Vol. 47, No. 9, pp.1343-1348.

Hochheim, K.P., D.G. Barber and P.R. Bullock. 1996. Spring wheat yield prediction for western Canada using weekly NOAA AVHRR composites. *Proceedings, IGARSS'96*, May 27-31, Lincoln, Nebraska, USA, pp. 1992-1994.

Holmes, M.G. 1990. Applications of radar in agriculture. *Applications of Remote Sensing in Agriculture*, edited by J.A. Clarke and M.D. Steven, London, Toronto: Butterworths.

Hoogeboom, P. 1983. Classification of agricultural crops in radar images. *IEEE Transection on Geoscience and Remote Sensing*, GE-21, No. 3, pp. 329-336.

Hoogeboom, P. 1986. Identifying agricultural crops in radar images. *Remote Sensing for Resource Development and Environmental Management.* Eds., M.C. J. Damen, G.S. Smit, and H.T. Verstappen, A.A. Balkema Rotterdam Brookfield. Vol. 1, pp. 131-135.

Horn, R. 1996. The DLR airborne SAR project E-SAR. *Proceedings, IGARSS'96*, May 27-31, Lincoln, Nebraska, USA, pp. 1624-1628.

Howarth, P.J. and R. Protz. 1991. Radar Imagery for an Agricultural Monitoring System. *ISTS Task Force on Remote Sensing Information for Resource Management*, pp. 1-5.

Hutchinson, C.F. 1991. Use of satellite data for famine early warning in sub-Saharan Africa. *International Journal of Remote Sensing*. Vol. 12, No. 6, pp. 1405-1421.

Hutton, C.A. and R.J. Brown. 1986. Comparison of space and airborne L-HH radar imagery in an agricultural environment. *Proceedings of the 10th Canadian Symposium on Remote Sensing*, Edmonton, Alberta, Vol. 1, pp. 171-181.

Hutton, C.A. and R.J. Brown. 1989. Effect of row aspect, and incidence angle on radar backscatter. *Proceedings IGARSS'89 / 12th Canadian Symposium on Remote Sensing*, Vancouver, British Columbia, Vol. 3, pp. 1156-1159.

Hutton, C., B. Brisco, R. Brown, and D. Lorente. 1990. *OXSOME: Oxford County Soil Moisture Experiment - Data Documentation*, Unpublished Report, Applications Division, Canada Centre for Remote Sensing, Ottawa, 16 pp.

Ishiguro, E., M.K. Kumar, Y. Hidaka, S. Yoshida, M. dato, M. Miyazato and J.Y. Chen. 1993. Use of rice response characteristics in area estimation by LANDSAT/TM and MOS-1 satellites data. *ISPRS Journal of Photogrammetry and Remote Sensing*, 48(I): 26-32.

Janssen, L.L.F. and H. Middelkoop. 1992. Knowledge-based crop classification of a Landsat Thematic Mapper image. *International Journal of Remote Sensing*, Vol. 13, No. 15, pp. 2827-2837.

Jensen, J.R. 1986. *Introductory Digital Image Processing: A Remote Sensing Prespctive*. Englewood Cliffs, New Jersey: Prentice-Hall.

Jordan, R.L., B.L. Huneycutt, and M. Werner. 1995. The SIR-C/X-SAR synthetic aperture radar system. *IEEE Transactions on Geoscience and Remote Sensing*, Vol. 33, No. 4, pp. 829-839.

JPL. 1996. *JPL Homepage*, http://southport.jpl.nasa.gov:80/scienceapps/instruments.html.

Kalensky, Z.D. 1992. Overview of FAO remote sensing activities. *Space in the Service of the Changing Earth*, Munich, Germany, March 30 - April 4, p.12.

Kanellopoulos I., A. Varfis, G.G. Wilkinson, and J. Mégier, 1991. Neural network classification of multi-date satellite imagery. *Proceedings, IGARSS'91*, June 3-6, Espoo, Finland, pp. 2215-2218.

Kauth, R.J. and G.S. Thomas. 1976. The tasselled cap, a graphic description of the spectral-temporal development of agricultural crops as seen by Landsat. *Proceedings, the 3rd Symposium on Machine Processing of Remote Sensing Data*, Purdue University, West Lafayette, IN, pp. 41-51.

Ketting, R.L. and D.A. Landgrebe. 1975. Classification of multispectral image data by extraction and classification of homogeneous objects. *Proceeding, Symposium on Machine Classification of Remotely Sensed Data.* West Lafayette, pp. 2A-1--2A-11.

Kleschenko, A.D. 1992. Applying of remote sensing data to agriculture. *Remote Sensing from Research to Operation*, Eds. A.P. Cracknell and R.A. Vaughan, the Remote Sensing Society, Department of Geography, University of Nottingham, Nottingham, England, pp.208-221.

Kohl, H., C. King and H.D. Groof. 1993. Agricultural statistics: comparison of ERS-1 and SPOT for the crop acreage estimation of the MARS-project. *Proceedings of the Second ERS-1 Symposium: Space at the Service of Our Environment*, ESA SP-361, Vol. 1, pp. 87-92, October 11-14, Hamburg, Germany.

Kohl, H., E. Nezry and H. De Groof. 1995. Crop acreage estimation with ERS-1 PRI images *Earth Observation Quarterly*, Nr. 46, http://esapub.esrin.esa.it/pointtoeoq/eoq46.html.

Kontoes, C., G.G. Wilkinson, A. Burrill, S. Goffredo, and J. Mégier. 1993. An experimental system for the integration of GIS data in knowledge-based image analysis for remote sensing of agriculture. *International Journal of Remote Sensing*, Vol.7, No. 3, pp. 247-262.

Kramer, H.J. 1992. *Earth Observation Remote Sensing: Survey of Missions and Sensors.* Springer-Verlag, 251pp.

Krul, L. 1987. The microwave remote sensing program for agriculture and forestry in the Netherlands. *Remote Sensing for Resources Development and Environmental Management, Proceedings of the 7th International Symposium for Resources Development and Environmental Management*, Ed. by Damen/G. Sicco SMIT/H.TH. Verstappen, ISPRS Commission VII, Enschede, August 25-29, pp. 1033-1040.

Krul, L. 1988. Some results of microwave remote sensing research in the Netherlands with a view to land applications in the 1990s. *International Journal of Remote Sensing.* 9:1553-1563.

Kühbauch, W., M.J.W. Davidson, R. Steingieber and K. Dockter. 1995. Investigation of agricultural land use in Italy and Germany by means of the multi-band/multi-frequency SIR-C/X-SAR system. *IGARSS'95*, Florence, Italy, pp. 1061-1063.

Kumar, R. 1977. Eveluation of spectral channles and wavelength regions for separability of agricultural cover types. *Proceedings, 11th International Symposium on Remote Sensing of Environment*, Vol. 2, pp. 1081-1090.

Kumar, R. and L.F. Silva. 1977. Separability of agricultural cover types by remote sensing in the visible and infrared wavelength regions. *IEEE Transections on Geoscience Electronics*, Vol GE-15, pp. 19-26.

Kurosu, T., M. Fujuta, and K. Chiba. 1995. Monitoring of rice crop growth from space using the ERS-1 C-band SAR. *IEEE Transactions on Geoscience and Remote Sensing*, Vol. 33, pp. 1092-1096.

Kurosu, T., T. Suitz, M. Fujita, K. Chiba, and T. Moriya. 1993. Rice crop monitoring with ERS-1 SAR: a first year result. *Proceedings, the Second ERS-1 Symposium: Space at the Service of Our Environment*, ESA Publication, SP-361, Vol. 1, pp. 97-101, October 11-14, Hamburg, Germany.

Kutzner, P.L. 1991. *World Hunger: A Reference Handbook.* Contemporary World Issues. ABC-CLIO: Santa Barbara, California, Oxford, England.

Laboratory for Applications of Remote Sensing. 1970. *Remote Multispectral Sensing in Agriculture.* Purdue University, Annual Report, Vol. 3.

Lannelongue, N. 1981. Agriculture and microwave remote sensing. *Application of Remote Sensing to Agricultural Production Forecasting*, Edited by A. Berg, A.A. Balkema: Rotterdam, pp. 231-260.

Lantieri, D. 1993. *Use of Remote Sensing for Development Projects Assisted by the World Food Programme*, FAO Brochure.

Laur, H. 1992. *ERS-1 SAR Calibration: Derivation of Backscattering Coefficient σ° in ERS-1.SAR.PRI Product*, ESRIN/ESA Document, Issue 1, Rev. 0, 17pp.

Laur, H., P. Meadows, J.I. Sanchez, and E. Dwyer. 1993. ERS-1 SAR radiometric calibration. Proceedings of *SAR Calibration Workshop: CEOS Calibration Working Group SAR Calibration Sub-Group*, pp. 257-281, September 20-24, ESTEC/ESA, Noordwijk, The Netherlands.

Laycock, J.E. and H. Laur. 1994. *ERS-1 SAR Antenna Pattern Estimation*, ESRIN/ESA Document, ES-TN-DPE-OM-JL01, Issue 1, Rev. 1.

Le Toan, T., and H. Laur. 1988. Multi-temporal and dual polarisation observations of agricultural crops by X-Band SAR images. *Proceedings, IGARSS'88*, Edinburgh, Scotland, Vol. 3, pp. 1291-1294.

Lechi, G.M., 1980. Survey of photointerpretation techniques in agricultural inventories; identification of crops, discrimination of species, biomass evaluation ECC typical results. *Remote Sensing Application in Agriculture and Hydrology*. Netherland: A.A. Balkema/Rotterdam, pp.17-24.

Lemoine, G.G., G.F. de Grandi, and A.J. Sieber. 1994. Polarimetric contrast classification of agricultural fields using MAESTRO 1 AIRSAR data. *International Journal of Remote Sensing*, Vol. 15, No. 14, pp. 2851-2869.

Lentz, H. 1993. German SAR calibration activities: devices and results. Proceedings of *SAR Calibration Workshop: CEOS Calibration Working Group SAR Calibration Sub-Group*, pp. 87-92, September 20-24, ESTEC/ESA, Noordwijk, The Netherlands.

Li, R. and H. Si. 1992. Multi-spectral image classification using improved backpropagation neural networks. *Proceedings, 1992 IGARSS International Space Year: Space Remote Sensing*, Vol. 2, pp.1078-1080.

Lillesand, T.M. and R. W. Kiefer. 1994. *Remote Sensing and Image Interpretation*, 3rd Edition. New York: John Wiley & Sons, Inc.

Liu, J.J.K. 1986. A GIS-based image processing system for agricultural purposes (GIPS/ALP) - a discussion on its concept. *Remote Sensing for Resource Development and Environmental Management.* Eds. M.C. J. Damen, G.S. Smit, H.T. Verstappen, A.A. Balkema Rotterdam Brookfield. Vol 1, pp. 27-30.

Livingstone, C.E., A.L. Gray, R.K. Hawkins, J.G. Halbertsma, R.A. Deane, and R.B. Olsen. 1987. CCRS C-band airborne radar system description and test results. *Proceedings of the 11th Canadian Symposium on Remote Sensing*, Waterloo, Ontario, pp. 15-21.

Livingstone, C.E., A.L. Gray, R.K. Hawkins, and R.B. Olsen. 1988. CCRS C/X- airborne synthetic aperture radar: an R&D tool for the ERS-1 time frame, *Proceedings of the 1988 IEEE National Radar Conference*, University of Michigan, Ann Arbor, Michigan.

Livingstone, C.E., D. Maxwell and J.R.C. Cafontaine. 1992. The ERS-1 /CV 580 SAR cross-calibration experiment: Sault Ste Marie, October 26 - November 2, 1991. *Proceedings of the First ERS-1 Symposium: Space at the Service of Our Environment*, Vol. 1, pp. 167-171, November 4-6, 1992, Cannes, France.

Lo, T.H.C. 1986. Use of multitemporal spectral profiles in agricultural land-cover classification. *Photogrammetric Engineering and Remote Sensing,* Vol. 52, No. 4, pp. 535-544.

Lukowski, T.I., R. St-Jean, and R.K. Hawkins. 1993. ERS-1 SAR calibration studies. *Proceedings of SAR Calibration Workshop.* CEOS Calibration Working Group SAR Calibration Sub-Group. September 20-24, ESTEC/ESA, Noordwijk, The Netherlands, pp247-254.

Luscombe, A.P., I. Ferguson, N. Shepherd, D.G. Zimcik, and P. Naraine. 1993. The RADARSAT synthetic aperture radar development. *Canadian Journal of Remote Sensing: Special Issues on RADARSAT,* Vol. 19. No. 4, pp. 298-310.

MacDonald, R.B. 1984. A summary of the history of the development of automated remote sensing for agricultural applications. *IEEE Transactions on Geoscience and Remote Sensing,* Vol. GE-22, No. 6, pp. 473-482.

MacDonald, R.B. and F.G.Hall. 1978. An experiment in global crop forecasting. *Large Area Crop Inventory Experiment Symposium,* Washington: National Aeronautics and Space Administration, JSC 14551, pp. 17-48.

Mack, A.R., F. Peet and L. Crosson. 1975. The cooperative Canada - US crop prediction project (crop classification). *Proceedings of the 3rd Canadian Symposium on Remote Sensing,* Edmonton, Alberta, pp. 449-456.

Mack, A.R., J. Schubert, C. Goodfellow, P. Chagarlamudi and H. Moore. 1977. *Proceedings of the 4th Canadian Symposium on Remote Sensing,* pp. 4-18.

Mahey, R.K., R. Singh, S.S. Sidhu, R.S. Narang, V.K. Dadhwal, J.S. Parihar, and A.K. Sharma. 1993. Pre-harvest state level wheat acreage estimation using IRS-1A LISS-I data in Punjab (India). *International Journal of Remote Sensing,* Vol. 14, No. 6, pp.1099-1106.

Malthus, T.J., B. Andrieu, F.M. Danson, K.W. Jaggard, and M.D. Steven. 1993. Candidate high spectral resolution infrared indices for crop cover. *Remote Sensing of Environment,* 46:204-212.

Mann, L.J., J.S. Salute, and G. R. Waddington Jr. 1991. Commerial application of remote sensing for columbia basin potato crop estimation. *Proceedings, IGARSS'91,* Vol. pp. 1931-1935.

Manore, M.J. and R.J. Brown. 1990. Remote sensing/GIS integration in the Canadian crop information system. *Geocarto International,* Vol.5, No. 1, pp. 74-76.

McCulloch, M.B. and W.B. Yates. 1992. The potential of polarimetric synthetic aperture radar for crop mapping and monitoring. *Remote Sensing from Research to Operation: Proceedings of the 18th Annual Conference of the Remote Sensing Society.* Eds. A.P. Cracknell and R.A. Vaughan, pp. 222-231.

McKeown, D. M. 1987. Role of artificial intelligence in the integration of remotely sensed data with geographic information systems. *IEEE Transactions on Geoscience and Remote Sensing.* Vol. GE-25, No. 3, pp. 330-348.

Mehta, N. 1983. Crop identification with airborne scatterometers. *Proceedings, IGARSS'83*, Vol. 1, PS-2, San Francisco, U.S.A.

Menenti, M., S. Azzali, D.A. Collado and S. Leguizamon. 1986. Multitemporal analysis of LANDSAT multispectral scanner (MSS) and thematic mapper (TM) data to map crops in the PO valley (Italy) and in Mendoza (Argentina). *Remote Sensing for Resource Development and Environmental Management.* Eds. M.C. J. Damen, G.S. Smit, H.T. Verstappen, A.A. Balkema Rotterdam Brookfield. Vol. 1 pp. 293-299.

Metzler, M.D., R.C. Cicone, and K.I. Johnson. 1983. Experiments with an expert-based crop area estimation techniques for corn and soybeans. *Proceedings, 17th International Symp. on Remote Sensing of Environment*, University of Michigan, Ann Arbor, Vol. III, pp. 965-972.

Meyer-Roux, J. and C. King. 1992. Agriculture and Forestry. *Internation Journal of Remote Sensing*, Vol. 13, Nos. 6 & 7, pp. 1329-1341.

Michelson, D.B. 1994. ERS-1 SAR backscattering coefficients from bare fields with different tillage row directions. *International Journal of Remote Sensing*, Vol 15, No. 13, pp. 2679-2685.

Morton, C.M. 1987. *Backscattering Behaviour of Agricultural Crops in the Microwave Region*, Unpublished M.Sc. thesis. University of Saskatchewan.

Mosher, P., R.A. Ryerson, and W.M. Stone. 1978. New Brunswick potato area estimation from Landsat. *Proceedings, 12th International Symposium on Remote Sensing of Environment*, Manila, Philippines, pp. 1415-1419.

Müller, U., Th. Löcherbach, W. Förstner, and W. Kühbauch. 1993. Suitability of ERS-1 SAR PRI data for multitemporal agricultural landuse mapping. *Proceedings, the Second ERS-1 Symposium: Space at the Service of Our Environment*, ESA SP-361, Vol. 1, pp. 69-74, October 11-14, Hamburg, Germany.

Myers, V.I. *et al.*, 1983. Remote sensing applications in agriculture. *Manual of Remote Sensing*, Vol. 2, pp.2111-2228.

NAS. 1970. *Remote Sensing: With Special Reference to Agriculture and Forestry*, National Academy of Sciences: Washington, D.C., 424pp.

NASA. 1988. *SAR - Earth Observing System Instrument Panel Report*, Vol. IIf, pp. 2-4.

NASA and JPL. 1994. *SIR-C/X-SAR*, NASA and JPL Brochure.

NASDA. 1993. *Japanese Earth Resources Satellite-1*, National Space Development Agency of Japan, Brochure.

Noetix Research Inc. 1993. *ERS-1 SGF Image Calibration Software User Manual - Draft*, Version 1.1, 29pp.

Odenweller, J.B. 1984. Crop identification using Landsat temporal-spectral profiles. *Remote Sensing of environment*, 14:39-54.

Pacheco, R.A. 1980. Application of remote sensing to agriculture development in tropical countries. *Remote Sensing Application in Agriculture and Hydrology*. Fraysse ED. A.A. Balkema, Rotterdam. pp. 299-308.

Paloscia, S. 1995. An empirical approach for retriving leaf area indix from multifrequency SAR dara. *Proceedings, IGARSS'95*, Florence, Italy, July 10-14, pp. 967-969.

Paola, J.D. and R.A. Schowengerdt. 1995. A review and analysis of backpropagation neural networks for classification of remotely-sensed multi-spectral imagery. *International Journal of Remote Sensing*, 16(16):3033-3058.

Parashar, S., D. Day, J. Ryan, D. Strong, R. Worsfold, and G. King. 1979. Radar discrimination of crops. *Proceedings, 19th International Symposium on Remote Sensing of Environment*, Ann Arbor, Michgan, Vol. 2, pp. 813-823.

Paris, J.F. 1982. Radar remote sensing of crops. *Proceedings, IGARSS'82*, Vol. 2, Munich, Germany.

Paris, J.F. 1983. Radar backscattering properties of cron and soybeans at frequencies of 1.6, 4.75, and 13.3 GHz. *IEEE Transactions on Geoscience and Remote Sensing*, Vol. GE-21, No. 3, pp. 392-400.

Paris, J.F. 1986. The effect of leaf size on the microwave backscattering by corn. *Remote Sensing of Environment*, 19:81-95.

Paris, J.F. 1990. On the uses of combined optical and active-microwave image data for agricultural applications. *Applications of Remote Sensing in Agriculture*, pp.355-374.

Park, A.B. 1978. Implementation of a crop monitoring system. *Proceedings of the W. Nordberg Memorial Symposium of the Twentieth Plenary Meeting of COSPAR*, Tel Aviv, Israel, Eds.: E.A. Godby and J Otterman, Vol. 2, pp. 105-120.

Park, A.B., R.E. Fries, and A.A. AAronson. 1980. Agricultural information systems for Europe. *Remote Sensing Application in Agriculture and Hydrology*. pp. 81-109.

PCI. 1994. *EASI/PACE Image Analysis System Manual*, PCI Incorporated, Toronto, Ontario, Canada.

Pei-yu, H. and De-li, G. 1983. Radar backscatter coefficients of paddy fields. *Proceedings, IGARSS'83*, Vol. 2, FP-5, San Francisco.

Petzinger, F.C. 1995. GlobeSAR: the CCRS airborne SAR in the era of RADARSAT. *Geocarto International*, Vol. 10, No. 3, pp. 9-17.

Philipson, W.R. and W.L. Teng. 1988. Operational interpretation of AVHRR vegetation indices for world crop information. *Photogrammetric Engineering and Remote Sensing*, Vol. 54, No. 1, pp. 55-59.

Pierce, L.E., F.T. Ulaby, K. Sarabandi, and M.C. Dobson. 1994. Knowledge-based classification of polarimetric SAR images. *IEEE Transactions on Geoscience and Remote Sensing*,Vol. 32, No. 5, pp. 1081-1086.

Pitts, S.E., G.D. Badhwar, D.R. Thompson, K.E. Henderson, S.S. Shen, C.T. Sorensen and J. G. Carnes. 1984. Evaluation of corn/soybeans separability using thematic mapper and thematic simulator data. *IEEE Transactions on Geoscience and Remote Sensing*, Vol. GE-22, No. 3, pp. 312-318.

Poirier, S., K.P.B. Thomson, A. Condal, and R.J. Brown. 1988. SAR applications in agriculture: a comparison of steep and shallow mode (30° and 53° incidence angles) data. *International Journal of Remote Sensing*, Vol.10, No. 6, pp. 1085-1092.

Proud, B., R. Protz, and B. Brisco. 1990. Temporal changes in radar backscatter of crop canopies due to soil effects. *Canadian Journal of Remote Sensing*, Vol. 16, No. 3, pp. 30-36.

Pultz, T.J. and R.J. Brown. 1987. SAR image classification of agricultural targets using first- and second-order statistics. *Canadian Journal of Remote Sensing*, Vol. 13, No. 2, pp. 85-91.

Pultz, T.J., R. Leconte, R.J. Brown, and B. Brisco. 1990. Quantitative soil moisture extraction from airborne SAR data. *Canadian Journal of Remote Sensing*, Vol. 16, No. 3, pp. 56-62.

Pultz, T.J., R. Leconte, R.J. Brown, B. Brisco, and T.I. Lukowski. 1989. SAR response to spatial and temporal variations in soil moisture and vegetation. *Proceedings IGARSS'89 / 12th Canadian Symposium on Remote Sensing*, Vancouver, British Columbia, Vol. 5, pp. 2755-2757.

Qiu, Z.C. and M. Goldberg. 1985. A new classification scheme based upon segmentation for remote sensing. *Canadian Journal of Remote Sensing*, Vol. 11, No. 1, pp. 59-69.

Rashid, A. 1996. *The FAO Global Information and Early Warning System on Food and Agriculture (GIEWS).* http://www.cirad.fr/EN/fao/smiar/giews.htm

RESTEC. 1996a. *Remote Sensing Data.* Brochure, Remote Sensing Technology Center of Japan.

RESTEC. 1996b. *JERS-1 Data for Global Monitoring.* Brochure, Remote Sensing Technology Center of Japan.

Robert P.C. 1996. Use of remote sensing imagery for precision farming. *Proceedings, Information Tools for Sustainable Development - 26th International Symposium on Remote Sensing of Environment/18th Annual Symposium of Canadian Remote Sensing Society*, May 25-29, Vancouver, BC, Canada, pp.596-599.

RSI. 1995a. Food stuff. Reflections, RADARSAT International Newsletter.

RSI. 1995b. *RADARSAT: Canada's Earth Observation Satellite*, RADARSAT International Brochure, 24pp.

Rundquist, D. C. and S.A. Samson. 1983. Application of remote sensing in agricultural analysis. *Introduction to Remote Sensing of the Environment. Ed. B.F. Richason, Jr.* Kendall/Hunt, pp. 317-337.

Ryerson, R.A., P.N. Mosher, V.R. Wallen, and N.E. Stewart. 1979. Three tests of agricultural remote sensing for crop inventory in Eastern Canada: results, problems and prospects. *Canadian Journal of Remote Sensing*, 5(1):53-66.

Ryerson, R.A., J. L. Tambay, R J. Brown, L. Murphy, and B. McLaughlin. 1981a. A timely and accurate potato acreage estimate from Landsat: results of a demonstration. *Proceedings, 15th International Symposium on Remote Sensing of Environment*, Ann Arbor, Michigan, Vol. II, pp. 587-597.

Ryerson, R.A., R.S. Sigman and R J. Brown. 1981b. Satellite remote sensing for domestic crop reporting in the United States and Canada: a look to the future. *Proceedings, 7th Canadian Symposium on Remote Sensing*, Winnipeg, Manitoba, pp.30-40.

Ryerson, R.A., R.N. Dobbins and C. Thibault. 1985. Timely crop area estimates from landsat. *Photogrammetric Engineering and Remote Sensing*, Vol. 51, No. 11, pp.1735-1743.

Satellitbild, 1996. *RESURS-01: Bridging the Gap.* Brochure, Satellitbild, Swedish Space Corporation.

Schadt, R., J. Kellndorfer and W. Mauser. 1993. Comparison of ERS-1 SLC and Landsat Thematic Mapper data for monitoring grassland and detecting changes in agricultural use. *Proceedings, the Second ERS-1 Symposium: Space at the Service of Our Environment*, ESA SP-361, Vol. 1, pp. 75 -78, October 11-14, Hamburg, Germany.

Schalkoff, R. 1992. *Pattern Recognition: Statistical, Structural and Neural Approaches*, John Wiley & Sons Inc., New York, Toronto, Singapore, pp. 204-258.

Schmullius, C. and J. Nithack. 1992. High-resolution SAR frequency and polarization dependent backscatter variations from agricultural fields. *IGARSS'92*, May 26-29, Houston, Texas, USA, pp. 930-932.

Schmullius, C. and R. Furrer. 1992a. Frequency dependence of radar backscattering under different moisture conditions of vegetation-covered soil. *International Journal of Remote Sensing*, Vol. 13, No. 12, pp. 2233-2245.

Schmullius, C. and R. Furrer. 1992b. Some critical remarks on the use of C-band radar data for soil moisture detection. *International Journal of Remote Sensing*, Vol. 13, No. 17, pp. 3387-3390.

Schmullius, C., J. Nithack and M. Kern. 1993. Comparison of multitemporal ERS-1 and airborne DLR E-SAR image data for crop monitoring. *Proceedings, the Second ERS-1 Symposium: Space at the Service of Our Environment*, ESA SP-361, Vol. 1, pp. 79-83, October 11-14, Hamburg, Germany.

Schmullius, C., J. Nithack, and M. Kern. 1994. Comparison of multitemporal ERS-1 and airborne E-SAR image data for crop monitoring. *ESA-Earth Observation Quarterly*, No. 43, pp. 9-12.

Schotten, C.G.J., W.W.L. Van Rooy and L.L.F. Janssen. 1995. Assessment of the capabilities of multi-temporal ERS-1 SAR data to discriminate between agricultural crops. *International Journal of Remote Sensing*, Vol. 16, No. 14, pp. 2619-2637.

Shanmugan, K.S., F.T. Ulaby, V. Narayana and C. Dobson. 1983. Identification of corn fields using multidate radar data. *Remote Sensing of Environment*, 13: 251-264.

Sharon, W.L., T.W. Randall, C.E. Brown, and E. H. Bauer. 1984. Landsat-based inventory system for agriculture in California. *Remote Sensing of Environment*, 14:267-278.

Shepherd, P., C. Morton, G. Sofko, J. Koehler, and A. Wacker. 1987. Crop separability with a 3-band microwave scatterometer. *Proceedings 11th Canadian Symposium on Remote Sensing*, Waterloo, Ontario, Vol. 1, pp. 173-180.

Shi, Z. and K.B. Fung. 1994. A comparison of digital speckle filters. *Proceedings, IGARSS'94*, pp. 2129-2133.

Sieber, A.J., B. Freitag, and K. Lawler. 1982. The aspect angle dependence of SAR images. *Proceedings, IGARSS'82*, Vol. 2, FA-4, Munich, Germnay.

Silleos, N., N., Misopolinos, and K. Perakis. 1992. Relationships between remote sensing spectral indices and crop discrimination. *Geocarto International*, (2): 41-51.

Simonett, D.S. 1976. Remote sensing of cultivated and natural vegetation: cropland and forest land. *Remote Sensing of Environment*, Eds. J.Lintz,Jr. and D.S.Simonett, Addison-Wesley, pp.442-467.

Simonett, D.S., J.E. Eagleman, A.B. Erhart, D.C. Rhodes, and D.E. Schwarz. 1967. *The Potential of Radar as A Remote Sensor in Agriculture*. University of Kansas Center for Research, Inc., CRES Tech. Rep. 61-21, pp. 1-13.

Staenz, K. and P.M. Teillet. 1993. MODIS data simulation from AVIRIS data. *Remote Sensing in Canada*, pp. 1-3.

Stakenborg, J.H.T.. 1986. Per-field classification of a segmented SPOT simulated image. *Remote Sensing for Resource Development and Environmental Management*, Eds. M.C. J. Damen, G.S. Smit, H.T. Verstappen, A.A. Balkema Rotterdam Brookfield. Vol. 1, pp. 73-78.

Statistics Canada. 1992. *Agricultural Profile of Ontario: Part 1&2 - 1991 Census and Recensement*, Government of Canada Publications, Catalogue 93-351, Ottawa:Statistics Canada, Agriculture Division.

Steinberg, B.D. and H.M. Subbaram. 1991. *Microwave Imaging Techniques*, Wiley Series in Remote Sensing, Ed. J.A. Kong, John Wiley and Sons, Inc. pp.75-96.

Taillade-Carriere, M. 1980. Satellite data collection system: agricultural applications. *Remote Sensing Application in Agriculture and Hydrology.* Netherland: A.A. Balkema/Rotterdam, pp. 269-284.

TELSAT. 1995. *NOAA / AVHRR - Technical Specifications Sensor*, http://www.belspo.be/telsat/avhrr/avts_001.htm.

Teng, W.L. 1990. AVHRR monitoring of U.S. crops during the 1988 drought. *Photogrammetric Engineering and Remote Sensing*, Vol. 56, No. 8, pp. 1143-1146.

Tennakoon, S.B., V.V.N. Murty, and A. Eiumnoh. 1992. Estimation of cropped area and grain yirld of rice using remote sensing data. *International Journal of Remote Sensing.* Vol. 13, No. 3, pp. 427-439.

The Toronto Star. 1993. *Population Outstripping Food Supply, Report Finds*, A14, Sunday, July 18.

Thiede, G. 1980. Agricultural statistics analysis of the main requirements; conventional and new methodologies. *Remote Sensing Application in Agriculture and Hydrology.* Netherland: A.A. Balkema/Rotterdam, pp. 9-16.

Thiede, G. 1981. Methods of crop production forecasting in the EEC present and expected trends in crop production. *Application of Remote Sensing to Agricultural Production Forecasting*, Edited by A. Berg. Netherland: A.A.Balkema/Rotterdam. pp. 1-10

Thomson, K.P.B., G. Edwards, R. Landry, A. Jaton, S.-P. Cadieux, and Q.H.J. Gwyn. 1990. SAR applications in agriculture: multiband correlation and segmentation. *Canadian Journal of Remote Sensing*, Vol. 16, No. 3, pp. 47-54.

Thomson, K.P.B., S. Poirier, G.B. Bénié, C. Gosselin, and G. Rochon. 1987. Filter selection and processing methodology for synthetic aperture radar (SAR) data in agricultural applications. *Canadian Journal of Remote Sensing* , Vol. 13, No. 1, pp. 6-10.

Treitz, P.M., P.J. Howarth, O. R. Filho, E.D. Soulis, and N. Kouwen. 1993. Proceedings, *16th Canadian Symposium on Remote Sensing*, Sherbrooke, Quebec, Canada, pp. 343-347.

Treitz, P.M., O. R. Filho, P.J. Howarth, and E.D. Soulis. 1996. Textural processing of multi-polarization SAR for agricultural crop classification. *Proceedings, IGARSS'96*, May 27-31, Lincoln, Nebraska, USA, pp. 1986-1988.

Tucker, C.J. J.H. Elgin, Jr., and J.E. McMurtrey III. 1979. Temporal spectral measurements of corn and soybeans crops. *Photogrammetric Engineering and Remote Sensing*, Vol. 45, No. 5, pp. 643-653.

Tucker, C.J., J.A. Gatlin, and S.R. Schneider. 1984. Monitoring vegetation in the Nile Delta with NOAA-6 and NOAA-7 AVHRR imagery. *Photogrammetric Engineering and Remote Sensing*, Vol. 50, No. 1, pp. 53-61.

Turner, B. 1986. LANDSAT temporal-spectral profiles of crops on the South African Highveld. *Remote Sensing for Resource Development and Environmental Management.* Eds. M.C. J. Damen, G.S. Smit, H.T. Verstappen, A.A. Balkema Rotterdam Brookfield. Vol. 1, pp. 325-330.

Ulaby, T.F. 1981. Microwave response of vegetation. *Advanced Space Research*, 1:55-70.

Ulaby, F.T. and P.P. Batlivala. 1975. Diurnal variations of radar backscatter from a vegetation canopy. *IEEE Transactions on Antenna and Propagation*, Vol. AP-24, No. 1, pp. 11-17.

Ulaby, F.T. and T.F. Bush. 1976. Monitoring wheat growth with radar. *Photogrammetric Engineering and Remote Sensing*, 42(4):557-568.

Ulaby, F.T. and E.A. Wilson. 1985. Microwave attenuation properties of vegetation canopies. *IEEE Transactions on Geoscience and Remote Sensing,* GE-23:746-753.

Ulaby, F.T., P.P. Batlivala and M.C. Dobson. 1978. Microwave backscatter dependence on surface roughness, soil moisture and soil texture, part I: bare soil. *IEEE Transactions on Geoscience and Electronics*, GE-16:286-295.

Ulaby, F.T., G.A. Bradley and M.C. Dobson. 1979. Microwave backscatter dependence on surface roughness, soil moisture, and soil texture: part II - vegetation-covered soil. *IEEE Transactions on Geoscience and Electronics*, GE-17:33-40.

Ulaby, F.T., P.P. Batlivala and J.E. Bare. 1980. Crop identification with L-band radar. *Phtothrammetric Engineering and Remote Sensing,* Vol. 46, No. 1, pp. 101-105.

Ulaby, F.T., M.C. Dobson and G.S. Bradley. 1981. Radar reflectivity of bare and vegetation-covered soil. *Advanced Space Research*, 1:91-104.

Ulaby, F.T., A. Aslam and M.C. Dobson. 1982. Effects of vegetation cover on the radar sensitivity to soil moisture. *IEEE Transactions on Geoscience and Electronics*, GE-20:476-481.

Ulaby, F.T., C.T. Allen, G. Eger III and E. Kanemasu. 1984. Relating the microwave backscattering coefficient to leaf area index. *Remote Sensing of the Environment*, 14:113-133.

Ulaby, F.T., R.K. Moore, and A.K. Fung. 1986a. *Microwave Remote Sensing: Active and Passive*, Vol. I, II & III, Addison-Wesley, Reading, Massachusetts.

Ulaby, F.T., T. Kouyate, B. Brisco and T.H. Lee. 1986b. Textural information in SAR images. *IEEE Transactions on Geoscience and Remote Sensing,* Vol. GE-24, No. 2, pp. 235-245.

Ulaby, F.T., K. Sarabandi, K. McDonald, M. Whitt, and M.C. Dobson. 1990. Michigan microwave canopy scattering model. *International Journal of Remote Sensing*, vol. 11, No. 7, pp. 1223-1253.

Vallée, L.B., K.P.B. Thomson, and G.B. Bénié. 1987. Segmentation and crop classification. *Proceedings, 11th Canadian Symposium on Remote Sensing*, Waterloo, Ontario, Vol. 1, pp. 147-154.

Van Kasteren, H.W.J. 1981. Radar signature of crops: the effect of weather conditions and the possibilities of crop discrimination with radar. *Signatures Spectrales D'Objets En Teledetection*, p. 407-414.

Wall, S.L., R.W. Thomas and C.E. Brown. 1984. Landsat-based inventory system for agriculture in California. *Remote Sensing of Environment*, 14:267-278.

Wang, J., E.T. Engman, J.C. Shiue, M. Rusek, and C. Steinmeier. 1986. The SIR-B observations of microwave backscatter dependence on soil moisture, surface roughness, and vegetation covers. *IEEE Transactions on Geoscience and Remote Sensing,* Vol. GE-24, No. 4, pp. 510-516.

Wang, J., E.T. Engman, T.J. Schmugge, and J.C. Shiue. 1987. The effects of soil moisture, surface roughness, and vegetation on L-band emission and backscatter. *IEEE Transections on Geoscience and Remote Sensing*, Vol. GE-25, pp. 825-833.

Welch, R., H.C. Lo, C.W. Pannell. 1979. Mapping China's new agricultural lands. *Photogrammetric Engineering and Remote Sensing*, Vol. 45, No. 9, pp.1211-1228.

Werle, D. 1992. *Radar Remote Sensing: A Training Manual*, 2nd Edition, Ottawa: Dendron Resource Surveys Ltd., under contract to the Application Division, Canada Centre for Remote Sensing.

Wever, T., J. Henkel, and B. Häfner. 1995. Crop identification using multifrequency and polarimetric SAR data. *Proceedings, IGARSS'95*, Florence, Italy, July 10-14, pp. 1213-1215.

Wicklund, R.E. and N.R. Richards. 1961. *The Soil Survey of Oxford County*, Report No. 27 of the Ontario Soil Survey, Canada Department of Agriculture and The Ontario Agricultural College, 56 pp.

Wiegand, C.L., A.J. Richardson, D.E. Escobar, and A.H. Gerbermann. 1991. Vegetation indices in crop assessments. *Remote Sensing of Environment*, 35:105-119.

Wooding, M.G. 1983. Preliminary results from the analysis of SAR-580 digital radar for the discrimination of crop types and crop condition, Cambridge, UK. *SAR-580 Investigators Preliminary Report*, ESA.

Wooding, M.G. 1995. Satellite Radar in Agriculture Experience with ERS-1. *Earth Observation Quarterly*, No. 49, http://esapub.esrin.esa.it/pointtoeoq/eoq49.html.

Wooding, M.G. and E. Attema. 1992. Results from MAESTRO-1 and AGRISCATT campaigns. *Earth Observation Quarterly*, No. 39, ESA.

Wooding, M.G. and H. Laur. 1993. Report on agriculture Session. *Proceedings, the Second ERS-1 Symposium: Space at the Service of Our Environment*, ESA SP-361, Vol. 1, pp. 49, October 11-14, Hamburg, Germany.

Wooding, M.G., A.D. Zmuda, and G.H. Griffiths. 1993. Crop discrimination using multi-temporal ERS-1 SAR data. *Proceedings, the Second ERS-1 Symposium: Space at the Service of Our Environment*, ESA SP-361, Vol. 1, pp. 51-56, October 11-14, Hamburg, Germany.

Wright, P., P. Saich, and R. Cordey. 1993. Crop monitoring with ERS-1 SAR in East Anglia. *Proceedings, the Second ERS-1 Symposium: Space at the Service of Our Environment*, ESA SP-361, Vol. 1, pp. 103-108, October 11-14, Hamburg, Germany.

Yanasse, C.C.F, S. Quegan, and R.J. Martin. 1992. Inferences on spatial and temporal variability of the backscatter from growing crops using AgriSAR data. *International Journal of Remote Sensing*, Vol. 13, No. 3, pp. 493-507.

Yates, H.W., J.D. Tarpley, and S.R. Schneider. 1984. The role of meteorological satellites in agricultural remote sensing. *Remote Sensing of Environment*, 14:219-233.

APPENDIX A: COSTS AND BENEFITS OF REMOTE SENSING

(Lantieri, 1993)

A.1 Costs

The cost of remote sensing studies depends on many factors. Costs per square kilometer generally increase when:

- *the scale is more detailed*, for example, at 1:200,000 scale, generally corresponds to a cost of US$2-4 per square kilometer; whereas at 1:25,000 scale, is US$8-15 per square kilometer.
- *the level of information required increases*, for example, land potential maps are more complex and therefore more expensive than general land cover maps.

A.2 Benefits

Compared to extensive traditional ground surveys or inquiries, the main benefits of remote sensing are:

- *the provision of an exhaustive view of the selected area:* in large areas this avoids major under- or over-estimation of phenomena or problems related to earth resources, which can not readily be detected by ground surveys alone;
- *the provision of objective and independent information:* data acquired from remote sensing are measured by very reliable instruments which are independent of scientific judgment and/or political influences;
- *the provision of updated and homogeneous information* over hundreds or thousands of square kilometers, particularly meaningful for evaluation exercises.

At small scale and medium scale - up to 1:50,000 *satellite remote sensing* can, in most situations, offer a number of advantages when compared to *aerial photography*, such as:

- *lower direct costs:* the cost of satellite imagery is only 10 to 50 percent of that of the airborne or ground surveys required for the traditional production of updated thematic maps;
- *shorter time scale and unimpeded acquisition:* while the collection of ground-based regional resource information may take months or even years for wide and complex areas, satellite remote sensing can provide results in weeks or months and hence can speed decision-making. Moreover, there are no political or administrative restrictions to

the acquisition of satellite data, which is not always the case with aerial photographs and sometimes even maps;

- *new activities:* thanks to their large vision of the earth surface, to the availability of specific spectral bands and to the acquisition of imagery on a regular basis all over the world, satellite data offer new possibilities over very wide areas, impossible with traditional aerial surveys;
- *high speed of delivery and high accuracy of information.*

APPENDIX B: SPOT - SEARCH RESULTS

SPOT Data is Copyright SPOT-R © CNES

No	HRV	Mode	Angle	K / J	Orb	Acq. Date	Scene Centre Longitude	Scene Centre Latitude	Cloud
2	2	XS	29.7	612/264	103	5-Jul-1996	80-44-59:W	42-42-24:N	0000
2	2	XS	2.3	612/264	117	6-Jul-1996	80-44-23:W	42-42-24:N	1110
2	1	XS	14.1	612/264	259	16-Jul-1996	80-43-12:W	42-42-24:N	6312
2	1	XS	-9.7	612/264	344	22-Jul-1996	80-42-59:W	42-42-24:N	2211
2	2	XS	-11.4	612/264	344	22-Jul-1996	80-59-38:W	42-42-24:N	3211
2	1	XS	-3.6	612/264	046	27-Jul-1996	80-41-35:W	42-42-24:N	4422
2	1	XS	2.6	612/264	117	1-Aug-1996	80-40-52:W	42-42-24:N	6722
2	1	XS	-26.2	612/264	131	2-Aug-1996	80-40-32:W	42-42-24:N	4122
2	1	XS	8.7	612/264	188	6-Aug-1996	80-39-22:W	42-42-24:N	1231
2	1	XS	-3.6	612/264	046	22-Aug-1996	80-41-03:W	42-42-24:N	1200
2	1	XS	30.0	612/264	103	26-Aug-1996	80-40-11:W	42-42-24:N	4421
2	1	XS	2.6	612/264	117	27-Aug-1996	80-40-18:W	42-42-24:N	3521
3	2	PD	-11.4	612/264	344	5-Jun-1995	80-56-02:W	42-42-24:N	2233
2	2	PD	-11.4	612/264	344	3-Jun-1994	80-57-12:W	42-42-24:N	0000
2	2	PD	6.3	612/264	188	18-Jun-1994	81-00-09:W	42-42-24:N	2210
2	2	PD	0.6	612/264	117	9-Jul-1994	81-01-17:W	42-42-24:N	5430
2	1	PL	-4.3	612/264	046	30-Jul-1994	80-46-30:W	42-42-24:N	4322
2	1	XS	-4.3	612/264	046	30-Jul-1994	80-47-05:W	42-42-24:N	3322
2	1	PL	-4.3	612/264	046	25-Aug-1994	80-47-15:W	42-42-24:N	7631
2	1	XS	-4.3	612/264	046	25-Aug-1994	80-47-50:W	42-42-24:N	7641
2	1	PL	29.3	612/264	103	29-Aug-1994	80-48-19:W	42-42-24:N	8882
1	1	PD	-11.0	612/264	344	18-Jul-1993	80-54-39:W	42-42-24:N	7432
2	1	PD	0.8	612/264	117	31-Aug-1993	80-59-55:W	42-42-24:N	8652
2	2	XS	3.0	612/264	117	31-Aug-1993	80-37-10:W	42-42-24:N	7713
2	2	XS	2.3	612/264	117	15-Jun-1992	80-41-49:W	42-42-24:N	0000
1	2	XS	-27.9	612/264	131	6-Jun-1990	80-59-03:W	42-42-24:N	2311
2	2	XS	28.3	612/264	103	17-Jun-1990	80-59-40:W	42-42-24:N	3824
2	1	XS	-20.6	612/264	202	15-Aug-1990	80-37-02:W	42-42-24:N	1100
2	2	PD	-20.9	612/264	202	15-Aug-1990	80-39-50:W	42-42-24:N	1100
1	1	PD	1.3	612/264	117	5-Jul-1987	80-52-44:W	42-42-24:N	5512
1	2	XS	1.0	612/264	117	5-Jul-1987	80-56-25:W	42-42-24:N	4623
1	1	PD	-10.4	612/264	344	21-Jul-1987	80-47-45:W	42-42-24:N	0000
1	2	XS	-10.7	612/264	344	21-Jul-1987	80-51-27:W	42-42-24:N	0000
1	1	XS	1.9	612/264	117	31-Jul-1987	80-45-50:W	42-42-24:N	0000
1	2	PD	1.0	612/264	117	31-Jul-1987	80-54-55:W	42-42-24:N	0000
1	1	PD	-10.4	612/264	344	16-Aug-1987	80-47-29:W	42-42-24:N	2114
1	2	XS	-10.7	612/264	344	16-Aug-1987	80-51-11:W	42-42-24:N	2112
1	2	XS	2.3	612/264	117	6-Jul-1986	80-42-26:W	42-42-24:N	0000

APPENDIX C: SPACEBORNE SAR SYSTEMS - PAST, PRESENT AND FUTURE

C.1 Spaceborne SAR Systems: Past

SEASAT (1978)

The first spaceborne imaging radar was the L-band SAR on SEASAT, an instrument package launched into an 800 km altitude near-polar orbit in June 1978. This horizontally polarized instrument operated at a fixed wavelength (23.5 cm) and at a fixed look angle (23° from nadir). The SEASAT swath width was 100 km and the resolution was approximately 25 m. It operated for three months. Although SAR was included in the SEASAT payload primarily for the purpose of ocean-wave imaging, imagery obtained over land areas clearly demonstrated its sensitivity to surface roughness, slope, land-water boundaries (NASA, 1988; Werle, 1992).

SIR-A (1981)

The next spaceborne SAR to follow SEASAT was the Shuttle Imaging Radar A (SIR-A), ferried into a 57° inclination, 240 km altitude orbit by the Space Shuttle Columbia in November 1981. The SIR-A SAR technology was derived from SEASAT SAR, again using the 23.5 cm wavelength (L-band) and HH polarization. The look angle, however, was changed to a fixed angle of 47° since the SIR-A mission was to be used principally for geological research. The swath width was approximately 50 km and the resolution was 40m. SIR-A provided much improved images for geological analysis as they were relatively free of the layover distortion that accompanied SEASAT SAR images of high-relief regions. One of the most exciting aspects of the experiment was the demonstration of the radar's ability to penetrate extremely dry surfaces, which resulted in the discovery of ancient river channels buried beneath the Sahara Desert (NASA, 1988, Werle, 1992).

SIR-B (1984)

The next NASA SAR mission was SIR-B, launched in October, 1984 on the Space Shuttle Challenger. The imaging altitude varied between 350 km, 272 km and 225 km. Wavelength and polarization of the SAR were the same as its predecessors on SEASAT and SIR-A; i.e. L-HH. The new feature was that SIR-B was equipped with an articulating antenna so that selectable incidence angles could be obtained over the 15° to 60° range. This capability provided the first multi-incidence angle data set for surface-feature (particularly forest) mapping and topographic mapping. SIR-B data were also the first to be digitally encoded and digitally processed, which represents a significant advance in SAR image processing technology. The swath width was 20 to 40 km. Range resolution was 58 to 16 m and azimuth resolution 20 to 30 m (4-look). The Mission Length was 8.3 days (NASA, 1988, Werle, 1992; JPL, 1996).

C.2 Spaceborne SAR Systems: Present

Russian ALMAZ-1 (1991)

The former Soviet Union (just prior to its dissolution) became the first country to operate a spaceborne radar system with the launch of ALMAZ-1 on March 31, 1991. Although this system initiated a new era in operational remote sensing from space with the ability to provide high resolution data independent of weather conditions and time of day, ALMAZ-1 was not well known in the SAR research and application community due to lack of promotion by Russia. ALMAZ-1 was launched with a nominal altitude of 300 km (it was changed to 360 km in an attempt to prolong its lifetime in orbit) and an orbit that ranged from 73° N to 73° S latitude. It returned to earth on October 17, 1992, after operating for about 18 months. The primary sensor on board ALMAZ-1 was S-band (10 cm) SAR with HH polarization. The look angle ranged from 30° to 60° and the spatial resolution varied from 10 to 30 m, depending on the range and

azimuth of the area imaged. The ALMAZ-1 SAR incorporated two antennas, which provided for eastward and westward looking swaths, each approximately 350 km wide (Lillesand and Kiefer, 1994).

European Earth Resources Satellites ERS-1&2 (1991 and 1995)

The European Space Agency (ESA)'s ERS-1 was launched into a sun-synchronous near-polar orbit at an altitude of 785 km in July 1991. The ERS-1 payload includes a C-band Active Microwave Instrument (AMI) with VV polarization and a 23° incidence angle in mid-range. In Image Mode, SAR obtains strips of imagery, 100 km in width, to the right side of the satellite track. The spatial resolution is about 30 m in range direction and about 30 m in azimuth direction. The SAR return signals are processed digitally on board and transmitted to receiving stations. The ERS-1 SAR operated for 3 years and 10 months (ESA, 1992; Eurimage, 1994; ESA, 1995). The second European Earth Resources Satellite was successfully launched in April, 1995, carrying the same SAR instrument as ERS-1.

Although most of the microwave instruments on board the ERS-1 are primarily designed for the study of oceans, ice and meteorology, this long-duration spaceborne SAR system provides the research community with an excellent opportunity to obtain a better understanding of our land environment and its dynamic processes. Since its launch, it has stimulated a lot of research activities in a wide range of applications including agriculture, forestry, geology, flood monitoring and sea-ice monitoring (ESA, 1992; Eurimage, 1994).

Japanese Earth Resources Satellite JERS-1 (1992)

The Japanese Earth Resources Satellite JERS-1 was launched in February, 1992 with an expected lifetime of four years. The satellite is in a sun-synchronous, 568 km high orbit. The payload of JERS-1 includes a L-HH SAR with a 38.5° incidence angle in mid-range. The image

swath is 75 km. The spatial resolution is 18 m at 3-looks in both range and azimuth directions. Like ESA's ERS-1&2, the JERS-1 is an experimental satellite. Its data are used for exploration of earth resources and monitoring land surfaces (ESA, 1995; RSI, 1995b).

SIR-C/X-SAR (1994)

The SIR-C/X-SAR mission represented a very important step forward. Not only was it the first spaceborne SAR system which simultaneously acquired multi-frequency SAR imagery, but also it was the first opportunity to use a multi-polarization capability from space. SIR-C/X-SAR is a joint project of the National Aeronautics and Space Administration (NASA), the German Space Agency (DARA) and the Italian Space Agency (ASI).

SIR-C/X-SAR is an imaging radar system launched aboard the NASA Space Shuttle in April and October 1994. SIR-C provided increased capability over SEASAT, SIR-A, and SIR-B by acquiring digital images simultaneously at two microwave wavelengths (L-band at 23.5 cm and C-band at 5.8 cm). These vertically and horizontally polarized transmitted waves were received on two separate channels, so that SIR-C provided images of the magnitude of radar backscatter for four polarization combinations: HH, VV, HV, and VH. Data on the relative phase differences between the HH, VV, VH, and HV returns were also acquired. This allowed derivation of the complete scattering matrix of a scene on a pixel by pixel basis. From this scattering matrix, every polarization configuration (linear, circular or elliptical) can be generated during ground processing. The radar polarimetric data will yield more detailed information about the surface geometric structure, vegetation cover and subsurface discontinuities than image brightness alone.

Germany/Italy's X-SAR operated at X-band (3.1 cm) with VV polarization, resulting in a three-frequency capability for the total SIR-C/X-SAR system. Because radar backscatter is most

strongly influenced by objects comparable in size to the radar wavelength, this multi-frequency capability has provided information about the earth's surface over a wide range of scales not discernible with previous single-wavelength experiments. Radar images generated by SIR-C/X-SAR have been used by scientists to help understand some of the processes which affect the earth's environment, such as deforestation in the Amazon, desertification south of the Sahara, and soil moisture retention in the Mid-West (JPL, 1996).

Canadian RADARSAT (1995)

The Canadian RADARSAT was successfully launched on November 4, 1995. RADARSAT is equipped with an advanced SAR with a planned lifetime of five years. Using a single-frequency, C-Band, the RADARSAT SAR has the unique ability to shape and steer its radar beam over a 500 km range. Users have access to a variety of beam selections that can image swaths from 35 km to 500 km with resolutions from 10 m to 100 m, respectively. Incidence angles range from less than 20° to more than 50°.

RADARSAT provides complete global coverage with the flexibility to support specific requirements. The satellite's orbit is repeated every 24 days. RADARSAT provides daily coverage of the Arctic, views any part of Canada within three days, and achieves complete coverage at equatorial latitudes every six days using a 500 km wide swath.

APPENDIX D: SPACEBORNE SAR FOR AGRICULTURAL CROP CLASSIFICATION - DISCUSSION OF SELECTED STUDIES

D.1 Early Spaceborne SAR Data for Crop Classification

Cihlar, Prévost and Vickers (1986) conducted a feasibility study to discriminate among various land-cover categories on SIR-B L-band data. The data were acquired over agricultural areas after harvest in southwestern Saskatchewan, Canada. The Hoosier area was imaged at an incidence angle of 34° and the Lake Diefenbaker area at two incidence angles (15° and 34°). Images were interpreted visually using prints. In order to facilitate the transfer of information between the SAR image and the ground map, and to determine digital values for the visually interpreted tones, digital SIR-B data were also processed. The images were co-registered with TM images, and a field-by-field analysis was conducted and image tones were assigned. Since the SIR-B data were acquired over areas with no corresponding ground observations, enhanced TM images were employed to determine land-cover types in those areas. The results show that general land-cover categories can be visually delineated on SIR-B images, but contextual interpretive parameters (shape and pattern) must be used to compensate for tonal overlap between categories. If image tone were used in isolation, it is likely that digital pixel-by-pixel analysis would not be successful. The main difference between the 34° and 15° images was the greater tonal variation within the latter. Similar trends were observed, however, in data collected at two incidence angles. Soil surface roughness was a dominant factor influencing radar backscatter at L-band in dry harvested agricultural areas.

Hutton and Brown (1986) conducted a comparative analysis of space and airborne L-HH radar imagery in an agricultural environment near Napierville, Quebec. They attempted to determine the extent to which agricultural ground features influenced radar returns and compared the

relative radar backscattering coefficients derived from both a SIR-B L-HH image (October 7, 1984) and an airborne SAR L-HH image (October 25, 1984). They also compared the results of this study with those derived from an analysis of sites in western Canada. The study was accomplished by carrying out a visual assessment of the images and by performing digital classifications. From visual analysis of both space and airborne SAR images, it was concluded that the radar returns from rows or ditches dominated those of the actual ground cover in the areas where row/field/ditch orientations were orthogonal to the sensor look direction. In all other cases, the radar returns from the ground-cover type dominated over the row/field/ditch orientation. Pasture, which is devoid of rows, showed no orientation dominance. The digital results indicated that pasture, ploughed fields and unharvested corn were separable on the airborne image in most of the classifications, but harvested corn was not consistently or accurately defined. On the spaceborne image, separability was *much poorer* and almost non-existent if backscattering values (i.e., training areas) were derived from orthogonal regions. Pasture had the highest classification accuracies of any of the ground-cover types studied. Post-classification filtering of both types of data increased the overall accuracies in most cases. The dissimilarities between the ground characteristics because of different farming practices did not allow for a relevant comparison from eastern Canada to western Canada.

Cihlar and Hirose (1984) and Cihlar (1986) conducted a qualitative and quantitative analysis of single-date digital airborne X- and L-band data, SEASAT SAR data, and LANDSAT MSS data for four agricultural sites in western Canada which represent sub-arid and semi-arid climatic regimes. MSS images were rectified to a UTM map and all SAR data were registered to these images. Filters were used to reduce speckle. The boundaries of each field were outlined and digital values for each cover type were extracted. Images were visually examined to establish possible relationships between features imaged by SAR and ground observations. Cihlar and Hirose (1984) also performed digital classifications for various SAR, VIR, and SAR plus VIR combinations. One classification using individual pixels as input and one classification using

field means as input was performed for each band combination. Results of the analysis demonstrated the importance of cover type for determining SAR backscatter. Several crop/site combinations exhibited distinct tones. Cover type was the single most important parameter, and other variables (such as surface roughness, cultivation direction) were also significant in some cases. Also highlighted was the complexity of the relationships between radar return and crop type, agroclimatic region, and SAR sensor parameters, and the need for further detailed studies of these relationships. A necessary part of such a study are data sets with detailed documentation of ground conditions over the growing season, preferably on a per-pixel basis. In addition to plant canopy development, soil surface roughness and its distribution within a field should be adequately characterized. Analysis indicated that SAR return from the soil surface is often a significant component of the total backscatter from cultivated fields, particularly under semi-arid agroclimatic conditions with lower total biomass. Cihlar and Hirose (1984) found that for all the combinations that included MSS data, the overall average classification accuracy of the per-field classification was higher than the accuracies obtained using the single-pixel values. Conversely, band combinations that included only SAR data gave mixed results in that per-field accuracies were higher than per-pixel accuracies for some sites and lower for other sites.

D.2 Multitemporal Spaceborne SAR Data for Crop Classification

Schotten *et al.* (1995) conducted an assessment of the capabilities of multitemporal ERS-1 SAR data to discriminate between agricultural crops and to determine the earliest possible stage in the growing season at which crop type can be distinguished. The test site is located in South Flevoland, an agricultural region in the Netherlands where 12 crop types are found. Fourteen ERS-1 SAR images were acquired during the 1992 growing season between May and November. The field-based classification yielded an overall classification accuracy of 80% with the optimal data set. For potatoes, winter wheat, grass, winter rape, spring barley, fruit trees and lucerne, an accuracy and reliability of over 80% was achieved. For sugar beet, maize,

onions, beans, and peas, the accuracy and reliability were below 80%. The stage at which the crop type could be assessed is crop dependent. Winter wheat, spring barley, potatoes, winter rape and lucerne could all be distinguished in the period between mid-June and mid-August. Grass and fruit orchards could only be distinguished using images acquired after the more seasonal crops had been harvested. Sugar beet, maize, onions, beans and peas could not be distinguished acceptably using SAR images.

Ban and Howarth (1995) investigated ERS-1 SAR temporal-spectral profiles for agricultural crop identification. During the growing season in 1992, six dates of ERS-1 C-VV SAR data were acquired over an agricultural area in Oxford County, southern Ontario, Canada. Radar backscatter characteristics for five major crops were analyzed for each date. ERS-1 temporal-spectral SAR profiles for the five major crops were generated and the earliest time of the year for identification of individual crop types was determined. The results showed that winter wheat could be successfully separated in the early season, but other crops could not be differentiated from one another until mid- and late season. The mean highest validation accuracy for four dates in early and mid- season using a per-field classifier reached 78.2%, which represents a 20% improvement over that of the single-date classification. Fields which display anomalous radar backscatter characteristics were identified and statistically described. It was found that these anomalies usually result from growing conditions and crop management practices. Soil drainage and soil roughness characteristics can also influence radar backscatter.

Aschbacher (1995a and 1995b) conducted an assessment of ERS-1 SAR for rice-crop mapping and monitoring. A study area of approximately 10 x 10 sq. km was selected in Kanchanaburi Province, West Thailand. Multitemporal ERS-1 SAR data were available for eight acquisition dates, namely 1991: November 22; 1992: October 7; 1993: February 24, May 7, June 11, August 20, October 29 and December 3. Extensive ground measurements were taken in parallel to ERS-1 data acquisitions during the main growth period in August to December 1993. Plant

height, plant moisture content, plant density, number and size of leaves, stalk diameters, and height of standing water were measured, together with more general observations regarding the state of the water/soil surface, state of plants, and weather at acquisition time. The analysis of ERS-1 SAR data was supported by aerial photographs and a SPOT panchromatic image. Irrigated or flooded rice fields showed a very characteristic radar backscatter signature. In radar imagery, rice fields appear very dark during the flooded, vegetative phase, and turn brighter during the reproductive and ripening phase. The radar backscattering coefficient σ° increases from about -15 dB to about -8 dB during plant growth, and thus covers a dynamic range which is significantly larger than that of any other agricultural crop. The relatively good correlation between σ° and plant-growth parameters makes the use of ERS-1 SAR data particularly suitable for crop-growth monitoring. As regards rice-field mapping, a simple, pixel-based maximum likelihood classification was carried out, based on multitemporal, Gamma MAP speckle filtered radar images (four dates, June 6, August 20, October 29, and December 3, 1993). It was found that:

- Multitemporal ERS-1 SAR data are highly suitable for rice-field mapping. The classification accuracy is 89% for rice fields versus other land covers.
- At least three images should be available during the growth cycle. The optimum acquisition dates are during the flooded vegetation phase, at the end of the reproduction phase and shortly before harvest.
- The use of a pixel-based standard maximum likelihood classifier is sufficient, although more sophisticated methods may yield slightly better results. Speckle filtering of the input data is mandatory.

As regards rice-crop monitoring, it was found that:

- Multitemporal ERS-1 SAR data are very suitable for rice-crop monitoring.

- The radar backscatter coefficient σ°[dB] of rice fields is highly correlated with rice-plant height (r=0.77). Consequently the use of radar data allows one to determine the approximate stage of plant growth.
- The radar signal shows a potential correlation with rice yield, but the relationship may be indirect.

D.3 Integration of Spaceborne SAR and VIR Data for Crop Classification

Ban and Howarth (1996b) investigated the synergistic effects of integrating SAR data and imagery acquired in the VIR portions of the spectrum. Combinations of ERS-1 SAR and Landsat TM data were used to evaluate classification accuracy for eight crop classes: winter wheat, corn (good growth), corn (poor growth), soybeans (good growth), soybeans (poor growth), barley/oats, alfalfa, and cut hay and pasture. The study area was situated in an agricultural area in Oxford County, southern Ontario, Canada. Three dates of early- and mid-season ERS-1 C-VV SAR data were acquired during the 1992 growing season (June 15, July 24 and August 5). July 24 SAR data were acquired in ascending mode, while others were acquired in descending mode. One date of Landsat TM data was also acquired on August 6, 1992. Both per-pixel and per-field classifications were performed on single-date SAR, multitemporal SAR, single-date TM and the combinations of SAR and TM data. Two post-segmentation classifiers (minimum distance and artificial neural network) were evaluated. Results showed that combinations of SAR and VIR improve classification accuracies, the best results showing overall accuracies in the mid-90% range. The per-field approach using an artificial neural network produced better accuracies than using a per-field minimum distance classifier or a per-pixel maximum likelihood classification.

Kohl *et al.* (1993) conducted a comparison of ERS-1 SAR and SPOT XS data for crop acreage estimation for agricultural statistics as part of the Monitoring Agriculture by Remote Sensing (MARS) pilot project. The study was performed on two test sites: Seville, Spain and Great Driffield, UK. Six ERS-1 Fast-Delivery (FD) scenes acquired between April and December 1992 over the Seville test site were analyzed. The information content extracted from those scenes was evaluated relative to a four-date SPOT XS data set acquired in the 1992 growing season and the results of a ground survey. The preprocessing of the FD data included 16- to 8-bit conversion, speckle reduction using G-MAP and Texture/Mean filter and geometric registration of the images. Maximum Likelihood Classifications (MLC) for 22 land-use and land-cover classes were performed based on five-date ERS-1 SAR, a single-date SPOT XS, and combined three-date ERS-1 SAR and a single-date SPOT XS data. The results showed a significant increase in classification accuracy of the combined ERS-1 and SPOT data sets in comparison to either ERS-1 or SPOT alone. For the Great Driffield site, five-date ERS-1 SAR data from April to October and single-date SPOT data in May were acquired and analyzed. The unfiltered FD data using a MLC showed that the classification accuracy of four-date ERS-1 is slightly better than that of five-date. This is probably because the late-October image is not significant for the crop in question. The work demonstrated that the information content of the ERS-1 data is complementary to the SPOT data and that multi-date SAR data performs better than a single-date SPOT data for certain classes.

APPENDIX E: GROUND INFORMATION - AN EXAMPLE OF GREEN SHEETS

BLOCK 4 - OXFORD COUNTRY - JULY 21, 1993

Field ID	Crop Type	Dev't Interval	Ground Cover	Canopy Height	Photos Roll	Frame	Row Direction	Comments
4-01	corn	3	5/0/5	14	2	2		
4-33	corn	3	4/0/6	10-14	1	2		
4-03	corn	3	4/0/6	10-14	1	4		9 stalks/squared metre
4-30	oats/barley	5	7/0/3	9	1	3		
4-34	corn	3	4/0/6	10-14				
4-04	perm. pasture	3	9/0/1	1	1	5		
4-05	corn	3	4/0/6	14	1	6/7		
4-06	soybeans	4	9/0/0	7	1	9		purple flowers
4-07	winter wheat	7	0/7/3	5	1	8	N/S	
4-08A	corn	4	6/0/4	22	1	10/11		
4-09	oats/barley	5	9/0/0	10	1	12/13		
4-10A	perm. pasture	3	9/0/0	1	1	14F		photo 4-10B in background
4-10B	corn	3			1	14B		photo 4-10A in foreground from distance
4-11	corn	3	8/0/2	17	1	15		11 stalks/squared metre
4-12	corn	3	8/0/2	17				
4-13	alfalfa/hay	3	5/1/4	2	1	16		weed infested (dandilions)
4-28	corn	3	5/0/5	16	1	17		
4-14edge	oats/barley	5	9/0/0	10	1	18		8m wide strip around edges
4-14centre	corn	3		17	1	18		
4-15A	hay/pasture	3	4/5/1	3	1	19		8m strip cut around edges
4-15B	alfalfa/hay	3	9/1/0	3	1	20		15m strip cut around edges
4-16	hay	3	7/2/1	2	1	21		whole field recently cut
4-31	oats/barley	5	9/0/0	12	1	23		
4-32	hay	3	6/2/2	2				whole field recently cut
4-18A	hay/pasture	3	6/3/1	2	1	24/25		whole field recently cut
4-18B	alfalfa/hay	3	9/0/1		1	24/25		field in process of being cut
4-19	winter wheat	7	1/5/4	12	1	27/28L/29R		colour is rustic
4-20A	winter wheat	7	0/5/5	11	1	29L		golden colour
4-20B	oats/alfalfa	6	4/4/2	8	1	30/31		height of alfalfa is 4
4-21A?	beans	4	7/0/3	4	1	32/33		white flower therefore could be white beans